UNIVERSITY COLLEGE LONDON

Pyridazinediones: A Novel Class of Tuneable Reagents for the Selective Dual Modification of Proteins

by

Antoine Maruani

A thesis submitted in partial fulfillment for the
degree of Doctor of Philosophy

in the
Faculty of Mathematical and Physical Sciences
Department of Chemistry

January 2016

Declaration of Authorship

I, Antoine Gabriel Félico Maruani, confirm that the work presented in this thesis is my own. Where information has been derived from other sources, I confirm that this has been indicated in the thesis.

Antoine Gabriel Félico Maruani

January 10, 2016

For papy Jacob and mamie Solange

In loving memory of papy Félix and mamie Hélène

Abstract

Faculty of Mathematical and Physical Sciences
Department of Chemistry

Doctor of Philosophy

by Antoine Maruani

Antibody–drug conjugates (ADCs) are a particularly promising class of antibody-based therapeutics. They are commonly referred to as "magic-bullet" therapy due to the ability to seek and destroy primarily diseased cells within the body (*e.g.* cancer cells). Critical to this strategy is the availability of effective methodologies to link an antibody to other molecules (*e.g.* cytotoxic drugs, prodrugs).

Although current approaches offer great promise for the development of ADC constructs, they often are not selective and yield heterogeneous product mixtures. Other strategies require mutations with natural or unnatural amino acids, which are generally associated with low expression yields and post-translational issues, whilst some result in the loss of vital disulfide bonds. Furthermore, most of the current peptide/payload linker technologies have the potential to attach only one moiety, greatly limiting their scope and flexibility.

To tackle these issues, a novel class of tuneable reagents based on pyridazinedione (PD) moieties was developed. These reagents are readily accessible from inexpensive starting materials in 3 – 4 scalable steps and overcome the problems stated above. Indeed, the PD-based reagents have exquisite selectivity towards cysteines over lysines, even at high temperature and/or with an excess of reagent. When reacted with reduced native disulfide bonds of antibodies or antibody fragments, PDs rapidly and quantitatively form a stable and rigid 2-carbon bridge between the two cysteines side-chains without affecting the structure and biological activity of antibodies. The resulting conjugates have also been demonstrated to have exceptional resistance to hydrolysis at various extreme pHs and temperatures over an extended period of time. Finally, the PD-conjugates possess two orthogonal handles that were readily modified with two different moieties to generate highly functionalised homogeneous constructs with application not only in antibody therapeutics but also in imaging and diagnostics.

Acknowledgements

This PhD represents an immensely rich experience which could not come to an end without acknowledging a number of people who supervised me, helped me and supported me over the past few years, or who simply left their fingerprints in one way or another in this thesis. Nevertheless, thanking all these people without forgetting anyone would probably be more challenging than writing the thesis itself! I therefore apologise to those whose names are inadvertently left out of the following lines.

First, I want to thank my supervisor Prof. Stephen Caddick for giving me the opportunity to carry out a variety of exciting research, for his constant enthusiasm, motivation and support and for the trust he placed in my (often very random) ideas. A very special thank you goes then to Dr Vijay Chudasama for his daily help and supervision, for our passionate discussions about life and chemistry, for his daily *joie de vivre* and for his friendship.

Further, I wish to acknowledge Prof. Benjamin Davis and Dr Tom Sheppard for accepting to be my examiners.

For their supervision, I would like to thank Dr Mark Smith and Dr Richard Fitzmaurice. I also thank Dr Jamie Baker for the chats about antibodies, bioconjugation and more generally, about science. Thanks to Dr Abil Aliev, Dr Lisa Haigh and all professional services staff from mass spectroscopy service for their help with NMR and LC-MS.

I am very grateful to those who had a direct or indirect impact on the choices I made that led to this PhD: Dr Adam Squires for the afternoon chat about proteins more than 10 years ago and my "classes préparatoires" professors at Louis-le-Grand, Emmanuel Goldsztejn, Dominique Zann, Gérard Mantin and Stéphane Olivier for teaching me scientific rigour as well as kindling a desire to always learn more and to observe the world with a sharper eye.

I would also like to thank past and present members of the Caddick group and the Chudasama group; in particular Brian for the afternoon cooking, the whisky tasting and the English lessons, Max for his "clever stupidity", that keeps surprising me, Ramiz for the great AoE evenings, Eifion for being such a great listener, Ahmed for sharing my passion for computers, Lourdes for sharing my pain with the BIAcore, João for the history and politics lectures, Rachel for all the quarto games, Felix for teaching me the delicate art of casting gels but also Emily, Paul, Maurício, Florian...
Thanks to all the chemists from the KLB, especially all those who have passed through KLB230, without whom the past 4 years would have been nowhere near as fun. A

particular mention must go to Laure, Sam, Rosemary, Valerija, Liz, Dan and Cristina for their great unique personalities.

To my family and to my friends in France and overseas, whom I wish I could spend more time with, who manage to make me feel as if I never left every time we meet, un énorme merci.

To Agnès for putting up with me in the past few years, I know it was not an easy job, wielkie podziękowania z witaminą M.

I am deeply grateful to my parents for their invaluable support, for their patience, for their advice, for being the best teachers one could hope to learn from.

A very special thank you to Emmanuel, my brother, for the depth of his insight on all things of life. Even if you were far away, you managed to be with me.

Finally, for their support, for their understanding and for their love, I want to thank my grandparents, papy Jacob and mamie Solange, to whom this thesis is dedicated.

אם אין אני לי, מי לי? וכשאני לעצמי, מה אני? ואם לא עכשיו, אימתי?

"If I am not for myself, then who will be for me? And if I am only for myself, then what am I? And if not now, when?"

Hillel the Elder

Contents

List of Figures

List of Tables

List of Schemes

Abbreviations

Ac	Acetyl
ADC	Antibody–Drug Conjugate
ADIBO	Aza-dibenzocyclooctyne
AIBN	Azobisisobutyronitrile
aq.	Aqueous
BBS	Borate Buffered Saline
b.p.	Boiling point
BCN	Bicyclo[6.1.0]nonyne
BME	2-Mercaptoethanol
Boc	*tert*-Butyloxycarbonyl
br.	Broad
calcd	Calculated
CI	Chemical Ionisation
CIAP	Calf intestine alkaline phosphatase
CMP	Cytidine monophosphate
CuAAC	Copper(I)-catalyzed Alkyne–Azide Cycloaddition
Cys	Cysteine
d	Doublet
DCC	*N,N'*-Dicyclohexylcarbodiimide
DCCU	Dicyclohexylurea
DCM	Dichloromethane
dhAA	Dehydroascorbic acid
DIBO	Dibenzocyclooctyne
DIFO	Difluorinated cyclooctyne
DIPEA	*N,N*-Diisopropylethylamine

DMF	Dimethylformamide
Dox	Doxorubicin
DTT	Dithiothreitol
EDC	1-Ethyl-3-(3-dimethylaminopropyl)carbodiimide
EDTA	Ethylenediaminetetraacetic acid
EI	Electron Ionisation
eq.	Equivalents
ES	Electrospray
Fab	Fragment antigen-binding
FAB	Fast Atom Bombardment
FcRn	Neonatal Fc Receptor
FDA	U.S. Food and Drug Administration
HATU	1-[Bis(dimethylamino)methylene]-1*H*-1,2,3-triazolo[4,5-*b*]pyridinium 3-oxid hexafluorophosphate
HBTU	*O*-Benzotriazole-*N,N,N',N'*-tetramethyl-uronium hexafluorophosphate
HIV	Human Immunodeficiency Virus
HOBt	Hydroxybenzotriazole
HRMS	High Resolution Mass Spectrometry
IR	Infrared
J	Coupling constant
KHMDS	Potassium bis(trimethylsilyl)amide
LCMS	Liquid Chromatography Mass Spectrometry
LRMS	Low Resolution Mass Spectrometry
M	Molar
m/z	Mass to charge ratio
mAb	Monoclonal Antibody
MAb	Murine Antibody
MFCO	Monofluorosubstituted Cyclooctyne
Me	Methyl
MOPS	3-(*N*-morpholino)propanesulfonic acid
Ms	Mesyl
MS	Mass Spectroscopy
MWCO	Molecular Weight Cut Off

NBS	*N*-Bromosuccinimide
NHS	*N*-Hydroxysuccinimide
NMR	Nuclear Magnetic Resonance
p	Para
PB	Phosphate Buffer
PBS	Phosphate Buffered Saline
PD	Pyridazinedione
PEG	Polyethylene Glycol
PFP	Pentafluorophenyl
Ph	Phenyl
PK	Pharmacokinetic
ppm	Parts per million
PyBOP	(Benzotriazol-1-yloxy)tripyrrolidinophosphonium hexafluorophosphate
rt	Room temperature
s	Singlet
sat.	Saturated
SDS-PAGE	Sodium Dodecyl Sulfate - Polyacrylamide Gel Electrophoresis
SPAAC	Strain-Promoted Alkyne–Azide Cycloadditions
SPANC	Strain-Promoted Alkyne–Nitrone Cycloadditions
SPATC	Strain-Promoted Alkyne–Tetrazine Cycloadditions
t	Triplet
TBAB	Tetra-*n*-butylammonium bromide
TBTA	Tris(benzyltriazolylmethyl)amine
TCEP	Tris(2-carboxyethyl)phosphine
Tf	Triflate
TFA	Trifluoroacetic Acid
THF	Tetrahydrofuran
THPTA	Tris(3-hydroxypropyltriazolylmethyl)amine
TLC	Thin Layer Chromatography
Tris	Tris(hydroxymethyl)aminomethane
TSTU	*N,N,N',N'*-Tetramethyl-*O*-(*N*-succinimidyl)uronium tetrafluoroborate
UCL	University College London
UDP	Uridine diphosphate

uPLC	Ultra Performance Liquid Chromatography
UV-Vis	Ultraviolet-Visible Spectrophotometry
wt	Weight

Chapter 1

Introduction

1.1 Chemical modification of proteins

Decoding the chemistry of life is the ultimate goal for biochemists and chemical biologists. The enormous complexity of chemical and biochemical pathways, however, represents a major obstacle towards achieving this aim. A significant step in this direction was the decoding of the entire human genome sequence, which provided a vast trove of genetic information.[1,2] Whilst the human genome consists of 25 000 – 30 000 genes,[1] the human proteome is much more complex, consisting of more than 1 million proteins.[3] It is therefore essential to understand the functions of these encoded proteins to gain a thorough understanding of the chemistry of life.[4]

To achieve that goal, proteins have been artificially modified and advances in protein modification by chemical means have led to the development of a range of protein conjugation methodologies.[5] These methodologies have been successfully applied to a number of fields such as the fluorescent tagging of proteins[6] or the development of therapeutic protein conjugates[7,8] to treat indications such as HIV,[9] cancer,[10] and malaria.[11] Chemically modified proteins have also been utilised as diagnostics.[12]

The use of synthetic methodology to modify proteins has to overcome many major obstacles, the most significant of which is the need for high selectivity. For example, modifying only one amino acid type by discriminating against all the other natural amino acids in a protein is essential for selective modification.[13] Moreover, these modifications must be carried out in aqueous media, at near-physiological pH and

at ambient temperature to prevent the denaturing of proteins. In addition, these reactions should be unaffected by surfactants, that are often required for protein stability.[14] Despite these challenges, a large number of approaches have been developed for protein modification over the years.[15] These approaches can be divided into two categories: (i) modification of natural amino acids; and (ii) modification of unnatural amino acids (uAAs). Each of these methods has their own unique advantages and disadvantages. As it is of most relevance, the modification of natural amino acids is described in further detail below. A detailed review on the modification of uAAs has been reported by Mastrobattista *et al.* and it will not be discussed in detail here.[16]

1.2 Modification of natural amino acids

There is an ever increasing interest in the development of methods for the "traditional" chemical modification of proteins,[13] which focuses on modifying the 20 available natural amino acids in a selective manner. Most of the residues have been explored in this context and reagents for the selective modification of cysteine, serine, lysine, histidine, tyrosine, aspartic acid, tryptophan, arginine, threonine as well as glutamate and even methionine, have been developed (Figure 1.1).

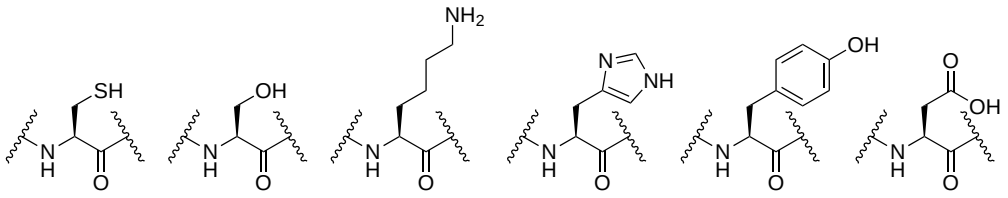

FIGURE 1.1: Some of the proteinogenic amino acids side chains targeted for chemical modification. Left to right: cysteine, serine, lysine, histidine, tyrosine and aspartic acid.

Classically, most of the work on the site-selective modification of natural amino acids has focused on reactions with cysteine and lysine[17] as these two residues bear the most nucleophilic side chain groups, a thiol and amine, respectively.

1.2.1 Modification of lysines

The majority of chemically modified biologicals that have obtained FDA approval to date have been prepared *via* lysine modification, typically through amine-reactive succinimidyl esters.[18] This amino acid is often targeted when site-selective modification

is not essential.[19] Lysine can form irreversible amide linkages with *N*-hydroxysuccinimide (NHS) esters at physiological pH in the absence of any exogeneous reagents. At higher pH (9 – 9.5), lysine residues react quantitatively with isothiocyanates or isocyanates, forming thioureas or ureas respectively. Over the years, a plethora of reagents have been developed to target lysines residues on the surface of proteins (Scheme 1.1).[20–23]

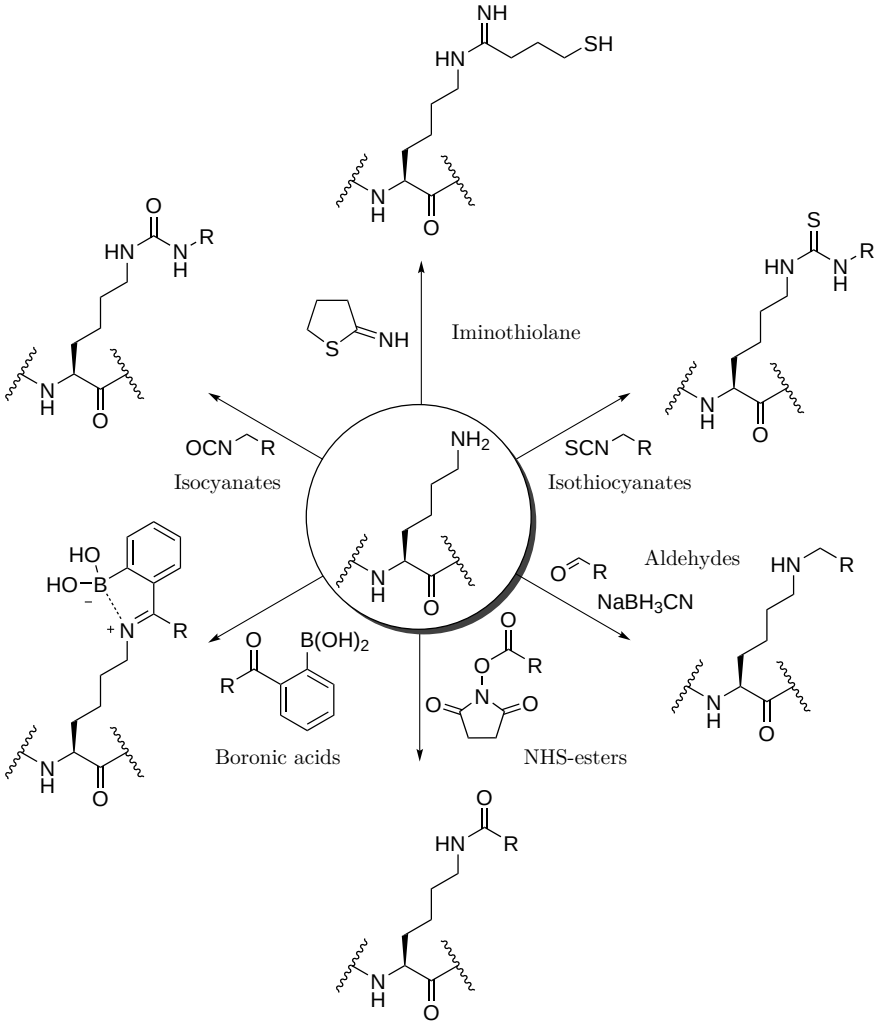

Scheme 1.1: Main reactions for lysine modification.

Nevertheless, this technique is now often considered to be non-ideal due to the high abundance of this amino acid.[24,25] Virtually all proteins contain many solvent exposed lysines in addition to the amine of the N-terminus, thus leading to a heterogeneous mixture of products upon conjugation with a wide distribution of loading levels.[26] When preparing therapeutics, for example, this would result in a narrow therapeutic window[27] as too many modifications per protein raise problems with solubility[28] and faster clearance rates from a patient's blood.[29] This is mainly due to the loss in surface charges upon conversion of the charged ammonium groups on lysine residues to neutral moieties.

In addition, lysine residues in or near the active or binding site of the protein might be targeted, which would lead to abrogation of activity.[30] Furthermore, heterogeneity complicates product analysis,[31] and the most widely used reagents for lysine-modification, NHS esters, have limited storage stability due to moisture sensitivity.[32] Moreover, control over the reaction at lysines is often limited and can only be achieved to a certain extent if carried out under strict pH control[33] or by the use of conditions that only allow reaction to take place at an extremely slow rate,[34] so that only the most reactive lysines react. Against this background, the naturally occurring amino acid that offers the greatest potential for site-specific modification is cysteine.

1.2.2 Modification of single cysteines

Free cysteines are extremely rare in proteins[35] and make up only 0.2% of all naturally occurring amino acids.[36] This, together with the fact that the thiol side chain has the highest reactivity of all proteinogenic groups at physiological conditions,[37] makes it a useful target for the selective and site-specific modification of proteins. Additionally, with the possibility of site-directed mutagenesis, cysteine residues can easily be inserted at a specific position on a protein.

Cysteine-targeting chemistry is well established and widely employed to create bioconjugates,[38–41] probe enzyme activity,[42] label proteins,[43] probe cellular oxidation status,[44] or obtain structural information.[45–47] A wide variety of cysteine modifying reagents are available from a number of leading biochemical companies (*e.g.* Pierce and Aldrich) with even more being synthesised in laboratories around the world for specific applications. The main reaction modes that are employed to modify cysteine residues are alkylation, disulfide formation and oxidation (Scheme 1.2).[48] The choice of reagent depends mostly on the specific application.

The most widely used compounds for alkylation are maleimides. These Michael acceptors tend to react more rapidly and selectively with thiols than α-halocarbonyls. As such, a number of chemical probes linked to maleimides (*e.g.* fluorophores, PEG chains, cytotoxic drugs and biotin) are now commercially available.[49] Recently, bromomaleimide and related derivatives have been developed which allow for reversible cysteine modification.[50] Bromomaleimides react as rapidly as conventional maleimides, but revert to free cysteines in the presence of a reducing agent such as 2-mercaptoethanol.[51] Novel pyridazinedione

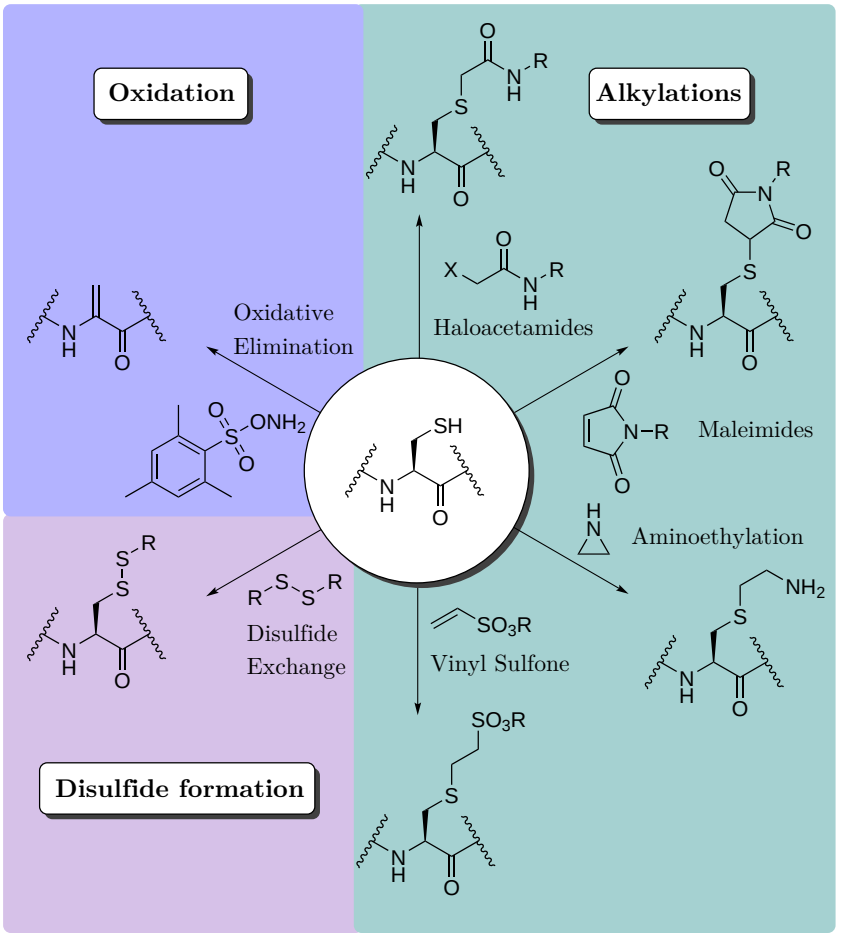

SCHEME 1.2: Main reactions for cysteine modification.

based reagents have also been developed.[52] These molecules offer the potential for four points of attachment and are stable to hydrolysis, unlike conventional maleimide reagents. Pyridazinedione-based reagents have also been shown to be highly selective for cysteine over lysine and the resultant conjugates are reversible in an environment of an excess of reducing reagent (Scheme 1.3).[52]

In proteins, free cysteine has an abundance of around 0.2% but the total proportion of this residue is 1.7%.[15] The remaining 1.5% are tied up in disulfide bonds. Due to their thiol reactivity and increased abundance, these disulfide bonds present themselves as an attractive target for the site-selective chemical modification of proteins.

1.2.3 Modification of disulfide bonds

The disulfide bonds of a protein are generally considered to be vital for protein stability and activity.[53] Accordingly, the rupture of these covalent links may destabilise many

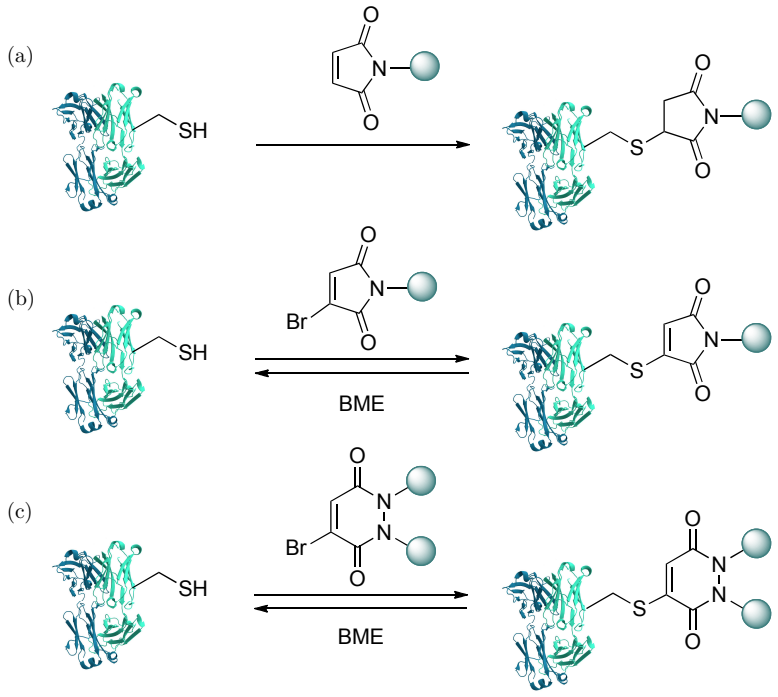

SCHEME 1.3: Cysteine modifications with (a) maleimide, (b) bromomaleimide and (c) bromopyridazinedione.

proteins.[54] When functionalising a reduced disulfide, it is therefore desirable to covalently re-connect the free thiols. This can be accomplished by the insertion of a non-natural bridge into the disulfide bond which would join the two thiols and also directly carry either a functional group of interest (*e.g.* a fluorophore or a drug) or a chemical handle allowing for further functionalisation. The first successful attempt to modify proteins *via* disulfide bonds whilst retaining their near-native structure was reported by Shaunak *et al.* in 2006.[55] In this work, an enone-sulfonyl reagent was synthesised. This reagent reacts with one of the two free thiols, generated from disulfide reduction, *via* a conjugate addition and elimination step, followed by a second conjugate addition reaction with the other free thiol, thereby re-connecting the side chains of the cysteines *via* a three-carbon bridge (Scheme 1.4).

An efficient and elegant approach to rebridge disulfide bonds has also been developed by Smith *et al.*[51] It was postulated that incorporation of two leaving groups on a maleimide double bond would enable two addition-elimination sequences to occur on reaction with the two free thiols to generate a bisthioether maleimide (Scheme 1.5).

Using the peptide somatostatin, a peptide hormone with poor *in vivo* stability, as a disulfide bearing protein model, Schumacher *et al.* selectively introduced a stabilising

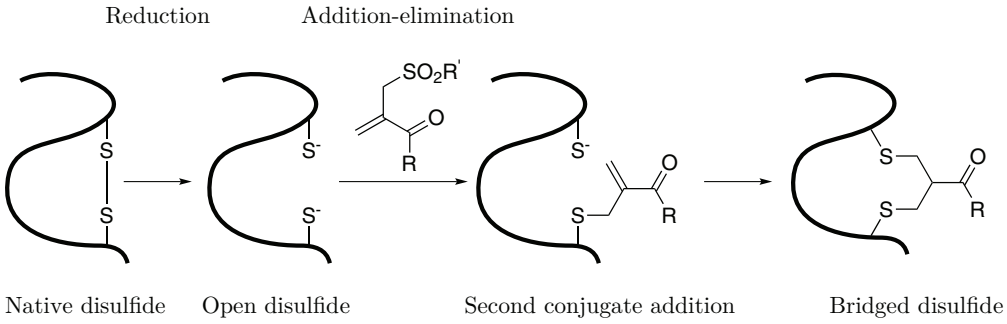

SCHEME 1.4: Mechanism of the insertion of a three-carbon bridge into a disulfide bond. Modified from Shaunak *et al.*[55]

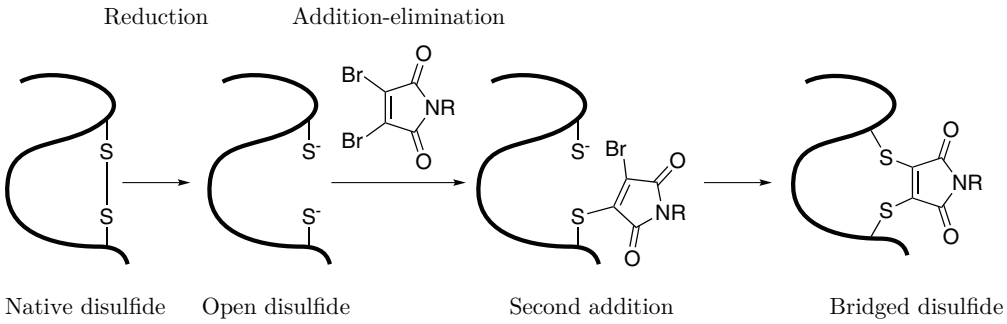

SCHEME 1.5: Bridging of a reduced disulfide bond with dibromomaleimide.[51]

group, PEG, whilst retaining the biological activity of unlabelled somatostatin.[56] This methodology allowed selective modification, and bridging, of a native disulfide bond yielding a homogeneous product. It is simple and inexpensive and under certain conditions the labelled peptide, or protein, could, in principle, be decoupled from its label in the cytoplasm of cells where there is a relatively high concentration of glutathione.[57] Although current approaches offer great promise, the current peptide/payload linker technologies only tend to attach one functional group of interest, thus limiting their scope. In recent years, proteins such as antibodies have been extensively modified for a variety of applications.

1.3 Antibodies and antibody fragments

1.3.1 Antibodies

Antibodies (also known as Ig because they were used historically to define the term immunoglobulin) are macromolecular Y-shaped protein complexes of *ca.* 150 kDa and above (*vide infra*, Figure 1.2, page 10). They are produced by B-cells in the blood upon

activation of the immune system. Antibodies target their specific antigen binding partner with exquisite selectivity and have therefore received much attention in recent years as targeted therapeutics alone, *via* antibody-dependent cell-mediated cytotoxicity (ADCC), and as vehicles for drug delivery and imaging.

Antibodies have differences in their biological properties, functional locations and ability to deal with different antigens. Therefore, they are subdivided into different varieties known as isotypes, or classes (Table 1.1). The isotype depends on the structure of the constant domains of the heavy chains (*vide infra*, Figure 1.2, page 10); in placental mammals, γ, α, μ, ε and δ chains correspond to IgG, IgA, IgM, IgE and IgD, respectively.[58] To reflect smaller differences in between heavy chains, some classes are also subdivided into Ig allotypes, or subclasses. For example, humans have 4 different types of IgG (IgG1, 2, 3 and 4) and 2 of IgA (IgA1 and IgA2) with more than 95% similarity in their sequences. Human light chains of antibodies also have isotypes named $\varkappa$ and λ.

	Location	Proportion	Valency	Function
IgG (γ)	Blood	$70\% - 75\%$	2	Immunity against invading pathogens
IgA (α)	Mucosal areas, gland secretions	$10\% - 15\%$	$2 - 4$[a]	Agglutination, immunity against invading pathogens
IgM (μ)	B cells, blood	10%	$2 - 10$[b]	Agglutination, initiation of classical complement pathway
IgE (ε)	Mast cells, basophils	$\leq 1\%$	2	Allergy, protection against parasitic worms
IgD (δ)	B cells	$\leq 1\%$	2	Activation of B cells

TABLE 1.1: Properties of the different antibody isotypes of placental mammals. [a]IgAs can be released as dimers. [b]The value of 10 is purely theoretical. Indeed, even if IgM are mostly pentameric, the steric hindrance generated when they are bound to the antigen epitopes makes the "real" valency closer to 5.

1.3.2 Antibody fragments

Specific enzymatic or chemical cleavage of antibodies allows for the isolation of different fragments (*vide infra*, Figure 1.2, page 10):

- **Fv fragment** (variable). It is the smallest fragment that retains the binding properties of the antibody to a specific antigen. It is composed of the variable regions (V_L and V_H). More specifically, in V_L and V_H, variable loops of β-strands are responsible for binding to the antigen. These loops are referred to as the *complementarity determining regions* (CDRs). Fv fragments are monovalent with a molecular weight of *ca.* 25 kDa.

- **Fab fragment** (antigen-binding). It has the same affinity for the antigen as that of the full antibody. It is composed of the whole light chain (V_L and C_L) and of part of the heavy chain (V_H and C_H1). Fab fragments are monovalent with a molecular weight of *ca.* 50 kDa.

- **F(ab')$_2$ fragment**. It corresponds to the association of two Fab fragments linked together by the disulfide-containing part of the C_H chains and, therefore, has the same affinity for the antigen as the full antibody. This small linking region is referred to as the *hinge region*. F(ab')$_2$ fragments are divalent with a molecular weight of *ca.* 110 kDa.

- **Fc fragment** (crystallisable). It carries some of the biological properties of the immunoglobulin, in particular its ability to be recognised by effectors of immunity (by interacting with cell surface receptors) or to activate the complement system. It is composed of two (or three, depending on the class of the antibody)[59] identical C_H2 fragments, derived from the heavy chains constant domains of the antibody. Fc fragments do not recognise the corresponding antigen. They bind monovalently to various cell receptors and complement proteins and have a molecular weight of *ca.* 50 kDa.

Antibody fragments have altered physiochemical features. For instance, smaller sized fragments can penetrate into tissues inaccessible to full-size monoclonal antibodies (mAbs).[60,61] Another advantage lies in the ability of prokaryotic systems to express antibody fragments when mAbs require more costly eukaryotic systems. However, most fragments lack the Fc domain that serves to both stabilise full-size antibodies and allow FcR-mediated recycling. As a consequence, fragments are rapidly degraded in humans and have short circulating half-lives.[62] Several strategies have been developed to extend the half-life of fragments and reduce immunogenicity; they include conjugation to proteins such as albumin[63] and PEGylation,[64–67] which was applied to the FDA-approved

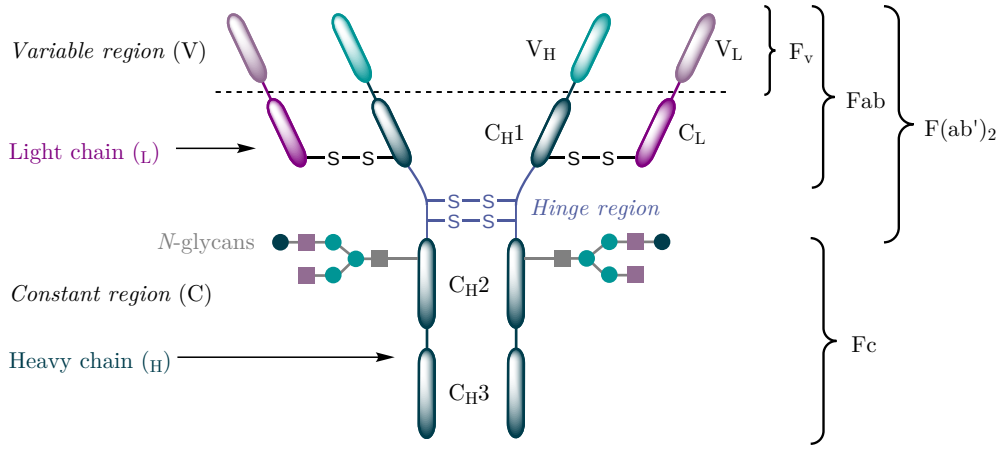

FIGURE 1.2: General structure of an IgG1 with its fragments highlighted.

anti-TNFα Fab, certolizumab pegol. However, any biomanufacturing advantage gained in operating with antibody fragments would be lost if the stabilising technology was expensive and/or excessively technically challenging.

From a more fundamental point of view, antibody fragments also offer several advantages over full-size antibodies for use in certain immunochemical techniques and experimental applications, including:

- Reduced non-specific binding from Fc interactions (many cells have receptors that bind to the Fc region).[68]
- Ability to control Fc-binding to Protein A or Protein G in experiments involving immunoprecipitation and Western blotting.[69]
- More efficient penetration of tissue sections.[60,61,70,71]
- Potentially higher sensitivity in antigen detection in solid phase applications as a result of reduced steric hindrance from large protein epitopes.
- Elimination of Fc-associated effector functions (*e.g.* complement fixation) in antigen-antibody binding studies.[72]
- Simpler system for studying the structural basis for immune recognition using X-ray crystallography or NMR.[73]

1.4 Antibody–drug conjugates

Antibody–drug conjugates (ADCs) are a type of targeted therapeutics. They consist of an antibody armed with potent cytotoxic drugs using various conjugation and linker technologies. The binding region of the antibody allows selective targeting of certain cell types (*i.e.* allowing for discrimination between healthy and diseased tissue) and the potent cytotoxic drug element effects cell-killing independent of antibody-dependent cell-mediated cytotoxicity (ADCC). Hence, ADCs offer the prospect for delivery of a toxic payload directly to a target, with minimisation of "off-target" toxicity. This in turn allows for the use of particularly toxic drug molecules that are conventionally excluded from use in chemotherapy.

The concept of delivering a toxic payload to cancer cells using a targeting agent dates back to 1913 when Paul Ehrlich described a "haptophore" that can deliver a "toxophore" selectively to a tumor.[74] However, it took 45 years for such a species to be constructed in the form of an ADC.[75] In the 1970's, ADCs were first tested on animals[76,77] and less than a decade later the first tests on humans showed promising results.[78] The first ADCs based on chimeric and humanised mAbs were reported in the 1990's,[79] and throughout this decade, ever increasing payload potency and improved target selection were achieved.[80] These advances finally led, in 2000, to the first US Food and Drug Administration (FDA) approved ADC (Mylotarg™, gemtuzumab ozogamicin).[81]

Despite promising preliminary results, Mylotarg™ was voluntarily withdrawn from the market in June 2010 as post-approval clinical trials for patients with acute myeloid leukemia showed that the ADC offered no clinical benefit over standard chemotherapy. Nevertheless, this class of targeted therapy showed considerable promise in the following years with two further ADCs gaining FDA approval (*i.e.* Adcetris™ **2**, brentuximab vedotin in 2011[82,83] and Kadcyla™ **1**, trastuzumab emtansine in 2013[84,85]). It is estimated that there are *ca.* 40 ADCs currently in the clinic and it is predicted that the market for ADCs will grow rapidly in coming years.[86]

Both Kadcyla™ **1** and Mylotarg™ were generated by modifying accessible lysine residues on the surface of the relevant antibody.[84,85] In fact, many ADCs are conjugated through lysine modification. However, with *ca.* 90 accessible lysines, any chemical modification strategy that is non-selective has the potential to generate complex mixtures, with

up to 10^6 distinct species statistically possible when targeting drug-to-antibody ratios (DARs) of 2 – 4. Such heterogeneous mixtures of ADCs may differ in both drug loading and conjugation site and this can result in a narrow therapeutic window with major pharmacokinetic implications. Although this non-specific conjugation technique has been used in FDA-approved ADCs, the use of non-selective approaches is now considered suboptimal in developing next generation ADCs.

In order for ADCs to deliver their full potential, sophisticated conjugation technologies to connect the cytotoxic drug to the antibody are needed. In a promising early development, Adcetris **2** was obtained by reacting some of the eight free cysteines generated by reduction of the four interchain disulfides of an antibody (*vide infra*, section 1.5.2.1, page 19). Whilst this approach still generates *ca.* 15 different species when targeting typical average DARs of 2 – 4, it offers a significant improvement over lysine modification strategies in terms of reduced heterogeneity.[87] There is a growing appreciation of the importance of developing site-specific methods, with several reports highlighting the advantages for generating near-homogeneous conjugates due to a better defined and improved pharmacokinetic (PK) profile.[87–89]

One of the keys to the ADC approach lies in the availability of effective methodologies to link an antibody to a payload. Most of the linking technologies in the clinical pipeline present drawbacks, such as lack of selectivity, poor yields and/or loss of structural integrity (Figure 1.3), limiting their usability and reducing their therapeutic index.

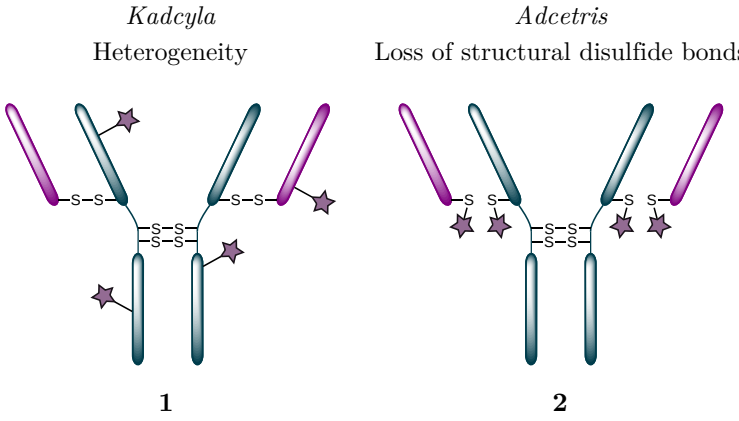

FIGURE 1.3: Main drawbacks in existing technologies.

1.5 Current methods for site-selective attachment of drugs to antibodies

1.5.1 Engineered antibody modification

With the rapid advances in protein engineering, methods to site-specifically functionalise antibodies have become more accessible in recent years. There are three main strategies to generate site-selectively modified ADCs with re-engineered mAbs: (i) insertion of cysteine residues in the antibody sequence by mutagenesis;[90,91] (ii) enzymatic conjugation (*e.g.* transglutaminases (TGs), formylglycine-generating enzymes (FGEs);[92] and (iii) insertion of an unnatural amino acid with a functional group that can be chemoselectively reacted.[93–95]

1.5.1.1 Engineered cysteines

The thiol moiety of the cysteine side chain has the highest nucleophilicity of all proteinogenic amino acid functional groups under physiological conditions. This makes it a useful target for the selective and site-specific modification of antibodies. Moreover, with the use of site-directed mutagenesis, cysteine residues can readily be inserted at a specific position on a protein. (*vide supra*, section 1.2.2, page 4).

In 2008, Junutula *et al.* (Genentech) described a method for the introduction of additional cysteine residues on a mAb using site-directed mutagenesis.[96] This procedure is non-trivial for an antibody as the engineered cysteine residues can pair with other free cysteines (*e.g.* to form protein dimers or to scramble disulfides), which could reduce or remove activity.[97,98] However, by screening conjugation sites on an antibody against the ovarian cancer antigen MUC16, an engineered thio-antibody (THIOMAB **3**) containing two new cysteine sites for attachment was generated successfully (Scheme 1.6).

Although the engineered cysteines were introduced successfully, they were mostly found as mixed disulfides with glutathione. As no reliable method to target reduction of these mixed disulfides over native disulfides was achieved, an alternative strategy was needed for engineered thiol unmasking. To do this, both the mixed and native interchain disulfides were reduced initially to yield **4**. This was followed by mild re-oxidation of the interchain disulfides with a gentle oxidant (*e.g.* $CuSO_4$) to afford antibody **5** with all of its native

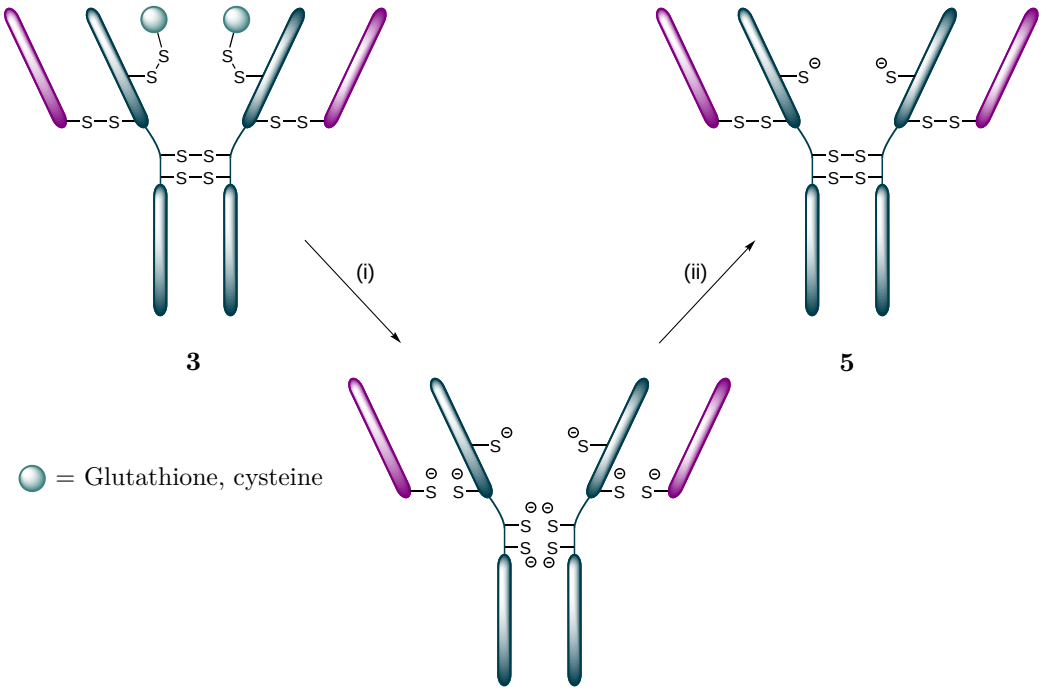

SCHEME 1.6: Preparation of THIOMAB.
Reagents and Conditions: (i) TCEP or DTT, PBS, 25 °C, 90 min; (ii) $CuSO_4$ or dhAA, PBS, 25 °C, 3 h.

disulfide bonds intact and two reduced engineered cysteines available for conjugation (Scheme 1.6).

Using this strategy, ADCs comprised of a monomethyl auristatin E (MMAE) derivative and an anti-MUC16 mAb were generated (Scheme 1.7). They were judged to have an average drug-to-antibody ratio (DAR) of 1.9 with more than 90% homogeneity and were active *in vitro* and *in vivo*.[91] The THIOMAB–drug conjugates were also shown to be significantly less toxic in rat and cynomolgus monkey models when compared with ADCs obtained by lysine conjugation with an average DAR of 4. Moreover, as described by Hamblett *et al.*, despite having half the average drug load, the THIOMAB–drug conjugates were as efficacious *in vivo*.[87,91]

1.5.1.2 Enzyme-directed modification

Another approach to achieving site-selective modification is *via* enzymes that react with a particular amino acid in a specific amino acid sequence. This has been used to site-selectively attach drugs to antibodies.

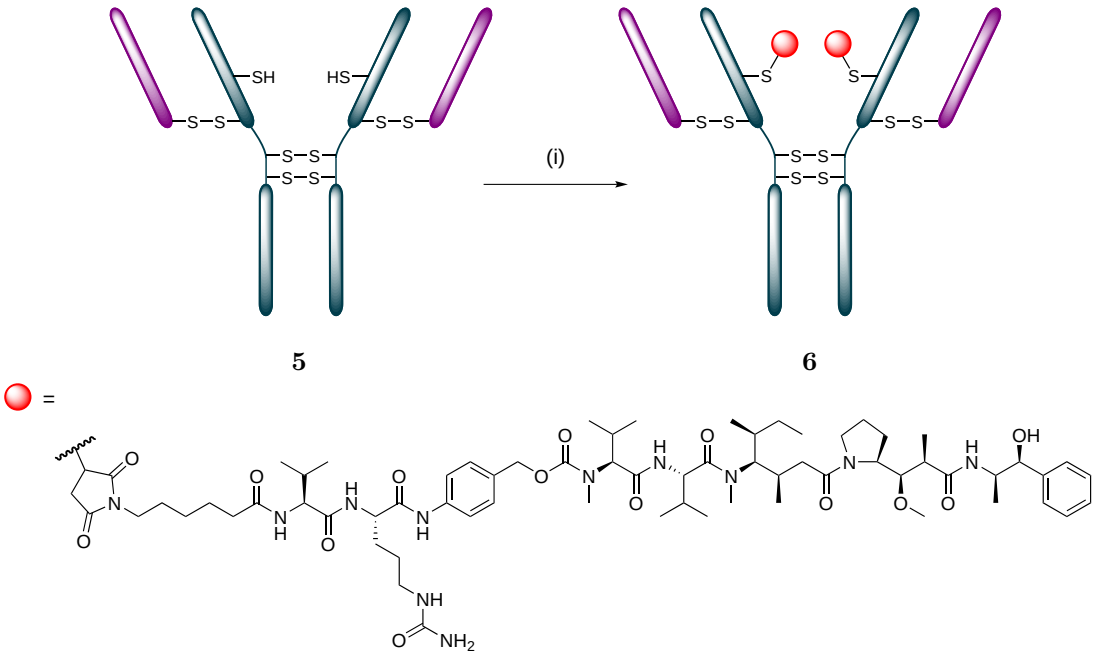

SCHEME 1.7: Conjugation to THIOMAB.
Reagents and Conditions: (i) MMAE derivative, 25 °C, 1 h.

Transglutaminases

Transglutaminases (TGs) play an important role in biological processes which depend on the covalent crosslinking of proteins,[99] where they catalyse the formation of amide bonds between the primary amine of a lysine and the amide group of a glutamine. However, bacterial TG isolated from *Streptoverticillium mobaraense* has an atypical catalytic site compared to other TGs.[100,101] It does not catalyse a reaction with any of the naturally occurring glutamine residues in the constant regions of an antibody, but will recognise a "glutamine tag" (*i.e.* LL**Q**G).[27]

By appraising the merits of incorporation of this sequence into 12 surface accessible regions of an anti-M1S1 IgG1, Strop *et al.* (Rinat-Pfizer) found two optimal locations for the "Q-tag". Two ADCs based on monomethyl dolastatin 10 (MMAD, a potent tubulin inhibitor) were then generated (Scheme 1.8).

These conjugates were found to have good biophysical properties and a DAR of *ca.* 1.9.[102] Furthermore, when compared with an analogous ADC with a higher drug loading (average DAR of 3.6) based on cysteine alkylation post-native interchain disulfide reduction, the glutamine-tagged ADCs showed similar activity *in vitro* and *in vivo* and were better tolerated *in vivo*. This differential in toxicity profile suggests that either the selected

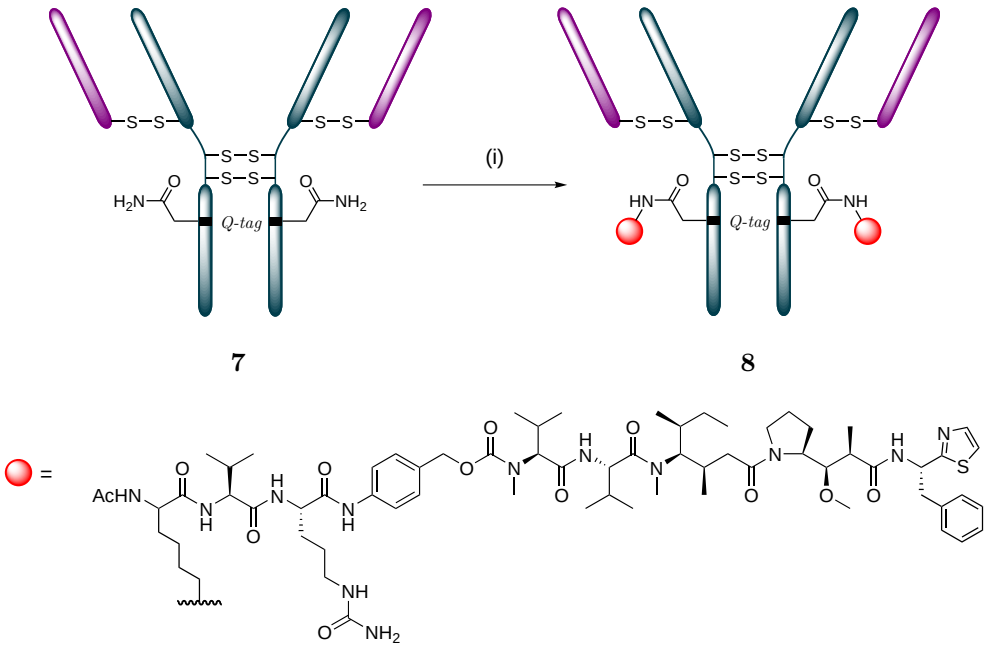

SCHEME 1.8: Conjugation with transglutaminase.
Reagents and Conditions: (i) MMAD derivative, TG (1 – 2%), TRIS·HCl pH 8.0, 25 – 37 °C, 16 h.

position of the drug and/or the lower loading offers the possibility for improvement of the therapeutic index of ADCs.

Formylglycine-generating enzymes

Formylglycine-generating enzymes (FGE) catalyse the selective conversion of a cysteine to an aldehyde when in a **C**XPXR sequence (where X is usually serine, threonine, alanine or glycine). The incorporated aldehyde can then be readily functionalised with aminooxy- or hydrazine-functionalised molecules.[103] Using this approach, Drake *et al.* (Redwood Bioscience) recently produced and characterised a series of functionalised antibodies bearing the aldehyde tag at different sites on trastuzumab.[104] They then used hydrazino-*iso*-Pictet-Spengler (HIPS) chemistry to conjugate a cytotoxic maitansine derivative (a potent microtubule-targeted agent) at three different positions (Scheme 1.9).

As observed with other methods, the site of conjugation had a significant impact on *in vivo* efficacy and PK profile in rats. Unfortunately, this method suffers from the hydration of the aldehyde from formyglycine in water to form an unreactive gem-diol, which lowers the yield of the process.[94]

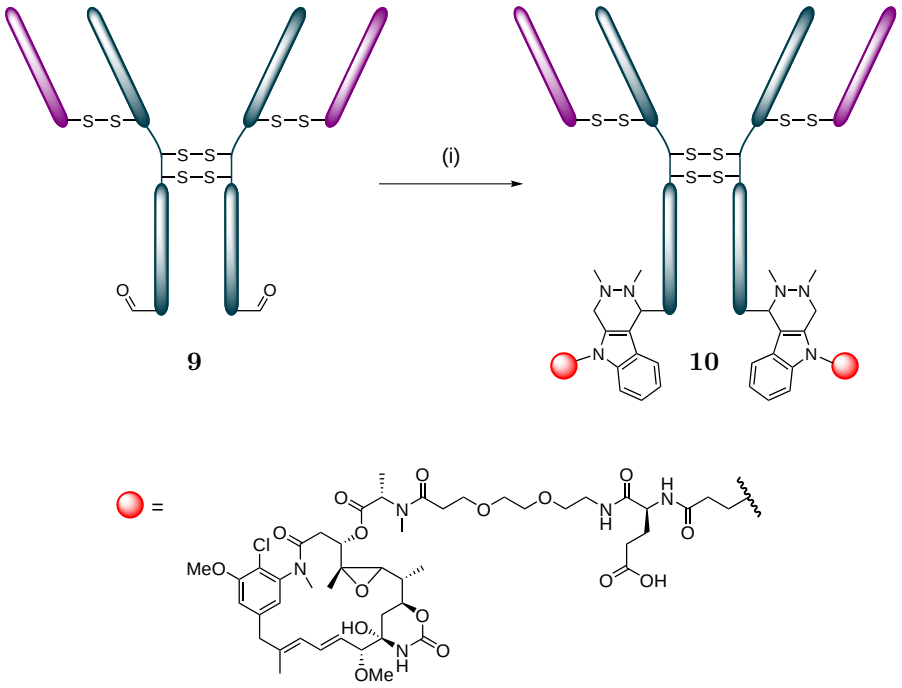

SCHEME 1.9: Conjugation by formylglycine-generating enzymes approach.
Reagents and Conditions: (i) Maitansine derivative, citrate buffer pH 5.5, 37 °C, 72 h.

1.5.1.3 Unnatural amino acid incorporation

Recent advances in development of methods for the incorporation of unnatural amino acids (uAAs) into proteins have presented opportunities for the site-selective modification of antibodies.[95,105] Three uAAs, *p*-acetylphenylalanine **11**, *p*-azidomethyl-phenylalanine **12** and azidohomoalanine **13** (Figure 1.4) have been particularly useful in generating conjugates through oxime ligation and classical click chemistry, respectively (*vide infra*, section 1.6, page 25).

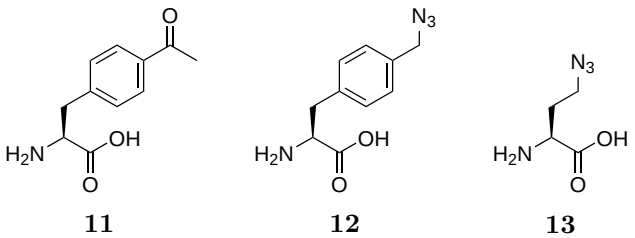

FIGURE 1.4: Common uAA used is site-specific modification of proteins.

Axup *et al.* described the incorporation of *p*-acetylphenylalanine into several residues in the constant region of trastuzumab to construct several modified antibodies ready for site-specific ADC synthesis.[95] Using this unique functional group, monomethyl auristatin F (MMAF), a potent tubulin inhibitor, was coupled through a stable oxime ligation

process to yield several near-homogeneous ADCs with a DAR of *ca.* 2.0 (Scheme 1.10). The resulting conjugates demonstrated good PK properties, potent *in vitro* cytotoxic activity against HER2-positive cancer cells and complete tumor regression in rodents. When compared with ADCs prepared by cysteine alkylation post-native interchain disulfide reduction, site-specific uAA-based ADCs were shown to have increased *in vitro* cytotoxicity and *in vivo* efficacy. They also had superior *in vitro* serum stability and an improved toxicology profile in rats.[106,107]

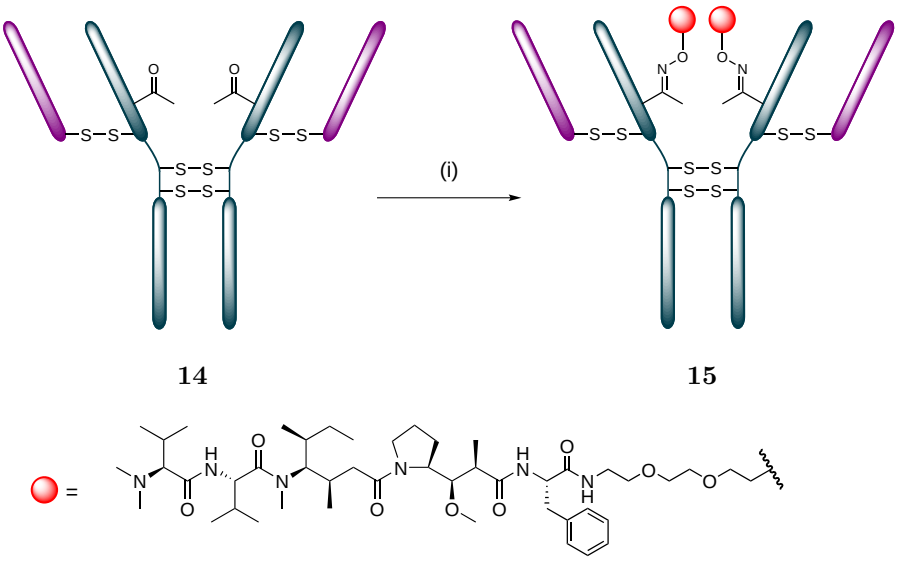

SCHEME 1.10: Conjugation by unnatural amino acid incorporation approach. *Reagents and Conditions*: (i) MMAF derivative, acetate buffer pH 4.5, 37 °C, 4 days.

Zimmerman *et al.* (SutroBiopharma) recently observed a similar trend *in vitro* by incorporating *p*-azidomethyl-phenylalanine into trastuzumab and using the strain-promoted azide–alkyne cycloaddition (SPAAC) reaction to conjugate an ADIBO-functionalised MMAF (Figure 1.5).[105]

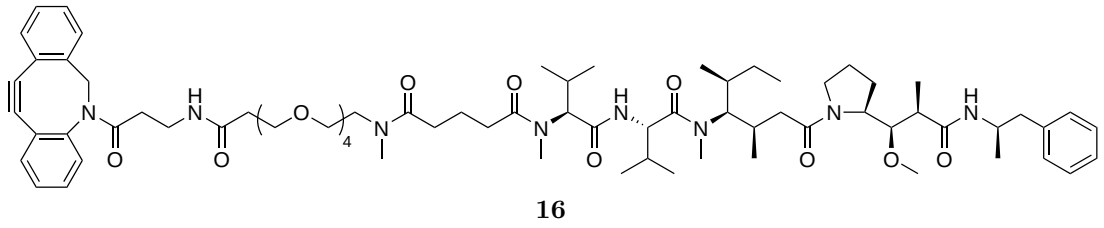

FIGURE 1.5: Structure of ADIBO-functionalised MMAF used by Zimmerman *et al.*

Even though these uAA methods offer the possibility of generating homogeneous conjugates by attachment of a drug at virtually any accessible site on a mAb, the potential immunogenicity of uAAs is not yet fully understood and more studies are needed to ensure the safety of these engineered ADCs.

1.5.2 Native antibody modification

Although the aforementioned methods offer the possibility to synthesise near-homogeneous ADCs they require site-directed mutagenesis and optimisation of cell culture conditions, which can increase the overall manufacturing cost of an ADC. The alternative is to develop methods which avoid the requirement for re-engineering by direct site-selective manipulation of native mAbs (*vide supra*, section 1.2, page 2).

1.5.2.1 Reduced inter-chain disulfides for site-selective modification

Whilst antibodies typically have approximately 90 accessible lysine residues, reduction of the 4 accessible interchain disulfides yields only 8 nucleophilic cysteine residues. Hence, conjugation to antibodies by reaction with cysteines thiols liberated from reduced interchain disulfides will inherently generate a smaller subpopulation of immunoconjugates compared with modification *via* lysine. Moreover, despite its known impact on complement-dependent cytotoxicity,[108] reduction of native interchain disulfide bonds was thought to have a limited effect on antibody structure and stability since assembly of light and heavy chains does not depend primarily on covalent disulfide linkages, but rather on non-covalent interactions.[109]

Conjugation of thiols liberated from reduced interchain disulfides

In 2003, Doronina *et al.* (Seattle Genetics) described the use of conjugation to thiols generated by reduction of the native interchain disulfides of a mAb as an ADC construction strategy. Initially, the 4 interchain disulfide bonds of a chimeric anti-CD30 mAb (*i.e.* cAC10) were reduced and the liberated thiols side chains were reacted with a MMAE derivative *via* a maleimide linker. This provided an ADC that was potent and selective for CD30-positive hematologic malignancies (Scheme 1.11).[110]

Originally, the 8 sulfhydryl groups generated by reduction of the interchain disulfides were alkylated using maleimide-MMAE, yielding a near-homogeneous conjugate with a DAR of 8. However, further analysis by Hamblett *et al.* and Beckley *et al.* showed that the high drug-loading had a significant impact on the conjugate PK (*i.e.* poor tolerability, high plasma clearance rate and decreased efficacy *in vivo*) and propensity to aggregate,[87,111] and that a lower DAR resulted in a larger therapeutic window.[87] In

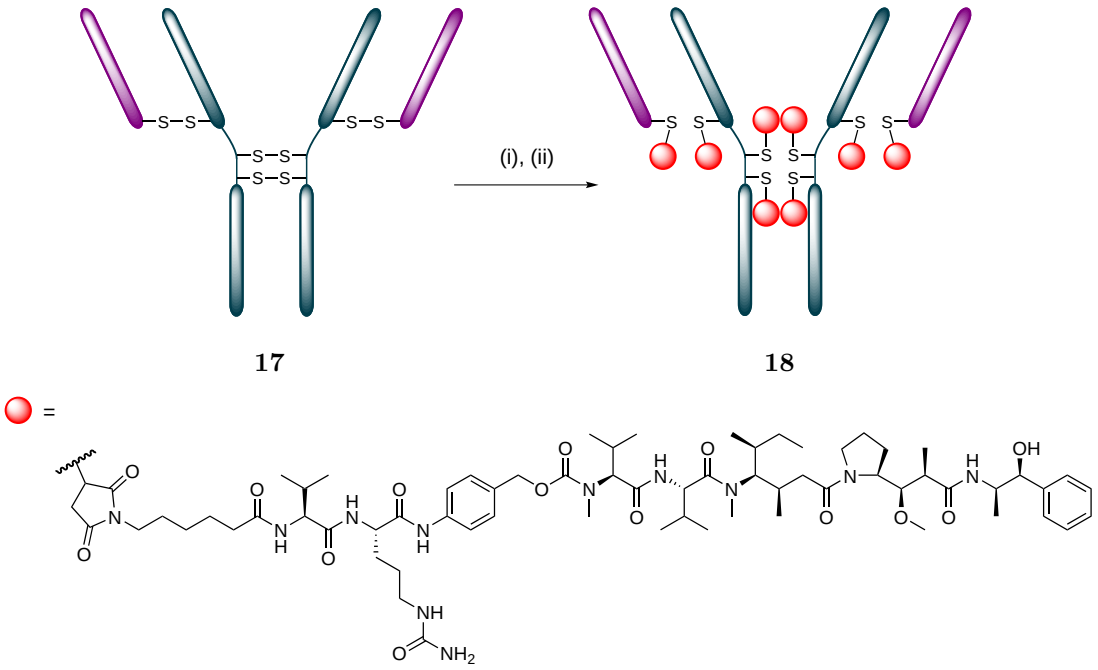

SCHEME 1.11: Alkylation of thiols liberated from reduced interchain disulfides. *Reagents and Conditions*: (i) DTT, PBS pH 8.0, 37 °C, 30 min; (ii) MMAE derivative, PBS/MeCN, 4 °C, 1 h.

particular, they showed that an ADC with a DAR of 4 was significantly less toxic to mice than higher loaded conjugates.

These observations, along with a screening of various reduction/re-oxidation strategies, resulted in a novel site-selectively modified antibody, Adcetris **2**, with an average DAR of 4 with isomeric homogeneities up to 75% (*vide supra*, Figure 1.3, page 12).[109] One of the main drawbacks of this strategy comes from the use of maleimide chemistry in that the generated conjugate is known to undergo retro-Michael reactions with blood thiols, resulting in the transfer of drug to thiol-bearing proteins and thus leading to off-site toxicity.[112–114] Recently, however, several strategies to overcome this issue and to obtain thiol-stable conjugates have been developed (*vide infra*, section 5.1, page 85).[113–117]

Re-bridging of cysteines liberated from reduced interchain disulfides

To target a DAR of 4 and increase the overall homogeneity of their conjugates, Badescu *et al.* (PolyTherics) explored the possibility that reduction of the interchain disulfide bridges could be followed by functional re-bridging of the disulfide. This would allow insertion of a single cytotoxic payload per disulfide and retain a covalent link between the protein chains. Their method is based on bis-cysteine-selective sulfone reagents that

allow for an addition-elimination-addition sequence onto the reduced disulfide bonds of either Fabs or mAbs (*vide supra*, Scheme 1.4, page 7).

Using MMAE as the toxic payload on both trastuzumab **19** and its Fab, Fab_{Her} **127**, they successfully demonstrated increased efficacy over drug alone whilst retaining binding and antigen-selective cytotoxicity *in vitro*, along with efficacy *in vivo* (Scheme 1.12).[118]

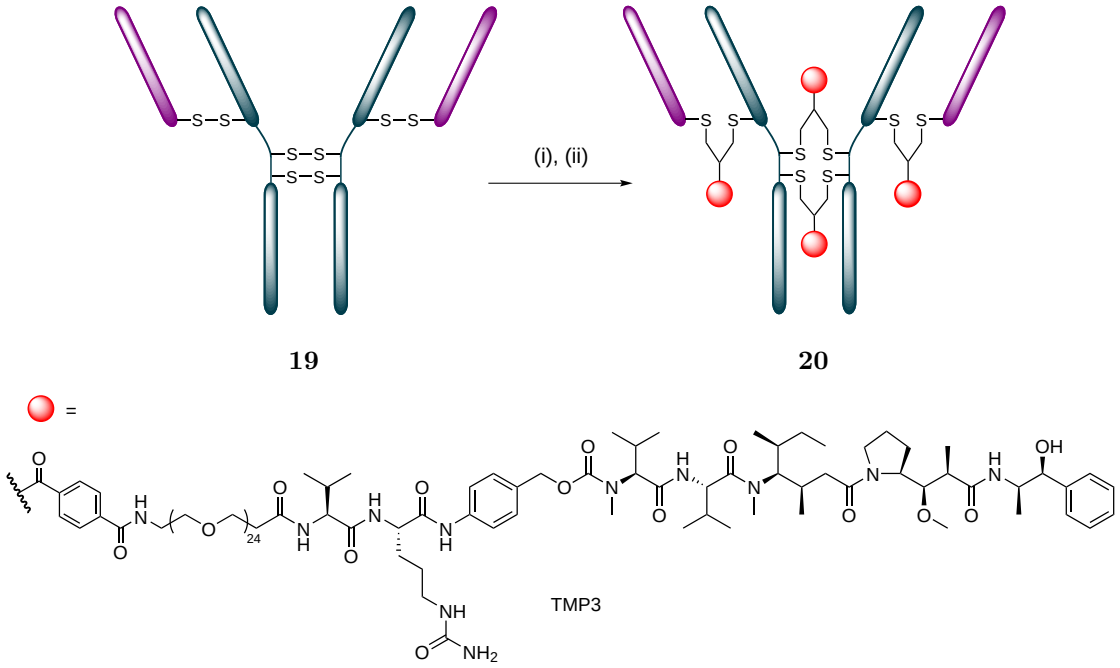

SCHEME 1.12: Rebridging reduced interchain disulfides.
Reagents and Conditions: (i) DTT, PB pH 7.4, rt, 30 min; (ii) MMAE derivative, PB pH 7.4, rt, 3 h.

Other groups (*i.e.* Chudasama, Baker and Caddick) have also developed reagents that allow for the efficient functional re-bridging of interchain disulfides (*vide supra*, Scheme 1.5, page 7).[119] Using these reagents on trastuzumab **19**, Nunes *et al.* have successfully generated near-homogeneous, MMAE-functionalised ADCs with *in vitro* efficacy.[120]

1.5.2.2 Glycan targeting for synthesis of antibody–drug conjugates

All antibodies are glycosylated at conserved positions in their constant regions; they possess an *N*-glycosylation site at the conserved Asn-297 residue of the Fc region (*vide supra*, Figure 1.2, page 10). Thus, this serves as a potentially interesting (and generic) site for antibody modification.

In this context, the use of hydrazone chemistry to attach a cytotoxic agent onto the glycans of an unmodified native antibody has found considerable utility.[121,122] Sodium periodate at high concentration has been used to oxidise carbohydrate residues in the native glycans to provide aldehydes which are used for ligation to afford relatively homogeneous ADCs (Scheme 1.13).[122]

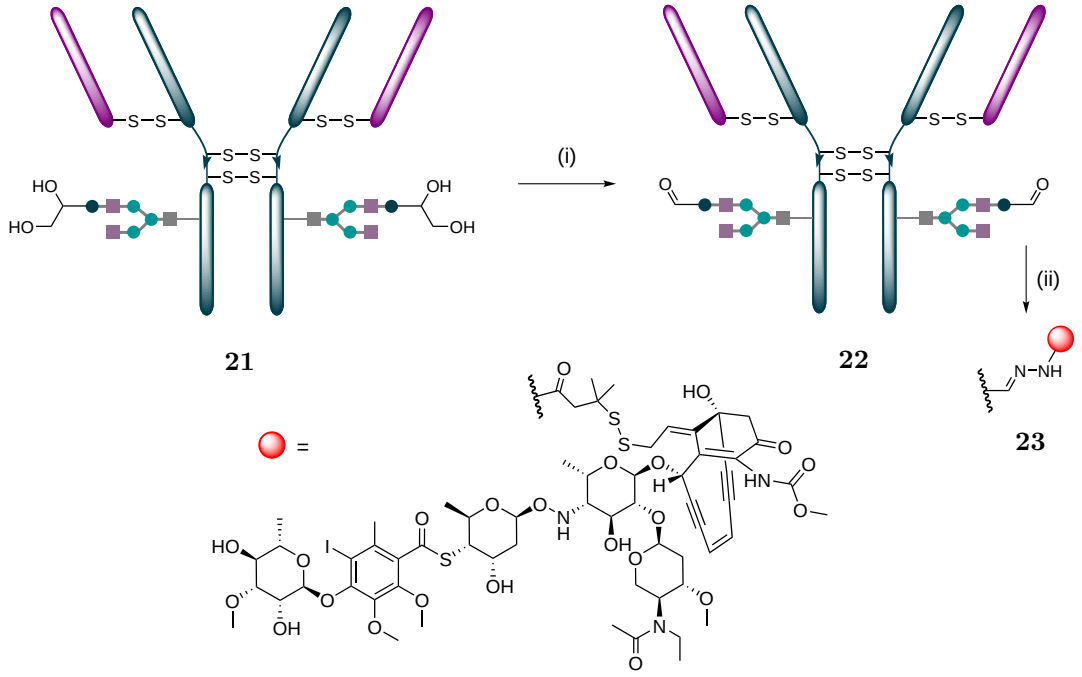

SCHEME 1.13: Oxidation and functionalisation of the glycans.
Reagents and Conditions: (i) $NaIO_4$, acetate buffer pH 5.5, 4 °C, 30 min;
(ii) Calicheamicin derivative, acetate buffer pH 5.5, rt, 3 h.

The main drawback of this approach arises from the harsh oxidation conditions required to generate the aldehydes, which can result in oxidation of methionine residues located close to FcRn binding site. This over-oxidation is known to affect FcRn binding and to generally reduce serum half-life (Scheme 1.14).[123] To alleviate this issue, milder enzymatic methods have been developed.

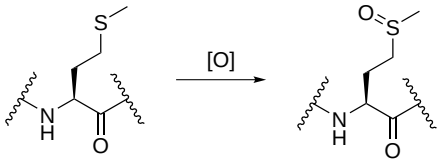

Methionine Methionine sulfoxide

SCHEME 1.14: Oxidation of methionine during glycans oxidation.

Neuraminidases

Through sequentially using neuraminidases to cleave the glycosidic linkages of neuraminic acids and Gal oxidase to oxidise the galactose residues of an anti-CEA mAb, Stan *et al.* site-selectively attached doxorubicin **143** *via* reductive amination on the generated aldehydes (Scheme 1.15).[88] The resulting ADC had a DAR of 3.7 and was four times more toxic *in vitro* than its counterpart generated by lysine conjugation with a DAR of 7.8. This demonstrates once again the importance of, and therapeutic opportunities for, site-specificity in ADC construction.

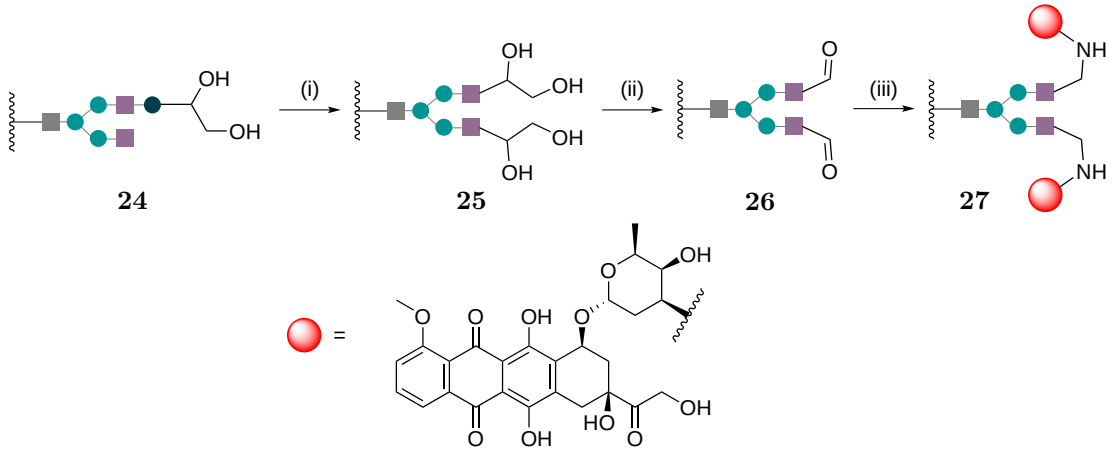

SCHEME 1.15: *Reagents and Conditions*: (i) Neuraminidases, PB pH 5.5, 37 °C, 16 h; (ii) Gal oxidase, PBS pH 7.4, 37 °C, 48 h; (iii) Doxorubicin **143**, pyridine borane, PBS pH 7.4, 37 °C, 48 h.

Glycosyltransferases

Recently, Zhou *et al.* (Sanofi-Genzyme) described another approach using post-translational modification of trastuzumab to introduce sialic acid moieties onto the native glycans on Asn-297.[124] To achieve site-specific modification, a mixture of galactosyltransferase and sialyltransferase was used to transfer galactose and sialic acid residues onto the native glycans. These sialic acid residues were then oxidised to yield aldehyde-functionalised trastuzumab.

Even though these conditions led to partial oxidation of the methionines proximal to the FcRn binding site, which compromised FcRn binding by *ca.* 25%, it had a negligible effect on serum half-life.[124] The enzymatically modified mAb was then conjugated by oxime ligation with aminooxy drug linkers to generate site-selectively modified ADCs. Using MMAE and MMAD, an average DAR of 1.6 was obtained and these glyco-conjugated ADCs exhibited antigen-dependent activity *in vitro* and were efficacious *in vivo*.

A similar strategy that avoids the oxidation step by utilising azido-modified sialic acid and SPAAC click chemistry with a suitable doxorubicin derivative has recently been applied to an anti-CD22 antibody. This resulted in a near-homogeneous ADC which has been shown to selectively target and kill lymphoma cells *in vitro* (Scheme 1.16).[125]

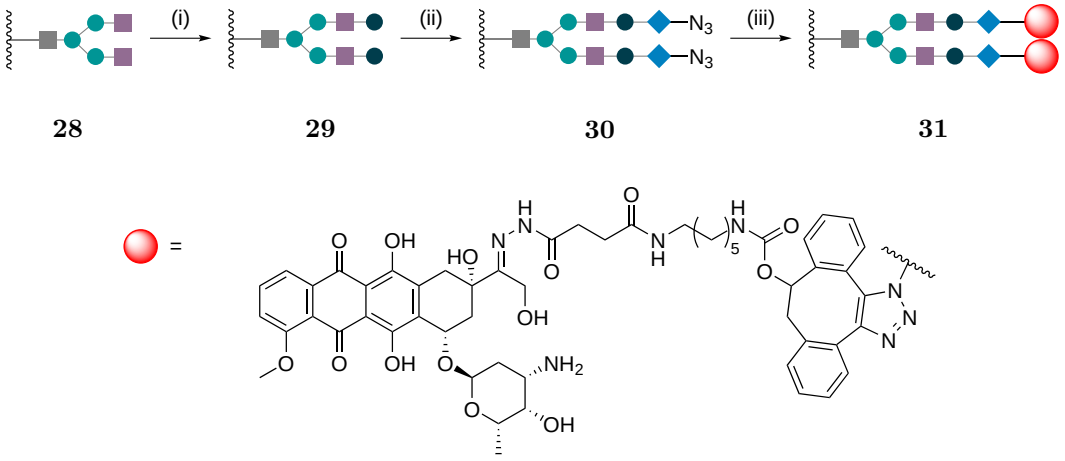

SCHEME 1.16: *Reagents and Conditions*: (i) UDP-Gal, galactosyltransferase, CIAP, MOPS buffer pH 7.2, 37 °C, 24 h; (ii) CMP sialic acid azide, sialyltransferase, CIAP, cacodylate buffer pH 7.6, 37 °C, 48 h; (iii) Doxorubicin derivative, cacodylate buffer pH 7.6, rt, 2 h.

The main limitations of these glycan-based modifications stem from the complex and heterogeneous population of glycans in mAbs, as well as their reliance on the presence of galactose on an IgG1. These characteristics of antibodies may reduce the homogeneity of the final ADC construct and/or mean that additional steps are required to homogenise the glycan population.[126]

1.5.3 Summary of the current methods used

A variety of methods have been developed for the site-selective modification of monoclonal antibodies to produce antibody–drug conjugates, each with their own advantages and limitations (Table 1.2).

		Advantages	Limitations	DAR
Engineered mAbs	THIOMAB	Homogeneity, ease of screening	Incorporation of non-orthogonal group leads to issues of ADC production	2
	Enzyme directed	Ease of incorporation, homogeneity	Efficiency is site and antibody-dependent	2
	uAA	Chemoselectivity, homogeneity	Technically challenging, potential immunogenicity issues	2
Native mAbs	Cys from native S–S	Ease of preparation, tuneable average DAR	Statistical mixture of products	0 – 8
	Bridging of native S–S	Homogeneity, no loss of covalent linkage between protein chains	Potential disulfide scrambling	4
	Glycan modification	Ease of preparation, enzymatically controlled selectivity	Heterogeneous glycan population, reduced FcRn binding due to undesired oxidation	2, 4

Table 1.2: Summary of the advantages and limitations of the main site-selective methods for antibody modification.

Although the use of engineered mAbs for ADC construction offers controlled homogeneity, this is offset by their construction and modification often being technically challenging. Modification of native mAbs, on the other hand, involves simple reaction protocols but with the caveat of difficulties in achieving homogeneous modification. Thus there is no leading technology at present for the site-selective attachment of drugs to antibodies and although recent methods for the construction of ADCs have gone some way to addressing the challenging issues of making homogeneous ADCs, significant hurdles still remain.

1.6 Bioorthogonal reactions and click chemistry

Bioorthogonal chemistry describes reactions between two groups with the following properties: (i) they are mutually reactive but do not cross-react or interact in noticeable ways with biological functionalities or reactions in a cell; (ii) they and their products are stable and non-toxic in physiological settings; and (iii) ideally, their reaction is highly specific and fast.[17]

Click chemistry has been defined as a set of reactions that are modular, stereospecific, wide in scope, high yielding, generate only inoffensive by-products, have simple reaction

conditions and generate products that are easy to purify.[127] Bioorthogonal chemistry and click chemistry therefore overlap significantly, reflecting the same underlying chemical principles. Indeed, click reactions generally offer water compatible chemistry and, their potential for bioorthogonal, regioselective and high-yielding conjugation under mild conditions make them ideal candidates for the functionalisation of proteins with effector moieties. For these reasons, click reactions have been used extensively in biological context.

Due to its ever-growing importance, click chemistry on proteins has been reviewed extensively in the past few years and will not be discussed in detail here.[128–133]

One of the most popular reactions within the bioorthogonal click chemistry concept is the copper-catalysed azide–alkyne Huisgen cycloaddition (CuAAC) or its strained-promoted, copper-free variant with strained alkynes (SPAAC). Both these reactions are compatible with water and have a very high degree of bioorthogonality.

1.6.1 Azide–alkyne Huisgen cycloaddition

In 1902, Dimroth was the first to describe the 1,3-dipolar cycloaddition between an azide and a terminal or internal alkyne to give a 1,2,3-triazole.[134] Some sixty years later, Huisgen realised the scope of this organic reaction which initially required heat to occur and applied it to a large variety of substrates.[135]

Four decades later, Sharpless *et al.* and Meldal *et al.* reported independently that Cu(I) catalysis resulted in a 1,4 regioselectivity along with an enormous rate acceleration of 10^7 to 10^8 compared to the uncatalysed 1,3-dipolar cycloaddition (Scheme 1.17).[136,137] However, the usefulness of this click reaction for bioconjugation was limited by the requirement for potentially toxic use of metal which could degrade proteins through oxidative damage from reactive oxygen species formed by the copper catalysts.[138]

There has been some development of ligands to prevent biomolecule damage and facilitate removal in *in vitro* applications.[138] However, it has been found that different ligand environments of complexes can still affect metabolism and uptake, introducing an unwelcome perturbation in cellular function.[139]

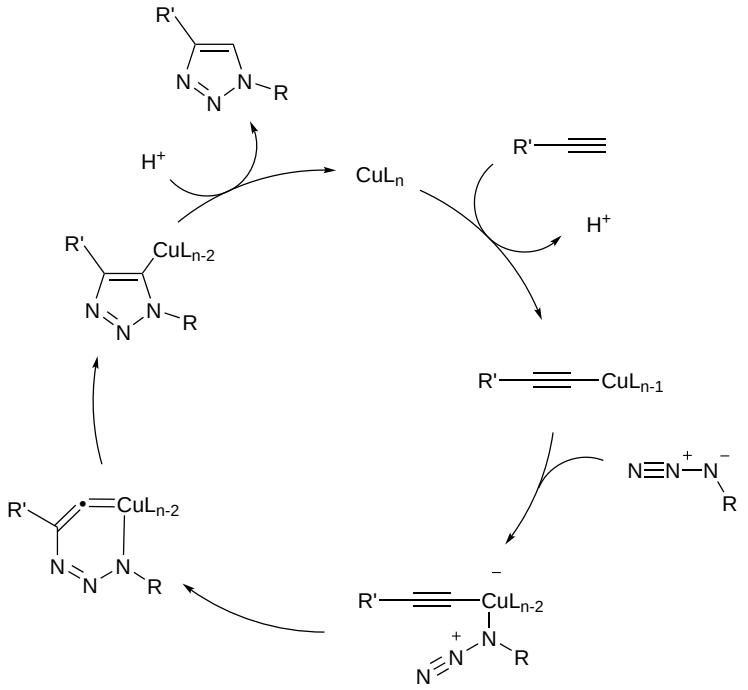

SCHEME 1.17: Mechanism of copper-catalysed azide–alkyne Huisgen cycloaddition (CuAAC).

1.6.2 Strain-promoted azide–alkyne cycloaddition

To tackle this limitation, Bertozzi *et al.* introduced the strain-promoted azide–alkyne cycloaddition (SPAAC) as a metal-free, activated variant of CuAAC.[140] Cyclooctynes were selected as the smallest stable alkyne ring which increases reactivity through ring strain to allow 1,3-dipolar cycloaddition with azides at room temperature. Importantly, in addition to being water-compatible, these reactions were found to have kinetics compatible with most of the biological applications (Scheme 1.18).

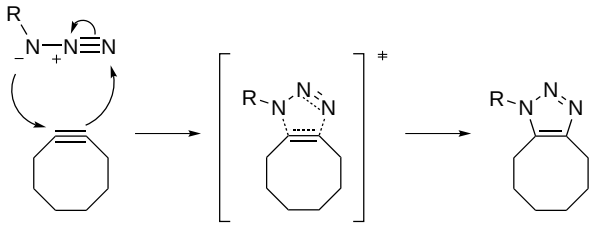

SCHEME 1.18: Mechanism of strain-promoted azide–alkyne cycloaddition (SPAAC).

CuAAC and SPAAC are orthogonal reactions as non-activated alkynes will not react with azides at room temperature without a catalyst, whereas strained alkynes will. This orthogonality makes the pair a suitable candidate to be used for dual modifications of proteins.

1.7 Dual modification of proteins

While a number of methods are available for site-selective *single* protein modification, the site-selective, orthogonal, *dual* modification of proteins has remained challenging. Nevertheless, certain applications require two different functional groups to be introduced into a protein, *e.g.* targeted theranostic biopharmaceuticals (*vide infra*, section 4.5.2, page 83)[141,142] or protein–drug therapeutics stabilised with conjugated half-life extension chemistry (*vide infra*, section 4.5.1, page 83).[143]

The main approaches to dually modify biomolecules can be classified in two separate categories (Figure 1.6). The first one involves the modification of two distinct amino acids on the proteins using various methods that include: exploiting the difference of accessibility or reactivity of amino acids,[144–146] functionalisation of the C- and N-terminus of proteins,[147] use of unnatural amino acids,[148–150] use of specific enzymes[150] or a combination of these strategies. The second category involves conjugation of a bifunctional linker to the protein of interest. The multifunctional scaffold can then be reacted to give a dually modified conjugate.[151–155]

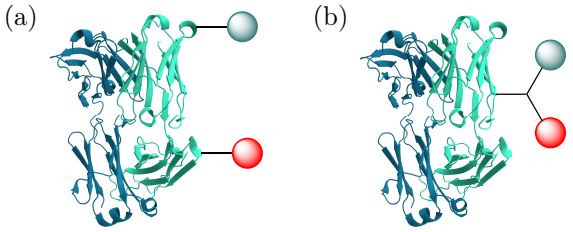

FIGURE 1.6: Different approaches for the introduction of two functional moieties to a protein. (a) *Via* two distinct amino acids; (b) *Via* a multifunctional scaffold containing the two reactive handles.

It is noteworthy that practically all the aforementioned approaches use click reactions for one or for the two modifications of the target biomolecule.

1.7.1 Amino acid-based dual-click approach

Dual functionalisation of biomolecules using click chemistry can be achieved by targeting directly amino acids with orthogonal reactivity. The insertion of two uAAs in proteins is often dependent on the availability of unnatural protein expression methods to incorporate orthogonal chemical handles for subsequent bioorthogonal reactions.[156,157]

A common strategy to introduce two orthogonal chemical handles is to combine nonsense and quadruplet codon suppressions.[158–161] Although recombinant expression strains have been engineered to improve incorporation efficiency, this dual-labelling approach is often associated with low protein yields.[162–164] The main reasons for these low yields are the competition of uAA incorporation with translational frame shifting or termination and low catalytic efficiency of engineered aminoacyl-tRNA synthetases.[165] Thus, strategies often comprised unnatural protein expression with the site-directed modification of canonical amino acids (*e.g.* cysteine).

Simon *et al.* reported a dual-labelling approach for Designed Ankyrin Repeat Proteins (DARPins) using a combination of uAA and cysteine functionalisation.[148] Azidohomoalanine was introduced at the N-terminus of the protein and a cysteine was introduced at a second position of interest *via* site-directed mutagenesis. SPAAC reaction was utilised for orthogonal functionalisation of azidohomoalanine, followed by maleimide modification of the single cysteine residue to obtain homogeneous dually functionalised DARPin (Scheme 1.19).

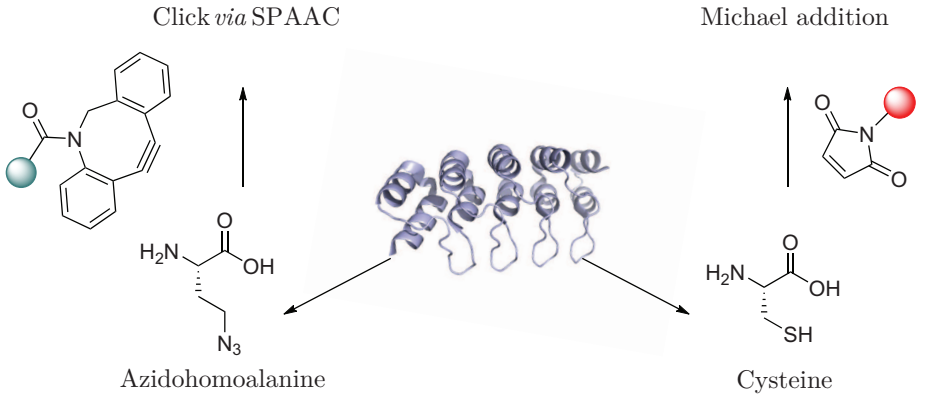

Scheme 1.19: DARPin dual functionalisation using SPAAC followed by thiol modification.

This uAA/cysteine pair has also been used by van Kasteren *et al.* to install two distinct moieties in β-glycosidase from the *archaeon Sulfolobus solfataricus* and reacting them using a sequential CuAAC and disulfide bond formation, respectively.[4] In addition, Brustad *et al.* successfully incorporated ketone-containing uAAs (*i.e.* *p*-azidomethyl-phenylalanine) and cysteines in a T4 lysozyme to generate mutants used in the study of T4 lysozyme folding at single-molecule resolution using fluorescence resonance energy transfer (FRET).[166]

To alleviate some issues associated with the incorporation and the reaction of cysteines (*e.g.* disulfide bond formation, reaction reversibility, side-reactions), Mühlberg *et al.* recently described a dual-labelling strategy for proteins that combines residue-specific incorporation of uAA with chemical oxidative aldehyde formation at the N-terminus of a protein.[149] They selectively introduced two different functional moieties in thermophilic lipase from *Thermoanaerobacter thermohydrosulfuricus via* CuAAC and oxime ligation (Scheme 1.20). This method was applied to the conjugation of biotin and β-linked galactose residues to yield an enzymatically active thermophilic lipase.

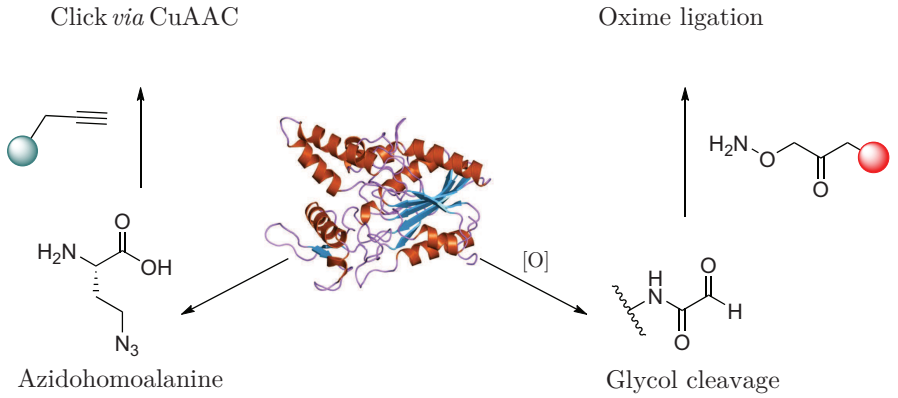

SCHEME 1.20: Lipase dual functionalisation using oxime ligation followed by thiol modification.

1.7.2 Reagent-based dual-click approach

A more straightforward approach to achieve dual modifications on proteins is to combine the reactive handles onto a single multifunctional scaffold that could be conjugated to proteins.[131] Although many commercially available scaffolds contain bifunctional linkers, relatively few of them possess three well-defined orthogonal handles to enable attachment to a protein followed by dual modification.

Efforts have been made towards the development of such platforms but with limited success, due to the potentially complex synthesis of a branched structure with orthogonal handles. Furthermore, these platforms have often been exemplified on small molecules or short peptides but rarely on proteins, which can represent an additional layer of difficulty. For example, trifunctional scaffold **32** was reacted with three small molecules (*i.e.* drug and fluorophores) and clickable decapeptide scaffold **33** was attached to a glucose derivative and two short peptides, but they were not trialled on larger proteins (Figure 1.7).

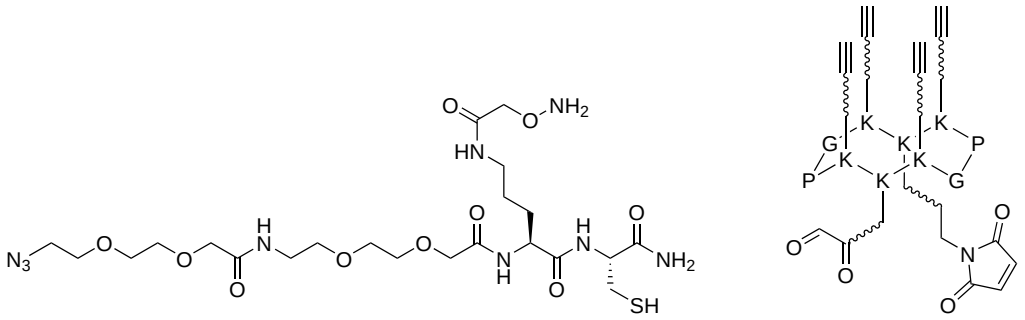

32 **33**

FIGURE 1.7: Multifunctional platforms with the potential to enable the dual functionalisation of proteins.

To date, there are very few examples of reagent-based dual modifications of proteins. Rashidian *et al.* described a method to site-specifically prenylate proteins containing a C-terminal CaaX-box amino acid sequence with various isoprenoids using Protein Farnesyl Transferase (PFTase). Triorthogonal reagent **34** was synthesised to allow incorporation of an alkyne and an aldehyde group simultaneously into a protein (Figure 1.8).[153]

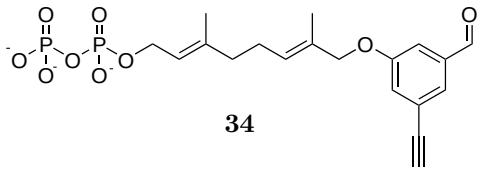

34

FIGURE 1.8: Triorthogonal prenylation reagent used by Rashidian *et al.*

To illustrate the capabilities of this approach, a model protein (*i.e.* GFP) and a therapeutically useful protein (*i.e.* ciliary neurotrophic factor) with engineered CaaX-box were enzymatically modified with **34** followed by oxime ligation and CuAAC reaction to incorporate a series of "clickable" molecules in a one-pot procedure (Scheme 1.21).[153]

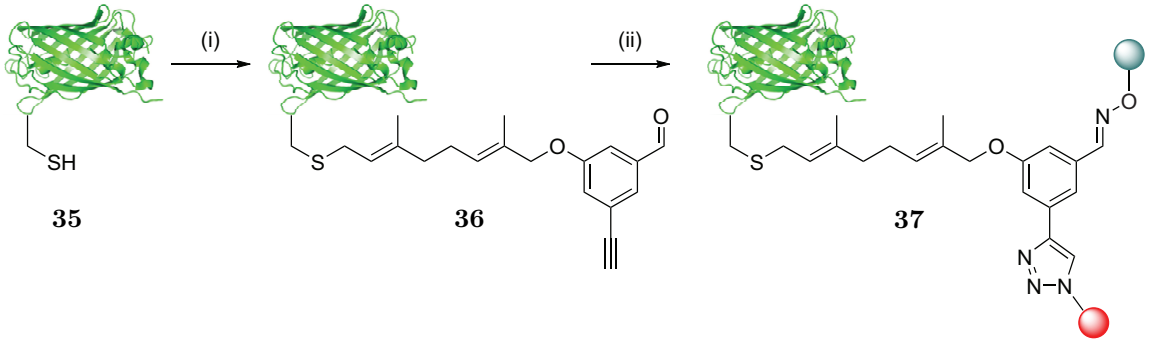

35 **36** **37**

SCHEME 1.21: Dual modification using triorthogonal prenylation reagent **34**. *Reagents and Conditions*: (i) Prenylation reagent **34**, PFTase, $MgCl_2$, $ZnCl_2$, KCl, DTT, Tris·HCl buffer pH 7.5, 30 °C, 4 h; (ii) Aminooxy-derivative, azido-derivative, $CuSO_4$, TCEP, TBTA, *m*-phenylenediamine, PB, DMSO, rt, 15 h.

Beal *et al.* developed a heterotrifunctional template that utilises click reactions (both copper-free and copper-mediated) to effect sequential biomolecule conjugations in a one-pot process.

The synthesis of the template was achieved using readily available Fmoc-Lys(Boc)-OH **38**. Initial amide formation to incorporate the terminal alkyne using HATU gave **39**. Fmoc deprotection of **39** using 4-methylpiperidine to give **40** was followed by amide coupling with *S*-acetylthioacetic acid to give **41**. Subsequent Boc deprotection of **41** followed by coupling to 1-fluorocyclooct-2-yne carboxylic acid **74** yielded the heterotrifunctional molecule **42**. This route enabled the preparation of the template in 5 steps with a 6.3% overall yield as a 1:1 mixture of diastereomers (Scheme 1.22).

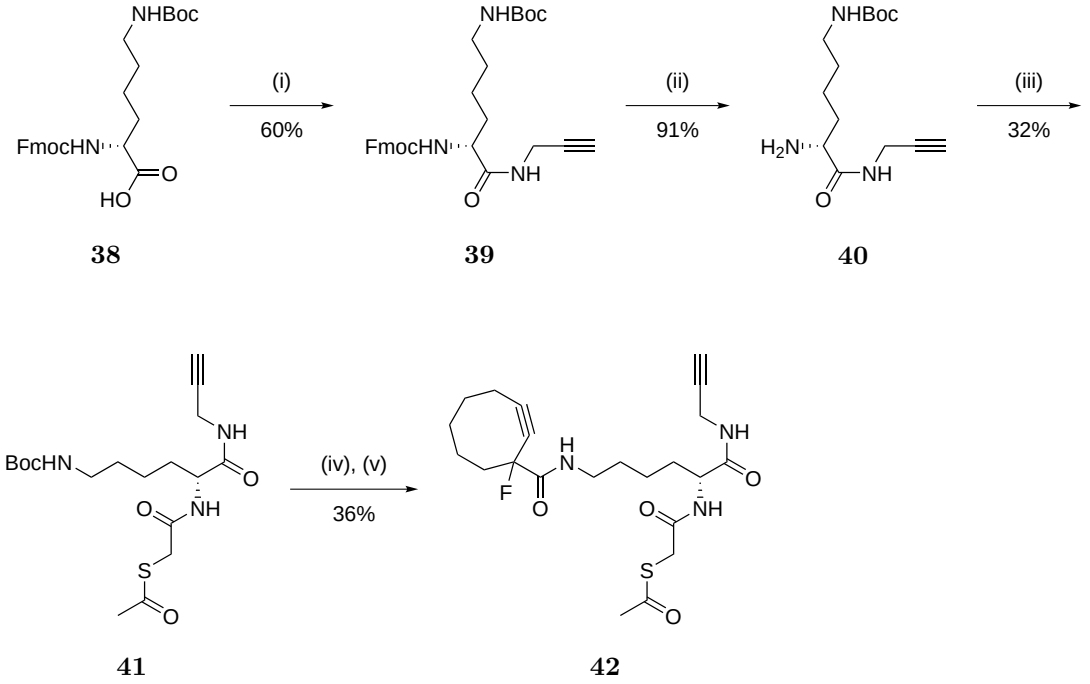

SCHEME 1.22: *Reagents and Conditions*: (i) HATU, propargylamine, DIPEA, CH_2Cl_2, rt, 12 h; (ii) 4-Methylpiperidine, CH_2Cl_2, rt, 12 h; (iii) $(COCl_2)_2$, 2-(acetylthio)acetic acid, NEt_3, DMF, CH_2Cl_2, rt, 12 h; (iv) 4 M HCl in dioxane, rt, 12 h; (v) HATU, 1-fluorocyclooct-2-yne carboxylic acid **74**, DIPEA, CH_2Cl_2, rt, 12 h.

Following the preparation of substrate **42**, SPAAC followed by CuAAC was used to react its two alkynes handles and give dually modified template **44** which was purified by HPLC. Finally, **44** was reacted with a maleimide-functionalised BSA modified *via* its lysines with an average of 15 – 25 maleimides per protein to yield heterogeneous dually modified BSA **45** (Scheme 1.23). The scope of compatible substrates was illustrated through conjugation of peptide, sugar, lipid, fluoroalkane, biotin and fluorophore molecules.[154]

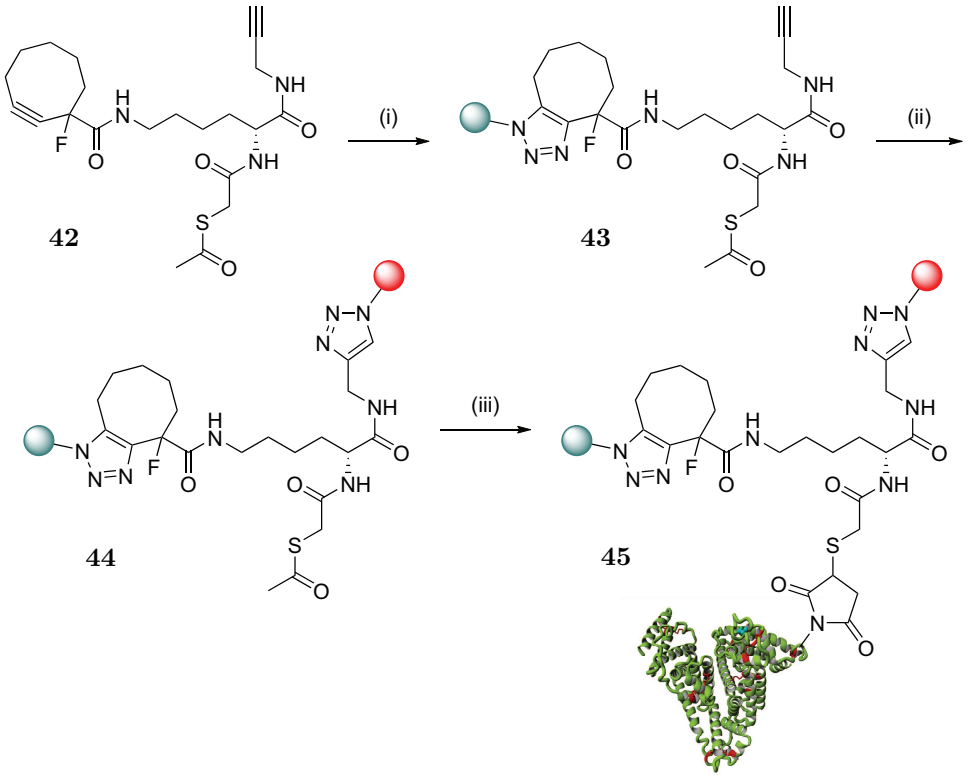

SCHEME 1.23: Dual modification using heterotrifunctional template **42**.
Reagents and Conditions: (i) Azido-dervative, DMSO, rt, 6 h; (ii) Azido-derivative, sodium ascorbate, $CuSO_4$, DMSO, rt, 2 h; (iii) BSA-maleimide, $NH_2OH \cdot HCl$, EDTA, PBS, pH 4, DMSO, rt, 2 h.

Temming *et al.* described a dual-functionalisation method where the two handles were introduced directly by modifying a serine residue on the N-terminus of a peptide (*i.e.* cell-penetrating peptide human lactoferrin) or proteins (*i.e.* enhanced GFP mutant and heat shock protein HspB2).[152] They argued that this approach potentially alleviates the need for lengthy syntheses of complex platforms used in exogeneous modification strategies.

The methods consists of a careful oxidation of the requisite N-terminal serine residue **46** with $NaIO_4$ as the oxidising agent followed by reaction of the resulting aldehyde **47** with 50 equivalents of *N*-propargylhydroxylamine to yield dually "clickable" protein **48** (Scheme 1.24).

Following this, the first functional label was introduced by strain-promoted alkyne–nitrone cycloaddition (SPANC) with a "clickable" BCN-biotin derivative. The terminal acetylene of **49** then served as the second anchor point for a CuAAC reaction with azido-containing fluorescein to give dually modified construct **50** (Scheme 1.25).

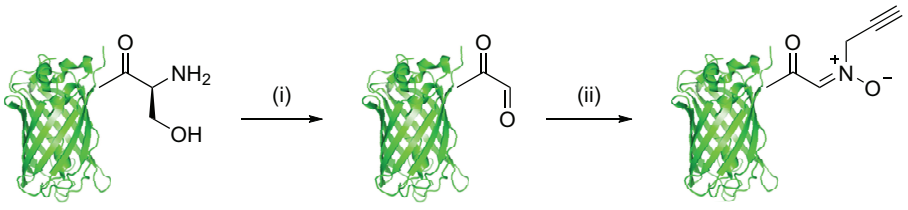

46 **47** **48**

SCHEME 1.24: Preparation of dually "clickable" GFP by terminal serine modification. *Reagents and Conditions*: (i) $NaIO_4$, NH_4OAc buffer pH 6.8, rt, 65 min then *p*-methoxybenzenethiol, MeCN, rt, 16 h; (ii) *p*-Anisidine, *N*-propargylhydroxylamine, NH_4OAc buffer pH 6.8, MeCN, rt, 65 min.

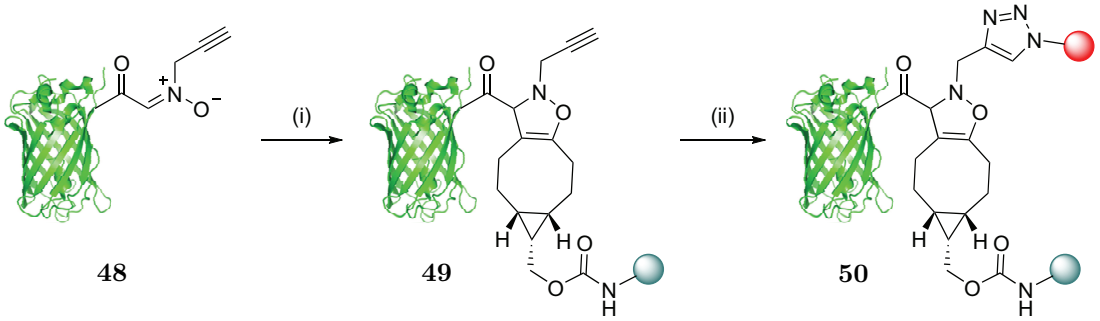

48 **49** **50**

SCHEME 1.25: Dual modification of GFP mutant using terminal serine modification. *Reagents and Conditions*: (i) BCN-biotin, NH_4OAc buffer pH 6.8, MeCN, rt, 4 h; (ii) Azido-fluorescein, ascorbate, $CuSO_4$, TBTA, PB pH 7.6; *t*-BuOH, DMSO, rt, 19 h.

Multifunctional scaffolds have a myriad of uses and can find significant utility in the biotherapeutic area. In the area of oncology, in particular, antibody–drug conjugates can benefit from the conjugation of monoclonal antibodies to multiple cytotoxic agents or stabilising groups (*vide supra*, section 1.4, page 11). The permutations and combinations for these functional molecules appear endless, but they rely heavily on the ability of chemistry to enable these "plug-and-play" strategies. Hence, there is great need for a straightforward and practical method for the simultaneous introduction of two functional moieties into proteins.

Recently, Chudasama *et al.* reported that pyridazinedione based reagents could be used as a platform to dually modify cysteine-containing biomolecules.[52] Indeed, in addition to the two cysteine-reactive centres, these compounds possess two additional points of attachment that can easily be functionalised (Figure 1.9).

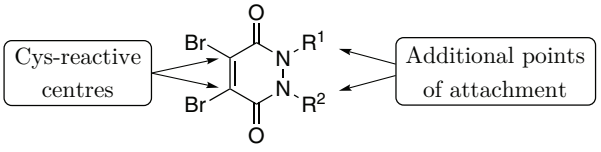

FIGURE 1.9: General structure of dibromopyridazinedione-based reagents.

1.8 Project aims

This project involves the development, synthesis and biological evaluation of new, stable and easy to use linker technologies based on pyridazinedione chemistry to site-selectively conjugate a peptide or protein to two functional units.

The strategy aims to introduce two orthogonal reactive handles onto proteins by modification of disulfide bonds or cysteines residues. The method should have the following features (Figure 1.10):

- The functionalisation should be fast, quantitative and should not require lengthy and complex purifications.
- The functionalisation should not impact the structure and biological activity of the peptide or protein of interest.
- The resulting conjugate should be stable under various conditions, depending on the desired application.
- The resulting conjugate should be able to undergo dual functionalisations using versatile chemistries such as click reactions.
- The dual functionalisation should be compatible with both small and large payloads (*i.e.* $> 10\,\text{kDa}$).
- The dual functionalisation should allow the payloads to retain their main characteristics (*e.g.* fluorescence, cytotoxicity).

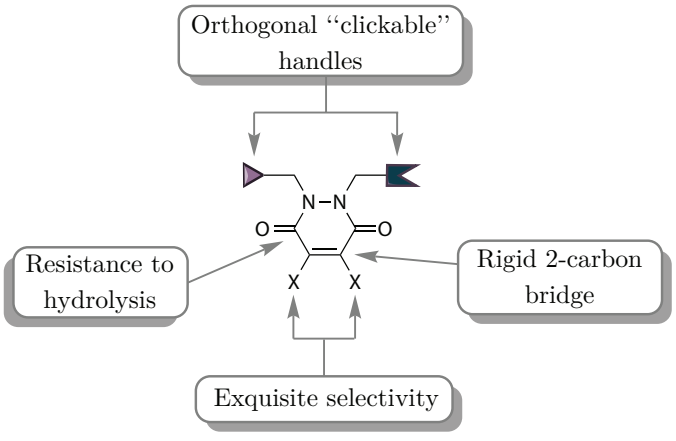

FIGURE 1.10: Structure and ideal characteristics of PD-based linkers.

Chapter 2

Synthesis of Pyridazinediones

2.1 Introduction

Pyridazinedione derivatives offer a similar and yet distinct reactivity profile for cysteine conjugation compared with maleimides. Recently, Chudasama *et al.* showed that both mono- and dibromo-1,2-dihydro-pyridazine-3,6-diones (PDs) derivatives are suitable for conjugation to proteins with cysteine residues and disulfide bonds, respectively (*vide supra*, Scheme 1.3, page 6).[52] Unlike maleimides, when a vast excess of PDs were used to effect conjugation (up to 100 equivalents at 37 °C for 16 h), no lysine modification was observed. Moreover, the conjugates generated demonstrated exceptional hydrolytic stability with the potential for four points of chemical attachment. In view of the project aims, it was decided to synthesise pyridazinedione derivatives containing "clickable" reactive handles (*e.g.* an azide and an alkyne moiety, and an alkyne and a strained alkyne moiety) to allow further functionalisation of the modified protein *via* two orthogonal, selective and sequential click reactions (*vide supra*, section 1.6, page 25).

2.2 Synthesis of Azide-Alkyne Pyridazinedione (Azal PD)

The azide fragment of Azal PD **61** was prepared *via* a Sandmeyer reaction on *p*-toluidine **51** to give azide **52** in 94% yield.[167] Azide **52** was then selectively brominated at the benzylic position using NBS and AIBN to give bromide **53** in 80% yield (Scheme 2.1).[168]

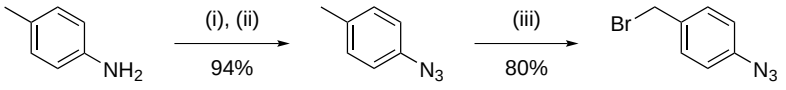

51 **52** **53**

SCHEME 2.1: *Reagents and Conditions*: (i) $NaNO_2$, $HCl_{(aq)}$, H_2O, −5 °C, 5 min; (ii) NaN_3, NaOAc, H_2O, 0 °C, 2 h; (iii) NBS, AIBN, C_6H_6, reflux, 8 h.

Treatment of Boc-protected hydrazine **54** with propargyl bromide under phase transfer conditions gave monoalkylated hydrazine derivative **55** in 86% yield. Gratifyingly, only a small amount of dialkylated product was observed despite the use of excess propargyl bromide.[169] Alkyne **55** was then alkylated with bromide **53** to give tetrasubstituted hydrazine **56** in 93% yield (Scheme 2.2).

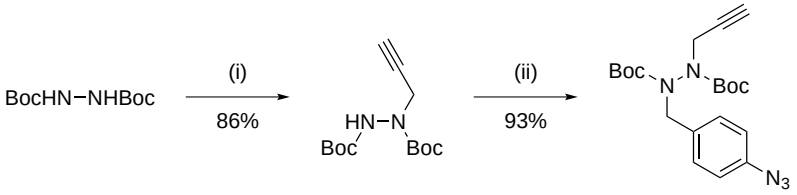

54 **55** **56**

SCHEME 2.2: *Reagents and Conditions*: (i) Propargyl bromide, TBAB, toluene/5% $NaOH_{(aq)}$, rt, 16 h; (ii) Azide **53**, Cs_2CO_3, DMF, rt, 16 h.

Bromopyridazinediones are commonly synthesised by either: (i) treating bromomaleic anhydride **58** with a hydrazine derivative and heating the reaction under reflux in AcOH to carry out dehydrative cyclisation;[50] (ii) treating maleic anhydride **57** with a hydrazine derivative and heating the reaction under reflux in AcOH, followed by a bromination-elimination sequence;[52] or (iii) using milder conditions and treating a hydrazine derivative with *N*-methoxycarbonylmaleimide **60**.[170] In this particular case the bromination-elimination sequence is not compatible with alkynes and was therefore not evaluated. As such, it was decided to attempt formation of PDs under both applicable conditions. For this purpose, dibromomaleic anhydride **58** and dibromo *N*-methoxycarbonylmaleimide **60** had to be synthesised. Treatment of maleic anhydride **57** with Br_2 gave dibromomaleic anhydride **58** in 83% yield and treatment of maleimide **59** with methyl chloroformate gave carbamate **60** in 97% yield (Scheme 2.3).

With precursors **58** and **60** in hand, it was decided to investigate the two methods for the formation of the pyridazinedione ring. Interestingly, the milder method involving reaction with carbamate **60** resulted in the formation of **61** in a low 21% yield whereas

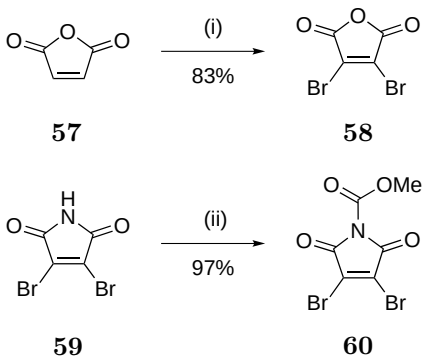

57 **58**

59 **60**

SCHEME 2.3: *Reagents and Conditions*: (i) Br_2, $AlCl_3$, 160 °C, 16 h; (ii) *N*-Methylmorpholine, methylchloroformate, THF, rt, 20 min.

reaction of deprotected **56** with maleic anhydride derivative **58** gave Azal PD **61** in a higher, although still limited, 35% yield (Scheme 2.4).

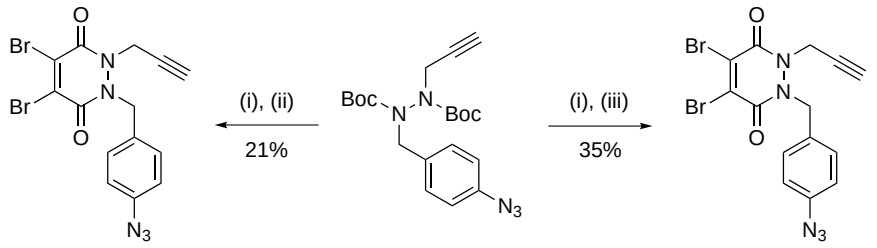

61 **56** **61**

SCHEME 2.4: *Reagents and Conditions*: (i) TFA, CH_2Cl_2, rt, 30 min; (ii) Carbamate **60**, NEt_3, CH_2Cl_2, rt, 16 h; (iii) Anhydride **58**, AcOH, reflux, 16 h.

Unfortunately, Azal PD **61** was poorly soluble in H_2O and thus was not ideal for reaction onto proteins as it required the use of a significant amount of organic solvent, which is often poorly tolerated by proteins. As such, it was decided to construct a more water soluble, dually "clickable" dibromopyridazinedione.

2.3 Synthesis of PEG-Azide-Alkyne Pyridazinedione (Pazal PD)

Organic molecules are known to have increased water solubility when linked to polyethylene glycol chains (PEGs). It was therefore decided to introduce a small PEG chain between the azide residue and the pyridazinedione ring to improve the solubility of the construct.

O-Mesylated azide **63** was prepared by mono-mesylation of PEG_4 **62** to obtain mesylate **63** in 64% yield. This was followed by displacement of the mesylate with sodium azide to obtain **64** in 95% yield. The remaining hydroxyl group of azide **64** was then mesylated to give azide-mesylate **65** in a quantitative yield (Scheme 2.5).[171]

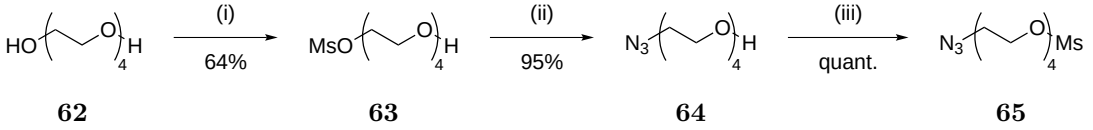

62 **63** **64** **65**

SCHEME 2.5: *Reagents and Conditions*: (i) MsCl, Ag_2O, CH_2Cl_2, rt, 16 h; (ii) NaN_3, DMF, 110 °C, 16 h; (iii) MsCl, NEt_3, CH_2Cl_2, 0 °C then rt, 2 h.

Trisubstituted hydrazine derivative **55** was next alkylated with mesylate **65** to give water soluble alkyne-azide precursor **66** in 94% yield (Scheme 2.6).

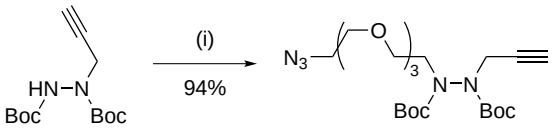

55 **66**

SCHEME 2.6: *Reagents and Conditions*: (i) Mesylate ester **65**, Cs_2CO_3, DMF, rt, 16 h.

The two applicable methods for the formation of the pyridazinedione ring were next investigated (*vide supra*, section 2.2, page 36). The high temperature used for the method involving refluxing the reaction in AcOH with maleic anhydride derivative **57** proved to be incompatible with substrate **66**. All that was identified under the reaction conditions, perhaps due to the flexibility of the PEG chain, was an inseparable mixture of regioisomers **67** and **68** derived from thermally promoted intramolecular azide–alkyne Huisgen cycloaddition (Scheme 2.7).

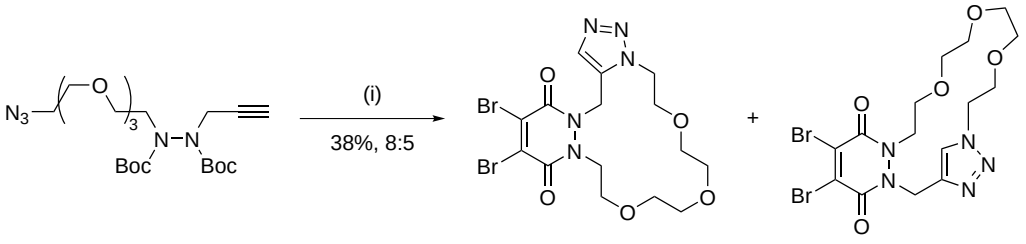

66 **67** **68**

SCHEME 2.7: *Reagents and Conditions*: (i) TFA, CH_2Cl_2, rt, 30 min then **57**, AcOH, reflux, 16 h.

The use of the mild method, however, afforded Pazal PD **69** in 27% yield with no azide–alkyne cycloaddition products observed (Scheme 2.8).

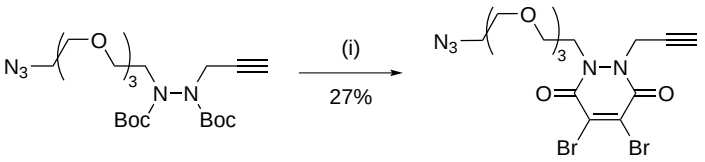

66 **69**

SCHEME 2.8: *Reagents and Conditions*: (i) TFA, CH_2Cl_2, rt, 30 min then carbamate **60**, NEt_3, CH_2Cl_2, rt, 16 h.

2.4 Synthesis of Alkyne-Strained Alkyne Pyridazinedione (Astra PD)

To expand the scope of this dual modification strategy, it was envisaged that **69** could be functionalised with a strained alkyne to form an alkyne/strained alkyne construct that could be sequentially dually functionalised *via* a SPAAC reaction, followed by a CuAAC reaction. Strained alkyne **74** was synthesised following literature procedure in a 56% overall yield (Scheme 2.9).[172]

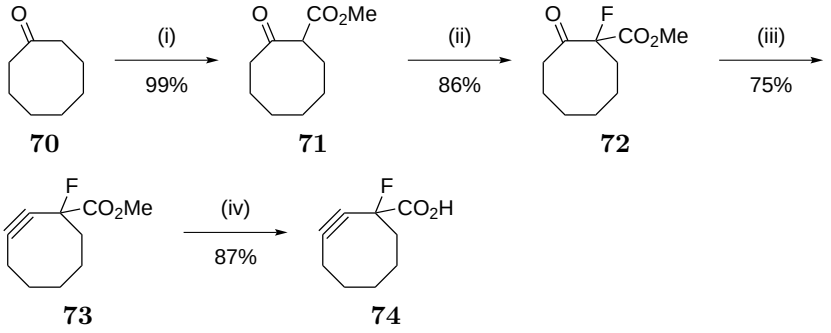

70 **71** **72** **73** **74**

SCHEME 2.9: *Reagents and Conditions*: (i) NaH, dimethylcarbonate, benzene, 90 °C, 2 h; (ii) Selectfluor™, CH_3CN, 55 °C, 8 h; (iii) KHMDS, Tf_2NPh, THF, −78 °C, 1 h then rt, 5 h; (iv) LiOH, MeOH, H_2O, 50 °C, 10 min then rt, 2 h.

It was envisaged that a Staudinger reduction of azide **69** would yield amine **75** which could then be coupled with acid **74**. Although reaction of triphenylphosphine with azide **69** resulted in complete conversion, it yielded a complex mixture of inseparable products (Scheme 2.10). It was thought that the resultant amine **75** might have undergone an intra and/or intermolecular Michael addition and that this would account for the complex mixture of products observed.

In order to prevent a possible Michael addition, attempts were made to trap the highly nucleophilic nitrogen atom of the iminophosphorane intermediate in the Staudinger reaction pathway with acid **74** which had been pre-activated *in situ* with DCC.

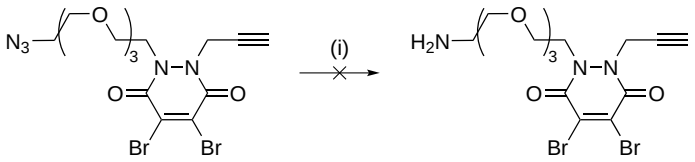

69 **75**

SCHEME 2.10: *Reagents and Conditions*: (i) PPh_3, H_2O, THF, rt, 16 h.

Unfortunately, this Staudinger ligation strategy returned a mixture of unidentified products (Scheme 2.11).

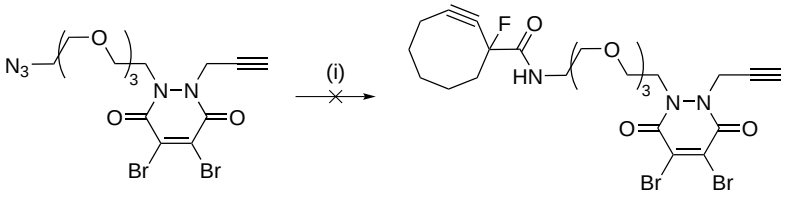

69 **76**

SCHEME 2.11: *Reagents and Conditions*: (i) PPh_3, THF, rt, 1 h then acid **74**, DCC, HOBt, MeCN, 0 °C, 1 h then rt, 16 h.

In view of the unsuccessful attempts to synthesise alkyne **76**, another approach was adopted for the synthesis of an alkyne-strained alkyne pyridazinedione (Astra PD) construct. It was then envisaged that Azal PD **61** could be converted into the desired construct as its azide moiety could undergo a mono SPAAC with a bis-strained alkyne. To construct a bis-strained alkyne, bis-amine-PEG_4 **77** was coupled to acid **74** and gave bis-cyclooctyne **78** in 54% yield (Scheme 2.12). The PEG spacer was chosen to improve the water solubility of the final construct as the two cyclooctyne rings would increase the hydrophobicity of the final construct once attached to the pyridazinedione moiety.

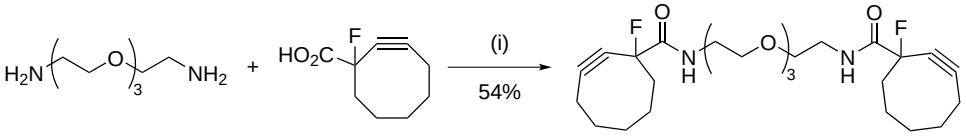

77 **74** **78**

SCHEME 2.12: *Reagents and Conditions*: (i) HBTU, DIPEA, DMF, rt, 4 h.

To form the desired Astra PD construct, Azal PD **61** was reacted with bis-cyclooctyne **78** to give Astra PD **79** in 36% yield as a mixture of regio- and diastereoisomers (Scheme 2.13).

Although the synthesis of an alkyne/strained alkyne pyridazinedione was successfully demonstrated, it was decided to improve upon the construct as it was a mixture of regio-

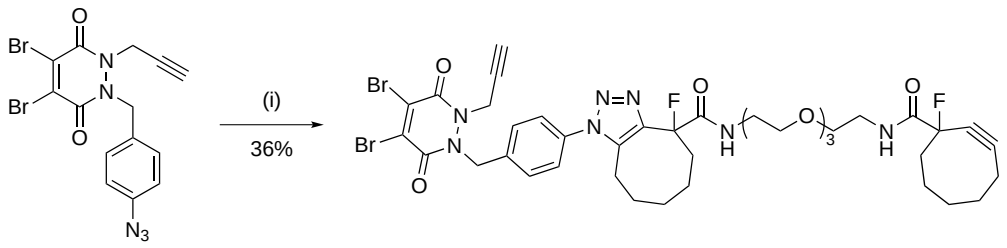

61 **79**

SCHEME 2.13: *Reagents and Conditions*: (i) Strained alkyne **78**, CH_2Cl_2, rt, 16 h.

and diastereoisomers. Furthermore, the route to Astra PD **79** proceeded in only 3% overall yield and, the aryl and cyclooctene moieties decrease the water solubility of the final construct, which may proved troublesome for future use in conjugation to protein. It was therefore envisaged to design alternative routes for the synthesis of dually "clickable" PDs.

2.5 Improved synthesis of Astra PD

2.5.1 Solastra PD — Direct attachment

The synthesis of a more water-soluble MFCO-Astra PD (Solastra PD) construct was initiated by alkylation of trisubstituted hydrazine derivative **55** with *tert*-butylbromoacetate to give ester **80** in 97% yield. Ester **80** was then deprotected with TFA and reacted with dibromomaleic anhydride **58** to give pyridazinedione derivative **81** in 67% yield (Scheme 2.14).

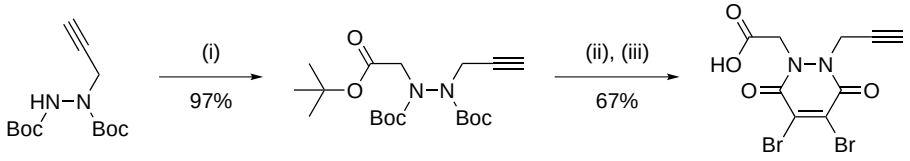

55 **80** **81**

SCHEME 2.14: *Reagents and Conditions*: (i) *Tert*-butyl bromoacetate, Cs_2CO_3, DMF, rt, 16 h; (ii) TFA, CH_2Cl_2, rt, 30 min; (iii) Anhydride **58**, AcOH, rt, 16 h then reflux, 2 h.

In order to improve water solubility of the final construct, mono-protected PEG_4-based diamine linker **83** was first prepared by slow addition of Boc anhydride to diamine **82** (Scheme 2.15).[173]

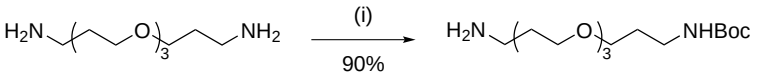

82 **83**

SCHEME 2.15: *Reagents and Conditions*: (i) Boc_2O, dioxane, rt, 24 h.

Amine **83** was then attached to acid **81** *via* EDC-mediated coupling to give Boc-protected PD **84** in 44% yield (Scheme 2.16).

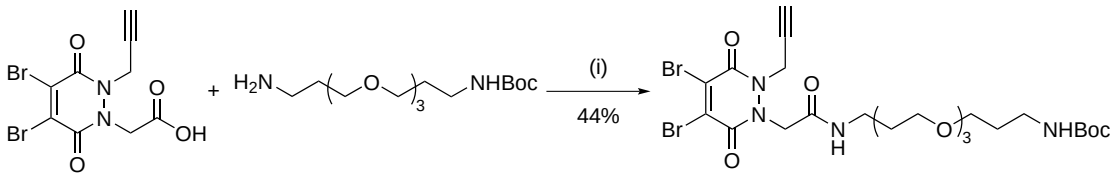

81 **83** **84**

SCHEME 2.16: *Reagents and Conditions*: (i) EDC·HCl, NEt_3, CH_2Cl_2, rt, 4 h.

To attach the strained alkyne part of the construct, Boc-protected PD **84** was first deprotected to yield a free primary amine which was then reacted with acid **74** using HBTU as coupling agent. Unfortunately these reaction conditions only returned traces of the desired product, Solastra PD **85**. As deprotected **84** as well as methyl ester **73** were oils, it was envisaged that a highly concentrated mixture of the two in NEt_3 could yield final construct **85** but after 5 days, no reaction between the two intermediates occurred (Scheme 2.17).[174]

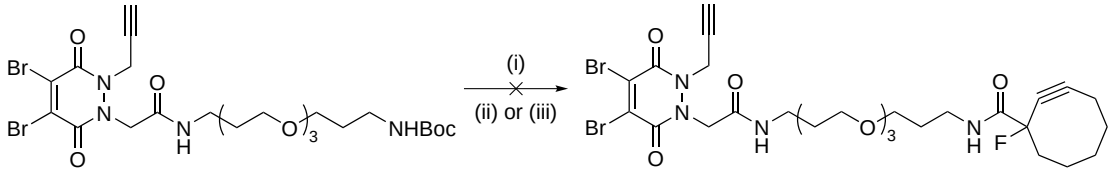

84 **85**

SCHEME 2.17: *Reagents and Conditions*: (i) TFA, CH_2Cl_2, rt, 30 min; (ii) Acid **74**, HBTU, DIPEA, DMF, rt, 4 h; (iii) **73**, NEt_3, 30 °C, 5 days.

This lack of reactivity was attributed to the low solubility of the deprotected PD in NEt_3; it was therefore thought that attaching the PEG-amine **83** to the strained alkyne moiety **73** prior to coupling with the PD core **81** could solve the solubility issue. Gratifyingly, nucleophilic acyl substitution with amine **83** and methyl ester **73** proceeded smoothly to give Boc-protected intermediate **86** in 72% yield (Scheme 2.18). This reaction was preferred to a more standard coupling between acid **74** and amine **83** as, in addition to reducing the number of steps needed to reach the final target molecule, acid **74** was found to be prone to decarboxylation which reduces the yield of the reaction.

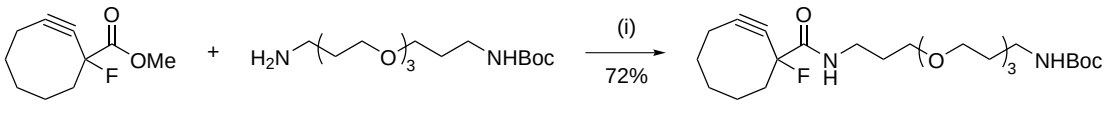

73 **83** **86**

SCHEME 2.18: *Reagents and Conditions*: (i) NEt_3, 30 °C, 36 h.

Attempts to deprotect **86** were then made using TFA/CH_2Cl_2 mixture in various dilutions at room temperature. However all ratios trialled returned TFA adduct **87**. Nevertheless, by lowering the temperature to −20 °C and careful monitoring of the degree of advancement of the reaction, amine **88** could be isolated in 82% yield (Scheme 2.19).[155]

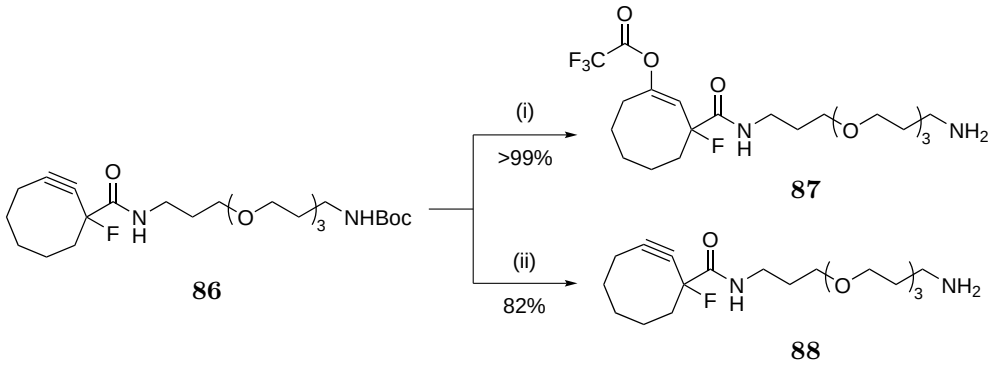

SCHEME 2.19: *Reagents and Conditions*: (i) TFA/CH_2Cl_2 (1 : 20 ↦ 1 : 1), rt, 1 h; (ii) TFA/CH_2Cl_2, −20 °C, 90 min.

Finally, EDC-mediated coupling of acid **81** and amine **88** afforded Solastra PD **85** although in a low 20% yield (Scheme 2.20). This yield was partially attributed to Cl^- (from EDC·HCl) displacement of a bromine from the PD core.

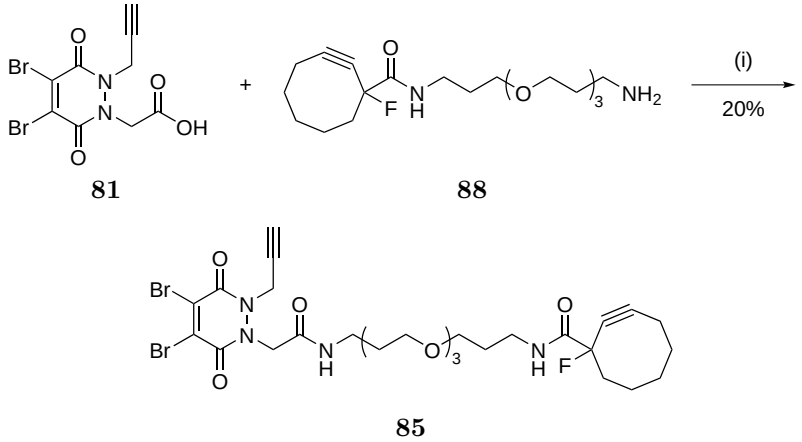

SCHEME 2.20: *Reagents and Conditions*: (i) EDC·HCl, NEt_3, CH_2Cl_2, rt, 4 h.

Although the synthesis of this alkyne/strained alkyne pyridazinedione with improved water-solubility was successfully demonstrated it was decided to improve upon the route

to Solastra PDs **79** as the last steps involving MFCO derivatives **73**, **86** and **88** were challenging and often low yielding, resulting in the synthesis proceeding in only 7% overall yield.

2.5.2 BCN-Astra PD

In view of the issues stated above, a new route was devised to construct an alkyne/strained alkyne PD moiety. To do this, it was decided to switch from Schultz/Pigge's MFCO strained alkyne **90** to van Delft's bicyclononynes (BCNs).[175] BCN **89** has the lowest calculated $\log P$ value amongst the other popular cyclooctynes in the literature and is therefore preferred if low lipophilicity is required (Figure 2.1).

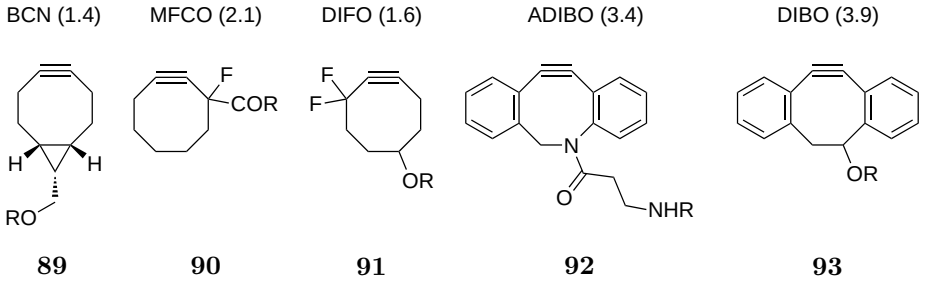

FIGURE 2.1: Structure of popular cyclooctynes and their calculated $c\log P$ for R = H (numbers in parenthesis).

Furthermore, BCNs have been shown to react with azides with better kinetics when compared to MFCOs ($k_{\mathrm{BCN}} = 0.29\,\mathrm{M}^{-1}\cdot\mathrm{s}^{-1}$ and $k_{\mathrm{MFCO}} \simeq 1.5\times10^{-3}\,\mathrm{M}^{-1}\cdot\mathrm{s}^{-1}$ respectively).[175] The addition of a BCN handle also opens the door to other click reactions orthogonal to alkynes as they have been shown to react rapidly with tetrazines and nitrones in aqueous media ($k \simeq 500\,\mathrm{M}^{-1}\cdot\mathrm{s}^{-1}$ and $k \simeq 1.67\,\mathrm{M}^{-1}\cdot\mathrm{s}^{-1}$ respectively) to form stable adducts (Figure 2.2).[175–177] In contrast, MFCOs **90** and DIBOs **93** have been shown to be poor dienophiles when reacted with tetrazines.[178,179]

Acid **81** was therefore coupled to commercially available BCN−PEG−NH_2 **97** resulting in new alkyne-strained alkyne pyridazinedione **98** as the sole isomer, with improved water solubility, and in an improved 25% overall yield (Scheme 2.21).

With 5 dibromo PDs successfully synthesised (Azal PD **61**, Pazal PD **69**, MFCO-Astra PD **79**, Solastra PD **85** and BCN-Astra PD **98**, *vide infra*, Figure 2.3, page 51) and ready to be used for conjugation onto proteins with disulfide bonds, it was decided to

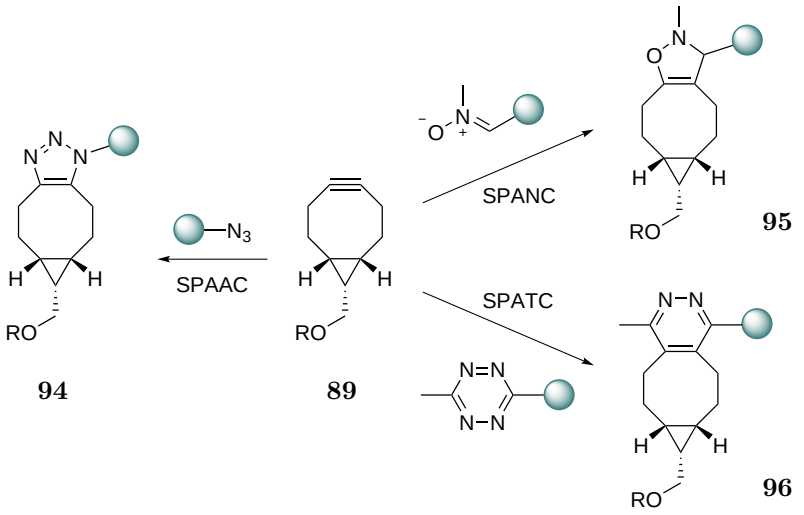

FIGURE 2.2: Click reactions with BCN and azide (SPAAC), nitrone (SPANC) and tetrazine (SPATC).

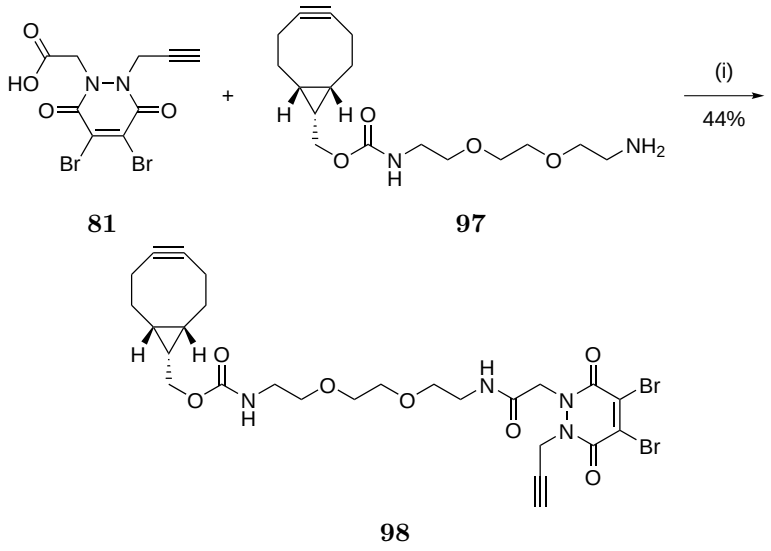

SCHEME 2.21: *Reagents and Conditions*: (i) HATU, DIPEA, DMF, rt, 16 h.

also investigate single cysteine modification. To this effect, mono bromo PD derivatives had to be prepared.

2.6 Synthesis of monobromo Azide-Alkyne Pyridazinedione (mBr-Azal PD)

With precursor **56** in hand, it was decided to synthesise the monobromo analogue of Azal PD **61**. Deprotection of hydrazine derivative **56** followed by reaction with bromomaleic anhydride **99** gave mBr-Azal PD **100** in 60% yield (Scheme 2.22).

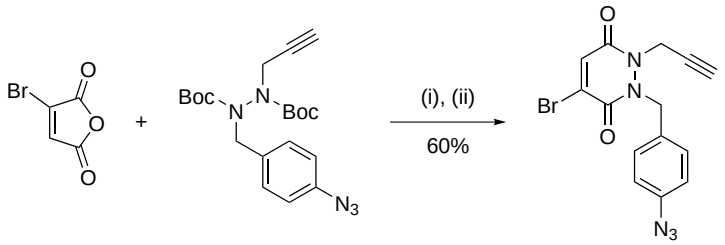

99 **56** **100**

SCHEME 2.22: *Reagents and Conditions*: (i) TFA, CH_2Cl_2, rt, 30 min; (ii) Bromomaleic anhydride **99**, AcOH, reflux, 16 h.

2.7 Synthesis of diethyl PD (Diet PD)

In order to optimise the conditions for the conjugation to proteins on both single cysteines and disulfides, monobromo and dibromo PDs where reactive handles are replaced with unreactive alkyl groups were prepared.[52] Synthesis of **m**ono**br**omo **diet**hyl PD **103** (mBr-Diet PD) and dibromo **diet**hyl PD **104** (Diet PD) were achieved in high yield by the initial condensation of maleic anhydride **57** with diethylhydrazine **101** followed by sequential dibromination/elimination steps (Scheme 2.23).

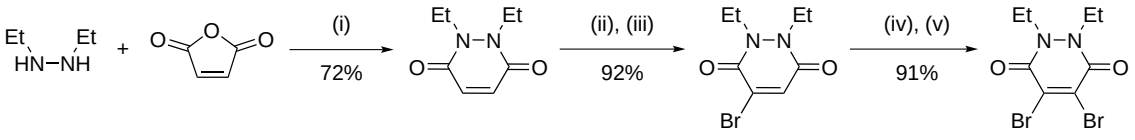

101 **57** **102** **103** **104**

SCHEME 2.23: *Reagents and Conditions*: (i) AcOH, reflux, 16 h; (ii) Br_2, CH_2Cl_2, rt, 16 h; (iii) Et_3N, CH_2Cl_2, rt, 16 h; (iv) Br_2, CH_2Cl_2, 50 °C, 72 h; (v) Et_3N, CH_2Cl_2, rt, 16 h.

Alternatively, mBr-Diet PD **103** and Diet PD **104** were prepared using the mild method involving carbamates (*vide supra*, section 2.2, page 36).[170] Monobromo maleimide **105** was reacted with methyl chloroformate to give carbamate **106** in > 99% yield (Scheme 2.24).

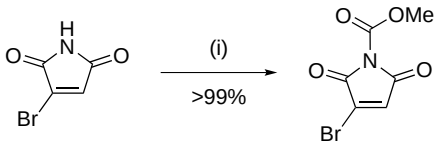

105 **106**

SCHEME 2.24: *Reagents and Conditions*: (i) *N*-Methylmorpholine, methylchloroformate, THF, rt, 20 min.

Both monobromo- and dibromo-PD precursors **106** and **60** were then reacted with diethylhydrazine **101** to give mBr-Diet PD **103** and Diet PD **104** in 64% and 57% yield, respectively (Scheme 2.25).

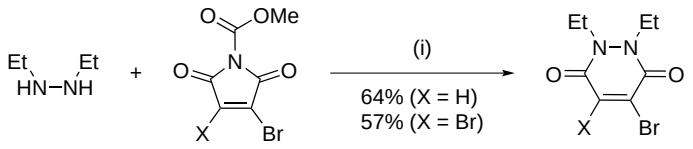

101 **106** X = H, **60** X = Br → **103** X = H, **104** X = Br

SCHEME 2.25: *Reagents and Conditions*: (i) CH_2Cl_2, rt, 16 h.

2.8 Synthesis of mono-functionalised PD

Finally, in order to optimise the conditions for the click reactions on proteins, PDs where one of the "clickable" handles (azide, alkyne or strained alkyne moiety) is replaced by an unreactive group were prepared.

2.8.1 Synthesis of mono-functionalised PD precursor

It was envisaged that a common PD precursor would facilitate the syntheses of mono-functionalised PDs. It was then postulated that a PD with an unreactive methyl group on one nitrogen and, on the other, an acid handle that could be further coupled to amines, was a suitable common precursor. Using previously developed routes, its synthesis was attempted. Unfortunately, monoalkylation of Boc-protected hydrazine **54** with methyl- or ethylhalide resulted in a mixture of starting material **54**, mono- and bisalkylated hydrazine (**109**, **110** and **111**, **112** respectively) which would greatly reduce the overall yield of the synthesis (Scheme 2.26). Thus, an alternative route towards **Met**hyl-**A**cid PD **116** (Meta PD) was needed.

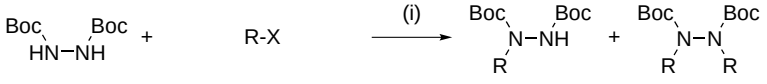

54 **107** R = Me, X = I; **108** R = Et, X = Br → **109** R = Me; **110** R = Et; **111** R = Me; **112** R = Et

SCHEME 2.26: *Reagents and Conditions*: (i) Cs_2CO_3, DMF, rt, 16 h.

The synthesis started from inexpensive methylhydrazine **113** which was fully Boc-protected to give hydrazine **114** in > 99% yield. Following a procedure by Stafford *et al.*, **114** was then selectively mono-deprotected by mild cleavage of Boc group catalysed by $Mg(ClO_4)_2$ to yield **109**.[180,181] The resulting hydrazine **109** was then alkylated to give *tert*-butyl ester **115** in 87% yield over three steps. Finally, **115** was deprotected

and condensed with dibromomaleic anhydride **58** to afford Meta PD **116** in 73% yield (Scheme 2.27).

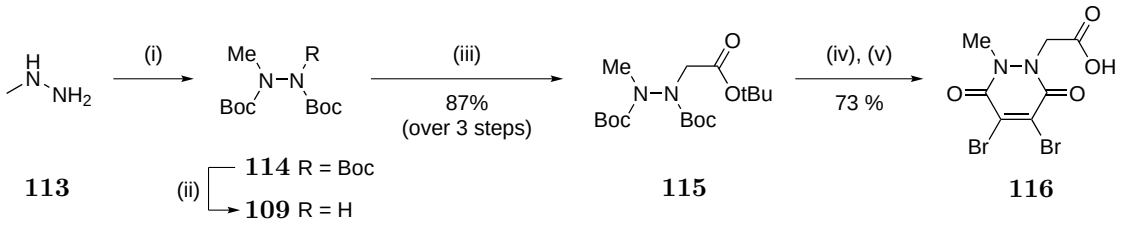

SCHEME 2.27: *Reagents and Conditions*: (i) Boc_2O, NEt_3, DMAP, CH_2Cl_2, rt, 16 h; (ii) $Mg(ClO_4)_2$, MeCN, 50 °C, 1 h; (iii) *tert*-Butyl bromoacetate, Cs_2CO_3, DMF, rt, 16 h; (iv) TFA, CH_2Cl_2, rt, 30 min; (v) Anhydride **58**, AcOH, rt for 16 h, then reflux, 2 h.

As alkyne **81** could already act as an alkyne-functionalised PD, it was decided to focus on the synthesis of PDs mono-functionalised with an azide and with a strained alkyne handle.

2.8.2 Functionalisation of Meta PD

Following the successful high-yielding synthesis of Meta PD **116** but keeping in mind the relatively modest yields obtained when acid **81** was coupled to amines using HBTU, HATU or EDC as coupling agent (*vide supra*, section 2.5, page 42), it was envisaged that the synthesis of isolable NHS- or PFP-activated ester would improve the overall yield of the coupling.

To this end, activation of acid **116** was first attempted using DCC/NHS and TSTU activation; but this returned a mixture of products with no trace of the expected NHS-activated ester **117** (Scheme 2.28). However, DCC/Pentafluorophenol activation resulted in complete conversion to PFP-ester **118** by NMR analysis of the crude mixture post-workup of the reaction. As the crude of the reaction was contaminated with DCCU, it was purified by column chromatography. Unfortunately, **118** partially degraded on the silica and was isolated in only 34% yield (Scheme 2.28).

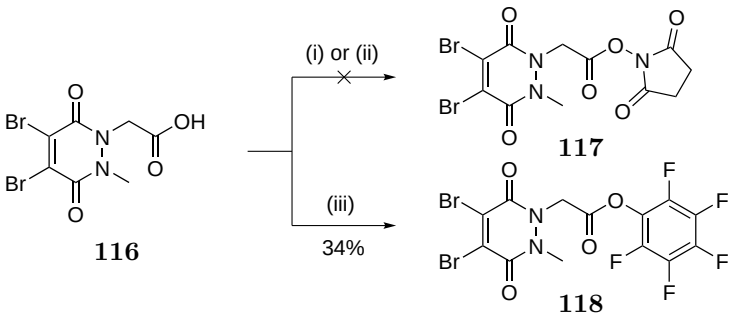

SCHEME 2.28: *Reagents and Conditions*: (i) TSTU, NEt_3, DMF, rt, 5 h; (ii) DCC, NHS, CH_2Cl_2, rt, 16 h; (iii) DCC, pentafluorophenol, dioxane, rt, 16 h.

Commercially available amine **119** was then reacted with **118** to give **Azi**de-**Me**thyl PD **120** (Azime PD) in 81% yield (Scheme 2.29).

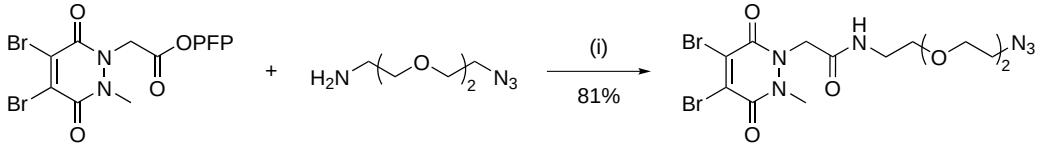

SCHEME 2.29: *Reagents and Conditions*: (i) NEt_3, CH_2Cl_2, rt, 16 h.

Owing to the instability of PFP-ester **118** upon purification and the overall low 28% yield for the coupling with amine **119**, it was decided to attempt a PyBOP-mediated direct coupling between commercially available BCN−PEG−NH_2 **97** (*vide supra*, section 2.5.2, page 45) and acid **116**. These new reaction conditions afforded BCN-based **Me**thyl-**Str**ained **A**lkyne PD **121** (BCN-Mestra PD) in 54% yield (Scheme 2.30).

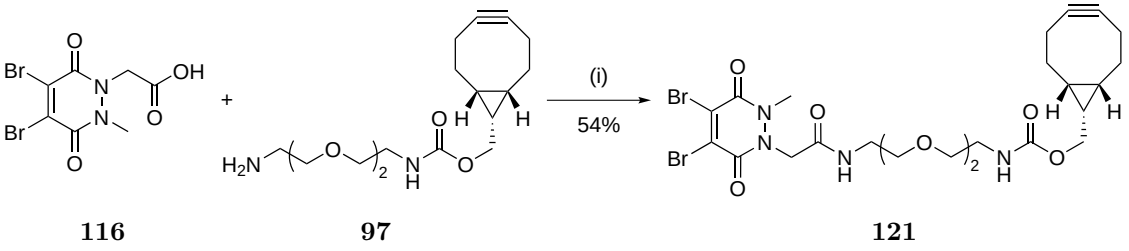

SCHEME 2.30: *Reagents and Conditions*: (i) PyBOP, DIPEA, CH_2Cl_2, rt, 16 h.

2.9 Conclusion

A library of monobromo- and dibromo-PD-based compounds with 0 – 2 clickable handles have been prepared in low to good overall yields (Figure 2.3 and Appendix B). The syntheses of dually "clickable" PDs have been optimised to generate constructs with

improved water solubility through the use of short PEG chains, which may prove essential when attempting conjugation onto proteins. A novel route has been developed for the preparation of mono-functionalised PDs to be used for optimisation of click reactions with alkynes, azides and strained alkynes. Finally, monobromo- and dibromo-PDs with two unreactive ethyl groups on the nitrogens in lieu of clickable handles were prepared to optimise the reaction conditions used for attachment of PDs to proteins.

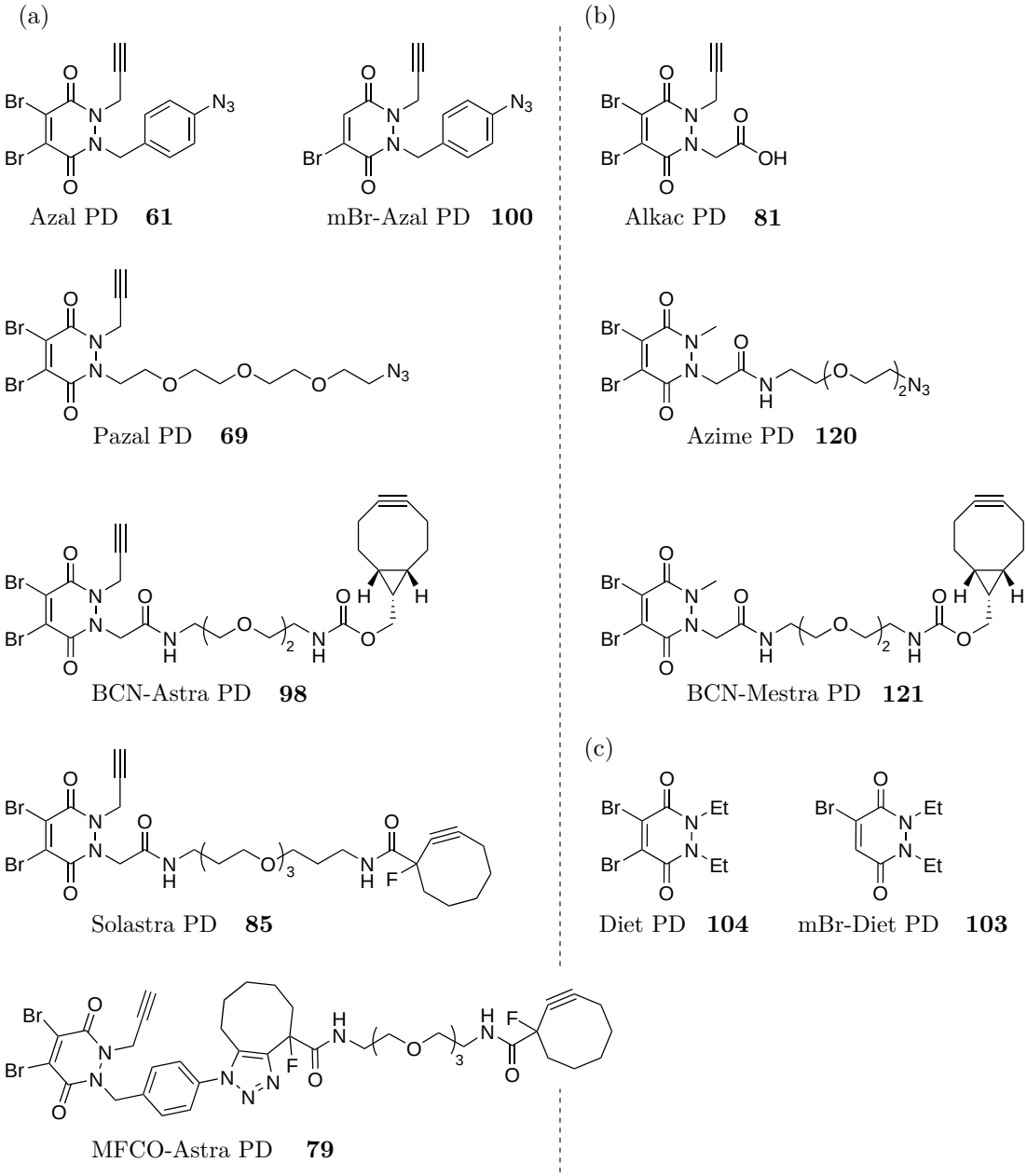

FIGURE 2.3: PDs synthesised with (a) two "clickable" handles; (b) one "clickable" handle; (c) no reactive handle.

Chapter 3

Antibody, Antibody Fragment and Protein Modification

3.1 Introduction

3.1.1 Trastuzumab

The HER receptors are proteins that are embedded in the cell membrane and communicate molecular signals from outside the cell to inside the cell, and turn genes on and off. They are known to stimulate cell proliferation. In some cancers, notably certain types of breast cancer, HER2 is over-expressed and causes cancer cells to reproduce uncontrollably.[182]

In order to inhibit tumor growth due to HER2 over-expression, mAbs specifically directed towards HER2 extracellular domains have been developed. One of the most potent is the murine antibody MAb 4D5. However, its immunogenicity in human has limited its use greatly. Thus, humanised recombinant monoclonal antibodies such as trastuzumab (Herceptin™) were developed.

Trastuzumab interferes with the HER2/neu receptor (also known as ErbB2) and its affinity towards this receptor is three times the affinity of MAb 4D5. Its mechanism of action is known (Figure 3.1).[183] It has been suggested that trastuzumab induces some of its effect by downregulation of HER2/neu, leading to disruption of receptor dimerisation and signalling.[184] In brief summary, trastuzumab binds to domain IV of the extracellular segment of the HER2/neu receptor and inhibits its ectodomain cleavage.[185,186] Cells

treated with trastuzumab undergo arrest during the G1 phase of the cell cycle so there is reduced proliferation. In addition, trastuzumab suppresses angiogenesis (the process through which new blood vessels form from pre-existing vessels) both by induction of antiangiogenic factors and repression of proangiogenic factors. A more detailed mechanism of action of trastuzumab may be found in a report by Hudis.[183]

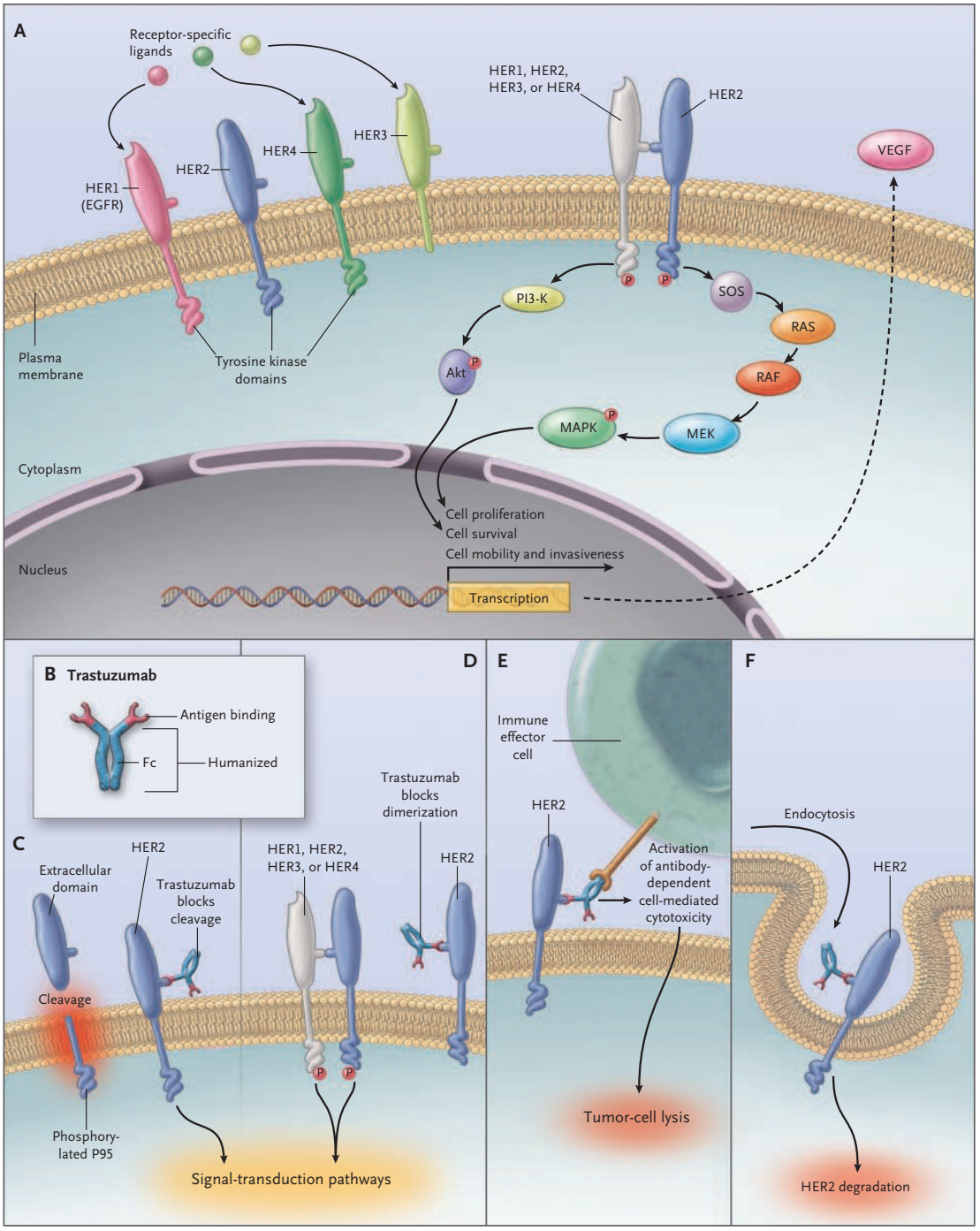

FIGURE 3.1: Mechanism of action of trastuzumab (reproduced from Hudis).[183]

Trastuzumab is mainly used in the treatment of certain breast cancers but it is also being studied for the treatment of other cancers such as gastric cancer[187] and uterine papillary serous carcinomas that also overexpress HER2/neu.[188] An ADC based on trastuzumab, trastuzumab emtansine (trade name Kadcyla™) has already been developed and recently approved by the FDA (*vide supra*, section 1.4, page 11). Kadcyla™ is used to treat patients with HER2-positive metastatic breast cancer which represents at least 20% of breast cancers (breast cancer is the second leading cause of cancer-related death among women). This treatment extends median overall survival by 5.8 months when compared with standard lapatinib + capecitabine treatment.[189] This, along with other results in the field, makes this antibody a suitable construct model for the study.

3.1.2 Fab fragments

Amongst all the antibody fragments, Fabs are the most thoroughly explored; knowledge and experience was generated during the development of 3 FDA-approved therapeutics (Table 3.1), 6 agents in active clinical development, and 20 discontinued programs, which collectively account for 49% of 54 identified antibody fragments that have entered the clinical pipeline.[70]

Generic (brand) names	Description	Indication of 1st approval	Year of 1st approval	Sponsor
Abciximab (Reopro)	Anti-GPIIb/IIIa chimeric Fab	Clot prevention in angioplasty	1994	Centocor
Ranibizumab (Lucentis)	Anti-VEGF-A humanised Fab	Macular degeneration	2006	Genentech
Certolizumab pegol (Cimzia)	Anti-TNFα pegylated humanised Fab	Moderate to severe Crohn disease	2008	UCB

Table 3.1: Monoclonal antibody fragments approved in the US.

Fab fragments of antibodies retain the targeting specificity of full antibodies but can be produced more economically. Indeed, there are significant differences between biomanufacturing fragments and full-sized antibodies, *e.g.* the smaller size of fragments permits cheaper, faster production in microbial systems. In addition, Fab fragments possess other advantages over full antibodies, such as improved tissue penetration.

However, Fab fragments are significantly less stable *in vivo* than full antibodies and as a consequence have relatively short circulating half-lives. Strategies have been developed, such as PEGylation, to extend the half-life of fragments and reduce immunogenicity.[64–67]

3.2 Digestion of antibodies

The shortest method to produce Fab fragments is to enzymatically digest their corresponding full antibody. For such a reaction, the protease of choice is papain. Indeed, when IgG molecules are incubated with papain in the presence of a reducing agent (papain is inactive in its oxidised form), the hinge region is split. This produces three fragments of similar size: two Fab fragments and one Fc fragment[190] that can be easily separated *via* protein A purification. Fab fragments from two different antibodies, rituximab and trastuzumab, were prepared *via* enzymatic digestion.

3.2.1 Rituximab

The Fab fragment of rituximab **123** (Fab_{rit}) was prepared from rituximab **122** using a thiol-free protocol where papain is reduced beforehand with DTT or cysteine. Pre-activated papain, washed from the reducing agent, at an enzyme/IgG ratio of 1/40 (wt/wt) was used to generate Fab_{rit} in an average 70% yield (determined by UV-Vis) after protein A purification (Scheme 3.1).

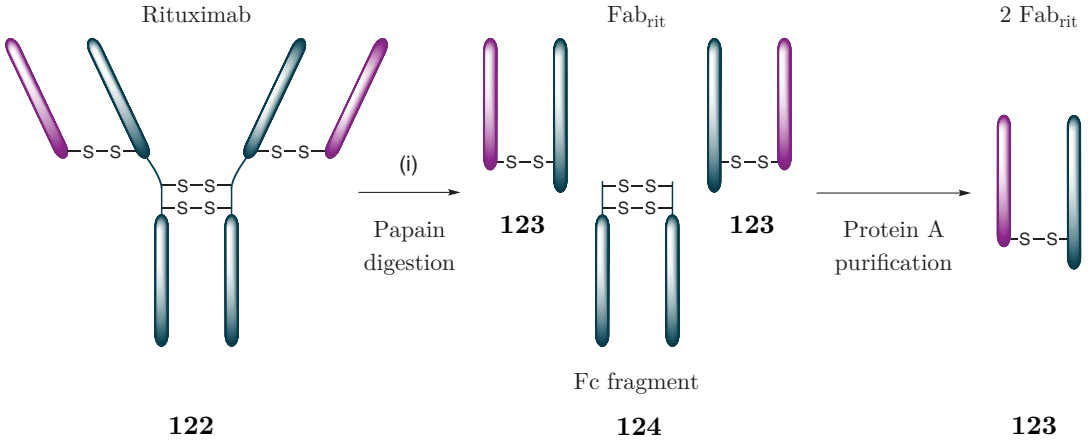

SCHEME 3.1: Fab_{rit} preparation by papain digestion and protein A purification. *Reagents and Conditions*: (i) Papain, phosphate buffer pH 6.8, 37 °C, 16 h.

The fragments obtained were analysed by SDS-PAGE and by LCMS to reveal highly pure Fab_{rit} **123** as the sole product (Figure 3.2).

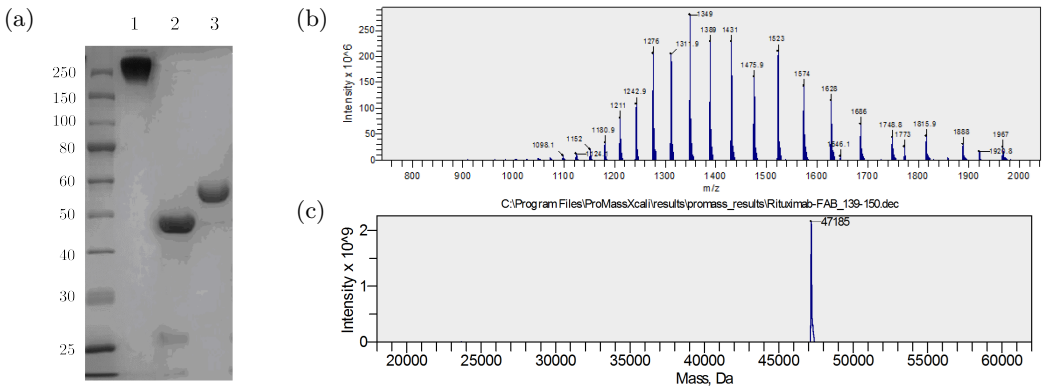

FIGURE 3.2: (a) SDS-PAGE of digested rituximab *via* a thiol-free protocol. Lane 1 – rituximab **122**; 2 – Fab_{rit} **123**; 3 – Fc_{rit} **124**; (b) Non-deconvoluted and (c) deconvoluted LCMS data for Fab_{rit} **123**.

3.2.2 Trastuzumab

The preparation of homogeneous Fab fragments of trastuzumab **127** (Fab_{Her}) proved to be more challenging; several enzymes and conditions had to be tried to yield Fab_{Her} **127** as a single species post-purification using standard techniques.

3.2.2.1 Direct method

In accordance with the report by K. L. Bennett *et al.*,[191] trastuzumab was reacted with various amounts of immobilised papain ranging from 1/40 to 1/10 (enzyme/IgG ratio, wt/wt) in the presence and in the absence of thiol (*vide supra*, section 3.2.1, page 55). At all tested ratios, the thiol-free protocol yielded a mixture of undigested trastuzumab **19**, Fc_{Her} **126**, and Fab_{Her} **127** (Figure 3.3 – lane 2). Attempts were made to purify the mixture using protein A but unfortunately Fab_{Her} **127** also binds to protein A and thus could not be isolated from the mixture (Figure 3.3 – lane 1).

In the presence of a reducing agent and at a high concentration of enzyme (1/10, enzyme/IgG ratio, wt/wt), the digestion went to completion. Gratifyingly, it was found that, when left for an extended period of time, reduced papain also digested Fc_{Her} into low-molecular-weight proteolytic contaminants thus allowing for the purification of Fab_{Her} by diafiltration without the use of protein A. The purified protein was then analysed by SDS-PAGE to reveal Fab_{Her} free of other fragments. Unfortunately, analysis by LCMS revealed a mixture of Fab_{Her} products with a mass difference of 367 Da consistent with

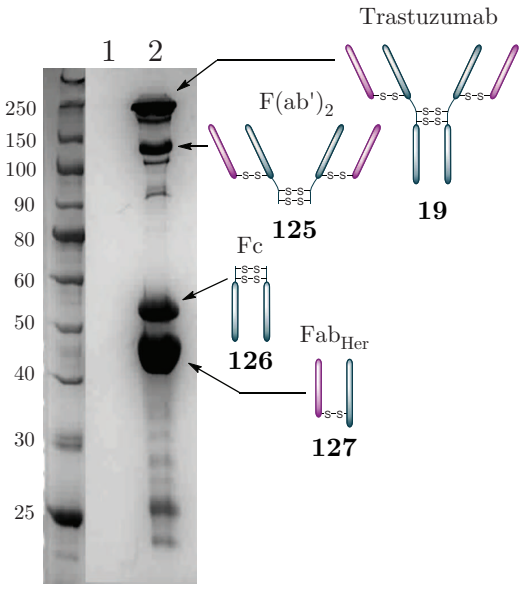

FIGURE 3.3: Failed digest of trastuzumab **19**. Lane 1 – mixture post-purification by protein A; 2 – incomplete digest of trastuzumab **19**.

the cleavage of the first three amino acids of the V_H region, thus most likely reducing the binding affinity of the fragment (Figure 3.4).[192]

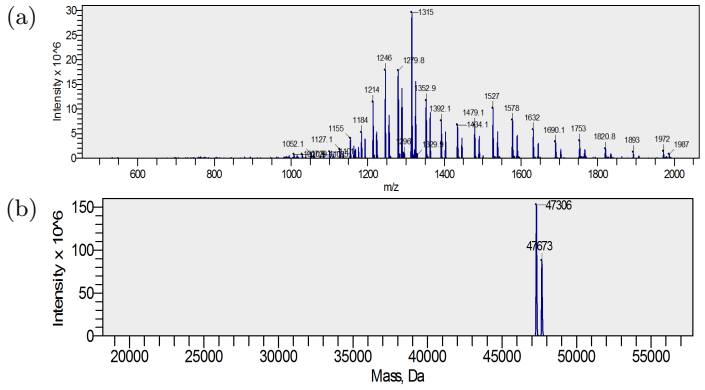

FIGURE 3.4: (a) non-deconvoluted and (b) deconvoluted LCMS data for attempted preparation of a trastuzumab Fab using the protocol outlined by K. L. Bennett *et al.*[191]

As no homogeneous Fab_{Her} **127** could be obtained *via* a direct approach, other conditions had to be found. On the one hand, these conditions had to be milder to avoid over-digestion of Fab_{Her} **127** but, on the other hand, they had to be harsher than the thiol-free protocol that did not reach completion; a two-step method was developed.[192]

3.2.2.2 Two-step method

The two-step method developed consists of pre-digestion of trastuzumab **19** with pepsin to give F(ab')$_2$ **125**, followed by thiol-free digestion with papain. Indeed, pepsin pre-digestion to F(ab')$_2$ **125** also cleaves the Fc in numerous small peptides that can be removed easily by diafiltration. This reduces the steric hindrance around the hinge region of the antibody (Figure 1.2) and allows the subsequent milder thiol-free papain digestion to reach completion within 10 h (Scheme 3.2).

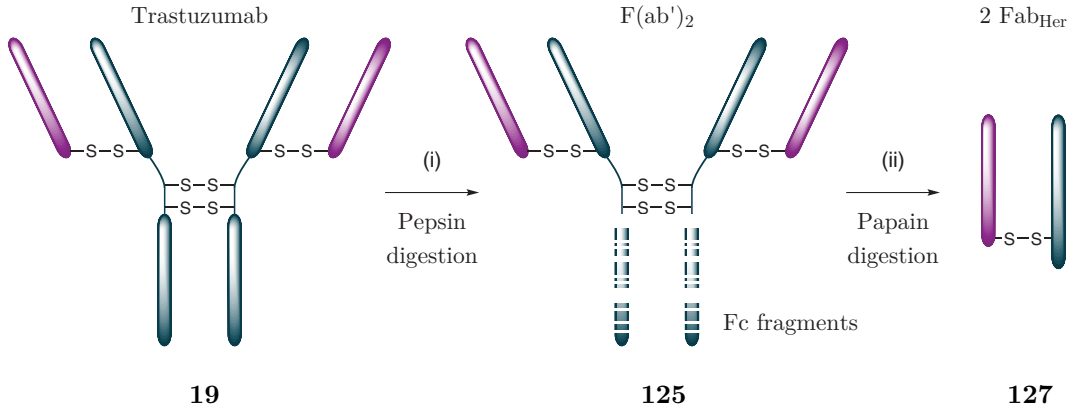

SCHEME 3.2: Fab$_{Her}$ preparation by pepsin digestion followed by papain digestion. *Reagents and Conditions*: (i) Pepsin, acetate buffer pH 3.1, 37 °C, 5 h; (ii) Papain, phosphate buffer pH 6.8, 37 °C, 16 h.

Gratifyingly, analysis of the digest by SDS-PAGE and LCMS revealed formation of a single Fab fragment **127** with an intact V_H region in an average 65% yield (Figure 3.5).

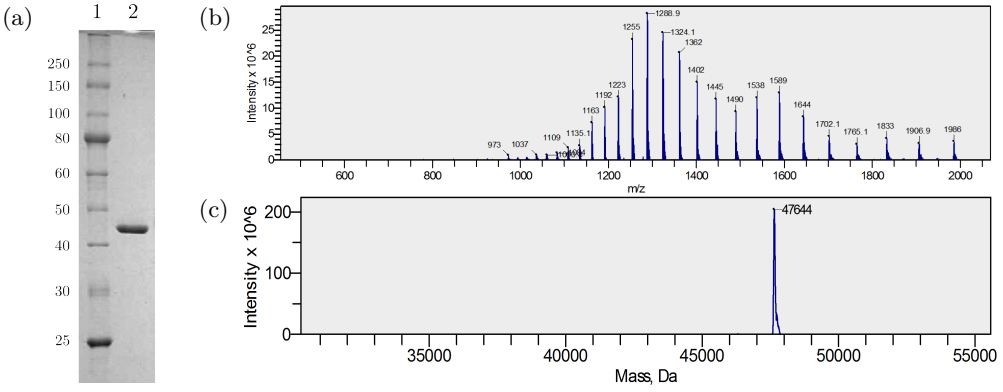

FIGURE 3.5: (a) SDS-PAGE of digested trastuzumab *via* the two-step protocol developed. Lane 1 – ladder; 2 – Fab$_{Her}$ **127**; (b) Non-deconvoluted and (c) deconvoluted LCMS data for the novel preparation of a Fab$_{Her}$ **127**.[192]

3.2.2.3 Conclusion

Direct, "classical" methods involving digestion with papain followed by purification with protein A or diafiltration failed to generate clean and homogeneous Fab fragments. However, a two-step method involving pre-digestion of trastuzumab with pepsin to give $F(ab')_2$ **125**, followed by digestion with papain and diafiltration to remove small proteolytic fragments resulted in clean and homogeneous Fab_{Her} **127**.

3.3 Modification of antibodies

The general strategy developed for the modification of mAbs and Fabs and the generation of constructs that can be functionalised using a "double click" strategy can be divided into two distinct steps (Figure 3.6).

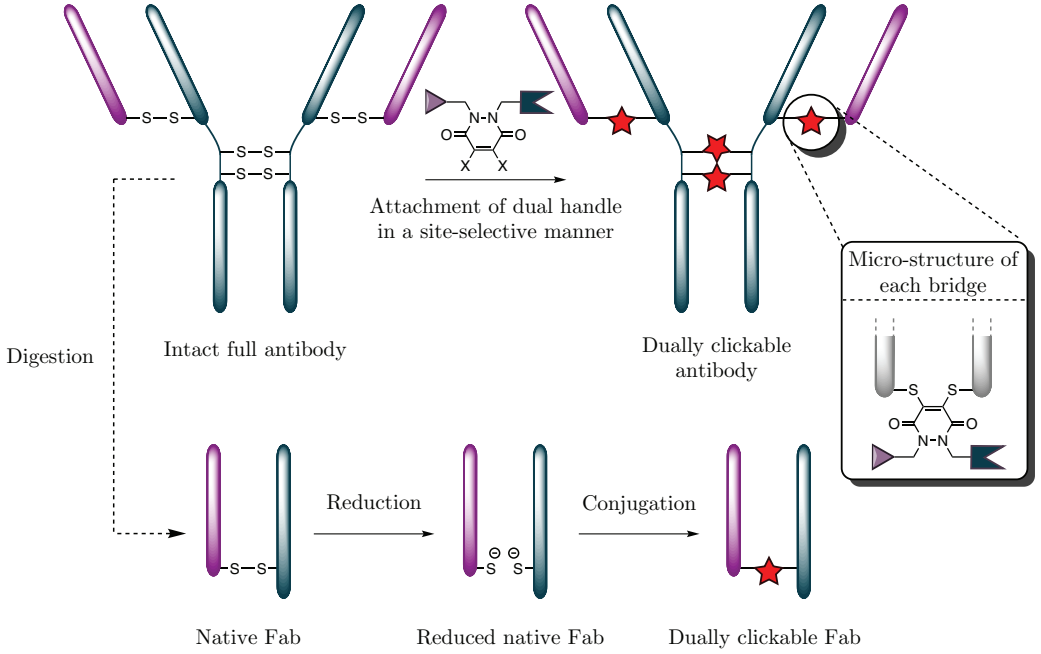

FIGURE 3.6: General strategy for IgG1 and Fab functionalisation.

When modifying mAbs, the four disulfides of a commercially available IgG1 are chemically reduced, leading to eight free thiols. These can be re-bridged by addition to four pyridazinedione-based reagents to give a conjugate with four bridging PDs, each bearing a set of orthogonal handles to be used for dual modification.

Fab fragments contains a single solvent accessible disulfide bond that can be reduced chemically and lead to two free cysteines. These residues can then be reacted in the

presence of the developed pyridazinedione-based reagents to give a dually "clickable" conjugate with two orthogonal handles. These two groups can then be independently reacted in a sequential manner.

3.3.1 Trastuzumab

3.3.1.1 Reduction study

In order to avoid the use of excess reducing agent, a reduction study was carried out with trastuzumab **19**. Two reducing agents (DTT and TCEP) in phosphate and borate buffer, at two different pHs (6.8 and 8), and at 37 °C were evaluated for the reduction of the disulfide bonds of **19**. For analysis purposes, the reaction was then stopped by addition of an excess of maleimide (Scheme 3.3).[119]

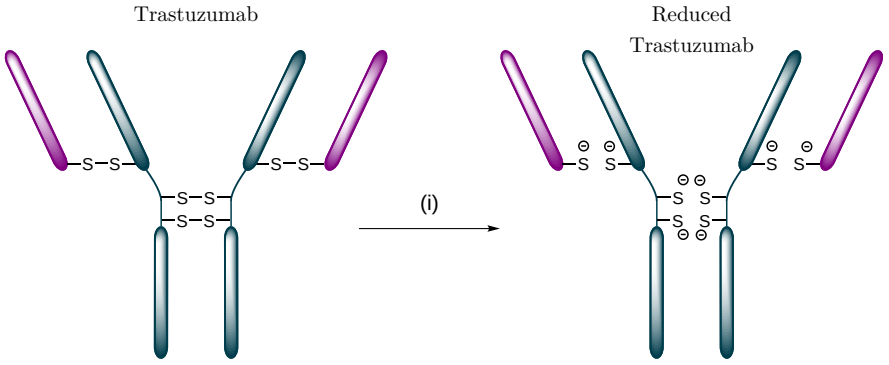

19 **128**

SCHEME 3.3: Reduction of trastuzumab **19**.
Reagents and Conditions: (i) TCEP or DTT for 90 min then maleimide, BBS pH 8.0 or PBS pH 6.8 – 8.0, 37 °C.

SDS-PAGE analysis revealed that 8 equivalents of TCEP in borate buffer pH 8.0 with 1 mM EDTA at 37 °C were sufficient to reduce the 4 disulfide bonds in 90 min, thus revealing the heavy chains (*ca.* 50 kDa) and the light chains (*ca.* 25 kDa) of the antibody (Figure 3.7).[119,155]

After removal of the excess TCEP by diafiltration, re-bridging conditions had to be optimised.

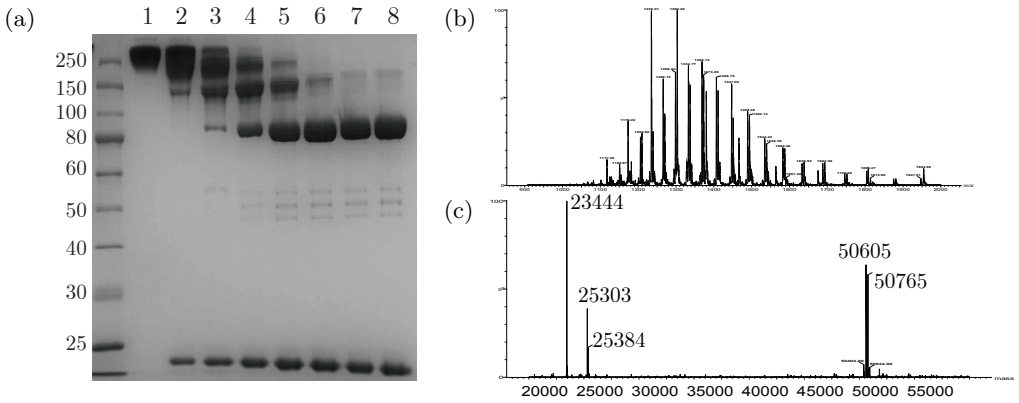

FIGURE 3.7: (a) SDS-PAGE of trastuzumab reduction by TCEP in borate buffer pH 8.0 at 37 °C for 90 min.[119] Lane 1 – trastuzumab **19**; 2 – 2 eq. of TCEP; 3 – 3 eq.; 4 – 4 eq.; 5 – 5 eq.; 6 – 6 eq.; 7 – 7 eq.; 8 – 8 eq.; (b) Non-deconvoluted and (c) deconvoluted LCMS data for trastuzumab **19** reduced with 8 eq. of TCEP.

3.3.1.2 Conjugation study

Using di-bromo Diet PD (Diet PD) **104** as a model, it was shown that 10 equivalents of pyridazinedione-based reagents were sufficient to react with the 8 accessible sulfhydryls of reduced antibody **128** within 1 h at 37 °C (Scheme 3.4).

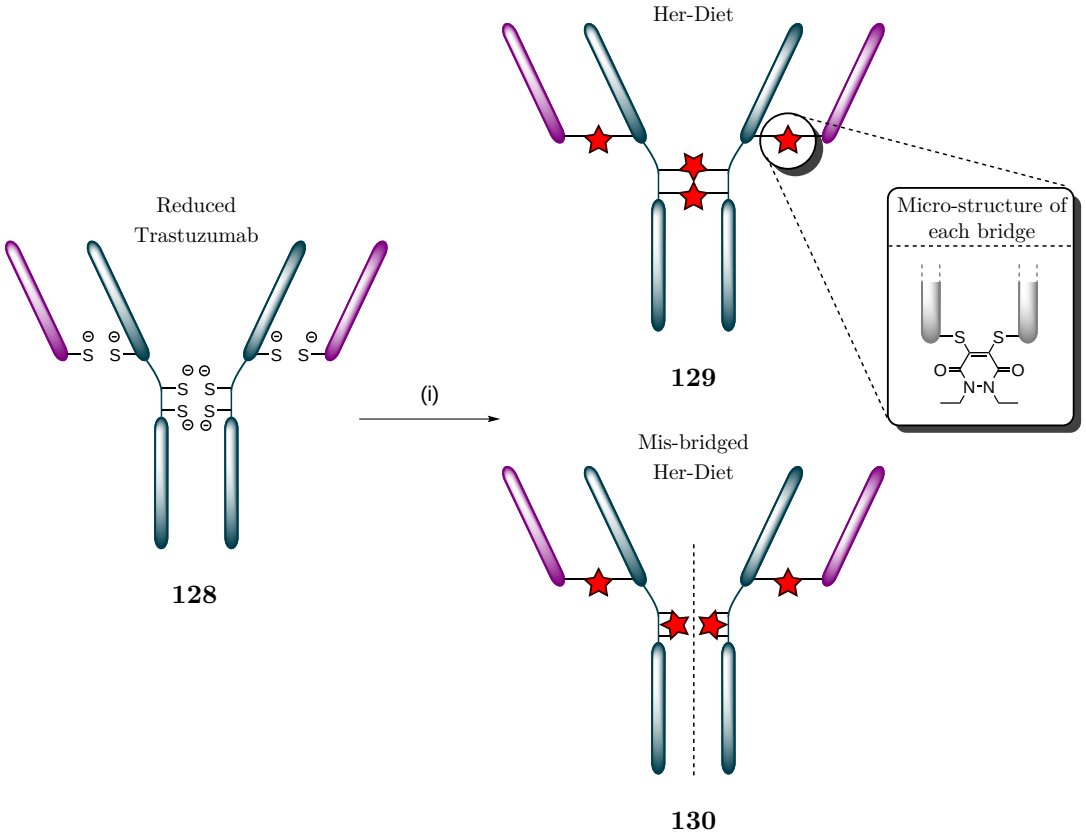

SCHEME 3.4: Modification of reduced trastuzumab **128** with Diet PD **104**. *Reagents and Conditions*: (i) Diet PD **104**, BBS pH 8.0, 37 °C, 1 h.

Unfortunately, SDS-PAGE analysis revealed that a mixture of two products had been obtained by sequentially reacting TCEP then Diet PD **104** with trastuzumab **19**. The high molecular weight species was attributed to the correctly bridged antibody whereas the *ca.* 80 kDa species was hypothesised to be result of a mis-bridging of the hinge region, where the two cysteines of the heavy chain are only separated by two amino acids, resulting in a "half-antibody" (Figure 3.8).

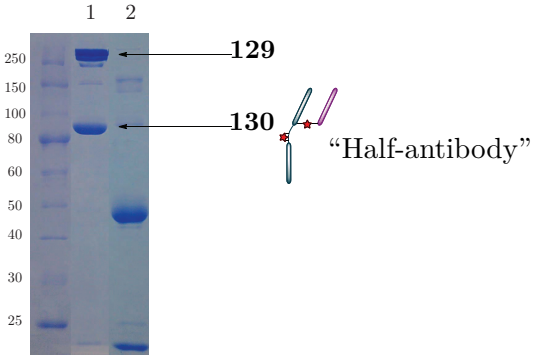

FIGURE 3.8: SDS-PAGE of a Diet-modified trastuzumab by sequential protocol. Lane 1 – re-bridged trastuzumab **129** and **130**; 2 – reduced trastuzumab **128**.

To confirm this hypothesis, a mixture of **129** and **130** was enzymatically digested by pepsin (*vide supra*, section 3.2.2.2, page 58) to yield a mixture of Fab_{Her}-Diet **131** and $F(ab)'_{Her}$-Diet **132** which were characterised by LCMS (Scheme 3.5 and *vide infra*, appendix A.3.1.6, page 150).

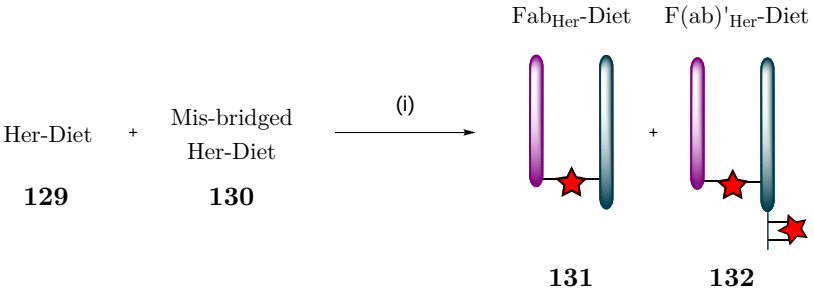

SCHEME 3.5: Pepsin digestion of mis-bridged Her-Diet **130**.
Reagents and Conditions: (i) Pepsin, acetate buffer pH 3.1, 37 °C, 5 h.

As the hinge region of IgG1s has been shown to be essential for certain effector functions of antibodies, it was decided to investigate further the issue of mis-bridging leading to "half-antibody".[108]

It was first envisaged that an *in situ* protocol where the reducing agent (*i.e.* TCEP) is slowly added in the presence of an excess of bridging reagent (*e.g.* Diet PD **104**) would alleviate the mis-bridging: the PD would rapidly trap an opened disulfide of the

hinge region before it can react with the adjacent one. As TCEP is known to react with dibromomaleimides, a class of heterocyles close to PDs (*vide supra*, section 2.1, page 36), before attempting such a protocol, it was first needed to check the absence of cross-reactivity between PDs and this reducing agent.[193,194] Gratifyingly, when Diet PD **104** was mixed with TCEP in a buffered solution at pH 8.0, no reaction was observed after 4 h at 37 °C (Scheme 3.6).

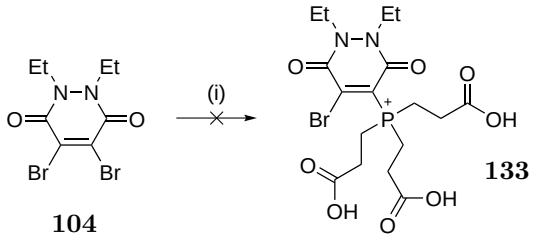

SCHEME 3.6: *Reagents and Conditions*: (i) TCEP, MeCN/BBS pH 8.0, 37 °C, 4 h.

Thus, to avoid half-antibody formation, *in situ* protocols were trialled. TCEP was added to a solution of trastuzumab **19** in BBS pH 8.0 containing 50 or 100 eq. of Diet PD **104** at two different rates, 0.5 eq./h and 0.5 eq./30 min over 16 h and 8 h respectively. The mixture was kept at 37 °C under mild agitation and samples were flash frozen for SDS-PAGE analysis every hour. The results obtained are summarised in Figure 3.9.

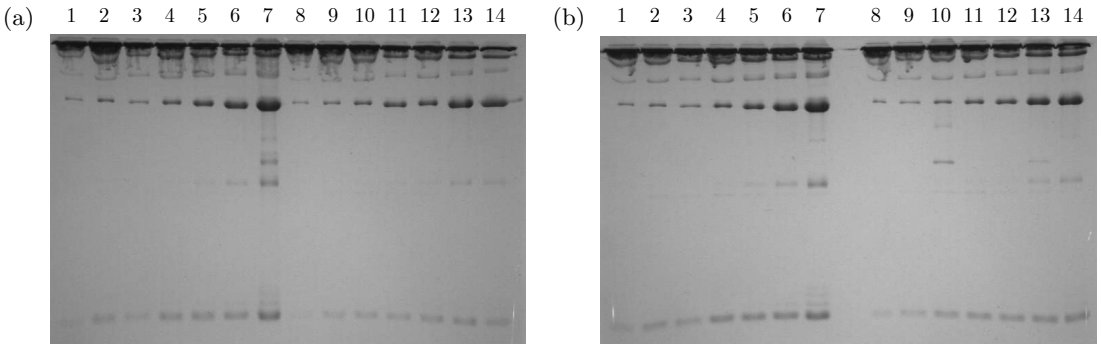

FIGURE 3.9: *In situ* protocol with slow addition of TCEP at 37 °C in borate buffer pH 8.0. (a) SDS-PAGE of reaction with 50 eq. of Diet PD **104**. Lane 1 – 7: 0.5 eq./h after 4, 6, 8, 10, 12, 14 and 16 h respectively; Lane 8 – 14: 1 eq./h after 2, 3, 4, 5, 6, 7 and 8 h respectively; (b) SDS-PAGE of reaction with 100 eq. of Diet PD **104**. Lane 1 – 7: 0.5 eq./h after 4, 6, 8, 10, 12, 14 and 16 h respectively; Lane 8 – 14: 1 eq./h after 2, 3, 4, 5, 6, 7 and 8 h respectively.

In view of these rather disappointing results, it seemed that the rate of addition of reducing agent had no influence over the correct bridging of Diet PD **104**. After addition of 8 eq. all conditions tested showed similar amounts of "half-antibody" **130** (Figure 3.9, lanes 7 and 14) when compared with the sequential protocol (Figure 3.8, lane 1). These results also showed that, at 37 °C, TCEP reduces the four disulfide bonds altogether as,

even with low amounts of reducing agent, "half-antibody" **130** was observed (Figure 3.9, lanes 3 and 10). Another strategy had to be devised to tackle this limitation.

As the *addition rate* did not have an impact on the bridging, it was then envisaged that lowering the temperature of the reaction would limit the *reduction rate* of TCEP while maintaining a high concentration of PD would allow for rapid trapping of an opened disulfide of the hinge region before the adjacent one is opened. It would also reduce thermal motion therefore allowing the antibody to remain close to its original templated structure where the cysteines residues are at a distance where they can be correctly linked together.

Thus, to avoid half-antibody formation, *in situ* protocols at low temperature were trialled. TCEP (8 eq.) was added to a solution of trastuzumab **19** in BBS pH 8.0 containing 50 eq. of Diet PD **104** and the mixture was kept at 4 °C for 16 h. Encouragingly, analysis by SDS-PAGE revealed very limited formation of the undesired "half-antibody" **130** (Figure 3.10a, lane 2). This protocol was then further optimised and it was found that pre-lowering the temperature to 4 °C before addition of TCEP allowed for complete correct re-bridging of trastuzumab **19** and afforded exclusive formation of **129** by SDS-PAGE (Figure 3.10b, lane 2). After removal of the excess unbound small molecules by diafiltration, no further purification was required and a yield in excess of 95% was obtained.

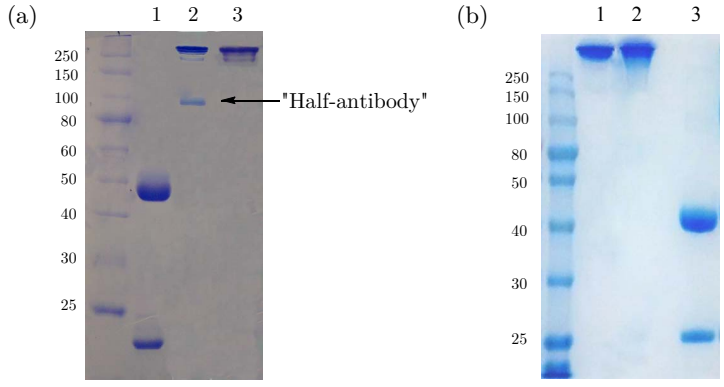

FIGURE 3.10: SDS-PAGE of a trastuzumab **19** re-bridged by *in situ* protocol at 4 °C in borate buffer pH 8.0. (a) Without pre-lowering of the temperature. Lane 1 – reduced trastuzumab **128**; 2 – re-bridged trastuzumab **129** and **130**; 3 – trastuzumab **19**; (b) With pre-lowering of the temperature. Lane 1 – trastuzumab **19**; 2 – re-bridged trastuzumab **129**; 3 – reduced trastuzumab **128**.

Having optimised the conjugation reaction with model compound Diet PD **104**, it was then decided to try these conditions with more relevant "clickable" PDs (*vide supra*,

Figure 2.3, page 51). Gratifyingly, the optimised conditions translated well with more complex PDs and "clickable" Her-PDs were obtained in 90 – 99% yields (Scheme 3.7). Analysis by SDS-PAGE revealed that these optimised conditions resulted in very limited amount of incorrect bridging in the hinge region (Figure 3.11).

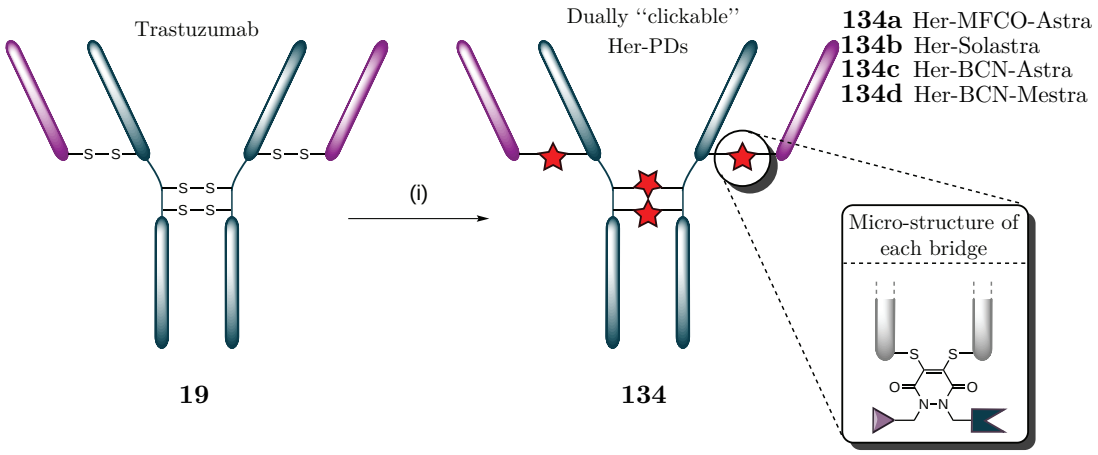

SCHEME 3.7: Modification of trastuzumab **19** with "clickable" PDs. *Reagents and Conditions*: (i) PD, TCEP, BBS pH 8.0, 4 °C, 16 h.

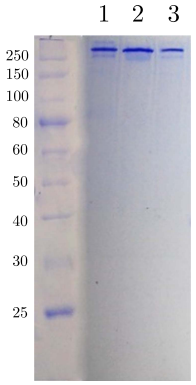

FIGURE 3.11: Typical SDS-PAGE of PD-modified trastuzumab by low temperature *in situ* protocol. Lane 1 – Her-Solastra **134b**; 2 – Her-Mestra **134d**; 3 – Her-BCN-Astra **134c**.

The main limitation of this approach lies in the competing Staudinger reduction when azide containing molecules are used. On the other hand, in addition to yielding correctly re-bridged antibody conjugates, this *in situ* protocol is close to being ideal and more general in that, contrary to the sequential protocol developed, as well as those which have been previously described, it does not rely on the fact that the reduced form of the protein is stable.[195–197] Indeed, it is well established that peptides and proteins that contain disulfide bonds can start to unfold or scramble upon opening of their bridge. Furthermore, protein complexes that are only connected by disulfide bonds would fall apart if a sequential reduction/re-bridging protocol is used. Thus, by minimising the

time a disulfide exists in its reduced form, the developed protocol has the potential to alleviate these issues.

3.3.2 Rituximab

In order to evaluate the compatibility of the method developed with other antibodies, similar conjugation reactions were carried out with rituximab **122**. Analysis by SDS-PAGE, UV-Vis and Ellman's test revealed a very similar profile of re-bridging and PAR for both antibodies. The main difference appeared to be the amount of TCEP needed to reduced rituximab. It was found that 20 eq. were enough to effect complete reduction of the 4 disulfide bonds (Figure 3.12).[194]

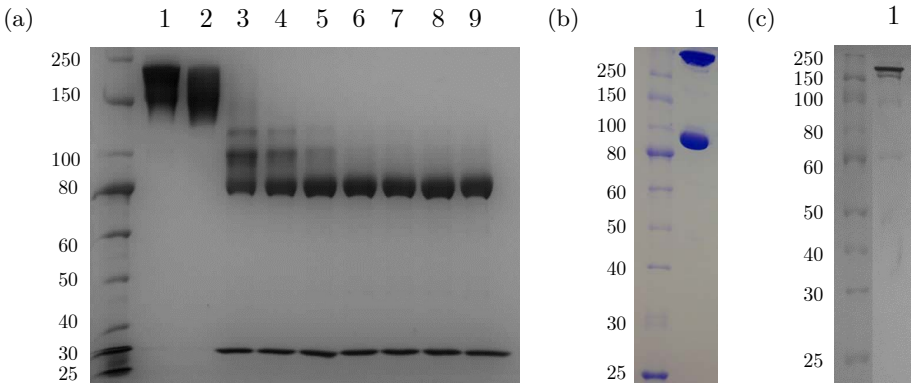

FIGURE 3.12: SDS-PAGE of rituximab **122** and rituximab conjugates showing profiles similar to trastuzumab **19**. (a) SDS-PAGE of rituximab reduction by TCEP in borate buffer pH 8.0 at 37 ℃ for 60 min.[119] Lane 1 – rituximab **122**; 2 – 2 eq. of TCEP; 3 – 4 eq.; 4 – 8 eq.; 5 – 15 eq.; 6 – 30 eq.; 7 – 50 eq.; 8 – 80 eq.; (b) SDS-PAGE of a Diet-modified rituximab by sequential protocol. Lane 1 – Reaction mixture; (c) SDS-PAGE of a Diet-modified rituximab by low temperature *in situ* protocol. Lane 1 – Reaction mixture.

Although it gives a qualitative idea of the efficiency of the bridging, analysis using SDS-PAGE combined with Ellman's test could not quantitatively indicate the number of PD per antibody. A more accurate method to access this value on a full antibody was therefore developed.

3.3.3 PD per antibody ratio

It was found that pyridazinediones absorb light around a $\lambda_{max} \simeq 345$ nm. Using di-cysteine Diet PD **135** as a model (Figure 3.13), a standard UV-Vis curve was obtained. From this curve, using the Beer–Lambert law, it was possible to calculate a molar extinction coefficient value at $\lambda_{max} = 345$ nm (ε_{345}) for the pyridazinedione-based reagents used.

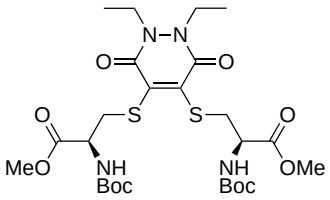

135

FIGURE 3.13: Protected di-cysteine derivative of Diet PD used for UV-Vis standard curve.

As shown in Figure 3.14, PD **135** also absorbs light at 280 nm, and the relation with its absorbance A_{345} at $\lambda_{max} = 345$ nm is given by:

$$A_{280}^{PD} = 0.28 A_{345}$$

Taking into account this correction, the PD/antibody ratio (PAR) for a conjugate is given by:

$$PAR = \frac{A_{345}/\varepsilon_{345}}{(A_{280} - A_{280}^{PD})/\varepsilon_{280}} = \frac{A_{345}/\varepsilon_{345}}{(A_{280} - 0.28A_{345})/\varepsilon_{280}}$$

with A_λ the absorbance of the conjugate at the wavelength λ, $\varepsilon_{345} \simeq 9100\,M^{-1}\cdot cm^{-1}$ and $\varepsilon_{280} = 215\,380\,M^{-1}\cdot cm^{-1}$ for trastuzumab **19**.

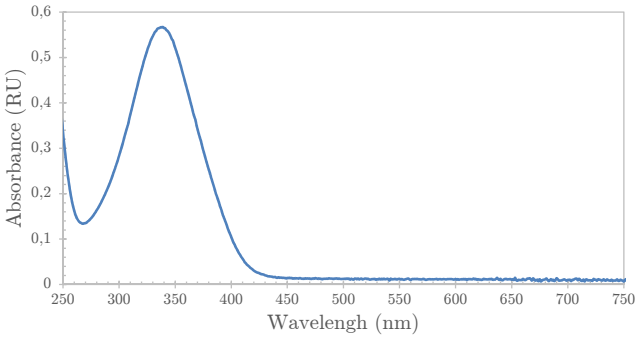

FIGURE 3.14: UV-Vis spectrum of di-cysteine Diet PD **135**.

As suggested by the SDS-PAGE analysis and by Ellman's test, using this formula the average calculated PAR for conjugates **134a–d** was *ca.* 4. This is consistent with the insertion of PDs into each of the disulfide bonds of trastuzumab **19** (Figure 3.15).

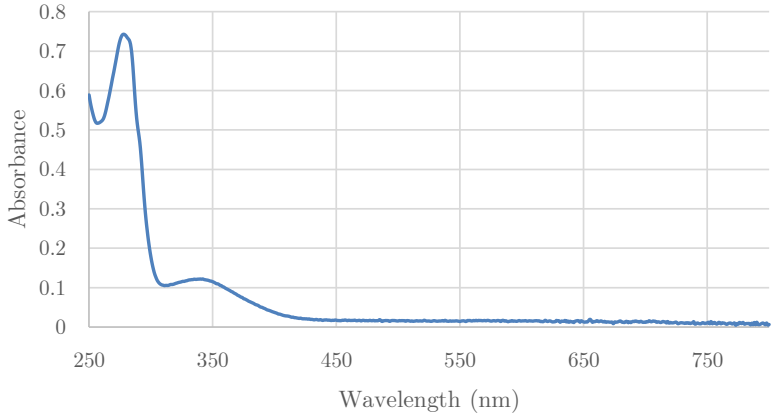

FIGURE 3.15: UV-Vis spectrum of Her-Solastra **134b**.

3.4 Modification of Fab fragments

3.4.1 Trastuzumab

3.4.1.1 Reduction study

As for the optimisation with a full antibody, a reduction study was carried out with Fab_{Her} **127**. Two reducing agents (DTT and TCEP) in phosphate and borate buffer, at two pH and 8, and at 37 °C were evaluated for the reduction of the disulfide bond of Fab_{Her} **127** (Scheme 3.8).

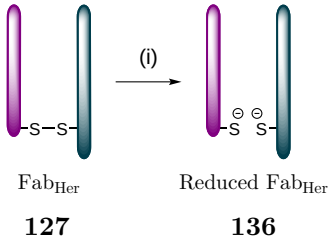

SCHEME 3.8: Reduction of Fab_{Her} **127**.
Reagents and Conditions: (i) TCEP or DTT, 90 min, BBS or PB pH 8.0, 37 °C.

SDS-PAGE together with LCMS analysis revealed that 3 equivalents of TCEP in borate buffer pH 8.0 with 1 mM EDTA at 37 °C were sufficient to reduce the disulfide bond in 90 min, thus revealing the free truncated heavy chains (observed mass 23 449 Da) and light chains (observed mass 24 209 Da) of reduced Fab_{Her} **136** (Figure 3.16).[155,192]

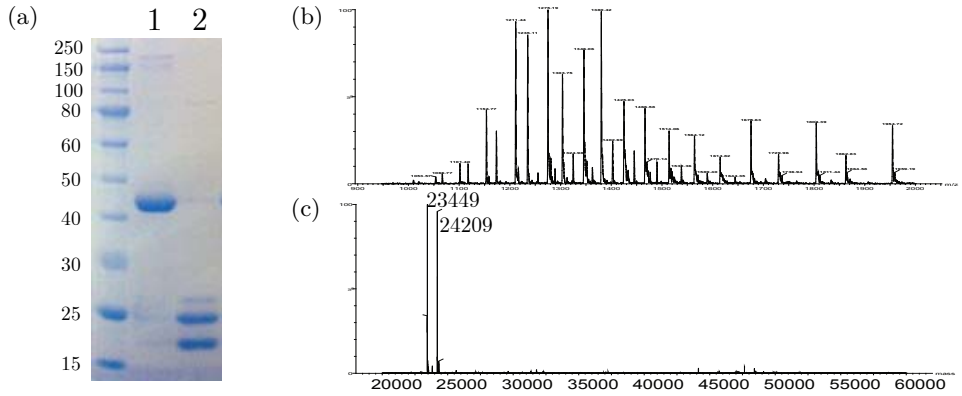

FIGURE 3.16: (a) SDS-PAGE of Fab_{Her} **127** reduction by TCEP in borate buffer pH 8.0 at 37 °C for 90 min. Lane 1 – Fab_{Her} **127**; 2 – reduction with 3 eq. of TCEP; (b) Non-deconvoluted and (c) deconvoluted LCMS data for reduced Fab_{Her} **136**.

3.4.1.2 Conjugation study

After removal of the excess TCEP by diafiltration, a small screening of conditions, using Diet PD **104** as a model, showed that 5 equivalents of pyridazinedione-based reagent were sufficient to re-bridge Fab_{Her} **127** within 1 h at 37 °C to afford the desired Fab_{Her}-Diet **131** covalently inserted (Scheme 3.9).

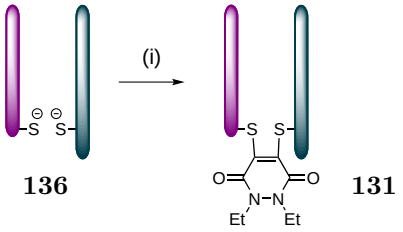

SCHEME 3.9: Modification of reduced Fab_{Her} **136** with Diet PD **104**. *Reagents and Conditions*: (i) Diet PD **104**, BBS pH 8.0, 37 °C, 1 h.

The insertion of the PD moiety was confirmed by SDS-PAGE, LCMS and UV-Vis analysis (Figure 3.17). The conjugate was obtained in high purity in $> 95\%$ yield.

Having optimised the conjugation reaction with model compound Diet PD **104**, it was then decided to try these conditions with more relevant "clickable" PDs (*vide supra*, Figure 2.3, page 51).

Fab_{Her} was therefore reduced to reduced Fab_{Her} **136** and re-bridged using the optimised conditions developed. The excess of unbound small molecules was removed by diafiltration to give "clickable" Fab_{Her}-Azal **137a**, Fab_{Her}-Pazal **137b**, Fab_{Her}-Alkac **137d**, Fab_{Her}-Astra **137c**, Fab_{Her}-Solastra **137e**, Fab_{Her}-BCN-Astra **137f** and Fab_{Her}-BCN-Mestra

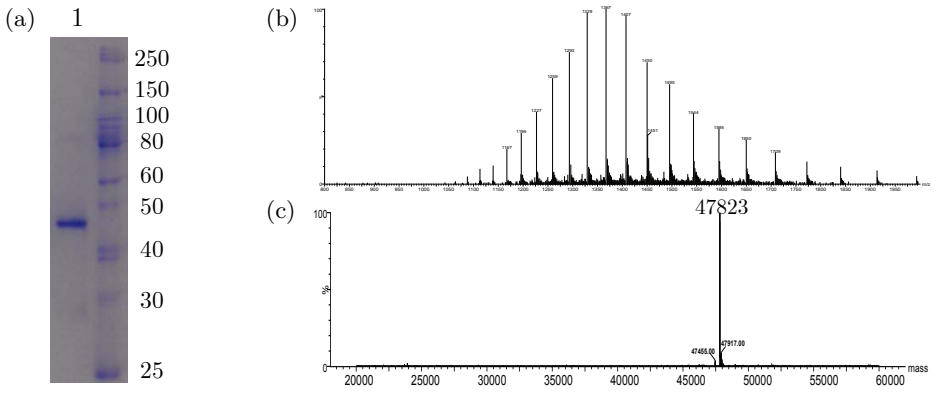

FIGURE 3.17: (a) SDS-PAGE of Fab_{Her}-Diet **131**. Lane 1 – Fab_{Her}-Diet **131**; (b) Non-deconvoluted and (c) deconvoluted LCMS data for Fab_{Her}-Diet **131**.

137g (Scheme 3.10), from PDs **61**, **69**, **81**, **79**, **85**, **98** and **121** respectively (*vide supra*, Figure 2.3, page 51).

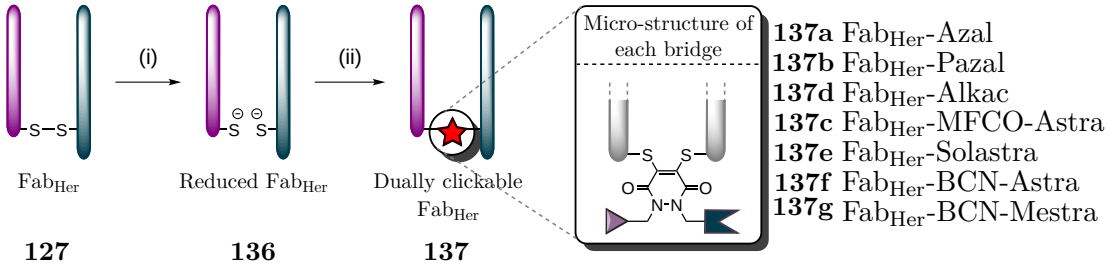

SCHEME 3.10: Modification of Fab_{Her} with PDs **61**, **69**, **81**, **79**, **85**, **98** and **121**. *Reagents and Conditions*: (i) TCEP, BBS pH 8.0, 37 °C, 1.5 h; (ii) PD, BBS pH 8.0, 37 °C, 1 h.

Pleasingly, the optimised conditions translated well with more complex PDs. Analysis by LCMS, UV-Vis and SDS-PAGE confirmed that "clickable" Fab_{Her}-PDs **137** were obtained in 90 – 99% yields in high purity without the need for lengthy purification or separation (Figure 3.18 and Appendix A.3).

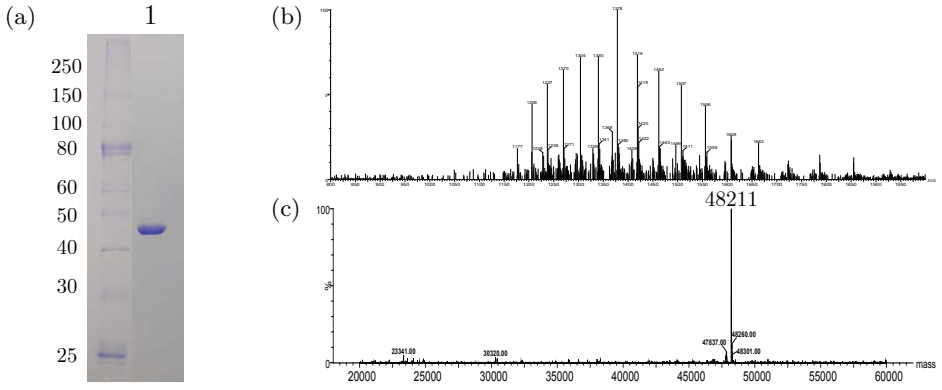

FIGURE 3.18: Typical SDS-PAGE and LCMS data for Fab_{Her}-PD **137**. (a) SDS-PAGE of Fab_{Her}-Solastra **137e**. Lane 1 – Fab_{Her}-Solastra **137e**; (b) Non-deconvoluted and (c) deconvoluted LCMS data for Fab_{Her}-Solastra **137e**.

3.4.2 Rituximab

In order to show the compatibility of the method with Fab fragments from other antibodies, Fab_{rit} **123** was modified following the same procedure with Diet PD **104**. SDS-PAGE and LCMS analysis revealed clean and complete conversion to the corresponding conjugate (Figure 3.19).

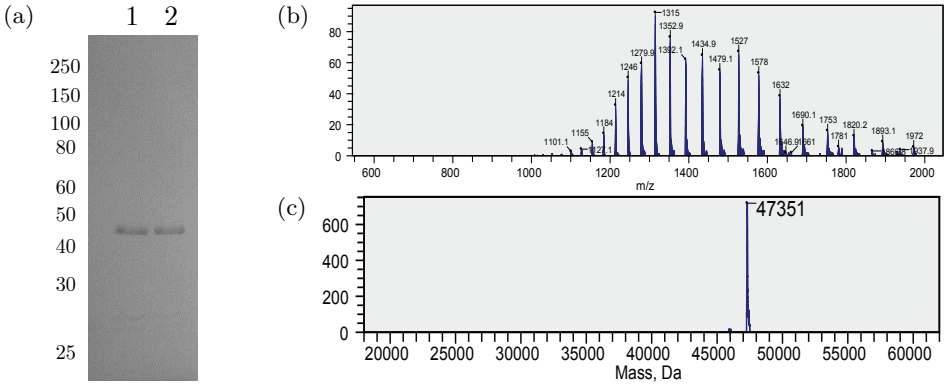

FIGURE 3.19: (a) SDS-PAGE of Fab_{rit}-Diet **183**. Lane 1 – Fab_{rit} **123**; 2 – Fab_{rit}-Diet **183**; (b) Non-deconvoluted and (c) deconvoluted LCMS data for Fab_{rit}-Diet **183**.

3.5 Conjugation with monobromo PDs

As free cysteines are extremely rare in proteins[35] and since the thiol side chain has the highest nucleophilicity of all proteinogenic groups at physiological conditions,[25] it is a very popular target for the selective and site-specific modification of proteins.[198] Moreover, with the possibility of facile cysteine introduction by site-directed mutagenesis, this is a leading approach. The most popular strategy for labelling the thiol moiety of cysteine residues is their alkylation with maleimides to form thioether-succinimides.[38–40,198]
As PDs offer a distinct reaction profile when compared with other standard cysteine-reactive reagents (*vide supra*, section 1.2.2, page 4), modification of single-cysteine-containing proteins was investigated.

Cysteine modification with mBr-Diet PD **103** has been previously described.[52] It was used as a model compound to modify a single cysteine mutant (L111C) of the SH2 domain of the Grb2 adapter protein **138** (Scheme 3.11).[51]

To make this approach modular and to further exemplify the use of monobromo PDs on other proteins and with PDs with reactive handles, conjugation on a single cysteine

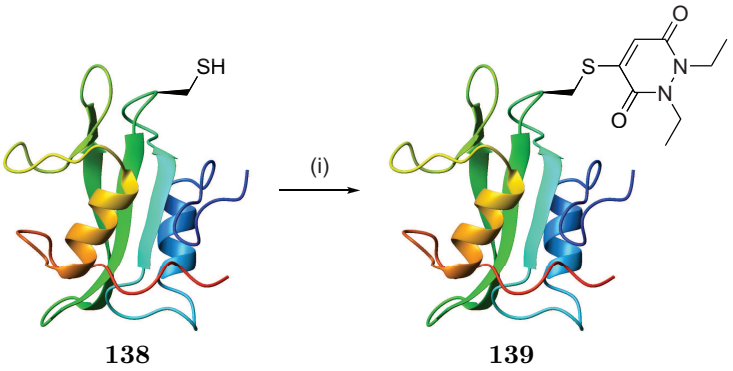

SCHEME 3.11: Conjugation to Grb2L111C described by Chudasama *et al.*[52]
Reagents and Conditions: (i) mBr-Diet PD **103**, PBS pH 8.0, 37 °C, 16 h.

mutant (S147C) of GFP was investigated.[199] Initially, single cysteine mutant GFP_{S147C} **140** was incubated with mBr-Diet PD **103** in sodium phosphate buffer (pH 8.0) for 1 h at 37 °C (Scheme 3.12).

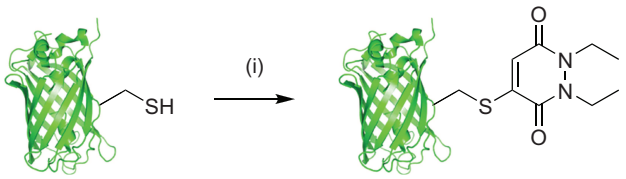

SCHEME 3.12: Modification of GFP_{S147C} **140** with mBr-Diet PD **103**.
Reagents and Conditions: (i) mBr-Diet PD **103**, PBS pH 8.0, 37 °C, 1 h.

As expected, LCMS analysis confirmed that this proceeded with complete conversion and afforded GFP-derivative **141** (Figure 3.20).

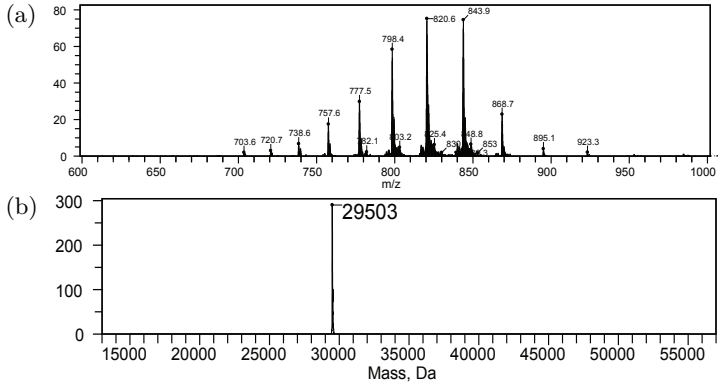

FIGURE 3.20: (a) Non-deconvoluted and (b) deconvoluted LCMS data for GFP-Diet derivative **141**.

Following these encouraging results with model compound mBr-Diet PD **103**, it was decided to expand the scope of this conjugation method and to appraise the protocol with "clickable" mBr-Azal PD **100** (*vide supra*, Figure 2.3, page 51). Thus, GFP_{S147C}

140 was incubated with 10 equivalents of mBr-Azal PD **100** in PBS pH 8 with 5% DMF for 1 h at 37 °C (Scheme 3.13).

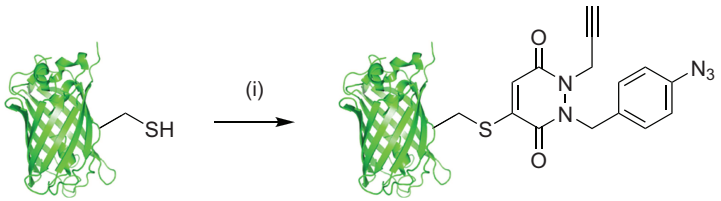

140 **142**

SCHEME 3.13: Modification of GFP_{S147C} **140** with mBr-Azal PD **100**.
Reagents and Conditions: (i) mBr-Azal PD **100**, PBS pH 8.0, DMF, 37 °C, 1 h.

Gratifyingly, SDS-PAGE and LCMS analysis confirmed that this proceeded with complete conversion and afforded GFP-Azal **142** (Figure 3.21).

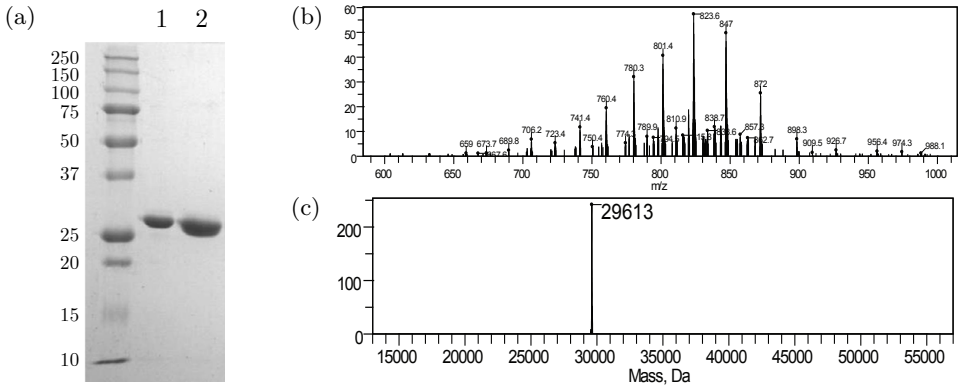

FIGURE 3.21: (a) SDS-PAGE of GFP-Azal **142**. Lane 1 – GFP_{S147C} **140**; 2 – GFP-Azal **142**; (b) Non-deconvoluted and (c) deconvoluted LCMS data for GFP-Azal **142**.

3.6 Conclusion

Methods for the successful attachment of PDs to either single cysteines or disulfide bonds have been developed. They have been optimised with model compounds Diet PD **104** and mBr-Diet PD **103** to give PD-conjugates in high yields, in high purity and in excellent homogeneity. The reaction conditions used are mild, rapid and limit greatly disulfide scrambling when used in challenging multi-disulfides systems such as IgG1s.

Following the optimised protocols, conjugates have then been successfully prepared by attaching monobromo and dibromo-PDs (*vide supra*, Figure 2.3, page 51) to antibodies **19**, **122**, antibody fragments **127**, **123** and a single cysteine mutant of GFP **140**. These conjugates are readily "clickable" and can be functionalised with various modalities.

Chapter 4

Functionalisation of the PD-modified Conjugates

4.1 Introduction

The term "theranostic" is defined as a biological entity (*e.g.* bioconjugate) that combines the modalities of therapy and diagnostic imaging.[200,201] Instead of using two separate conjugates for two related objectives, theranostics combine these features into one platform. As the payloads will reach the target simultaneously, this has the potential to alleviate undesirable differences that exist between distinct therapeutic and imaging agents (*e.g.* biodistribution, selectivity).[202–204] There are plentiful opportunities in multimodal imaging and theranostics, which can be made available through a dual-click approach by attachment of a fluorophore and a radiolabel or cytotoxic drug, respectively.[200,205,206]

Furthermore, this method allows for the construction of novel ADC fragment-based products. In terms of therapeutics, antibody fragments offer potential advantages over full antibodies (*e.g.* fragments are smaller and offer greater tissue penetration; many lack the antibody Fc region and can therefore be expressed in bacterial cell lines as there is no requirement for post-translational glycosylation).[61,207–209] However, antibody fragments below the *ca.* 60 – 70 kDa size cut-off for glomerular filtration lack the stability afforded by the antibody Fc region; therefore, they often have a lifetime in blood serum below what is required to elicit a beneficial therapeutic effect without intensive and frequent therapy.[209–214]

It was envisaged that the technology developed in this project would allow antibody fragment-based therapeutics to be far more accessible by delivering long lifetime antibody fragment–drug conjugates (FDC). This could be achieved by the attachment of an antibody fragment to: (i) a suitable toxic drug; and (ii) a blood serum-stabilising functionality (*e.g.* PEG, albumin or albumin-binding functionality) to increase lifetime *in vivo*, using the dual-click approach. It would generate an ideal "ADC" that would benefit from all the advantages of antibody fragments with an increased half-life and stability. Moreover, as the chemistry allows for the controlled stoichiometric addition of each moiety, it would allow for the construction of well-characterised products.

4.2 "Clickable" molecules for functionalisation of PD-Conjugates

In order to optimise the conditions for the functionalisation of the "clickable" proteins prepared, suitable "clickable" components on which to evaluate the technology needed to be selected. In addition to being biologically relevant, these components should ideally be commercially available or easily prepared and water-soluble; they should also enable facile reading of their loading by a means other than LCMS which is often challenging on full antibody or with polymers. Moreover, their molecular weights should cover a broad spectrum (*i.e.* from small molecule size to protein size: below 1 kDa to more than 10 kDa) to best explore the scope of the click conjugation.

Anti-cancer drug doxorubicin (Dox **143**) has been previously used as a cytotoxic model payload; it has a relatively distinctive absorbance maximum at 495 nm which facilitates determination of drug-to-antibody ratios (DAR) by UV-Vis absorption.[192] As such, Dox was chosen as the cytotoxic platform (Figure 4.1).

To appraise the effectiveness of the dual-click approach on a full antibody scaffold, where accurate mass spectrometry analysis is limited, a second light absorbing moiety that absorbs at a wavelength sufficiently distinct to Dox's was needed to enable facile analysis by UV-Vis of the loading of each cargo. To this end, a commercially available, clickable, water-soluble, cyanine-based fluorophore with a maximum absorbance at 646 nm (sulfo-Cy5 **145**) was selected (Figure 4.1).

Finally, to expand the scope of the dual-click approach to high molecular weight payloads, a commercially available life extension module comprised of a 20 kDa water-soluble PEG chain functionalised on one end with an azide and, on the other, with an unreactive methyl group was selected (Figure 4.1). In addition to enabling facile analysis by SDS-PAGE, the choice of the 20 kDa PEG **144** was motivated by the fact that its effects on half-life are well-characterised *in vivo*. Indeed, attachment of such PEGs can endow proteins with many desirable attributes, such as improved circulating half-life *in vivo* and also enhanced water-solubility, reduced immunogenicity, enhanced proteolytic resistance and improved thermal and mechanical stability without significantly compromising the penetration ability of a Fab fragment.[64,215–218]

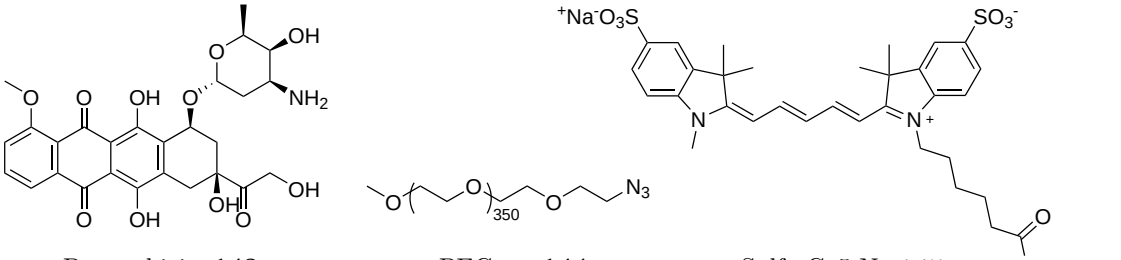

Doxorubicin **143** PEG$_{20k}$ **144** Sulfo-Cy5-N$_3$ **145**

FIGURE 4.1: Molecules used to appraise the dual-click approach.

4.2.1 Synthesis of "clickable" doxorubicin

As Dox **143** did not have a commercially available "clickable" analogue, it had to be prepared. The derivative should ideally be water-soluble; thus, it was decided to prepare acid PEG$_4$−N$_3$ **146** to incorporate an azide handle and to increase water-solubility of the final "clickable" molecule.

Azide **64** was converted to acid **146** which was then reacted with Dox **143** using HBTU as coupling agent. This afforded "clickable" Dox **147** in good overall yield (Scheme 4.1).[155]

4.2.2 Synthesis of water-soluble tetrazines

Some of the tetrazines with the fastest kinetics can undergo rapid 1,4 additions with nucleophiles such as H_2O and are therefore not suitable for conjugation on proteins.[219] To alleviate this issue, a variety of water-compatible tetrazines with reduced reactivities

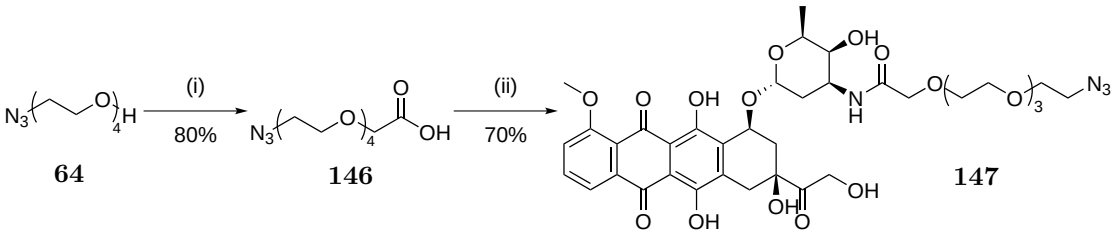

SCHEME 4.1: *Reagents and Conditions*: (i) *Tert*-butyl bromoacetate, NaOH, toluene/H_2O, rt, 16 h; (ii) Dox **143**, HBTU, DIPEA, DMF, rt, 3 h.

have been developed. While being still highly reactive towards bicyclononynes (BCNs) **89**,[176,177] pyrimidinyl-substituted tetrazine **150** has been shown to remain stable in aqueous buffer for extended period of time.[220,221] Nevertheless, it is not soluble in water above 0.2 mM.[222] To explore further this bioorthogonal reaction with BCNs, derivatives with increased solubility were prepared.

Tetrazine **150** was synthesised following a procedure described by Chen *et al.*[220] Hydrazine, 4-cyanobenzoic acid and 2-pyrimidinecarbonitrile where reacted to give a dihydrotetrazine which was oxidised by $NaNO_2$ to yield pyrimidinyl-substituted tetrazine **150** in 8% yield (Scheme 4.2). This low yield can be explained by the challenging separation of the statistical mixture of symmetrical and unsymmetrical by-products formed during the reaction (*vide infra*, Appendix A.2, page 112).[220]

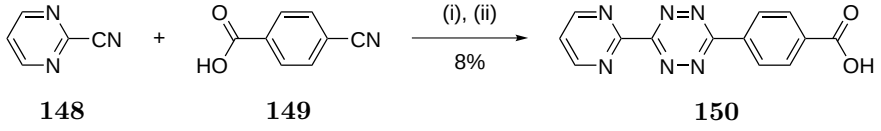

SCHEME 4.2: *Reagents and Conditions*: (i) Hydrazine hydrate, EtOH, reflux, 2 h; (ii) $NaNO_2$, AcOH, 10 °C, 10 min.

Acid **150** was then activated with NHS and reacted with diamine PEGs of various lengths (NH_2−PEG_4−NH_2 **82**, NH_2−PEG_{18}−NH_2 **184** and NH_2−PEG_{38}−NH_2 **185**) to yield tetrazines **152a**–**c** in 41%, 71% and 26% yield respectively (Scheme 4.3).

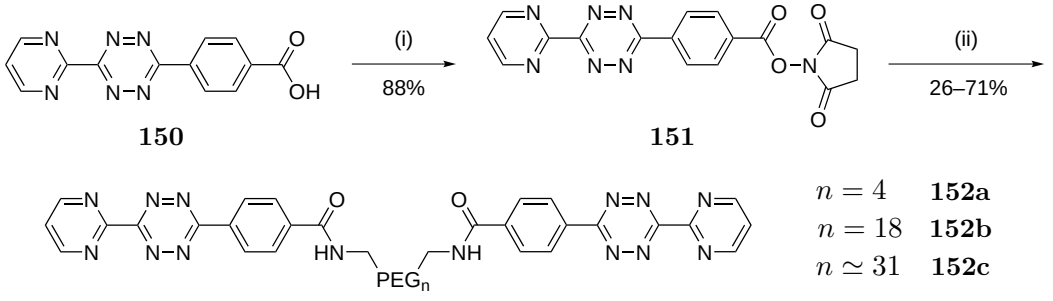

SCHEME 4.3: *Reagents and Conditions*: (i) NHS, EDC, pyridine, DMSO, 40 °C, 3 h; (ii) **82**, **184** or **185**, pyridine, DMSO, rt, 24 h.

With this small library of "clickable" reagents available, copper(I)-catalysed Azide–Alkyne Cycloaddition (CuAAC), Strain-Promoted Azide–Alkyne Cycloaddition (SPAAC) and Strain-Promoted Alkyne–Tetrazine Cycloaddition (SPATC) protocols were developed and optimised for the generation of dually functionalised constructs.

4.3 Copper-free functionalisation

4.3.1 SPATC — Tetrazines

Using Fab_{Her}-BCN-Mestra **137g** as the "clickable" protein model and tetrazine **152a** as the tetrazine model, SPATC conditions were optimised. It was found that incubation for 1 h at room temperature of 5 equivalents of tetrazine **152a** was sufficient to convert **137g** to clicked Fab_{Her} **153** in near quantitative yield and in high purity (Scheme 4.4). The buffer used and pH (6.2 – 8.0) were found to have no measurable impact on the reaction.

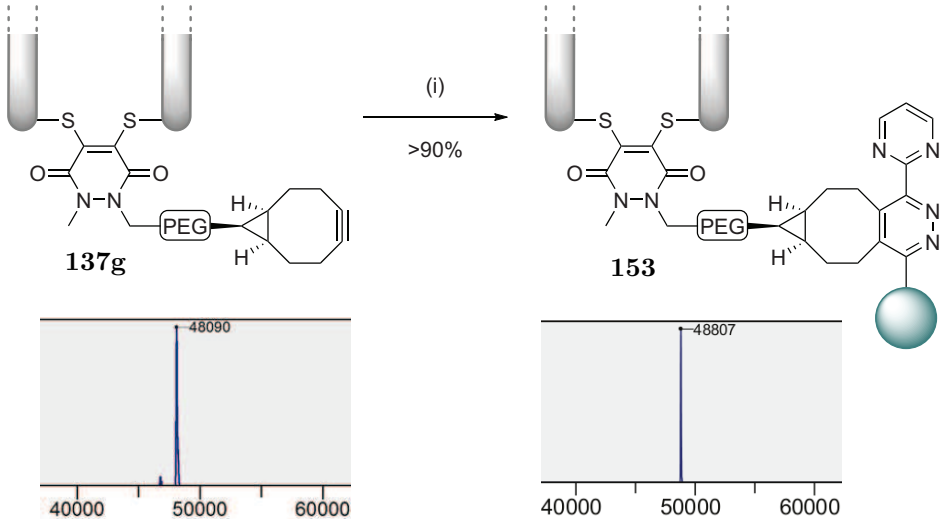

SCHEME 4.4: Modification of Fab_{Her}-BCN-Mestra **137g** with tetrazine **152a**. *Reagents and Conditions*: (i) Tetrazine **152a**, DMSO, PBS pH 7.0, rt, 1 h.

Unfortunately, upon repeating this reaction after storage of the stock solution of BCN-Mestra PD **121** kept at −20 °C in DMSO for a week, only a partial conversion to **153** was observed. An additional fragment which mass corresponds to Fab_{Her}-BCN-Mestra **137g** + *ca.* 32 was observed by LCMS, which indicates degradation of the BCN residue overtime upon storage (Scheme 4.5).

This side product has been previously observed and it was suggested that over time, the small amount of molecular oxygen present in the stock solution would react with the

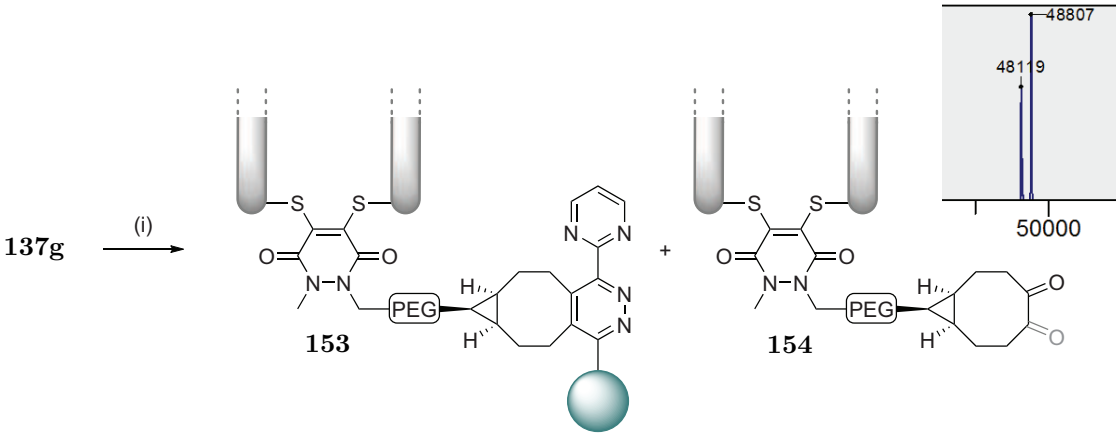

SCHEME 4.5: Modification of degraded Fab_{Her}-BCN-Mestra **137g** with tetrazine **152a**. *Reagents and Conditions*: (i) Tetrazine **152a**, DMSO, PBS pH 7.0, rt, 1 h.

strained alkyne to give the corresponding cyclooctanedione.[223–225] Although an LC-MS analysis with increased resolution would be needed to confirm this hypothesis, this could explain the lack of reactivity with a highly reactive tetrazine.

4.3.2 SPAAC — Cyclooctynes

4.3.2.1 Bicyclo[6.1.0]nonyne (BCN)

Fab_{Her}-BCN-Mestra **137g** was also used as the "clickable" protein model with azide $NH_2-PEG_4-N_3$ **119** as the azide model. Similarly, conditions for SPAAC were optimised. It was found that incubation for 3 h at room temperature of 5 equivalents of azide **119** was sufficient to convert **137g** to clicked Fab_{Her} **155** in near quantitative yield and in high purity. Here again, the buffer used and pH (6.2 – 8.0) were found to have no measurable impact on the reaction. Unfortunately, and as expected, the same degradation pathway was observed and a mixture of products was obtained when the stock solution of BCN-Mestra PD **121** was not prepared freshly before use (Scheme 4.6).

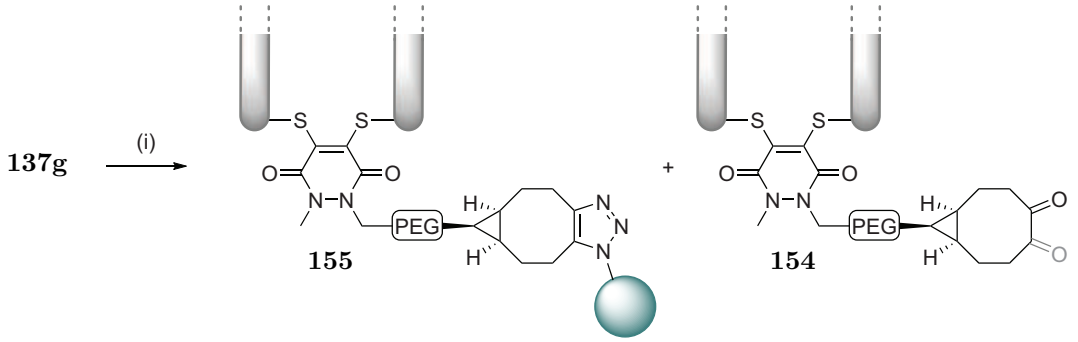

SCHEME 4.6: Modification of degraded Fab_{Her}-BCN-Mestra **137g** with azide **119**. *Reagents and Conditions*: (i) Azide **119**, DMSO, PBS pH 7.0, rt, 3 h.

4.3.2.2 Monofluorosubstituted Cyclooctyne (MFCO)

In view of the limitations of BCN-base PDs and in spite of the slower kinetics associated with MFCOs, it was decided to focus on Solastra PD **85** as the bridging platform. It was hypothesised that the lower reativity of **85** would limit its degradation in organic solvent and therefore allow for more consistent results between repeats.

Thus, click reactions on the strained alkyne **137e** were also conducted in various buffers, at different pHs, and at various temperatures using model azide **119**. In the presence of 5 equivalents of "clickable" molecule, the conversion of Fab_{Her}-Solastra **137e** was complete in 6 h at room temperature (Scheme 4.7). The pHs and buffers tested (PBS pH 6.8 and BBS pH 8) did not have a measurable impact on the outcome or the rate of the reaction.

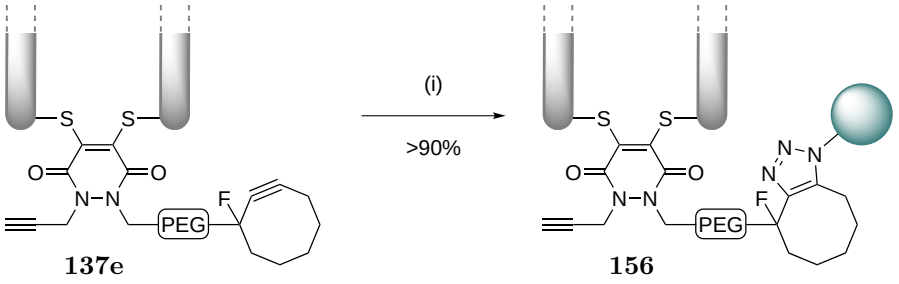

SCHEME 4.7: Modification of Fab_{Her}-Solastra **137e** with azide **119**. *Reagents and Conditions*: (i) Azide **119**, DMF, PBS pH 7.0, rt, 1 h.

Gratifyingly, PD **85** was stable in DMF at −20 °C over an extended period of time. Indeed, repeating the reaction with the same stock solution of bridging molecule two months later resulted in the same outcome (Figure 4.2).

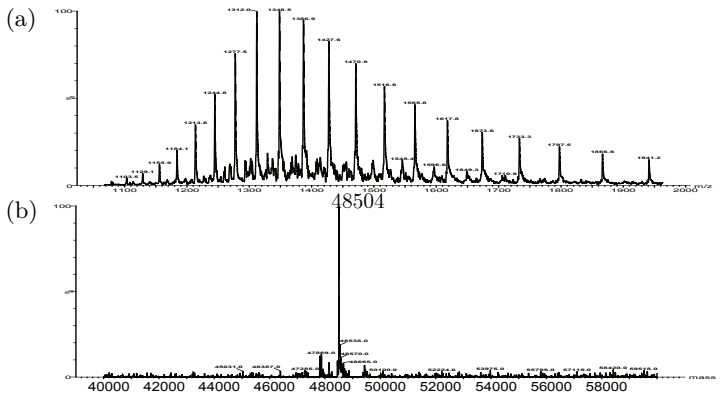

FIGURE 4.2: (a) Non-deconvoluted and (b) deconvoluted LCMS data for Fab_{Her}-Solastra-PEG_4 **137e** after 2 months of storage of **85** in DMF.

4.4 Copper-catalysed functionalisation

Two ligands (TCEP and THPTA) in acetate, phosphate and borate buffers, at different pHs (5 – 8.5) and at various temperatures (4 °C, 21 °C or 37 °C) were evaluated for the CuAAC of the model PEG_4-azide **119** on alkyne Fab_{Her}-Alkac **137d**. It was found that 500 µM of THPTA (*ca.* 10 eq.), 100 µM of $CuSO_4$ (*ca.* 2 eq.), and 5 mM sodium ascorbate were sufficient for the reaction to reach completion at room temperature within 1 h when at least 5 equivalents of "clickable" molecule were used (Scheme 4.8). When TCEP was used as a ligand or when no ligand was used, no reaction was observed. The pH did not have a measurable impact on the outcome or the rate of the reaction and the only requirement for the buffer was the strict absence of EDTA; indeed, EDTA would inhibit the reaction by complexing copper.

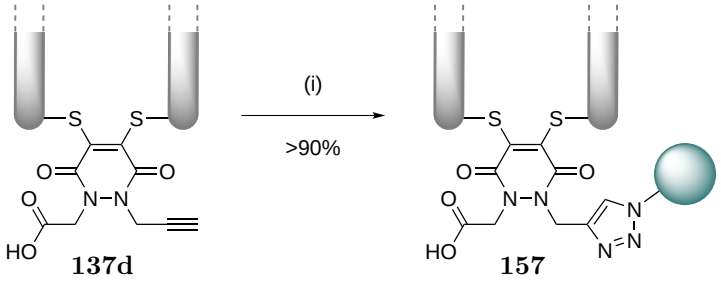

SCHEME 4.8: Modification of Fab_{Her}-Alkac **137d** with azide **119**.
Reagents and Conditions: (i) Azide **119**, $CuSO_4$, THPTA, sodium ascorbate, PBS pH 7.0, rt, 1 h.

Alternatively, a protocol where Cu(I)Br was used instead of generating the Cu(I) source from $CuSO_4$/sodium ascorbate, was developed for proteins where the Cu(II)-based protocol failed to result in full conversion (*vide infra*, section 5.4.4, page 94).

4.5 Dually functionalised proteins — Proof of concept

With both the conditions for CuAAC and SPAAC in hand, it was decided to prepare a dually functionalised Fab_{Her}. As modification *via* Azal PD **61**, Pazal PD **69** and Solastra PD **85** (*vide supra*, Figure 2.3, page 51) proved to be equally facile, at this juncture it was decided to proceed with Solastra PD **85** only owing to the commercial availability of a large library of modalities bearing an azide handle.

Thus, starting from Fab_{Her}-Solastra **137e**, PEG_4-azide **119** and sulfo-Cy5 **145** were sequentially clicked onto the conjugate using SPAAC to give Fab_{Her}-Solastra-PEG_4 **156** quantitatively, followed by CuAAC with sulfo-Cy5 **145** resulting in dually modified Fab_{Her}-Solastra-PEG_4-Cy5 **158**. The reaction was followed by LCMS and complete and clean conversion of Fab_{Her}-Solastra **137e** to dually functionalised Fab_{Her}-Solastra-PEG_4-Cy5 **158** was observed (Scheme 4.9).

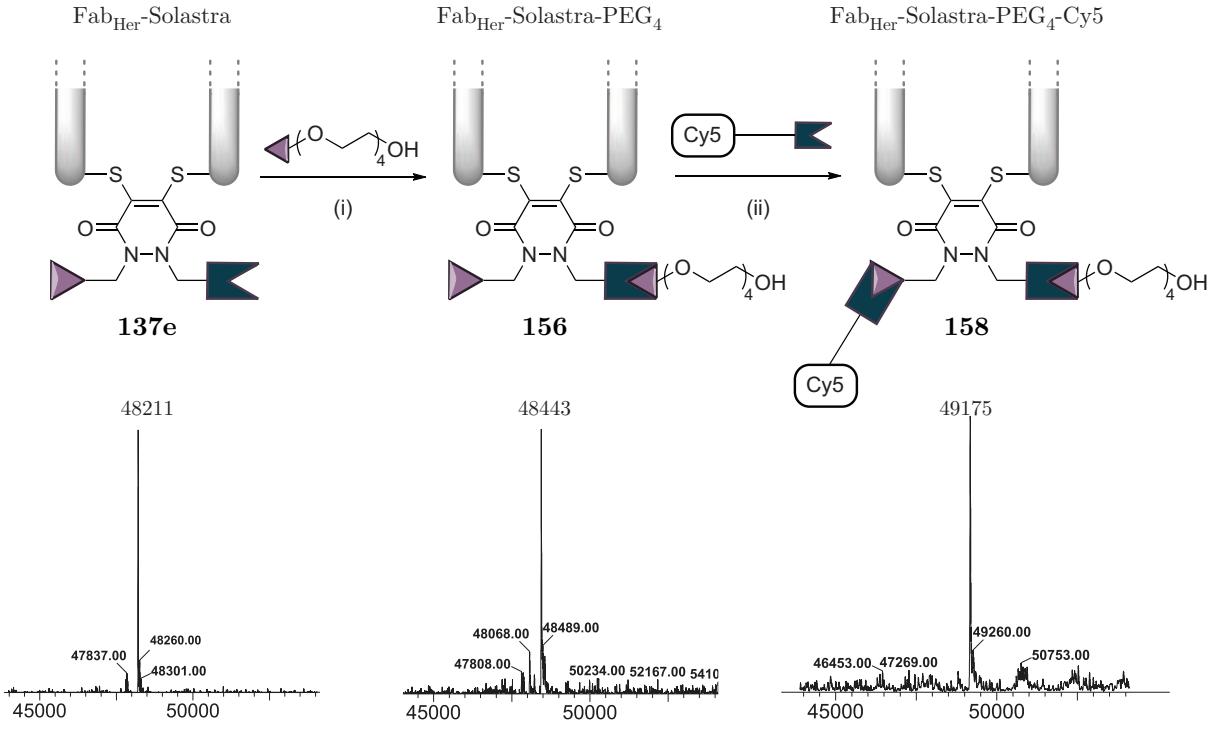

Scheme 4.9: Dual functionalisation of Fab-pyridazinedione conjugate **137c**. *Reagents and Conditions*: SPAAC (i) Azide **64**, BBS pH 8.0, rt, 6 h; CuAAC (ii) Cy5 derivative **145**, $CuSO_4$, THPTA, sodium ascorbate, PB pH 7.0, rt, 1 h.

4.5.1 Antibody Fragment–Drug Conjugate (FDC)

A dually modified Fab with both a half-life extension moiety and a cytotoxic agent is a highly valuable target (*vide supra*, sections 1.4, page 11 and 4.1, page 74); the construction of such a conjugate was therefore of interest. As such, a clinically relevant FDC preparation was attempted.

Fab_{Her}-Solastra **137e** was sequentially modified with PEG_{20k} **144** by SPAAC followed by CuAAC with doxorubicin derivative **147**. Gratifyingly, the final conjugate was analysed by UV-Vis and SDS-PAGE and revealed clean conversion to the desired product Fab_{Her}-Solastra-PEG_{20k}-Dox **159** (Figure 4.3). This further demonstrates the flexibility of this chemistry to allow for the facile attachment of large constructs such as a PEG_{20k} **144** moiety.

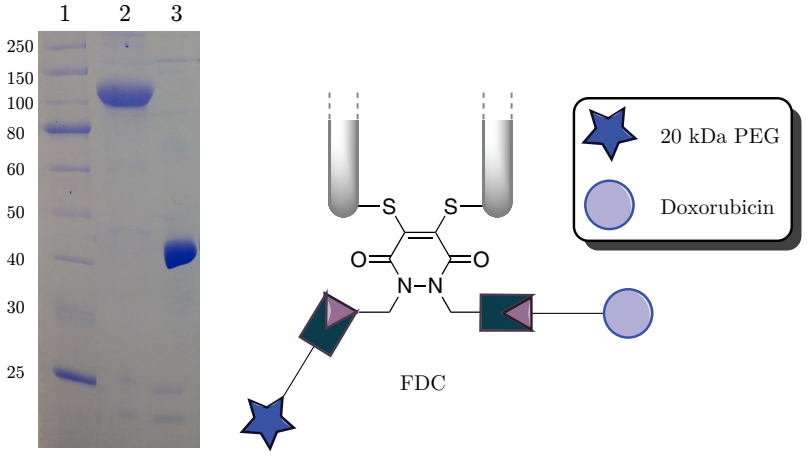

FIGURE 4.3: SDS-PAGE analysis of Fab_{Her}-PEG_{20k}-Dox **159**. Lane 1 – Ladder; 2 – FDC; 3 – Fab_{Her}.

4.5.2 Antibody–drug conjugate — Theranostics

A theranostic based on a dually modified antibody with both a fluorophore and a cytotoxic agent is also a highly valuable target (*vide supra*, section 4.1, page 74). As a proof of concept, the preparation of a theranostic based on doxorubicin and Cy5 was attempted.

Her-Solastra **134b** was sequentially modified with doxorubicin derivative **147** by SPAAC followed by CuAAC with sulfo-Cy5 **145**. As the four components of the reaction (*i.e.* the antibody, the PD moiety, doxorubicin and sulfo-Cy5) have a maximum of absorption at four distinct wavelengths (λ_{max} = 280, 340, 495 and 646 nm respectively), the reaction

could easily be followed by UV-Vis and the loading of each payload could be measured at every step of the protocol (*vide infra*, appendix A.1.8, page 108). Gratifyingly, the analysis by UV-Vis and SDS-PAGE of the final conjugate revealed clean conversion to the desired product Her-Solastra-Dox-Cy5 **161**. UV-Vis also revealed a drug loading of *ca.* 4 per antibody and a fluorophore loading of *ca.* 4 per antibody consistent with modification of the four disulfides of the antibody with complete conversion of the "clickable" handles to their corresponding module (Scheme 4.10).

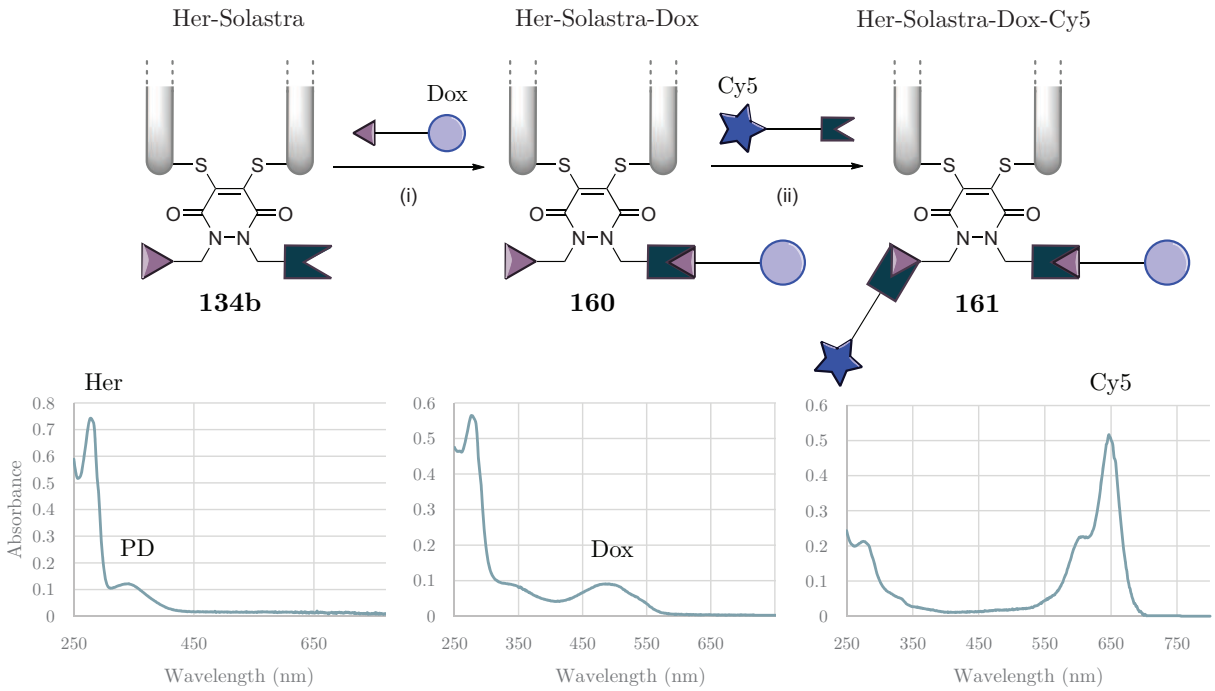

SCHEME 4.10: Dual functionalisation of Her-Solastra **134b** with **147** and **145**. *Reagents and Conditions*: SPAAC (i) Doxorubicin derivative **147**, BBS pH 8.0, rt, 6 h; CuAAC (ii) Cy5 derivative **145**, $CuSO_4$, THPTA, ascorbate, PB pH 7.0, rt, 1 h.

4.6 Conclusion

Both Copper(I)-catalyzed Azide–Alkyne Cycloaddition (CuAAC) and Strain-Promoted Cycloaddition protocols were developed and optimised for the generation of dually functionalised constructs based on native antibody and antibody fragment. By clicking the reactive handles on the PD conjugate with a series of "clickable" PEG-azide (*e.g.* PEG_4 **64** and PEG_{20k} **144**), fluorophores and/or cytotoxic construct (*e.g.* doxorubicin-azide **147**), functionalised proteins were prepared in a selective, rapid and efficient manner. As the functionalisation *via* this dual-click approach is distal from the antigen-binding site of the proteins modified, it was envisaged that the impact on the activity would be minimal, therefore allowing for a plethora of applications.

Chapter 5

Activity and Stability of PD-Conjugates

5.1 Introduction

The most popular strategy for labelling the thiol moiety of cysteine residues is by alkylation with maleimides to form thioether-succinimides.[38–40,198] However, it has recently come to light that such an appendage is suboptimal, owing to issues of hydrolysis and thiol exchange with reactive thiols in the blood (*e.g.* albumin).[112–114] Indeed, the succinimide **169** obtained upon reaction can revert back to maleimide and free thiol **168** *via* a retro-Michael pathway (Figure 5.1).

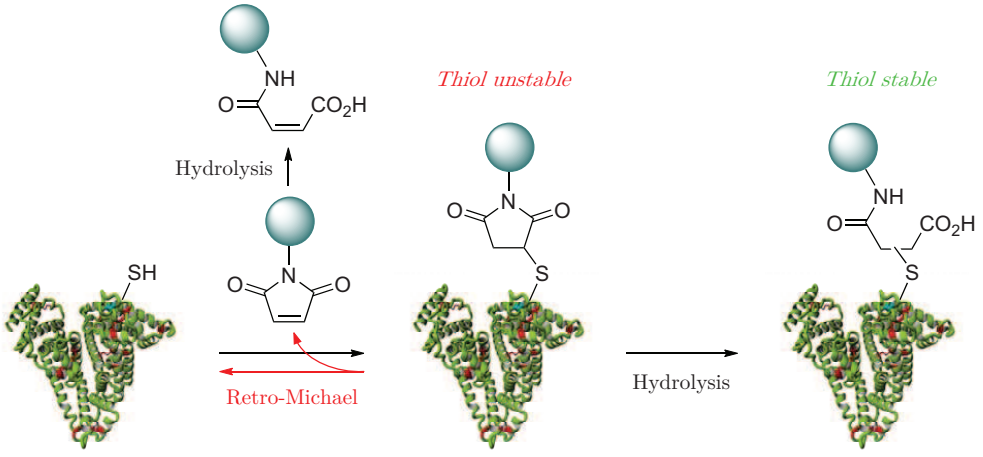

FIGURE 5.1: Albumin reaction with maleimide.

The lack of control over these reactions poses thorny reliability issues when it comes to the development of therapeutically relevant conjugates as the construct may not reach the target intact or as expected. This has major implications for therapeutics that employ a maleimide motif to functionalise a protein thiol for *in vivo* applications. For example, in ADCs, the use of maleimides to attach cytotoxic drugs to an antibody is not ideal as thiol exchange onto human serum albumin in the blood can result in lowered activity and/or off-target toxicity.[113,226,227] Although recent advances have been made in this area through the use of hydrolysed maleimides and succinimides,[113–117] a strong drive to develop novel reagents for reliable, chemoselective, stable and irreversible thiol labelling remains, particularly for the construction of ADCs.[228,229]

Indeed, the ADC is exposed to different conditions whilst circulating in the blood. The mode of action at cellular or molecular level is complex, with each step adding an additional layer of difficulty. Thus, several factors, activity and stability-related, are key when designing an ADC:[230]

- **Circulation**. The ADC must behave like a naked antibody when circulating in the plasma. In particular, the linker must be stable in the bloodstream to limit damage to healthy tissue. Decomposition or decay would release the cytotoxin before being delivered to the target site and result in off-site toxicity.
- **Antigen Binding**. It is necessary that the conjugated antibody retains high immunoaffinity. Ideally, attaching the cytotoxic compound to the antibody should not disturb its binding specificity.
- **Internalisation**. A sufficient intracellular concentration of the drug must be achieved. This is challenging because antigen targets on cell surfaces are often present in limited numbers and the internalisation process for antigen-antibody complexes is frequently inefficient.
- **Cytotoxicity**. The inherent potency of the released drug must be sufficient to kill the tumor cell, even at low concentration. To achieve significant cytotoxicity, use of very potent drugs with subnanomolar IC_{50} (as free drug) becomes necessary. It has been shown that compounds found to be too toxic when tested as a stand-alone chemotherapy agent are suitable candidates for ADC payloads. These toxins can be 100 to 1000 times more cytotoxic than traditional anticancer agents.

It has also been shown that for most ADCs, overall efficacy is hindered by linker instability[79,231–234] and compositional heterogeneity.[89,91,232–234] In this context, the selectivity, stability and activity of the PD-based conjugates were investigated.

5.2 Selectivity

To demonstrate the selectivity towards thiols of PDs on a small molecule model, monobromo Diet PD **103** and dibromo Diet PD **104** were incubated with lysine. After 72 h of incubation at 20 °C in a THF/BBS pH 8.0 mixture with a stoichiometric amount of the amino acid, the reaction was analysed and no trace of addition product was observed thus confirming the exquisite selectivity of PDs towards thiols over amines (Scheme 5.1)

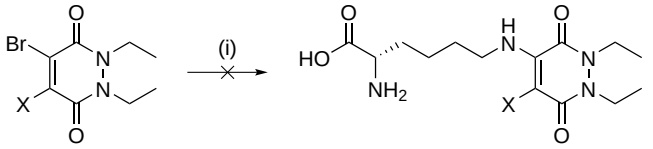

SCHEME 5.1: *Reagents and Conditions*: (i) L-lysine, THF/BBS pH 8.0, 20 °C, 72 h.

5.3 Stability of dibromo PD-based conjugates

5.3.1 Hydrolytic stability in buffered solutions

Fab_{Her}-Diet **131** was used as a model to assess the hydrolytic stability of the PD constructs. It was buffer-exchanged into solution with pHs of 3.1 and 9.0 and the conjugate was incubated at 37 °C for 24 h. To assess its hydrolytic stability over an extended period of time, Fab_{Her}-Diet **131** was also incubated in PBS at 4 °C for 8 months. Gratifyingly, LCMS and SDS-PAGE analysis revealed that the conjugate had exceptional hydrolytic stability as no trace of hydrolysis was observed for the range of conditions tested (Figure 5.2).

Similarly, Fab_{Her}-PEG_{20k}-Dox **159** and Her-Solastra-Dox-Cy5 **161** were subjected to the forcing conditions described above for Fab_{Her}-Diet **131**. SDS-PAGE analysis revealed that the conjugates showed no degradation for the range of conditions tested (Figure 5.3).

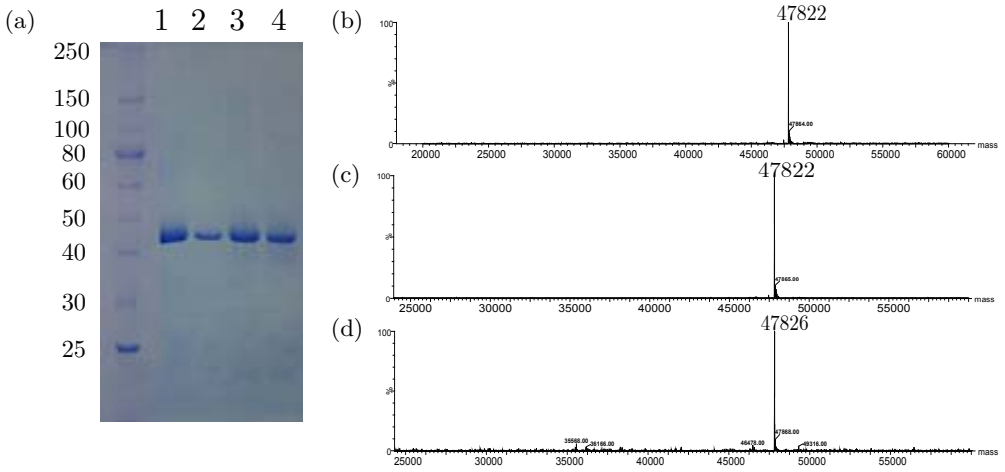

FIGURE 5.2: (a) SDS-PAGE of Fab_{Her}-Diet **131**. Lane 1 – Fab_{Her}-Diet **131**; 2 – After 8 months of storage at 4 °C in PBS; 3 – After 24 h at 37 °C in buffer pH 3.1; 4 – After 24 h at 37 °C in buffer pH 9.0; (b) Deconvoluted LCMS data for lane 2; (c) Deconvoluted LCMS data for lane 3; (d) Deconvoluted LCMS data for lane 4.

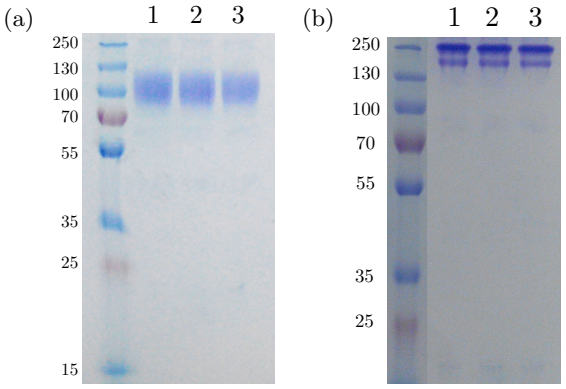

FIGURE 5.3: (a) SDS-PAGE analysis of Fab_{Her}-PEG_{20k}-Dox **159**. Lane 1 – after two months of storage at 4 °C in PBS; 2 – After 24 h at 37 °C in buffer pH 3.1; 3 – After 24 h at 37 °C in buffer pH 9.0; (b) SDS-PAGE analysis of Her-Solastra-Dox-Cy5 **161**. Lane 1 – after two months of storage at 4 °C in PBS; 2 – After 24 h at 37 °C in buffer pH 3.1; 3 – After 24 h at 37 °C in buffer pH 9.0.

5.3.2 Stability towards thiol exchange

Dibromopyridazinediones were also tested for potential thiol exchange with glutathione (GSH), a small molecule present at an average concentration of 5 µM in blood plasma and of 1 – 10 mM in the cytoplasm of mammalian cells.[235]

To demonstrate stability in blood plasma, Fab_{Her}-Diet **131** was buffer exchanged into a simulated body fluid solution (SBF)[236] by repeated diafiltration into fresh buffer. Then, human serum albumin (HSA) (final concentration 600 µM) and GSH (final concentration 20 µM) were added. The solution was incubated at 37 °C for 7 days. The reaction was monitored by SDS-PAGE (Figure 5.4) and the analysis revealed no trace of reaction of

conjugate **131** with GSH (expected resulting mass *ca.* 23 kDa) or with HSA (expected resulting mass *ca.* 90 kDa).

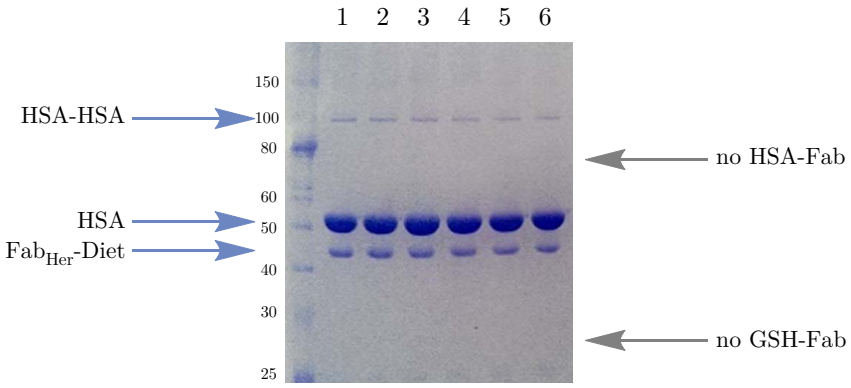

FIGURE 5.4: SDS-PAGE gel following incubation of Fab$_{Her}$-Diet **131** in blood plasma mimicking conditions for 0, 1, 2, 3, 5 and 7 days (lanes 1 – 6 respectively).

Similarly, Fab$_{Her}$-PEG$_{20k}$-Dox **159** and Her-Solastra-Dox-Cy5 **161** were incubated in a SBF for 7 days. SDS-PAGE analysis revealed that the conjugates showed no trace of unwanted reaction with GSH or HSA (Figure 5.5).

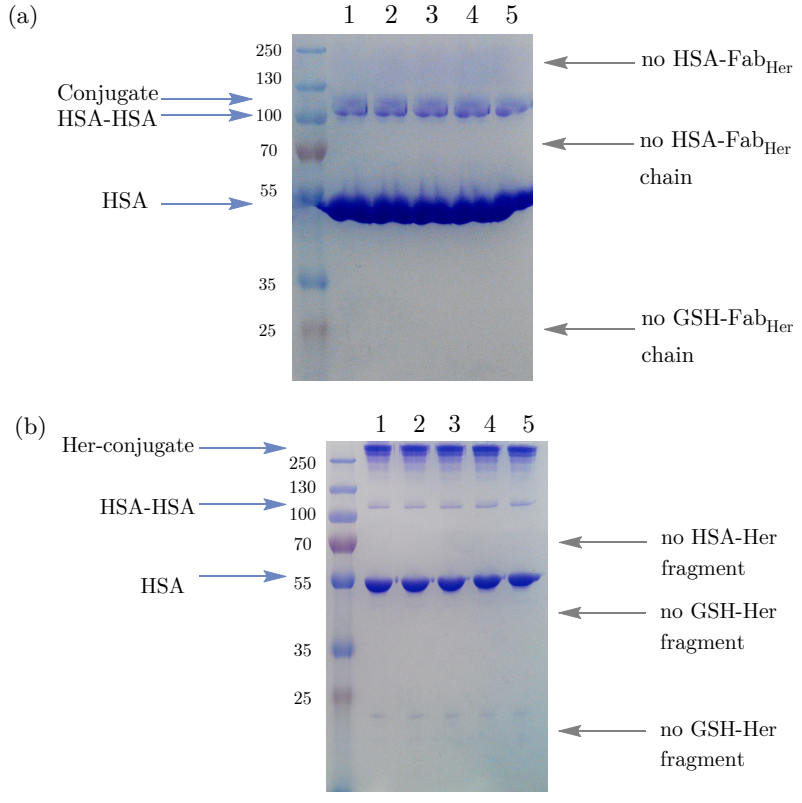

FIGURE 5.5: (a) SDS-PAGE gel following incubation of Fab$_{Her}$-PEG$_{20k}$-Dox **159** in blood plasma mimicking conditions for 0, 1, 3, 5 and 7 days (lanes 1 – 5 respectively); (b) Her-Solastra-Dox-Cy5 **161** in blood plasma mimicking conditions for 0, 1, 3, 5 and 7 days (lanes 1 – 5 respectively).

Interestingly, when Fab_{Her}-Diet **131** was incubated at 37 °C in the presence of a intracellular relevant concentration of thiol *e.g.* 1 mM GSH, LCMS analysis showed no trace of GSH-exchange after 4 h but when incubated for a further 12 h, Fab_{Her}-Diet **131** reverted back to unmodified Fab_{Her} **127**. This feature can potentially be used to form the core of novel prodrug systems where the drug in only released when internalised inside a diseased cell.[52,57]

5.4 From reversible to irreversible cysteine modification

During the course of developing bromopyridazinediones for *reversible* cysteine conjugation (*vide supra*, section 5.3.2, page 88), the prospect of pyridazinediones (PDs) as *irreversible* cysteine functionalisation reagents was explored. Previously, Chudasama *et al.* showed that if one of the nitrogen atoms on the PD core is unsubstituted, the molecule does not react with thiols at physiological pH (or higher).[52] It was postulated that this lack of reactivity is a consequence of such a structure existing as its enol-like tautomer, which is likely to be significantly deprotonated under physiological pH (or higher). Indeed, the reported pK_a of 1-methyl-3,6-(1*H*,2*H*)-pyridazinedione is *ca.* 5.7 in H_2O and the calculated pK_a of its thioether analogue, 1-methyl-4-(methylthio)-3,6-(1*H*,2*H*)-pyridazinedione is *ca.* 5.9.[237–239] Thiol reactivity will therefore be greatly reduced as the electrophilicity of the resulting PD-core moiety will be tuned down considerably. As such, the development of a strategy that would enable the generation of a mono-alkylated PD species post-conjugation to a cysteine thiol to afford a thiol-stable construct was set about (Figure 5.6).

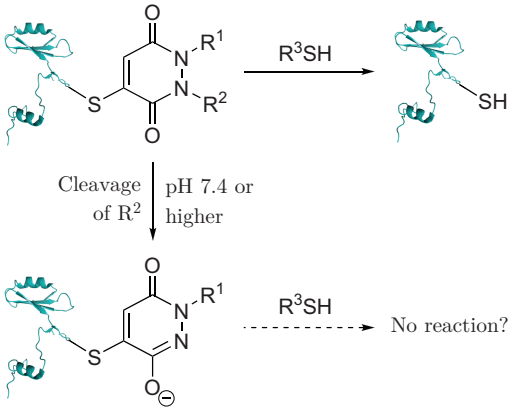

FIGURE 5.6: General strategy towards irreversible cysteine modification.

5.4.1 Strategy

The appraisal of this strategy began with the reaction of model protein GFP_{S147C} **140** with PDs **102** and **173** to confirm observations by Chudasama *et al.* when using protein $Grb2_{L111C}$ **138** (Scheme 5.2).[52,199] These results were consistent with previously reported work and confirmed that a mono-alkylated PD is unreactive to thiols (or other nucleophilic functional groups on amino acid side-chains).

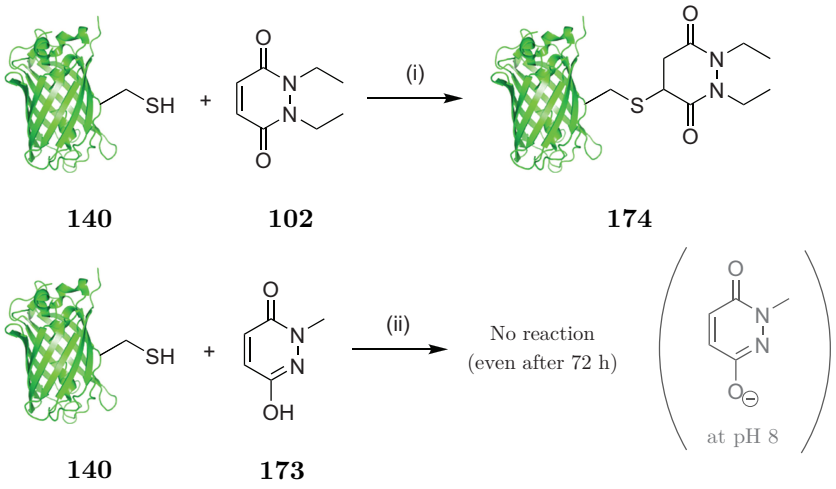

SCHEME 5.2: Incubation of GFP_{S147C} **140** with PD **102** and monoalkylated PD **173**. *Reagents and Conditions*: (i) PBS pH 8.0, 37 °C, 1 h; (ii) PBS pH 8.0, 37 °C, 72 h.

These initial studies paved the way to appraise the use of a novel strategy to develop irreversible pyridazinedione conjugates (Figure 5.6). To achieve this goal, a selective method for cleavage of R_2 from the PD core was needed. Although many strategies could have been applied, it was decided, at this juncture, to take the opportunity to develop a novel, mild and simple method based on an azide trigger.

The desire to use an azide-based cleavable handle originates from the bioorthogonality of the azide functional group. Taking inspiration from the well-documented work on *p*-aminobenzyloxycarbonyl (PABC) linkers,[240] a *p*-azidobenzyl cleavage strategy was developed (Scheme 5.3).

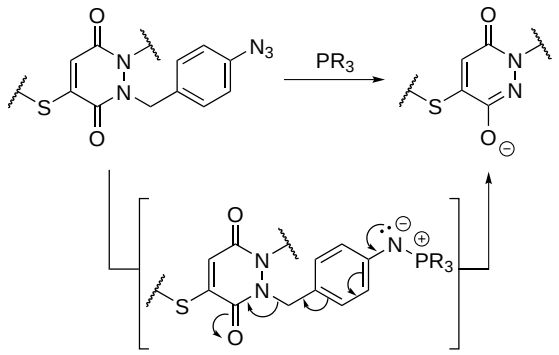

SCHEME 5.3: Use of a *p*-azidobenzyl cleavage strategy to generate a PD-based thiol-stable conjugate.

5.4.2 Small molecule study

Initially the *p*-azidobenzyl cleavage strategy was evaluated in a small molecule study through the use of cysteine derivative **175**. The stability of cysteine derivative **175** was first appraised. It was prepared in high yield by reacting *N*-(*tert*-butoxycarbonyl)-L-cysteine methyl ester **186** with mBr-Azal PD **100** in the presence of NEt_3. Cysteine derivative **175** was then incubated with 15 equivalents of 1-hexanethiol in THF/PBS buffer (pH 7.4) which led to thiol exchange and yielded PD derivative **176** in 71% yield (Scheme 5.4).

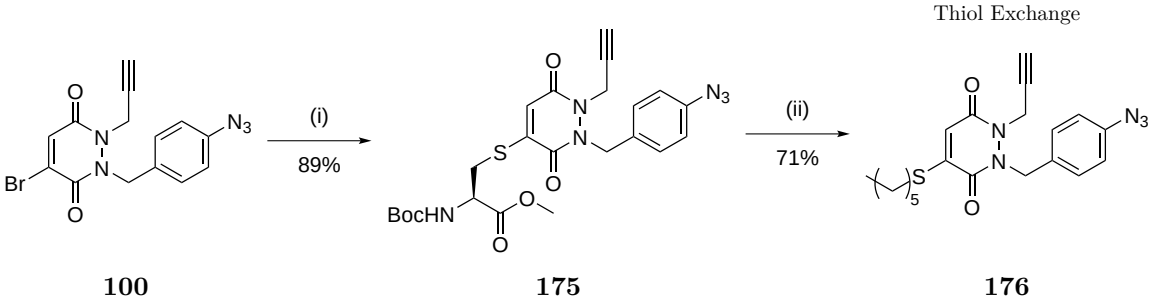

SCHEME 5.4: *Reagents and Conditions*: (i) Thiol **186**, CH_2Cl_2, rt, 2 h; (ii) 1-Hexanethiol, THF/PBS at pH 7.4, rt, 72 h.

The cleavage strategy was then assessed by treating PD **175** with TCEP. Gratifyingly, this led to clean conversion to derivative **177**, thus providing proof of concept for this novel cleavage strategy. Moreover, incubation of derivative **177** with 15 equivalents of 1-hexanethiol in THF/PBS buffer (pH 7.4) did not lead to thiol exchange (Scheme 5.5).

This provided support for the hypothesis of a mono-alkylatedPD being thiol unreactive under physiological pH or higher (*vide supra*, Scheme 5.2, page 91).

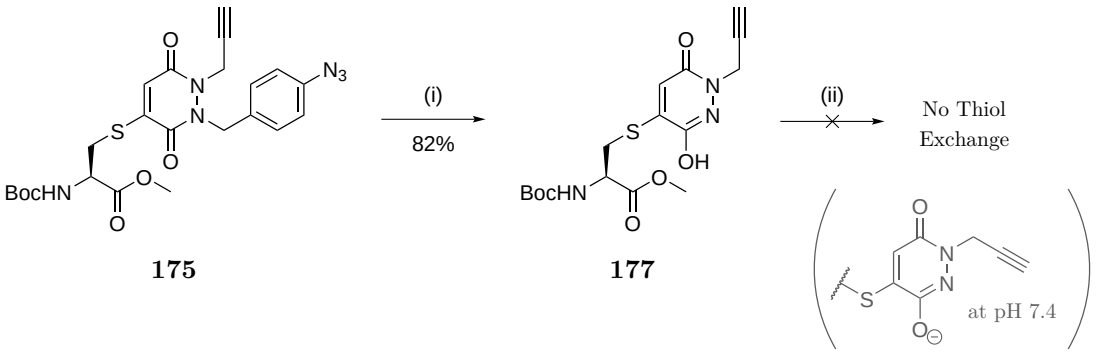

175 **177**

SCHEME 5.5: *Reagents and Conditions*: (i) TCEP, DMF, rt, 2 h; (ii) 1-Hexanethiol, THF/PBS at pH 7.4, rt, 72 h.

5.4.3 Protein study

Following these encouraging results on a small molecule study, the strategy was appraised on model protein GFP_{S147C} **140**. Initially, GFP_{S147C} **140** was incubated with mBr-Azal PD **100** in PBS (pH 8.0) for 1 h at 37 °C. This proceeded with complete conversion and afforded GFP-Azal **178** (Scheme 5.6). Next, the TCEP cleavage strategy was applied by incubating this derivative with 10 equivalents of TCEP in PBS pH 8.0. Satisfyingly, clean conversion to conjugate **179** was observed, which is consistent with the small molecule study results (Scheme 5.6 and Figure 5.7).

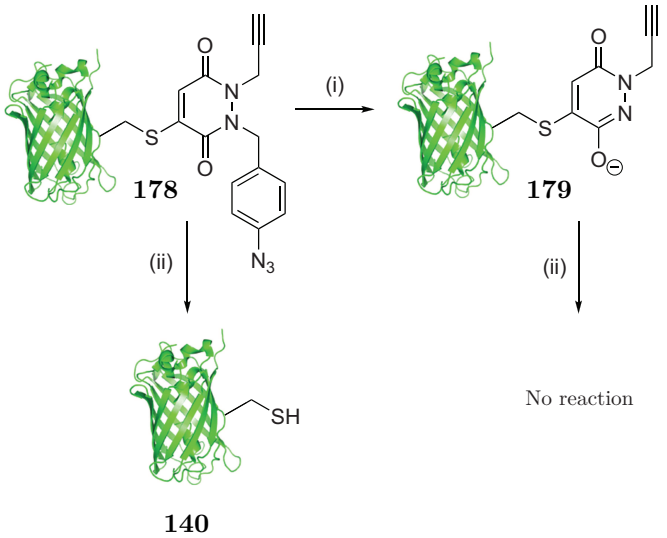

178 **179** **140**

SCHEME 5.6: Appraisal of cleavage strategy on GFP-Azal **178**.
Reagents and Conditions: (i) TCEP, PBS pH 8.0, 37 °C, 1.5 h; (ii) GSH, PBS at pH 7.4, 37 °C, 72 h.

Having established that this cleavage strategy is applicable on a protein, the thiol stability of GFP-Azal **178** and conjugate **179** was then compared by incubation with GSH (0.5 mM) for 72 h in PBS pH 7.4 and at 37 °C. Gratifyingly, GFP-derivative **179**

was completely stable under the reaction conditions, whereas derivative **178** showed complete thiol exchange with glutathione (Scheme 5.6).

It is also noteworthy that analysis by LCMS revealed that no hydrolysis occurred under these conditions, which is consistent with previous observations on the PD core being hydrolytically stable (Figure 5.7). This therefore validated the cleavage strategy on a model protein scaffold.

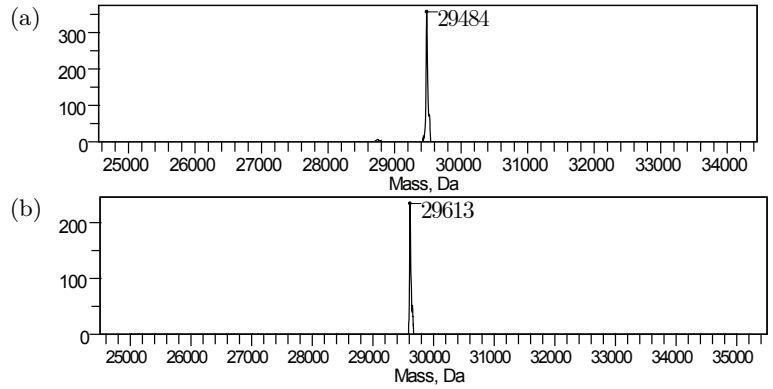

FIGURE 5.7: (a) Deconvoluted LCMS data for GFP-Azal **178**; (b) Deconvoluted LCMS data for alkyne **179**.

5.4.4 Functionalisation

The use of an alkyne handle, which is retained post *p*-azidobenzyl cleavage, allows for the resulting construct to be readily functionalised by CuAAC. Thus, protein scaffold **179** was functionalised by the use of click chemistry. The optimised conditions previously developed were trialled using benzyl azide as the model azide (*vide supra*, section 4.4, page 81). The most promising conditions were the use of Cu(I)Br as copper source with THPTA as ligand. These conditions gave complete conversion of starting material alkyne **179** to triazole conjugate **180a**. Moreover, these conditions allowed for clean reaction of the alkyne derivative with dansyl azide **162** and sulfo-Cy5 **145** to afford **180b** and **180c**, respectively (Scheme 5.7 and Figure 5.8). This strategy also highlights the versatility of the PD platform with a facile shift from reversible to irreversible constructs achieved under mild conditions.

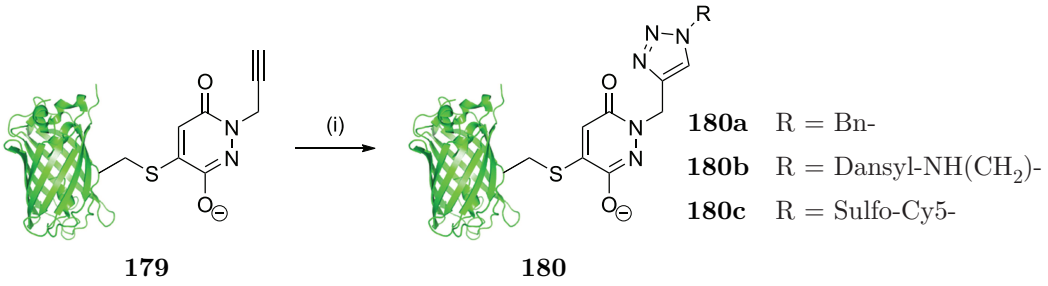

179 **180**

SCHEME 5.7: Functionalisation of alkyne **179**.
Reagents and Conditions: (i) Cu(I)Br/MeCN, THPTA, PBS pH 8.0, 37 °C, 4 h.

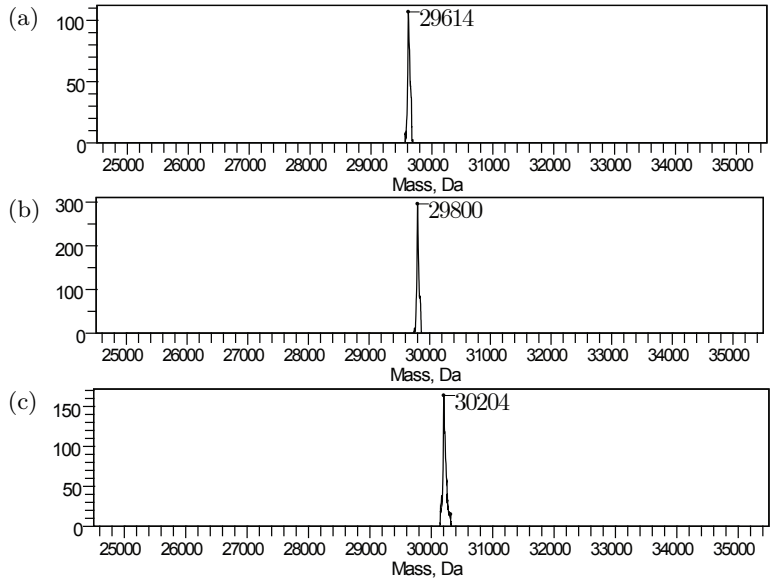

FIGURE 5.8: (a) Deconvoluted LCMS data for benzyl derivative **180a**;
(b) Deconvoluted LCMS data for dansyl derivative **180b**;
(c) Deconvoluted LCMS data for Cy5 derivative **180c**.

5.5 Activity

5.5.1 Binding affinity: ELISA

The impact on antibody/antigen binding of conjugating PDs to Fab_{Her} **127** was first appraised on model Fab_{Her}-Diet **131**. It was rationalised that, as the interchain disulfide is distal from the antigen-binding site of the Fab fragment, this impact should be minimal (*vide supra*, Figure 1.2, page 10). To appraise it, the binding profile of Fab_{Her}-Diet **131** around the reported value of dissociation constant ($K_D \simeq 5$ nM) was evaluated against unmodified Fab_{Her} **127** using ELISA.[241] Encouragingly, comparable antigen binding was observed across the two constructs with K_D values for Fab_{Her} **127** and Fab_{Her}-Diet **131** of 5.2 ± 0.5 nM and 6.1 ± 0.6 nM, respectively; even though a broader range of concentration could be trialled to measure the K_D of the constructs prepared with better accuracy, this

gives good indication that the conjugation does not affect the affinity of the modified fragment (Figure 5.9).

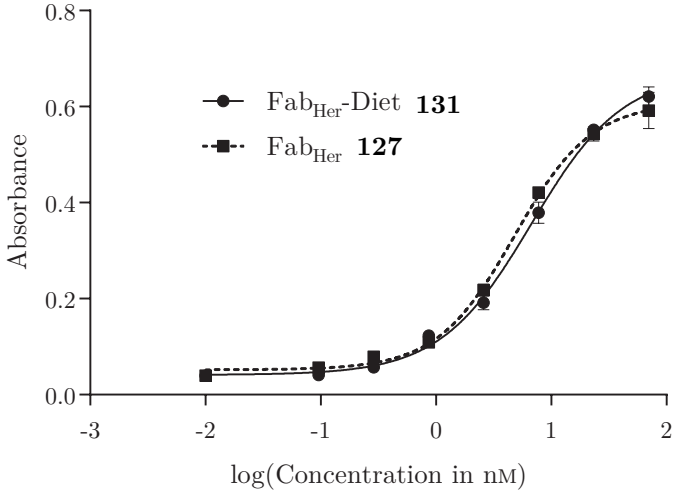

FIGURE 5.9: ELISA analysis of Fab$_{Her}$ **127** and Fab$_{Her}$-Diet **131** binding to the HER2.

The impact of the dual-click sequence on both dually modified fragment Fab$_{Her}$-Solastra-PEG$_{20k}$-Dox **159** and full antibody Her-Solastra-Dox-Cy5 **161** was then evaluated (Figure 5.10). As expected, no significant difference was observed between the respective binding activities across the four constructs with measured K_D of 7.9 ± 0.8 nM and 8.2 ± 0.8 nM for Fab$_{Her}$ **127** and Fab$_{Her}$-Solastra-PEG$_{20k}$-Dox **159** respectively, and 6.3 ± 0.7 nM and 7.7 ± 0.7 nM for trastuzumab **19** and Her-Solastra-Dox-Cy5 **161** respectively; this again indicates that neither the conjugation nor the dual functionalisation affect the affinity of the PD-modified conjugates.

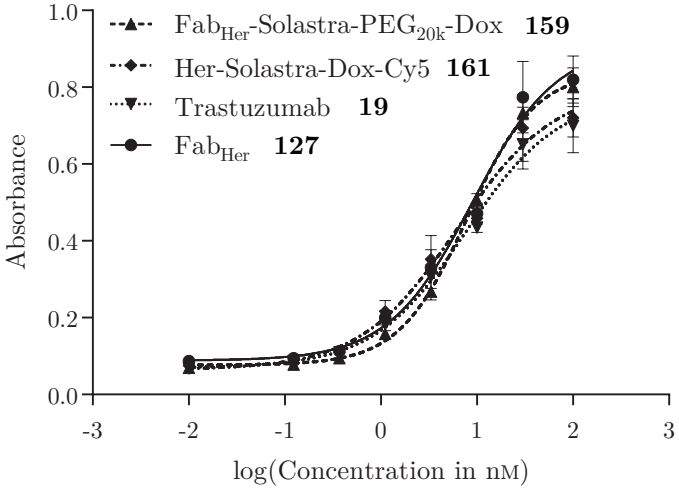

FIGURE 5.10: ELISA analysis of Fab$_{Her}$ **127**, Fab$_{Her}$-Solastra-PEG$_{20k}$-Dox **159**, trastuzumab **19** and Her-Solastra-Dox-Cy5 **161** binding to the HER2.

5.5.2 Internalisation study

The effect of the conjugation chemistry on the internalising properties of trastuzumab **19** and Fab_{Her} **127** was next appraised. For this purpose, Fab_{Her}-Solastra **137e** and Her-Solastra **134b** were directly conjugated to an azide derivative of AlexaFluor488 *via* SPAAC to form Fab_{Her}-Solastra-AlexaFluor488 **181** and Her-Solastra-AlexaFluor488 **182** respectively (Figure 5.11).

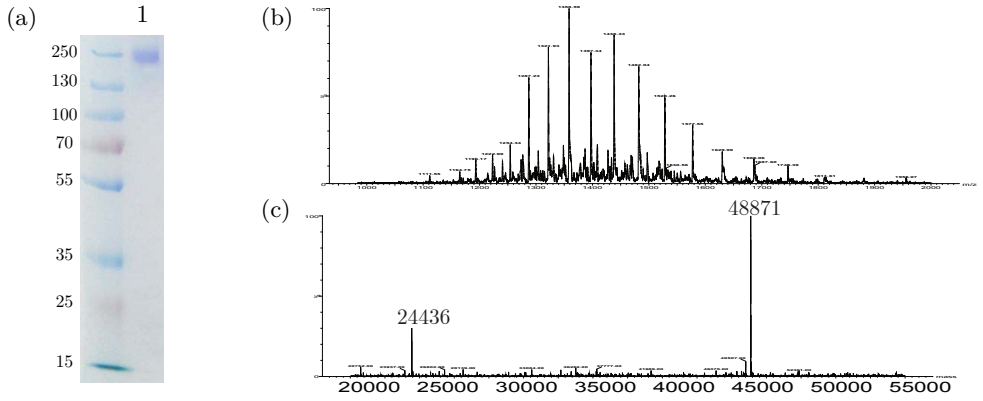

FIGURE 5.11: (a) SDS-PAGE of Her-Solastra-AlexaFluor488 **182**. Lane 1 – Her-Solastra-AlexaFluor488 **182**; (b) Non-deconvoluted and (c) deconvoluted LCMS data for Fab_{Her}-Solastra-AlexaFluor488 **181**.

These two constructs were then incubated with breast cancer cell lines BT-474 (HER2-positive) and MDA-MB-468 (HER2-negative). Initially, incubation was performed at 4 °C, a temperature allowing binding but not internalisation; analysis by confocal microscopy revealed that Her-Solastra-AlexaFluor488 **182** and Fab_{Her}-Solastra-AlexaFluor488 **181** bound to BT-474 cells (Figure 5.12a) but not to MDA-MB-468 cells (Figure 5.12b), indicating the specificity of these constructs to HER2-positive cell lines. Internalisation of the bound antibodies occurred when the temperature was increased to 37 °C; incubation under these conditions for 1 h resulted in cytoplasmic localisation of the labelled constructs in BT-474 cells (Figure 5.12a), thus indicating that the chemistry employed does not interfere with the internalising properties of trastuzumab **19** or Fab_{Her} **127**.

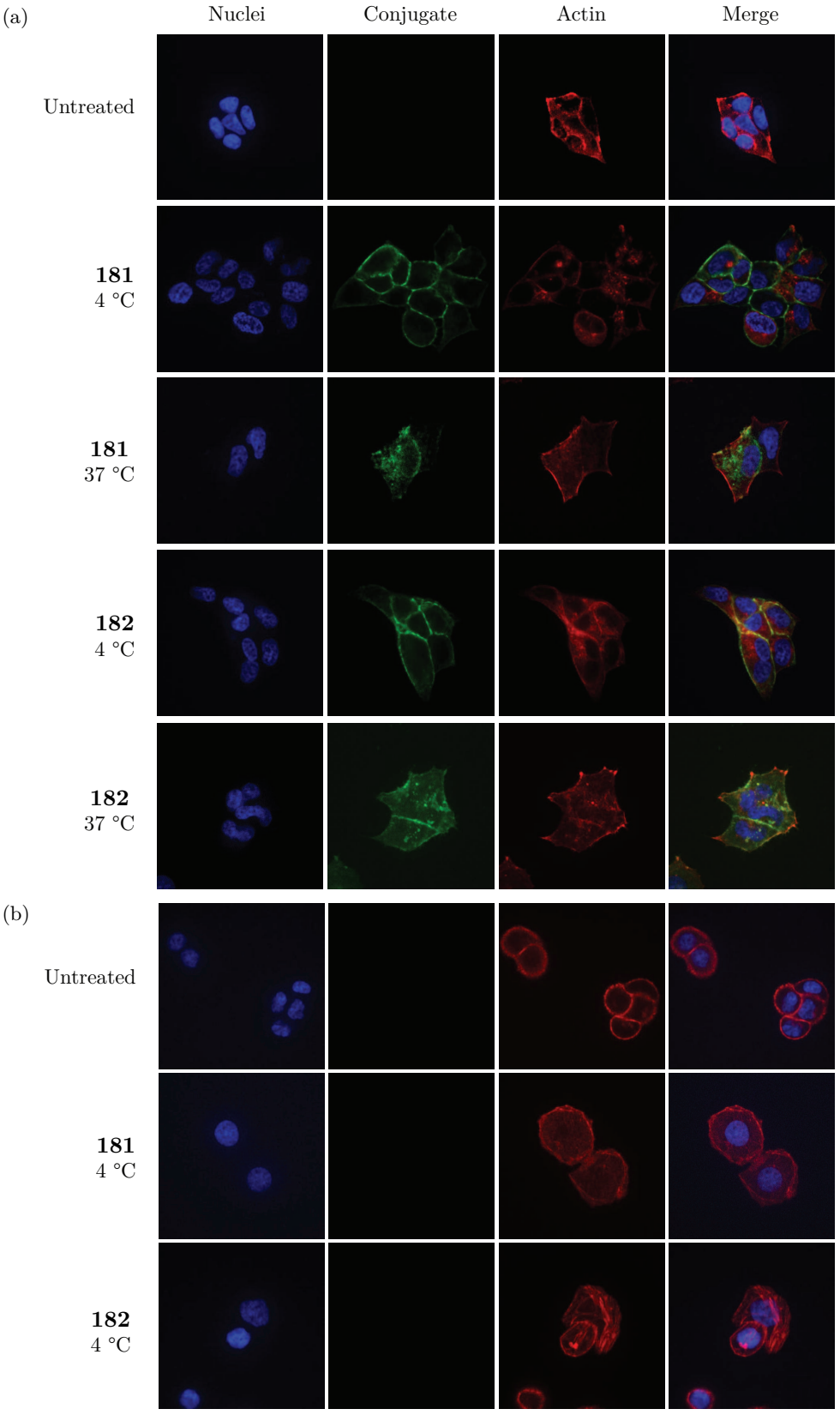

FIGURE 5.12: Internalisation analysis by confocal microscopy.
(a) BT474 treated with **181** and **182**; (b) MDA-MB-468 treated with **181** and **182**.

5.5.3 Cytotoxicity assay

Finally, the selectivity and cytotoxicity of constructs Fab_{Her}-Solastra-PEG_{20k}-Dox **159** and Her-Solastra-Dox-Cy5 **161** in *in vitro* studies, using the same HER2-positive and negative cell lines in the microscopy studies (*i.e.* BT-474 and MDA-MB-468), were evaluated. Initially, the sensitivity of both cell lines to doxorubicin was appraised to assess their suitability in a cytotoxicity assay. A comparable reduction in cell viability was observed for both cell lines at similar concentrations of the toxic payload (IC_{50} = 39 nM and 10 nM for BT-474 and MDA-MB-468 respectively), thus paving the way for toxicity studies with doxorubicin conjugates Fab_{Her}-Solastra-PEG_{20k}-Dox **159** and Her-Solastra-Dox-Cy5 **161** (Figure 5.13).

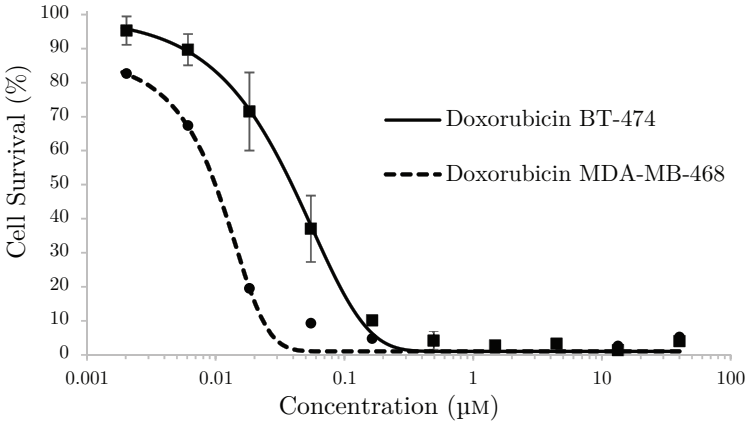

FIGURE 5.13: Inhibition of cell proliferation in cancer cell lines with different levels of HER2 expression, *i.e.* BT-474 (HER2-positive) and MDA-MB-468 (HER2-negative), with doxorubicin **143**.

Gratifyingly, BT-474 cell viability was reduced significantly when incubated with the conjugates (IC_{50} = 2.8 µM and 2.1 µM for conjugates Fab_{Her}-Solastra-PEG_{20k}-Dox **159** and Her-Solastra-Dox-Cy5 **161** respectively), especially when compared to the controls of native trastuzumab **19** and Fab_{Her} **127** where the reduction in cell survival was minimal at high concentrations (Figure 5.14).

Additionally, highlighting the targeted delivery aspect of the work, no toxicity was observed in analogous studies with MDA-MB-468 cells incubated with either conjugate Fab_{Her}-Solastra-PEG_{20k}-Dox **159** and Her-Solastra-Dox-Cy5 **161** (Figure 5.15). This is consistent with the observations by confocal microscopy, *i.e.* trastuzumab and Fab_{Her} conjugates **182** and **181** do not appear to bind to these cells, and hence doxorubicin could not be internalised and thereby cause a toxic effect.

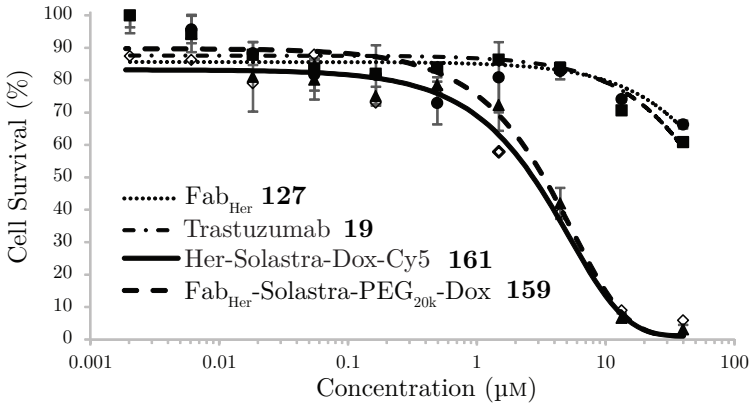

FIGURE 5.14: Inhibition of cell proliferation in cancer cell lines with high levels of HER2 expression with conjugates **159** and **161** (at similar concentration in doxorubicin) in comparison with trastuzumab **19** and Fab$_{Her}$ **127**.

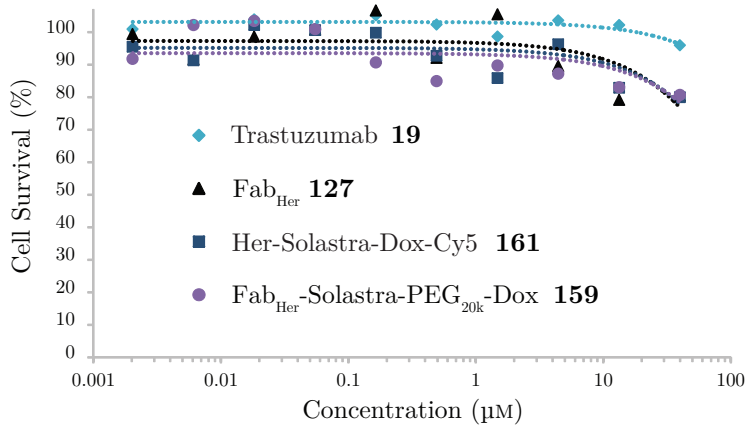

FIGURE 5.15: Inhibition of cell proliferation in cancer cell lines with low levels of HER2 expression with conjugates **159** and **161** (at similar concentration in doxorubicin) in comparison with trastuzumab **19** and Fab$_{Her}$ **127**.

These results clearly highlight the selectivity of conjugates **159** and **161** over doxorubicin alone, and indicate that the toxic drug in conjugates **159** and **161** is delivered by an HER2-dependent internalisation mechanism.

5.6 Conclusion

By assessing the selectivity, activity and stability of the conjugates in a broad range of conditions, it was demonstrated that PD reagents and conjugates show:

- a unique and exquisite chemoselectivity towards reaction with cysteines in the presence of all other amino acids, even under forcing conditions;

- complete retention of binding and internalisation activity, even post-conjugation to a large construct;
- exceptional resistance to hydrolysis at various extreme pHs and temperatures;
- tunable reactivity towards exogenous thiols: from stable in blood to irreversible in cytoplasm.

Chapter 6

Conclusion

6.1 Summary

A series of novel pyridazinedione-based reagents with various orthogonal handles have been synthesised in 3 – 5 scalable steps.
These molecules have shown exquisite selectivity towards cysteine thiols with no side reactions observed even at high temperature and/or after a prolonged period of time.
The adducts generated are hydrolytically stable and have been dually functionalised, selectively using two "click reactions" to generate a range of constructs (*vide supra*, Figure 2.3, page 51).

By the introduction of PD molecules bearing orthogonal "clickable" handles into the native disulfide bonds of antibodies, it was possible to demonstrate:

- the opportunity to synthesise multifunctionalised Fab fragments in a rapid and facile manner;
- the complete retention of binding activity post-conjugation and functionalisation;
- the potential of the method to generate a novel Fab-based ADC candidate with extended half-life;
- a new approach to a multifunctionalised, homogeneous full antibody to open the door to next-generation full antibody-based drug conjugate therapeutics;

- selective internalisation into HER2 positive cells with conjugates **181** and **182** of trastuzumab and Fab_{Her} that were directly conjugated to AlexaFluor488 *via* a PD-linker;
- selective cell killing over doxorubicin alone on appropriate HER2 cell lines.

By the introduction of PD molecules into a protein with an engineered cysteine, a novel *p*-azidobenzyl cleavage strategy was developed and demonstrated on both a small molecule system and on a model protein. This resulted in a route to thiol-stable conjugates with clear advantages over conventional conjugation chemistries (*e.g.* maleimides).

6.2 Future outlook

Having demonstrated the facile conjugation of PDs across various platforms and the rapid and clean dual functionalisation of the resulting conjugates with a range of biologically relevant molecules, an exciting next step would be to use PDs to generate clinically relevant protein–protein conjugates. For example, this would enable the generation of bispecific antibodies armed with cytotoxic drugs or bispecific T-cell engagers (BiTEs) with extended half-life *in vivo*. One could also envisage the reconstruction of a full antibody where a tailored Fc and two different Fabs could be attached together in a stepwise fashion using click reactions.

Another interesting next step would be the attachment on the same targeting entity of two drugs that operate by an orthogonal mechanism of action, which is a concept that is gathering increasing momentum.[242–245]

Owing to the plethora of fields where thiol functionalisation needs to be robust and reliable (*e.g.* in antibody–drug conjugates) it is believed that this work will find use in a variety of domains where irreversible/reversible protein modification is needed.
The modular "plug-and-play" approach enabled by PDs has broader applications in fields outside the scope of antibody modification (for example, dual warhead antibiotics, folic acid conjugates, tetrablock polymersomes);[243–246] then, one can envisage numerous applications for such a linker technology (*e.g.* multi-labelling of protein conjugates, cleavable fluorophores, radiolabels and quantum dots for imaging) with the possibility of combining two different functions. Hence, this will potentially be a highly versatile

platform (Figure 6.1) which could open the door to a valuable and novel range of conjugates.

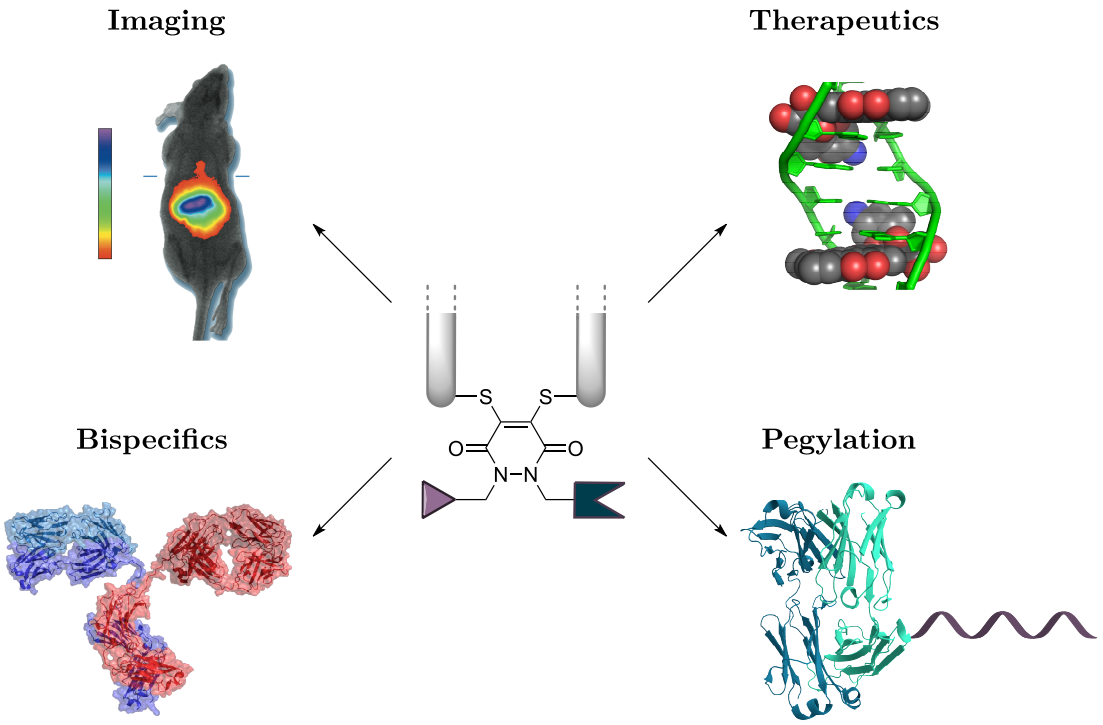

FIGURE 6.1: Potential applications of PD-conjugates.

Appendix A

Experimental

A.1 General experimental

A.1.1 Chemicals

All reagents were purchased from Sigma Aldrich, Alfa Aesar, Acros, Synaffix, Lumiprobe and Avocado and used as received unless otherwise stated. Trastuzumab was purchased from UCLH pharmacy.

A.1.2 Solvents

Solvents were used as received unless otherwise stated. Petrol refers to petroleum ether (b.p. 40 – 60 °C).

A.1.3 Chromatography

Reaction progress was monitored by analytical TLC using Merck aluminium coated plates covered with a 0.2 mm layer of silica gel 60 F254. Product spots were visualised by UV irradiation at 254 nm and subsequent staining with potassium permanganate solution, followed by heating. Column chromatography was carried out with silica gel (33 – 70 µm) supplied by VWR.

A.1.4 Spectroscopy

^{1}H NMR spectra were recorded at 300 MHz, 400 MHz, 500 MHz and 600 MHz and ^{13}C NMR at 75 MHz, 100 MHz, 125 MHz and 150 MHz on Bruker AMX300, AMX400, AMX500 and AMX600 at 25 °C as described below. The chemical shifts (δ) for ^{1}H and ^{13}C are quoted relative to residual signals of the solvent on the parts per million (ppm) scale. NMR peaks are reported as singlet (s), doublet (d), triplet (t), quartet (q), quint. (quintet), m (multiplet), br (broad), dd (doublet of doublet). Coupling constants (J values) are reported in Hertz (Hz) and are reported as $J_{\text{H-H}}$ couplings unless otherwise stated. Infrared spectra were obtained on a Perkin Elmer Spectrum 100 FTIR Spectrometer operating in ATR mode. Mass spectra were obtained at UCL on either a VG70-SE (FAB), Thermo Finnigan MAT900Xp (EI and CI) or Waters LCT Premier XE (ES) mass spectrometer.

A.1.5 Miscellaneous

Unless stated otherwise, all reaction mixtures were stirred magnetically. Melting points were measured with a Gallenkamp apparatus and are uncorrected. Compound **65** was synthesised following literature procedure and all data were consistent with literature data.[171] All reactions involving moisture sensitive techniques were performed under an atmosphere of dry argon *via* standard vacuum line techniques and glassware was flame dried and allowed to cool under reduced pressure. Within this text, room temperature is defined as between 19 – 22 °C. Reactions described as being performed at −78 °C were cooled by an acetone bath with submerged solid CO_2 pellets. Reactions performed at 0 °C were cooled with an ice and water bath. Concentration *in vacuo* refers to distillation on a Büchi rotary evaporator, and where appropriate under high vacuum.

A.1.6 General remarks on conjugation experiments

Conjugation experiments were carried out in standard polypropylene micro test tubes 3810X at atmospheric pressure with mixing at room temperature unless otherwise stated. All buffer solutions were prepared with double-deionised water and filter-sterilised. BBS was 25 mM sodium borate, 25 mM NaCl and 0.5 mM EDTA at pH 8.0 unless stated otherwise. PBS was 140 mM NaCl and 12 mM phosphates at pH 7.4. Ultrapure DMF

was purchased from Sigma-Aldrich and kept under dry and inert conditions. Solutions of TCEP 20 mM were prepared in BBS. Ultrafiltration was carried out in vivaspin 500 polyethersulfone (PES) membrane concentrators with a molecular weight cut-off (MWCO) of 10 kDa or 30 kDa. Centrifugation was carried out on an eppendorf 5415R fixed angle rotor centrifuge operating at 14 000 rcf at room temperature. Purification by size exclusion chromatography (SEC) was carried out on an ÄKTA Purifier HPLC system (GE Healthcare), equipped with a HiLoad Superdex 75 16/60 column (GE Healthcare) equilibrated in PBS, running at a flow rate of 0.5 mL/min. Detection was by absorption at 280 nm. Trastuzumab was obtained in its clinical formulation (lyophilised). The powder was dissolved in 10 mL sterile water and the buffer exchanged completely for digest buffer (50 mM phosphate, 1 mM EDTA, pH 6.8) *via* ultrafiltration (MWCO 50 kDa, Sartorius). The concentration after the exchange was determined by UV-Vis absorbance and adjusted to 23 µM and was stored in flash frozen aliquots at −18 °C or −80 °C. For experiments, aliquots were thawed, buffer swapped into the buffer of choice and concentration was corrected to 23 µM.

A.1.7 Protein mass spectroscopy

LC-MS was performed on protein samples using one Thermo Scientific uPLC connected to MSQ Plus Single Quad Detector (SQD) with the following parameters. Column: Hypersil Gold C4 1.9 µm, 2.1 µm × 50 µm. Wavelength: 254 nm. Mobile Phase: 99:1 Water (0.1% formic acid): MeCN (0.1% formic acid) to 1:9 Water (0.1% formic acid): MeCN (0.1% formic acid) gradient over 4 min. Flow Rate: 0.3 mL/min. MS Mode: ES^+. Scan Range: $m/z = 100 - 2000$. Scan time: 1.5 s. Data obtained in continuum mode. The electrospray source of the MS was operated with a capillary voltage of 3.5 kV and a cone voltage of 50 V. Nitrogen was used as the nebulizer and desolvation gas at a total flow of 600 L/h. Total mass spectra for protein samples were reconstructed from the ion series using the pre-installed ProMass software using default settings for large proteins in m/z range 500 – 2000.

Alternatively, LC-MS was performed on protein samples using a Waters Acquity uPLC connected to Waters Acquity Single Quad Detector (SQD) with the following parameters. Column: Hypersil Gold C4, 1.9 µm, 2.1 µm × 50 µm. Wavelength: 254 nm. Mobile Phase: 95:5 Water (0.1% Formic Acid): MeCN (0.1% Formic Acid) Gradient over 4 min (to

5:95 Water (0.1% Formic Acid): MeCN (0.1% Formic Acid). Flow Rate: 0.6 mL/min. MS Mode: ES^+. Scan Range: $m/z = 250-2000$. Scan time: 0.25 s. Data obtained in continuum mode. The electrospray source of the MS was operated with a capillary voltage of 3.5 kV and a cone voltage of 50 V. Nitrogen was used as the nebulizer and desolvation gas at a total flow of 600 L/h. Ion series were generated by integration of the total ion chromatogram (TIC) over the appropriate range. Total mass spectra for protein samples were reconstructed from the ion series using the MaxEnt 1 algorithm pre-installed on MassLynx software.

It is noteworthy to mention that the accuracy of the LC-MS was highly dependent upon the instrument used, its state at the time of the experiment (*e.g.* unclean column affecting signal-to-noise ratio) as well as the algorithm used to deconvolute.

A.1.8 UV-Vis spectroscopy

UV-Vis spectra were recorded on a Varian Cary 100 Bio UV/Visible spectrophotometer, operating at room temperature. Sample buffer was used as blank for baseline correction. Calculation of the molecule over antibody ratio, r, follows the formula below with $\varepsilon_{280} = 215\,380\,\text{M}^{-1}\cdot\text{cm}^{-1}$ for trastuzumab derivatives, $\varepsilon_{280} = 68\,590\,\text{M}^{-1}\cdot\text{cm}^{-1}$ for Fab_{Her} derivatives, $\varepsilon_{345} = 9100\,\text{M}^{-1}\cdot\text{cm}^{-1}$ for PDs, $\varepsilon_{495} = 8030\,\text{M}^{-1}\cdot\text{cm}^{-1}$ for Dox derivatives, $\varepsilon_{646} = 271\,000\,\text{M}^{-1}\cdot\text{cm}^{-1}$ and 0.724, 0.28, and 0.13 as a correction factor (CF) for Dox derivatives, PDs, and sulfo-Cy5 derivatives respectively for the absorbance at 280 nm.

$$r = \frac{\text{A}_\lambda/\varepsilon_\lambda}{\left(\text{A}_{280} - \sum_\lambda \text{CF}_\lambda \times \text{A}_\lambda\right)/\varepsilon_{280}}$$

With A_λ the absorbance at wavelength λ, and ε_λ the extinction coefficient of the molecule of interest.

A.1.9 SDS-PAGE

Non-reducing glycine-SDS-PAGE at 12% acrylamide (16% for GFP conjugates) gels were performed following standard lab procedures. A 4% stacking gel was used and a broad-range MW marker (10 – 250 kDa, BioLabs) was co-run to estimate protein weights. Samples (3 – 5 µL at *ca.* 20 µM) were mixed with loading buffer (1 – 2 µL, composition for 6×SDS: 1 g SDS, 1 mL glycerol, 6 mL 0.5 M Tris buffer pH 6.8, 2 mg R 250 dye) and

heated at 75 °C for 2 min. The gel was run at constant current (30 – 35 mA) for 40 min (150 V for 60 min for GFP conjugates) in 1×SDS running buffer. All gels were stained with Coomassie dye. Gel photographs were taken with a Wiko-Stairway device.

A.1.10 Enzyme-linked immunosorbent assay (ELISA)

Binding affinity to HER2 receptor was determined by ELISA. A 96-well plate was coated for 1 h at room temperature with HER2 (Human HER2/ErbB2 Protein (His Tag) from Sino Biological) (100 µL of a 0.25 µg·mL^{-1} solution in PBS), including coating one row of wells with PBS only for negative controls. Next, the coating solutions were removed and each well washed with PBS twice. Then, the wells were coated with a 1% BSA solution in PBS (200 µL) overnight at 4 °C. Next, the wells were washed with 0.1% Tween 20 in PBS twice and with PBS three times. Solutions of trastuzumab **19**, Fab_{Her} **127** and relevant Fab_{Her}-PD and Her-PD conjugates in PBS were prepared with the following dilution series: 100 nM, 30 nM, 10 nM, 3.3 nM, 1.1 nM, 0.37 nM, and 0.12 nM. Wells were coated with the dilution series solutions in triplicate, including a PBS only at 30 nM in the absence of HER2 as negative controls, and incubated for 2 h at room temperature. Then, the solutions were removed and the wells washed with 0.1% Tween 20 in PBS twice and with PBS three times. Detection antibody (100 µL of anti-human IgG, Fab-specific-HRP solution, prepared by taking 4 µL of a 1:5000 diluted solution and further diluting with 20 mL of PBS) was then added and incubated for 1 h at room temperature. Then, the solutions were removed and the wells washed with 0.1% Tween 20 in PBS twice and with PBS three times. OPD solution (100 µL of 10 mg/20 mL OPD in phosphate-citrate buffer with sodium perborate, prepared by dissolving 1 capsule in 100 mL water) was added to each well. After 30 s the reaction was stopped through addition of 4 M HCl (50 µL). The absorption was measured at 490 nm and corrected by subtracting average of negative controls. The results obtained were analysed with GraphPad Prism using a regression with variable slope (four parameters).

A.1.11 Ellman's test

To a solution of the protein of interest (50 µL, 40 µM, 1 eq.) in phosphate buffer (100 mM sodium phosphate, 1 mM EDTA, pH 8.0) was added TCEP (final concentration 400 µM, 10 eq.) and the reaction mixture incubated at 37 °C for 2 h. The excess reagents were then

removed by repeated diafiltration into fresh buffer using VivaSpin sample concentrators (GE Healthcare, 10 000 MWCO). The concentration of protein was then adjusted to 40 µM. Following this, a solution of Ellman's reagent (5,5'-dithiobis-(2-nitrobenzoic acid)) in phosphate buffer (100 mM sodium phosphate, 1 mM EDTA, pH 8.0) (final concentration 1.6 mM, 40 eq.) was added and the reaction mixture was incubated at 21 °C for 30 min. The mixture was then analysed by UV-Vis after a 10-fold dilution and the absorption at 412 nm was measured ($\varepsilon_{412} = 14\,150\,\mathrm{M}^{-1} \cdot \mathrm{cm}^{-1}$).

A.1.12 Cell lines

Breast cancer cell lines BT-474 and MDA-MB-468 were purchased from ATCC. BT-474 cells were maintained at 37 °C, 5% CO_2 in Hybricare Medium (ATCC) complemented with 10% foetal calf serum (Labtech International, Ringmer, UK). MDA-MB-468 cells were maintained at 37 °C, 5% CO_2 in Dulbecco's modified Eagle's medium complemented with 10% foetal calf serum and 2 mM L-glutamine (PAA Laboratories, UK).

A.1.13 Internalisation analysis by confocal microscopy

Analysis by Dr Enrique Miranda Rota.
Cells on coverslips at 70% confluency were incubated with AlexaFluor488-conjugated constructs at 10 mg/mL for 1 h at 4 °C. Cells were extensively washed with PBS to remove unbound antibodies and incubated at 37 °C in growth media. Internalisation was allowed for 1 h, followed by extensive washing and fixation with 4% formaldehyde for 10 min at 4 °C. Coverslips were then blocked with 5% goat serum in 0.3% Triton-X100 (Sigma). Actin was detected with phalloidin-568 (Invitrogen) and Hoechst trihydrochloride (Invitrogen) was used to stain cell nuclei. Coverslips were mounted on slides using ProLong Gold Antifade (Invitrogen) and examined using Perkin Elmer Spinning Disc Confocal microscope and Volocity Visualization software.

A.1.14 Toxicity assays

Cells were seeded in 96-well plates at 10^4 cells/well and allowed to attach for 24 h. Serial dilution of trastuzumab **19**, Fab_{Her} **127**, Dox **143**, Fab_{Her}-PEG_{20k}-Dox **159** and Her-Solastra-Dox-Cy5 **161** were added to the cells at concentrations ranging from 40 to 0 µM

in complete growth medium. After 96 h, cell viability was measured using the CellTiter 96 Aqueous Non-radioactive cell proliferation assay (Promega) following manufacturer's instructions. Cell viability was plotted as percentage of untreated cells. The results obtained were analysed with GraphPad Prism using a regression with variable slope (four parameters).

A.2 Characterisations

1-Azido-4-methylbenzene 52[167]

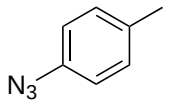

To a solution of *p*-toluidine (2.0 g, 18 mmol) in 2 M HCl (28 mL) at −5 °C was added slowly a solution of sodium nitrite (1.5 g, 22 mmol) in H_2O (5 mL) over 5 min making sure that the internal temperature did not rise above 0 °C. After completion of addition, the reaction mixture was stirred at −5 °C for 5 min to form a diazonium salt. Then urea (0.13 g, 2.2 mmol) was added to neutralise the diazonium salt solution. Following this, the diazonium salt solution was added to a solution of sodium azide (2.4 g, 37 mmol) and sodium acetate (4.6 g, 56 mmol) in 30 mL of H_2O at 0 °C over 5 min. The mixture was stirred for 2 h at 0 °C. The mixture was extracted into Et_2O (2×60 mL), the combined organic layers dried ($MgSO_4$) and concentrated *in vacuo* to afford 1-azido-4-methylbenzene **52** (2.3 g, 17 mmol, 94%) as a yellow oil: ^{1}H NMR (500 MHz, $CDCl_3$) δ 7.15 (d, J = 8.4 Hz, 2H), 6.92 (d, J = 8.4 Hz, 2H), 2.33 (s, 3H); ^{13}C NMR (125 MHz, $CDCl_3$) δ 137.2 (C), 134.7 (C), 130.4 (CH), 118.9 (CH), 21.0 (CH_3); IR (thin film) 2104, 1609, 1521 cm^{-1}.

1-Azido-4-(bromomethyl)benzene 53[168]

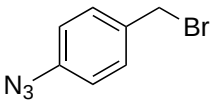

A solution of 1-azido-4-methylbenzene **52** (0.85 g, 6.4 mmol), *N*-bromosuccinimide (1.5 g, 8.3 mmol) and azobis(isobutyronitrile) (0.31 g, 1.9 mmol) in dry benzene (20 mL) was heated under reflux under argon in the dark for 8 h. After this time, the mixture was poured onto H_2O (20 mL), extracted into Et_2O (2×20 mL), the combined organic layers dried ($MgSO_4$) and concentrated *in vacuo*. Purification by flash column chromatography (neat petrol) yielded 1-azido-4-(bromomethyl)benzene **53** (1.1 g, 5.1 mmol, 80%) as a light brown solid: ^{1}H NMR (300 MHz, $CDCl_3$) δ 7.38 (d, J = 8.4 Hz, 2H), 7.00 (d, J = 8.4 Hz, 2H), 4.48 (s, 2H); ^{13}C NMR (150 MHz, $CDCl_3$) δ 140.3 (C), 134.6 (C), 130.7 (CH), 119.5 (CH), 33.0 (CH_2); IR (solid) 2107, 1607, 1505 cm^{-1}; LRMS (EI) 213 (100,

$[M^{81}Br]^{+\bullet}$), 211 (100, $[M^{79}Br]^{+\bullet}$); HRMS (EI) calcd for $C_7H_6N_3Br$ $[M^{79}Br]^{+\bullet}$ 210.9740, observed 210.9743.

Di-*tert*-butyl 1-(prop-2-yn-1-yl)hydrazine-1,2-dicarboxylate 55[169]

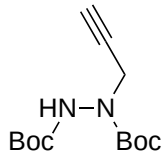

To a solution of di-*tert*-butyl hydrazine-1,2-dicarboxylate (300 mg, 1.29 mmol) in a mixture of toluene (2 mL) and 5% aq. NaOH (2 mL) were added tetra-*n*-butylammonium bromide (13 mg, 0.03 mmol) and propargyl bromide (461 mg, 3.87 mmol). The reaction mixture was stirred at 20 °C for 16 h. After this time, H_2O (20 mL) was added and the mixture was extracted with ethyl acetate (3×15 mL). The combined organic layers were washed with brine (15 mL), dried ($MgSO_4$), and concentrated *in vacuo*. Purification by flash column chromatography (20 % EtOAc/petrol) yielded di-*tert*-butyl 1-(prop-2-yn-1-yl)hydrazine-1,2-dicarboxylate **55** (437 mg, 1.62 mmol, 86%) as a white solid: m.p. 101 – 103 °C (*lit. m.p.*[169] 103.1 – 103.4 °C); ^{1}H NMR (500 MHz, $CDCl_3$) δ 6.47 (br. s, 0.78H), 6.18 (br. s, 0.22H,), 4.27 (s, 2H), 2.24 (t, J = 2.4 Hz, 1H), 1.48 (s, 18H); ^{13}C NMR (150 MHz, $CDCl_3$) δ 155.0 (C), 82.2 (C), 81.7 (C), 79.0 (C), 77.7 (C), 72.5 (CH), 39.5 (CH_2), 28.5 (CH_3), 28.5 (CH_3); IR (solid) 3310, 2109, 1703 cm^{-1}.

Di-*tert*-butyl 1-(4-azidobenzyl)-2-(prop-2-yn-1-yl)hydrazine-1,2-dicarboxylate 56

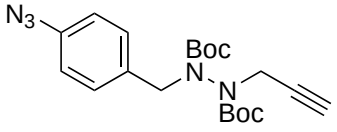

To a solution of di-*tert*-butyl 1-(prop-2-yn-1-yl)hydrazine-1,2-dicarboxylate **55** (0.20 g, 0.70 mmol) in DMF (10 mL) were added caesium carbonate (0.48 g, 1.5 mmol) and 1-azido-4-(bromomethyl)benzene **53** (0.23 g, 1.1 mmol). The reaction mixture was stirred at 20 °C for 16 h. After this time, the reaction mixture was diluted with H_2O (20 mL) and extracted with EtOAc (3×20 mL). The combined organic layers were washed with brine (15 mL), dried ($MgSO_4$), and concentrated *in vacuo*. Purification by flash column chromatography (20% Et_2O/petrol) yielded di-*tert*-butyl 1-(4-azidobenzyl)-2-(prop-2-yn-1-yl)hydrazine-1,2-dicarboxylate **56** (0.26 g, 0.65 mmol, 93%) as a viscous dark yellow

liquid: ^{1}H NMR (500 MHz, $CDCl_3$) δ 7.38 (d, J = 8.4 Hz, 2H), 6.97 (d, J = 8.4 Hz, 2H), 4.63 – 3.98 (m, 4H), 2.19 (t, J = 2.4 Hz, 1H), 1.47 (s, 9H), 1.30 (s, 9H); ^{13}C NMR (150 MHz, $CDCl_3$) δ 154.6 (C), 154.3 (C), 139.5 (C), 133.6 (C), 131.4 (CH), 118.9 (CH), 81.7 (C), 81.6 (C), 78.5 (C), 72.9 (CH), 52.6 (CH_2), 39.3 (CH_2), 28.3 (CH_3), 28.1 (CH_3); IR (thin film) 3257, 2110, 1705, 1600, 1507 cm^{-1}; LRMS (CI) 424 (100, $[M+Na]^+$), 365 (70); HRMS (CI) calcd for $C_{20}H_{27}N_5O_4Na$ $[M+Na]^+$ 424.1961, observed 424.1965.

3,4-Dibromo-furan-2,5-dione 58[247]

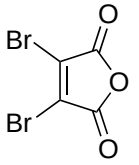

A mixture of maleic anhydride (1.5 g, 15 mmol), $AlCl_3$ (28 mg, 0.21 mmol) and Br_2 (1.6 mL, 4.9 g, 31 mmol) was heated at 160 °C in a sealed ampoule for 20 h. After this time, the reaction mixture was allowed to cool to room temperature and diluted with EtOAc (25 mL). The reaction mixture was then filtered and the solid washed thoroughly with EtOAc (3 × 25 mL). The filtrate was then concentrated *in vacuo* to afford 3,4-dibromo-furan-2,5-dione **58** as a yellow solid (3.3 g, 13 mmol, 83%): m.p. 108 – 111 °C (*lit. m.p.*[247] 113 – 114 °C); ^{13}C NMR (MeOD, 150 MHz) δ 164.4 (C), 125.9 (C); IR (solid) 1769, 1706, 1590 cm^{-1}.

1-(4-Azidobenzyl)-4,5-dibromo-2-(prop-2-yn-1-yl)-1,2-dihydropyridazine-3,6-dione 61

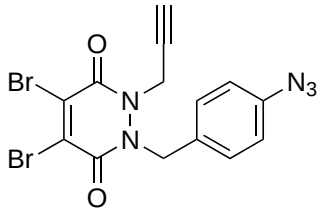

To a solution of di-*tert*-butyl 1-(4-azidobenzyl)-2-(prop-2-yn-1-yl)hydrazine-1,2-dicarboxylate **56** (1.8 g, 4.5 mmol) in CH_2Cl_2 (55 mL) was added TFA (18 mL) and the reaction mixture stirred at 20 °C for 30 min. After this time, all volatile materials were removed *in vacuo*. The crude residue was added to a solution of 2,3-dibromomaleic anhydride **58** (1.4 g, 5.4 mmol) in glacial AcOH (125 mL), and the reaction mixture heated at 130 °C for 16 h. Then the reaction mixture was concentrated *in vacuo*, and purification by

flash column chromatography (15% to 50% Et_2O/petrol) yielded 1-(4-azidobenzyl)-4,5-dibromo-2-(prop-2-yn-1-yl)-1,2-dihydropyridazine-3,6-dione **61** (0.69 g, 1.6 mmol, 35%) as a yellow solid: m.p. 79 – 81 °C; ^{1}H NMR (500 MHz, $CDCl_3$) δ 7.25 (d, J = 8.5 Hz, 2H), 7.02 (d, J = 8.5 Hz, 2H), 5.46 (s, 2H), 4.75 (d, J = 2.5 Hz, 2H), 2.45 (t, J = 2.5 Hz, 1H); ^{13}C NMR (125 MHz, $CDCl_3$) δ 153.5 (C), 153.0 (C), 140.8 (C), 136.7 (C), 135.8 (C), 130.9 (C), 128.5 (CH), 120.0 (CH), 75.7 (C), 75.2 (CH), 50.3 (CH_2), 37.1 (CH_2); IR (solid) 3251, 2111, 1636, 1507 cm^{-1}; LRMS (CI) 442 (50, $[M^{81}Br^{81}Br+H]^+$), 440 (100, $[M^{81}Br^{79}Br+H]^+$), 438 (50, $[M^{79}Br^{79}Br+H]^+$); HRMS (CI) calcd for $C_{14}H_{10}{}^{79}Br_2N_5O_2$ $[M^{79}Br^{79}Br+H]^+$ 437.9196, observed 437.9197.

Methyl 3,4-dibromo-2,5-dioxo-2,5-dihydro-1*H*-pyrrole-1-carboxylate 60[170]

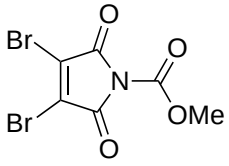

To a solution of dibromomaleimide (1.0 g, 3.9 mmol) and *N*-methylmorpholine (0.43 mL, 3.9 mmol) in THF (35 mL) was added methylchloroformate (0.31 mL, 3.9 mmol) and the reaction mixture stirred at 20 °C for 20 min. After this time, CH_2Cl_2 (40 mL) was added, and the reaction mixture was washed with H_2O (50 mL), dried ($MgSO_4$) and concentrated *in vacuo* to afford methyl 3,4-dibromo-2,5-dioxo-2,5-dihydro-1*H*-pyrrole-1-carboxylate **60** (1.2 g, 3.8 mmol, 97%) as a pink power: m.p. 114 – 116 °C; ^{1}H NMR (500 MHz, $CDCl_3$) δ 4.00 (s, 3H); ^{13}C NMR (125 MHz, $CDCl_3$) δ 159.3 (C), 147.0 (C), 131.5 (C), 54.9 (CH_3); HRMS (EI) calcd for $C_6H_3O_4N^{79}Br_2$ $[M^{79}Br^{79}Br]^{+\bullet}$ 310.8423, observed 310.8427.

***tert*-Butyl 14-azido-3-(*tert*-butoxycarbonyl)-2-(prop-2-yn-1-yl)-6,9,12-trioxa-2,3-diazatetradecan-1-oate 66**

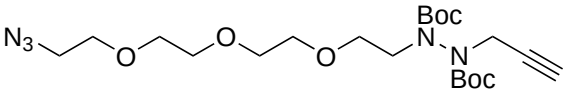

To a solution of di-*tert*-butyl 1-(prop-2-yn-1-yl)hydrazine-1,2-dicarboxylate **55** (0.11 g, 0.40 mmol) in DMF (3 mL) were added caesium carbonate (0.16 g, 0.48 mmol) and 2-(2-(2-(2-azidoethoxy)ethoxy)ethoxy)ethyl methanesulfonate **65** (0.13 g, 0.44 mmol) and the reaction mixture stirred at 20 °C for 16 h. After this time, the reaction mixture was diluted with H_2O (10 mL), extracted with Et_2O (5 × 10 mL), the combined organic layers washed

with sat. aq. LiCl (2 × 10 mL), dried ($MgSO_4$), and concentrated *in vacuo*. Purification by flash column chromatography (30% EtOAc/petrol) yielded *tert*-butyl 14-azido-3-(*tert*-butoxycarbonyl)-2-(prop-2-yn-1-yl)-6,9,12-trioxa-2,3-diazatetradecan-1-oate **66** (0.18 g, 0.38 mmol, 94%) as a yellow oil: ^{1}H NMR (500 MHz, $CDCl_3$) δ 4.61 – 3.41 (m, 16H) 3.38 (t, J = 5.0 Hz, 2H), 2.27 – 2.21 (m, 1H) 1.51 – 1.42 (m, 18H); ^{13}C NMR (150 MHz, $CDCl_3$) (rotamers) δ 155.3 (C), 155.3 (C), 154.8 (C), 154.7 (C), 154.5 (C), 154.3 (C), 153.9 (C), 82.2 (C), 82.0 (C), 81.7 (C), 81.7 (C), 81.4 (C), 81.3 (C), 79.3 (C), 79.3 (C), 78.9 (C), 72.5 (CH), 72.3 (CH), 72.1 (CH), 70.8 (CH_2), 70.8 (CH_2), 70.7 (CH_2), 70.5 (CH_2), 70.4 (CH_2), 70.3 (CH_2), 70.1 (CH_2), 68.6 (CH_2), 68.5 (CH_2), 68.4 (CH_2), 50.8 (CH_2), 50.7 (CH_2), 50.7 (CH_2), 49.8 (CH_2), 49.8 (CH_2), 41.3 (CH_2), 41.2 (CH_2), 39.7 (CH_2), 39.6 (CH_2), 28.3 (CH_3), 28.3 (CH_3), 28.3 (CH_3), 28.2 (CH_3), 28.1 (CH_3), 28.0 (CH_3), 28.0 (CH_3), 27.8 (CH_3); IR (thin film) 3258, 2100, 1708 cm^{-1}; LRMS (CI) 494 (50, $[M+Na]^+$), 272 (100); HRMS (CI) calcd for $C_{21}H_{37}N_5O_7Na$ $[M+Na]^+$ 494.2591, observed 494.2582.

18,19-Dibromo-5,6,8,9,11,12,14,15-octahydro-22*H*-pyridazino[1,2-*g*][1,2,3]triazolo[5,1-*j*][1,4,14]trioxa[7,8,11]triazacyclohexadecine-17,20-dione 67

(*Z*)-1^4,1^5-Dibromo-1^1,1^2,1^3,1^6-tetrahydro-3^1*H*-6,9,12-trioxa-1(1,2)-pyridazina-3(4,1)-triazolacyclotetradecaphane-1^3,1^6-dione 68

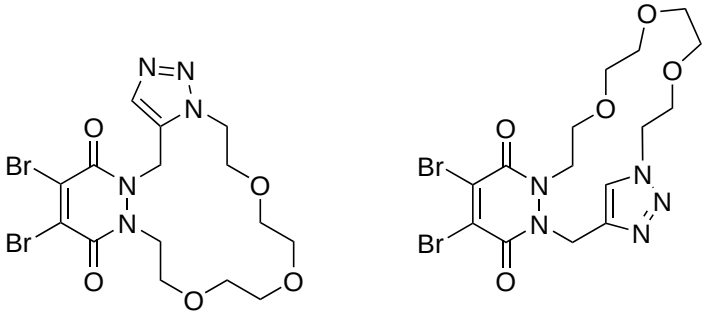

To a solution of *tert*-butyl 14-azido-3-(*tert*-butoxycarbonyl)-2-(prop-2-yn-1-yl)-6,9,12-trioxa-2,3-diazatetradecan-1-oate **66** (54 mg, 0.11 mmol) in CH_2Cl_2 (1 mL) was added TFA (0.5 mL) and the reaction mixture stirred at 20 °C for 30 min. After this time, all volatile materials were removed *in vacuo*. The crude residue was added to a solution of 2,3-dibromomaleic anhydride **58** (30 mg, 0.11 mmol) in glacial AcOH (2 mL), and the reaction mixture heated at 130 °C for 16 h. Then the reaction mixture was concentrated *in vacuo*, and purification by flash column chromatography (0 – 2%

MeOH/CH_2Cl_2) yielded 18,19-dibromo-5,6,8,9,11,12,14,15-octahydro-22*H*-pyridazino[1,2-*g*][1,2,3]tri azolo[5,1-*j*][1,4,14]trioxa[7,8,11]triazacyclohexadecine-17,20-dione **67** and (*Z*)-1^4,1^5-dibromo-1^1,1^2,1^3,1^6-tetrahydro-3^1*H*-6,9,12-trioxa-1(1,2)-pyridazina-3(4,1)-tri azolacyclotetradecaphane-1^3,1^6-dione **68** as an inseparable mixture of regioisomers (21 mg, 42 µmol, 38%) as a yellow oil: ^{1}H NMR (500 MHz, $CDCl_3$) (major regioisomer) δ 7.52 (s, 1H), 5.75 (s, 2H), 4.80 (t, J = 4.6 Hz, 2H), 4.43 (t, J = 4.5 Hz, 2H), 3.88 (t, J = 4.5 Hz, 2H), 3.77 (t, J = 4.6 Hz, 2H), 3.68 – 3.43 (m, 8H); ^{13}C NMR (125 MHz, $CDCl_3$) (major regioisomer) δ 152.9 (C), 152.8 (C), 142.0 (C), 136.3 (C), 136.0 (C), 131.8 (CH), 70.6 (CH_2), 70.3 (CH_2), 70.2 (CH_2), 69.8 (CH_2), 67.9 (CH_2), 53.5 (CH_2), 50.8 (CH_2), 49.2 (CH_2).

1-(2-(2-(2-(2-Azidoethoxy)ethoxy)ethoxy)ethyl)-4,5-dibromo-2-(prop-2-yn-1-yl)-1,2-dihydropyridazine-3,6-dione 69

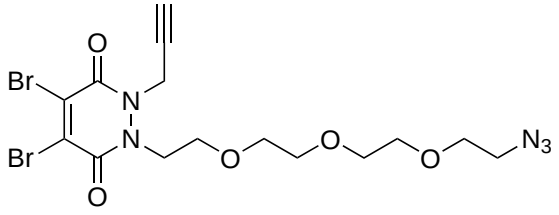

To a solution of *tert*-butyl 14-azido-3-(*tert*-butoxycarbonyl)-2-(prop-2-yn-1-yl)-6,9,12-trioxa-2,3-diazatetradecan-1-oate **66** (0.10 g, 0.21 mmol,) in CH_2Cl_2 (2 mL) was added TFA (1 mL) and the reaction mixture stirred at 20 °C for 30 min. After this time, all volatile materials were removed *in vacuo*. The crude residue was added to a solution of *N*-methoxycarbonyl-dibromomaleimide **60** (73 mg, 0.23 mmol) and NEt_3 (47 mg, 0.47 mmol) in CH_2Cl_2 (5 mL) and the reaction mixture stirred at 20 °C for 16 h. Then the reaction mixture was concentrated *in vacuo*, and purification by flash column chromatography (0.2% MeOH/CH_2Cl_2) yielded 1-(2-(2-(2-(2-azidoethoxy)ethoxy)ethoxy)ethyl)-4,5-dibromo-2-(prop-2-yn-1-yl)-1,2-dihydropyridazine-3,6-dione **69** (29 mg, 0.06 mmol, 27%) as a yellow oil: ^{1}H NMR (600 MHz, $CDCl_3$) δ 5.15 (d, J = 2.4 Hz, 2H), 4.45 (t, J = 4.7 Hz, 2H), 3.77 (t, J = 4.7 Hz, 2H), 3.67 – 3.64 (m, 2H), 3.63 – 3.54 (m, 8H), 3.39 (t, J = 5.1 Hz, 2H), 2.38 (t, J = 2.4 Hz, 1H); ^{13}C NMR (150 MHz, $CDCl_3$) δ 152.9 (C), 152.5 (C), 136.4 (C), 135.8 (C), 76.6 (C), 74.5 (CH), 70.8 (CH_2), 70.8 (CH_2), 70.7 (CH_2), 70.6 (CH_2), 70.2 (CH_2), 68.3 (CH_2), 50.7 (CH_2), 48.4 (CH_2), 37.3 (CH_2); IR (thin film) 3243, 2099, 1634, 1574 cm^{-1}; LRMS (CI) 512 (50, [M^{81}Br^{81}Br+H]$^+$), 510 (100, [M^{81}Br^{79}Br+H]$^+$),

508 (50, $[M^{79}Br^{79}Br+H]^+$); HRMS (CI) calcd for $C_{15}H_{20}O_5N_5{}^{79}Br_2$ $[M^{79}Br^{79}Br+H]^+$ 507.9831, observed 507.9835.

(*Z*)-Methyl 2-hydroxycyclooct-1-enecarboxylate 71[172]

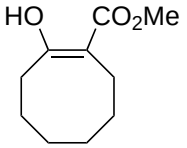

To a solution of dimethyl carbonate (1.4 g, 16 mmol) in toluene (20 mL) was added sodium hydride (0.88 g, 24 mmol). The resulting mixture was heated to 90 °C and a solution of cyclooctanone **70** (1.0 g, 7.9 mmol) in toluene (5 mL) was added dropwise over 30 min. The resultant mixture was stirred at reflux for 4 h. The reaction mixture was cooled down to 20 °C and AcOH (2 mL) was added. The resulting precipitate was then dissolved by addition of 2 M HCl (6 mL). The mixture was extracted with toluene (3×30 mL) the combined organic layers washed with sat. aq. $NaHCO_3$ (20 mL), H_2O (20 mL), dried ($MgSO_4$), and concentrated *in vacuo*. Purification by flash column chromatography (10% Et_2O/petrol) yielded (methyl 2-oxocyclooctanecarboxylate **71** (1.4 g, 7.9 mmol, 99%) as a clear liquid: ^{1}H NMR (500 MHz, $CDCl_3$) (major tautomer) δ 12.51 (s, 1H), 3.75 (s, 3H), 2.42 – 2.32 (m, 4H), 1.77 – 1.66 (m, 2H), 1.56 – 1.42 (m, 6H); ^{13}C NMR (125 MHz, $CDCl_3$) (major tautomer) δ 176.3 (C), 173.5 (C), 99.2 (C), 51.5 (CH_3), 32.4 (CH_2), 30.0 (CH_2), 28.8 (CH_2), 26.6 (CH_2), 26.2 (CH_2), 24.0 (CH_2); IR (thin film) 2960, 2940, 2860, 1740, 1700 cm^{-1}.

Methyl 1-fluoro-2-oxocyclooctanecarboxylate 72[172]

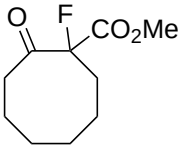

To a solution of (*Z*)-methyl 2-hydroxycyclooct-1-enecarboxylate **71** (4.5 g, 25 mmol) in dry MeCN (80 mL) was added Selectfluor™ (10 g, 29 mmol) at 0 °C. The resulting mixture was stirred at 55 °C for 16 h. The reaction mixture was poured into water (200 mL), extracted with EtOAc (3×200 mL), washed with brine (3×100 mL), dried ($MgSO_4$), and concentrated *in vacuo*. Purification by flash column chromatography (10% Et_2O/petrol) yielded methyl 1-fluoro-2-oxocyclooctanecarboxylate **72** (4.2 g, 21 mmol,

86%) as a white solid: m.p. 42 – 44 °C (*lit. m.p.*[172] 42 – 45 °C); ^{1}H NMR (500 MHz, $CDCl_3$) δ 3.75 (s, 3H), 2.69 – 2.46 (m, 3H), 2.22 – 2.16 (m, 1H), 1.84 – 1.79 (m, 2H), 1.69 – 1.56 (m, 3H), 1.47 – 1.33 (m, 3H); ^{13}C NMR (125 MHz, $CDCl_3$) δ 208.5 (d, $^{2}J_{\text{C-F}}$ = 22.1 Hz, C), 167.4 (d, $^{2}J_{\text{C-F}}$ = 24.9 Hz, C), 99.0 (d, $J_{\text{C-F}}$ = 200.6 Hz, C), 53.0 (CH_3), 38.7 (CH_2), 33.3 (d, $^{2}J_{\text{C-F}}$ = 22.1 Hz, CH_2), 27.3 (CH_2), 26.4 (CH_2), 24.3 (CH_2), 21.1 (CH_2); IR (thin film) 2924, 2853, 1751, 1713 cm^{-1}.

Methyl 1-fluorocyclooct-2-ynecarboxylate 73[172]

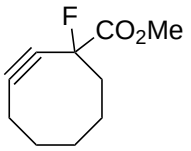

To a solution of methyl 1-fluoro-2-oxocyclooctanecarboxylate **72** (2.0 g, 9.9 mmol) in dry THF (200 mL) stirred at −78 °C was added a solution of KHMDS (0.91 M in THF, 33 mL, 30 mmol) dropwise over 10 min. After the addition was complete the reaction mixture was maintained for 30 min at −78 °C. Then a solution of Tf_2NPh (3.9 g, 11 mmol) in THF (30 mL) was added dropwise over 10 min. The reaction was stirred at −78 °C for 1 h. The reaction mixture was then warmed up to 20 °C and stirred for an additional 16 h. Methanol (15 mL) was then added and the reaction mixture was concentrated *in vacuo*. Purification by flash column chromatography (0 – 20% EtOAc/petrol) yielded methyl 1-fluorocyclooct-2-ynecarboxylate **73** (1.3 g, 7.4 mmol, 75%) as a yellow oil: ^{1}H NMR (500 MHz, $CDCl_3$) δ 3.83 (s, 3H), 2.41 – 2.20 (m, 4H), 2.06 – 1.85 (m, 4H), 1.77 – 1.66 (m, 1H), 1.50 – 1.42 (m, 1H); ^{13}C NMR (125 MHz, $CDCl_3$) δ 168.8 (d, $^{2}J_{\text{C-F}}$ = 27.8 Hz, C), 108.5 (d, $^{3}J_{\text{C-F}}$ = 9.6 Hz, C), 91.7 (d, $J_{\text{C-F}}$ = 186.2 Hz, C), 86.9 (d, $^{2}J_{\text{C-F}}$ = 31.7 Hz, C), 53.4 (CH_3), 46.2 (d, $^{2}J_{\text{C-F}}$ = 25.0 Hz, CH_2), 33.9 (CH_2), 29.2 (CH_2), 25.6 (CH_2), 20.7 (CH_2); IR (thin film) 2930, 2854, 2222, 1751 cm^{-1}.

1-Fluorocyclooct-2-yne-1-carboxylic acid 74[172]

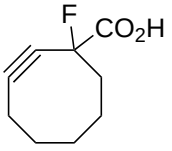

To a solution of methyl 1-fluorocyclooct-2-ynecarboxylate **73** (0.15 g, 0.82 mmol) in MeOH (2 mL) was added LiOH (69 mg, 1.6 mmol) in H_2O (2 mL). The reaction

mixture was heated at 50 °C for 10 min. Then the reaction was stirred at 20 °C for an additional 2 h. The reaction mixture was then cooled to 0 °C and diluted with water, acidified to pH 2 with diluted aq. HCl solution. The reaction mixture was extracted with EtOAc (3 × 10 mL), washed with brine (2 × 10 mL), dried ($MgSO_4$), and concentrated *in vacuo*. Purification by flash column chromatography (50% EtOAc/petrol) yielded 1-fluorocyclooct-2-yne-1-carboxylic acid **74** (0.12 g, 0.71 mmol, 87%) as a yellow liquid: ^{1}H NMR (300 MHz, $CDCl_3$) δ 2.45 – 2.30 (m, 4H), 2.07 – 1.86 (m, 4H), 1.78 – 1.68 (m, 1H), 1.52 – 1.45 (m, 1H); ^{13}C NMR (75 MHz, $CDCl_3$) δ 173.7 (d, $^2J_{C\text{-}F}$ = 29.1 Hz, C), 109.6 (d, $^3J_{C\text{-}F}$ = 9.9 Hz, C), 91.6 (d, $J_{C\text{-}F}$ = 185.8 Hz, C), 86.2 (d,$^2J_{C\text{-}F}$ = 31.7 Hz, C), 46.4 (d, $^2J_{C\text{-}F}$ = 24.6 Hz, CH_2), 33.9 (CH_2), 29.1 (CH_2), 25.6 (CH_2), 20.7 (CH_2); IR (thin film) 3474, 2932, 2850, 2220, 1732 cm^{-1}; HRMS (ES$^-$) calcd for $C_9H_{10}FO_2$ [M−H]$^-$ 169.0665, observed 169.0666.

_N,N'_-(((Oxybis(ethane-2,1-diyl))bis(oxy))bis(ethane-2,1-diyl))bis(1-fluoro cyclooct-2-ynecarboxamide) 78

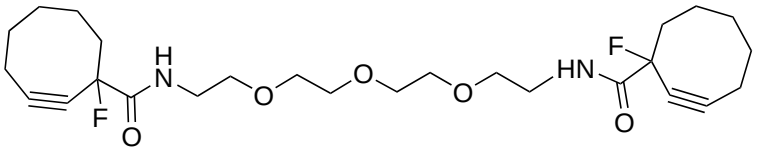

To a solution of 1-fluorocyclooct-2-ynecarboxylic acid **74** (0.23 g, 1.4 mmol) and DIPEA (0.48 mL, 2.7 mmol) in DMF (10 mL) was added HBTU (0.61 g, 1.6 mmol) and the reaction mixture stirred at 20 °C for 5 min. After this time, was added 1,11-diamino-3,6,9-trioxaundecane (0.13 g, 0.68 mmol) and the reaction mixture stirred at 20 °C for 4 h. Then the reaction mixture was diluted with H_2O (30 mL), extracted with EtOAc (3 × 15 mL), the combined organic layers were dried ($MgSO_4$) and concentrated *in vacuo*. The crude residue was purified by flash column chromatography (50% EtOAc/Et_2O) to afford *N,N'*-(((oxybis(ethane-2,1-diyl))bis(oxy))bis(ethane-2,1-diyl))bis(1-fluorocyclooct-2-ynecarboxamide) **78** (0.18 g, 0.37 mmol, 54%) as a yellow oil: ^{1}H NMR (600 MHz, $CDCl_3$) δ 7.21 (br. s, 2H), 3.62 – 3.50 (m, 12H), 3.50 – 3.35 (m, 4H), 2.35 – 2.15 (m, 8H), 2.05 – 1.74 (m, 8H), 1.64 – 1.55 (m, 2H), 1.42 – 1.30 (m, 2H); ^{13}C NMR (150 MHz, $CDCl_3$) δ 169.4 (d, $^2J_{C\text{-}F}$ = 24.0 Hz, C), 109.6 (d, $^3J_{C\text{-}F}$ = 10.6 Hz, C), 93.6 (d, $J_{C\text{-}F}$ = 186.2 Hz, C), 86.9 (d, $^2J_{C\text{-}F}$ = 31.6 Hz, C), 70.1 (CH_2), 70.0 (CH_2), 69.8 (CH_2), 46.5 (d, $^2J_{C\text{-}F}$ = 24.0 Hz, CH_2), 39.3 (CH_2), 33.8 (CH_2), 28.9 (CH_2), 25.6 (CH_2), 20.5 (CH_2); IR (thin

film) 3414, 1672 cm^{-1}; LRMS (ES^-) 495 (60, $[M-H]^-$), 475 (80), 455 (100); HRMS (ES^-) calcd for $C_{26}H_{37}O_5N_2F_2$ $[M-H]^-$ 495.2671, observed 495.2668.

1-(4-((4,5-Dibromo-3,6-dioxo-2-(prop-2-yn-1-yl)-2,3-dihydropyridazin-1(6*H*)-yl)methyl)phenyl)-4-fluoro-*N*-(1-(1-fluorocyclooct-2-yn-1-yl)-1-oxo-5,8,11-trioxa-2-azatridecan-13-yl)-4,5,6,7,8,9-hexahydro-1*H*-cycloocta[*d*][1,2,3]triazole-4-carboxamide 79

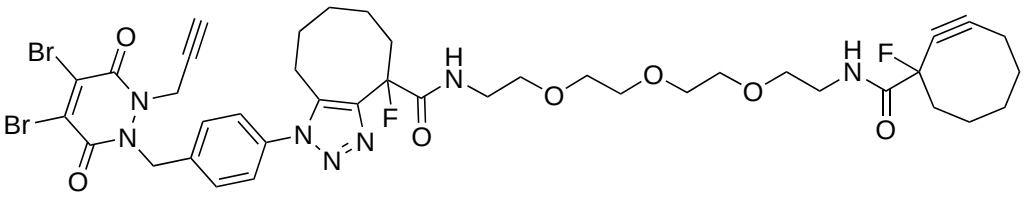

To a solution of *N,N'*-(((oxybis(ethane-2,1-diyl))bis(oxy))bis(ethane-2,1-diyl))bis(1-fluorocyclooct-2-ynecarboxamide) **78** (0.14 g, 0.28 mmol) in CH_2Cl_2 (5 mL) was added slowly a solution of 1-(4-azidobenzyl)-4,5-dibromo-2-(prop-2-yn-1-yl)-1,2-dihydropyridazine-3,6-dione **61** (50 mg, 0.11 mmol) in CH_2Cl_2 (3 mL) and the reaction mixture stirred at 20 °C for 16 h. After this time, the reaction mixture was concentrated *in vacuo* and the crude residue purified by flash column chromatography (1% MeOH/EtOAc) to afford 1-(4-((4,5-dibromo-3,6-dioxo-2-(prop-2-yn-1-yl)-2,3-dihydropyridazin-1(6*H*)-yl)methyl)phenyl)-4-fluoro-*N*-(1-(1-fluorocyclooct-2-yn-1-yl)-1-oxo-5,8,11-trioxa-2-azatridecan-13-yl)-4,5,6,7,8,9-hexahydro-1*H*-cycloocta[*d*][1,2,3]triazole-4-carboxamide **79** (33 mg, 0.04 mmol, 36%) as an inseparable mixture of diastereo- and regioisomers as a yellow oil: ^{1}H NMR (600 MHz, $CDCl_3$) δ 7.44 (d, J = 8.7 Hz, 2H), 7.42 (d, J = 8.7 Hz, 2H), 7.32 (br. s, 1H), 6.88 (br. s, 1H), 5.57 (t, J = 2.4 Hz, 2H), 4.77 (s, 2H), 3.71 – 3.51 (m, 14 H), 3.48 (t, J = 6.0 Hz, 2H), 3.02 – 2.92 (m, 1H), 2.92 – 2.84 (m, 1H), 2.73 – 2.58 (m, 1H), 2.48 (t, J = 2.4 Hz, 1H), 2.44 – 2.22 (m, 5H), 2.02 – 1.39 (m, 12H); ^{13}C NMR (150 MHz, $CDCl_3$) δ 170.9 (d, $^2J_{C\text{-}F}$ = 24.5 Hz, C), 168.6 (d, $^2J_{C\text{-}F}$ = 24.0 Hz, C), 153.5 (C), 153.0 (C), 143.1 (d, $^2J_{C\text{-}F}$ = 23.9 Hz, C), 136.7 (C), 136.4 (C), 136.2 (d, $^3J_{C\text{-}F}$ = 4.6 Hz, C), 135.4 (d, $^3J_{C\text{-}F}$ = 4.6 Hz, C), 128.2 (CH), 127.0 (CH), 126.9 (CH), 109.4 (d, $^3J_{C\text{-}F}$ = 10.5 Hz, C), 95.2 (C), 95.2 (C), 94.5 (d, $J_{C\text{-}F}$ = 186.7 Hz, C), 93.9 (C), 93.9 (C), 93.4 (C), 87.4 (d, $^2J_{C\text{-}F}$ = 31.5 Hz, C), 75.6 (C), 75.4 (CH), 70.7 (CH_2), 70.6 (CH_2), 70.6 (CH_2), 70.5 (CH_2), 70.4 (CH_2), 70.4 (CH_2), 69.7 (CH_2), 69.5 (CH_2), 50.2 (CH_2), 46.5 (d, $^2J_{C\text{-}F}$ = 24.5 Hz, CH_2), 39.4 (CH_2), 39.3 (CH_2), 37.4 (CH_2), 34.0 (CH_2), 33.3 (CH_2), 33.1 (CH_2), 29.0 (CH_2), 26.5 (CH_2), 25.8 (CH_2), 24.0 (CH_2), 22.3 (CH_2), 22.3 (CH_2), 21.8

(CH_2), 21.2 (CH_2), 20.7 (CH_2), 20.7 (CH_2); IR (thin film) 3440, 2107, 1677, 1647, 1574, 1518 cm^{-1}; LRMS (ES^+) 960 (50, $[M^{81}Br^{81}Br+Na]^+$), 958 (100, $[M^{81}Br^{79}Br+Na]^+$), 956 (50, $[M^{79}Br^{79}Br+Na]^+$); HRMS (ES^+) calcd for $C_{40}H_{48}O_7N_7{}^{79}Br_2F_2$ $[M^{79}Br_2+H]^+$ 934.1989, observed 934.1950.

Di-*tert*-butyl 1-(2-(*tert*-butoxy)-2-oxoethyl)-2-(prop-2-yn-1-yl)hydrazine-1,2-dicarboxylate 80

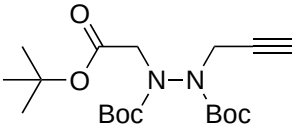

To a solution of di-*tert*-butyl 1-(prop-2-yn-1-yl)hydrazine-1,2-dicarboxylate **55** (0.50 g, 1.9 mmol) in DMF (15 mL) were added caesium carbonate (0.72 mg, 2.2 mmol) and *tert*-butyl bromoacetate (0.54 g, 2.8 mmol) and the reaction mixture stirred at 20 °C for 16 h. After this time, the reaction mixture was diluted with H_2O (50 mL), extracted with EtOAc (4 × 50 mL), the combined organic layers washed with sat. aq. LiCl (2 × 30 mL), dried ($MgSO_4$), and concentrated *in vacuo*. Purification by flash column chromatography (10% EtOAc/petrol) yielded di-*tert*-butyl 1-(2-(*tert*-butoxy)-2-oxoethyl)-2-(prop-2-yn-1-yl)hydrazine-1,2-dicarboxylate **80** (0.71 g, 1.9 mmol, 97%) as a colourless oil: ^1H NMR (600 MHz, $CDCl_3$) δ 4.58 – 4.35 (m, 2H), 4.16 – 4.01 (m, 1H), 3.67 – 3.64 (m, 1H), 2.18 (t, J = 2.3 Hz, 1H), 1.53 – 1.41 (m, 27H); ^{13}C NMR (150 MHz, $CDCl_3$) (major rotamer) δ 168.1 (C), 166.3 (C), 153.9 (C), 83.0 (C), 81.9 (C), 81.8 (C), 79.4 (C), 71.9 (CH), 53.5 (CH_2), 40.1 (CH_2), 28.3 (CH_3), 28.3 (CH_3), 28.1 (CH_3); IR (thin film) 3265, 2108, 1714 cm^{-1}; LRMS (CI) 385 (55, $[M+H]^+$), 329 (65), 273 (100); HRMS (CI) calcd for $C_{19}H_{33}O_6N_2$ $[M+H]^+$ 385.2333, observed 385.2319.

2-(4,5-Dibromo-3,6-dioxo-2-(prop-2-yn-1-yl)-2,3-dihydropyridazin-1(6*H*)-yl) acetic acid 81

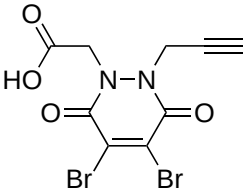

To a solution of di-*tert*-butyl 1-(2-(*tert*-butoxy)-2-oxoethyl)-2-(prop-2-yn-1-yl)hydrazine-1,2-dicarboxylate **80** (0.50 g, 1.3 mmol) in CH_2Cl_2 (10 mL) was added TFA (10 mL)

and the reaction mixture stirred at 20 °C for 2 h. After this time, all volatile materials were removed *in vacuo*. The crude residue was added to a solution of 2,3-dibromomaleic anhydride **58** (0.40 g, 1.6 mmol) in glacial AcOH (40 mL), and the reaction mixture was stirred at 20 °C for 16 h then heated at 130 °C for 2 h. Then the reaction mixture was concentrated *in vacuo*, and purification by flash column chromatography (3% MeOH/CH_2Cl_2 with 1% AcOH) yielded 2-(4,5-dibromo-3,6-dioxo-2-(prop-2-yn-1-yl)-2,3-dihydropyridazin-1(6*H*)-yl)acetic acid **81** (0.32 g, 0.87 mmol, 67%) as a white solid: m.p. 108 – 110 °C; ^{1}H NMR (600 MHz, MeOD) δ 4.95 (s, 2H), 4.91 (s, 2H), 2.98 (s, 1H); ^{13}C NMR (150 MHz, $CDCl_3$) δ 170.1 (C), 155.6 (C), 154.3 (C), 137.1 (C), 136.8 (C), 77.2 (C), 76.2 (CH), 50.3 (CH_2), 38.7 (CH_2); IR (solid) 3444, 3287, 2109, 1729, 1631 cm^{-1}; LRMS (CI) 369 (50, [M^{81}Br^{81}Br+H]$^+$), 367 (100, [M^{81}Br^{79}Br+H]$^+$), 365 (50, [M^{79}Br^{79}Br+H]$^+$); HRMS (CI) calcd for $C_9H_7N_2O_4{}^{79}Br_2$ [M^{79}Br^{79}Br+H]$^+$ 364.8767, observed 364.8762.

***Tert*-butyl (3-(2-(2-(3-aminopropoxy)ethoxy)ethoxy)propyl)carbamate 83**[173]

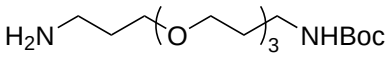

To a solution of 4,7,10-trioxa-1,13-tridecanediamine **82** (5.0 g, 23 mmol) in dioxane (100 mL) was added di-*tert*-butyl dicarbonate (0.85 g, 3.9 mmol) dropwise over 3 h. The reaction mixture was then stirred at 20 °C for 16 h and then poured into water (100 mL), extracted with CH_2Cl_2 (3 × 100 mL). The organic layer was then washed with brine (3 × 100 mL), dried ($MgSO_4$) and concentrated *in vacuo* to yield *tert*-butyl(3-(2-(2-(3-aminopropoxy)ethoxy)ethoxy)propyl)carbamate **83** (6.7 g, 21 mmol, 90 %) as a clear oil: ^{1}H NMR (500 MHz, $CDCl_3$) δ 5.12 (br. s, 1H), 3.62 – 3.49 (m, 12H), 3.21 – 3.18 (m, 2H), 2.78 – 2.75 (t, J = 6.7 Hz, 2H), 1.75 – 1.66 (m, 4H), 1.40 (s, 9H); ^{13}C NMR (125 MHz, $CDCl_3$) δ 156.1 (C), 78.9 (C), 70.7 (CH_2), 70.6 (CH_2), 70.3 (CH_2), 70.2 (CH_2), 69.6 (CH_2), 69.5 (CH_2), 39.7 (CH_2), 38.6 (CH_2), 33.5 (CH_2), 29.7 (CH_2), 28.5 (CH_3); LRMS (CI) 321 (50, [M+H]$^+$), 220 (100, [M-$C_5H_8O_2$]$^+$).

Tert-butyl (1-(cyclooct-2-yn-1-yl)-1-oxo-6,9,12-trioxa-2-azapentadecan-15-yl) carbamate 86

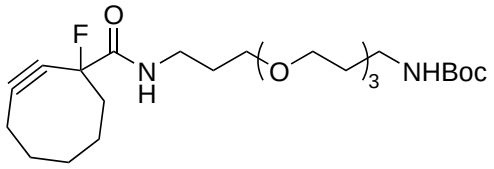

To a solution of methyl 1-fluorocyclooct-2-ynecarboxylate **73** (1.0 g, 5.0 mmol) in NEt_3 (6 mL) was added *tert*-butyl (3-(2-(2-(3-aminopropoxy)ethoxy)ethoxy)propyl)carbamate (4.8 g, 15 mmol). The reaction mixture was stirred at 20 °C for 48 h. After this time, all volatile materials were removed *in vacuo*. Purification by flash column chromatography (0% to 50% EtOAc/petrol) yielded *tert*-butyl (1-(cyclooct-2-yn-1-yl)-1-oxo-6,9,12-trioxa-2-azapentadecan-15-yl)carbamate **86** (1.7 g, 3.6 mmol, 72%) as a yellow oil: ^{1}H NMR (600 MHz, $CDCl_3$) δ 7.00 (br. s, 1H), 4.98 (br. s, 1H), 3.62 – 3.58 (m, 4H), 3.58 – 3.52 (m, 6H), 3.49 (t, J = 6.0 Hz, 2H), 3.37 (q, J = 6.0 Hz, 2H), 3.18 (q, J = 5.5 Hz, 2H), 2.43 – 2.16 (m, 4H), 2.07 – 1.98 (m, 1H), 1.98 – 1.87 (m, 2H), 1.86 – 1.66 (m, 5H), 1.66 – 1.58 (m, 1H), 1.44 – 1.33 (m, 10H); ^{13}C NMR (150 MHz, $CDCl_3$) δ 168.1 (d, $^2J_{C\text{-}F}$ = 24.1 Hz, C), 155.9 (C), 108.8 (d, $^3J_{C\text{-}F}$ = 10.5 Hz, C), 94.3 (d, $J_{C\text{-}F}$ = 186.4 Hz, C), 87.4 (d, $^2J_{C\text{-}F}$ = 31.6 Hz, C), 78.7 (C), 70.5 (CH_2), 70.4 (CH_2), 70.3 (CH_2), 70.1 (CH_2), 70.1 (CH_2), 69.5 (CH_2), 46.2 (d, $^2J_{C\text{-}F}$ = 24.1 Hz, CH_2), 38.5 (CH_2), 38.1 (CH_2), 33.8 (CH_2), 29.5 (CH_2), 28.8 (CH_2), 28.6 (CH_2), 28.3 (CH_3), 25.6 (CH_2), 20.5 (CH_2); IR (thin film) 3345, 2927, 2864, 2228, 1685, 1679 cm^{-1}; LRMS (CI) 473 (25, $[M+H]^+$), 373 (100, $[M\text{-}C_5H_8O_2]^+$); HRMS (CI) calcd for $C_{24}H_{42}FO_6N_2$ $[M+H]^+$ 473.3027, observed 473.3023.

Tert-butyl (1-(4,5-dibromo-3,6-dioxo-2-(prop-2-yn-1-yl)-3,6-dihydropyridazin-1(2*H*)-yl)-2-oxo-7,10,13-trioxa-3-azahexadecan-16-yl)carbamate 84

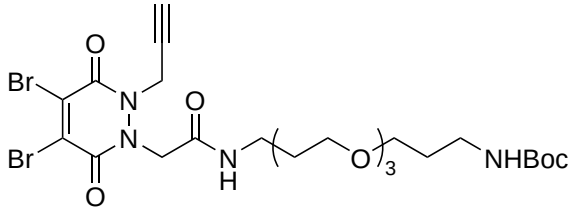

To a solution of 2-(4,5-dibromo-3,6-dioxo-2-(prop-2-yn-1-yl)-2,3-dihydropyridazin-1(6*H*)-yl)acetic acid **81** (93 mg, 0.26 mmol) in CH_2Cl_2 (5 mL) were added EDC·HCl (54 mg,

0.28 mmol) and NEt_3 (28 mg, 0.28 mmol). The resulting solution was stirred at 20 °C for 5 min. After this time, *tert*-butyl (3-(2-(2-(3-aminopropoxy)ethoxy)ethoxy)propyl) carbamate **83** (90 mg, 0.28 mmol) was added and the resulting solution was stirred at 20 °C for 4 h. Then, the reaction mixture was diluted with H_2O (15 mL), extracted with EtOAc (3 × 15 mL), the combined organic layers were dried ($MgSO_4$) and concentrated *in vacuo*. The crude residue was purified by flash column chromatography (5% MeOH/CH_2Cl_2) to afford *tert*-butyl (1-(4,5-dibromo-3,6-dioxo-2-(prop-2-yn-1-yl)-3,6-dihydropyridazin-1(2*H*)-yl)-2-oxo-7,10,13-trioxa-3-azahexadecan-16-yl)carbamate **84** (77 mg, 0.11 mmol, 44%) as a yellowish oil: ^{1}H NMR (500 MHz, $CDCl_3$) δ 7.07 (s, 1H), 5.00 (d, J = 2.5 Hz, 2H), 4.95 (t, J = 5.7 Hz, 1H), 4.87 (s, 2H), 3.68 – 3.63 (m, 4H), 3.62 – 3.56 (m, 6H), 3.52 (t, J = 6.0 Hz, 2H), 3.39 (q, J = 6.0 Hz, 2H), 3.19 (q, J = 6.4 Hz, 2H), 2.44 (t, J = 2.5 Hz, 1H), 1.84 – 1.69 (m, 4H), 1.48 – 1.36 (m, 9H); ^{13}C NMR (125 MHz, $CDCl_3$) δ 165.2 (C), 156.2 (C), 153.5 (C), 152.4 (C), 136.3 (C), 135.8 (C), 79.1 (C), 76.3 (C), 74.8 (CH), 70.5 (CH_2), 70.4 (CH_2), 70.2 (CH_2), 69.9 (CH_2), 69.5 (CH_2), 50.4 (CH_2), 38.5 (CH_2), 37.2 (CH_2), 29.8 (CH_2), 28.5 (CH_3). 89 ***N*-(1-(4,5-Dibromo-3,6-dioxo-2-(prop-2-yn-1-yl)-2,3-dihydropyridazin-1(6*H*)-yl)-2-oxo-7,10,13-trioxa-3-azahexadecan-16-yl)-1-fluorocyclooct-2-ynecarboxamide 85**

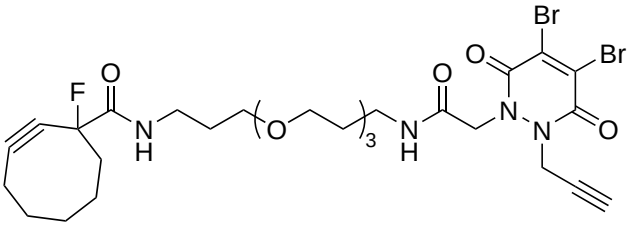

To a solution of *tert*-butyl (1-(cyclooct-2-yn-1-yl)-1-oxo-6,9,12-trioxa-2-azapentadecan-15-yl)carbamate **86** (50 mg, 0.11 mmol) in CH_2Cl_2 (3 mL) was added TFA (1.5 mL) dropwise at −20 °C and the reaction mixture stirred at −20 °C for 2 h. After this time, all volatile materials were removed *in vacuo*. The crude residue was then dissolved in CH_2Cl_2 (2 mL) and was added to a solution of 2-(4,5-dibromo-3,6-dioxo-2-(prop-2-yn-1-yl)-2,3-dihydropyridazin-1(6*H*)-yl)acetic acid **81** (39 mg, 0.11 mmol), EDC·HCl (22 mg, 0.12 mmol), and NEt_3 (24 mg, 0.23 mmol) in CH_2Cl_2 (3 mL). The resulting solution was stirred at 20 °C for 4 h. Then the reaction mixture was diluted with H_2O (15 mL), extracted with EtOAc (3 × 15 mL), the combined organic layers were dried ($MgSO_4$) and concentrated *in vacuo*. The crude residue was purified by flash column chromatography (5% MeOH/CH_2Cl_2) to

afford *N*-(1-(4,5-dibromo-3,6-dioxo-2-(prop-2-yn-1-yl)-2,3-dihydropyridazin-1(6*H*)-yl)-2-oxo-7,10,13-trioxa-3-azahexadecan-16-yl)-1-fluorocyclooct-2-ynecarboxamide **85** (16 mg, 0.02 mmol, 20%) as a yellowish oil: ^{1}H NMR (600 MHz, MeOD) δ 7.10 (br. s, 1H), 7.00 (br. s, 1H), 5.01 (d, J = 2.4 Hz, 2H), 4.88 (s, 2H), 3.69 – 3.64 (m, 4H), 3.63 – 3.55 (m, 8H), 3.40 (q, J = 5.8 Hz, 4H), 2.44 (t, J = 2.4 Hz, 1H), 2.42 – 2.20 (m, 4H), 2.11 – 2.03 (m, 1H), 2.02 – 1.89 (m, 2H), 1.89 – 1.75 (m, 6H), 1.49 – 1.39 (m, 1H); ^{13}C NMR (150 MHz, $CDCl_3$) δ 168.5 (d, $^{2}J_{C\text{-}F}$ = 24.1 Hz, C), 165.3 (C), 153.6 (C), 152.4 (C), 136.4 (C), 135.9 (C), 109.4 (d, $^{3}J_{C\text{-}F}$ = 10.6 Hz, C), 94.6 (d, $J_{C\text{-}F}$ = 186.4 Hz, C), 87.5 (d, $^{2}J_{C\text{-}F}$ = 31.6 Hz, C), 76.3 (C), 74.9 (CH), 70.5 (CH_2), 70.5 (CH_2), 70.4 (CH_2), 70.1 (CH_2), 70.1 (CH_2), 69.9 (CH_2), 50.5 (CH_2), 46.5 (d, $^{2}J_{C\text{-}F}$ = 24.5 Hz, CH_2), 38.8 (CH_2), 38.2 (CH_2), 37.3 (CH_2), 34.0 (CH_2), 29.0 (CH_2), 28.9 (CH_2), 28.5 (CH_2), 25.8 (CH_2), 20.7 (CH_2); IR (thin film) 3301, 2927, 2867, 2123, 1646 cm^{-1}; LRMS (ES^{+}) 723 (50, [M^{81}Br^{81}Br+H]$^{+}$), 721 (100, [M^{81}Br^{79}Br+H]$^{+}$), 719 (50, [M^{79}Br^{79}Br+H]$^{+}$); HRMS (ES^{+}) calcd for $C_{28}H_{38}O_7N_4{}^{79}Br_2F$ [M^{79}Br$_2$+H]$^{+}$ 719.1091, observed 719.1084.

((1*R*,8*S*,9*s*)-Bicyclo[6.1.0]non-4-yn-9-yl)methyl (2-(2-(2-(2-(4,5-dibromo-3,6-dioxo-2-(prop-2-yn-1-yl)-3,6-dihydropyridazin-1(2*H*)-yl)acetamido)ethoxy) ethoxy)ethyl)carbamate 98

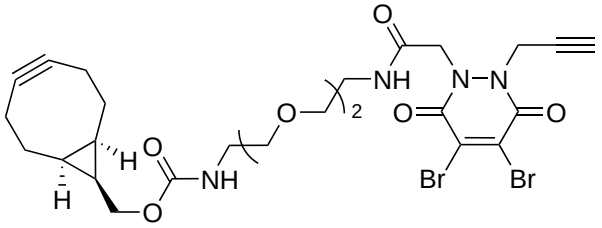

To a solution of 2-(4,5-dibromo-3,6-dioxo-2-(prop-2-yn-1-yl)-2,3-dihydropyridazin-1(6*H*)-yl)acetic acid **81** (38 mg, 0.10 mmol), HATU (44 mg, 0.12 mmol), and DIPEA (15 mg, 0.12 mmol) in DMF (2 mL). The resulting solution was stirred at 20 °C for 16 h. Then the reaction mixture was diluted with H_2O (15 mL), extracted with EtOAc (3 × 15 mL), the combined organic layers were dried ($MgSO_4$) and concentrated *in vacuo*. The crude residue was purified by flash column chromatography (neat EtOAc) to afford ((1*R*,8*S*,9*s*)-bicyclo[6.1.0]non-4-yn-9-yl)methyl (2-(2-(2-(2-(4,5-dibromo-3,6-dioxo-2-(prop-2-yn-1-yl)-3,6-dihydropyridazin-1(2*H*)-yl)acetamido)ethoxy)ethoxy)ethyl)carbamate **98** (30 mg, 46 µmol, 44%) as a yellowish oil: ^{1}H NMR (600 MHz, $CDCl_3$) δ 8.32 (br. s, 0.5H), 6.90 (br. s, 0.5H), 5.94 (br. s, 0.5H), 5.29 (br. s, 0.5H), 5.05 – 4.91 (m, 4H),

4.14 – 4.10 (m, 2H), 3.70 – 3.54 (m, 8H), 3.50 – 3.44 (m, 2H), 3.40 – 3.30 (m, 2H), 2.45 (s, 1H), 2.31 – 2.17 (m, 6H), 1.61 – 1.51 (m, 2H), 1.41 – 1.24 (m, 1H), 1.01 – 0.85 (m, 2H); ^{13}C NMR (150 MHz, $CDCl_3$) (major rotamer) δ 165.6 (C), 157.0 (C), 153.6 (C), 152.4 (C), 136.5 (C), 135.8 (C), 98.9 (C), 76.2 (C), 75.0 (CH), 70.7 (CH_2), 70.5 (CH_2), 70.3 (CH_2), 69.4 (CH_2), 63.0 (CH_2), 50.6 (CH_2), 40.9 (CH_2), 39.8 (CH_2), 38.7 (CH_3), 37.4 (CH_2), 29.1 (CH), 21.5 (CH_2), 20.2 (CH), 17.8 (CH_2); IR (thin film) 3304, 2916, 2111, 1680, 1644 cm^{-1}; LRMS (ES$^+$) 675 (50, [M^{81}Br^{81}Br+H]$^+$), 673 (100, [M^{81}Br^{79}Br+H]$^+$), 671 (50, [M^{79}Br^{79}Br+H]$^+$); HRMS (ES$^+$) calcd for $C_{26}H_{33}N_4O_7{}^{79}Br_2$ [M^{79}Br^{79}Br+H]$^+$ 671.0716, observed 671.0740.

_N_-Doxorubicin-14-azido-3,6,9,12-tetraoxatetradecan-1-amide 147

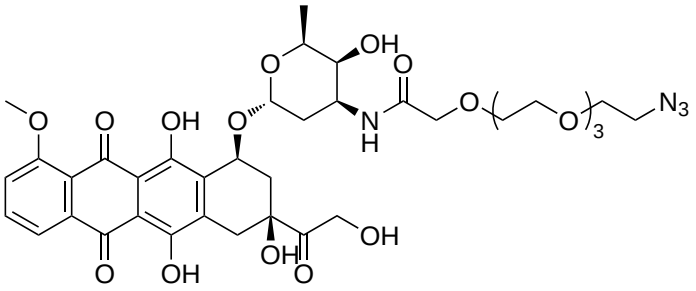

To a solution of 14-azido-3,6,9,12-tetraoxatetradecan-1-oic acid (4.4 mg, 16 µmol) and DIPEA (6.2 µL, 35 µmol) in DMF (1 mL) was added HBTU (6.7 mg, 18 µmol) and the reaction mixture stirred at 20 °C for 5 min. After this time, doxorubicin **143** (9.3 mg, 16 µmol) was added and the reaction mixture stirred at 20 °C for 3 h. Then the reaction mixture was diluted with H_2O (10 mL) and CH_2Cl_2 (10 mL), extracted with CH_2Cl_2 (3 × 15 mL), the combined organic layers washed with sat. aq. LiCl (2 × 10 mL) and acetate buffer pH 5.0, dried ($MgSO_4$) and concentrated *in vacuo*. The crude residue was purified by flash column chromatography (5% MeOH/EtOAc) to afford 14-azido-*N*-((2*S*,3*S*,4*S*,6*R*)-3-hydroxy-2-methyl-6-(((1*S*,3*S*)-3,5,12-trihydroxy-3-(2-hydroxyacetyl)-10-methoxy-6,11-dioxo-1,2,3,4,6,11-hexahydrotetracen-1-yl)oxy)tetrahydro-2*H*-pyran-4-yl)-3,6,9,12-tetraoxatetradecan-1-amide **147** (9.0 mg, 11 µmol, 70%) as a red solid: m.p. 61 – 64 °C; ^{1}H NMR (600 MHz, MeOD) δ 13.84 (1H, s), 13.05 (1H, s), 7.79 (1H, d, J = 7.5 Hz), 7.75 (1H, apt. t, J = 7.9 Hz), 7.48 (1H, d, J = 8.3 Hz), 5.38 – 5.42 (1H, m), 5.03 – 5.07 (1H, m), 4.74 (2H, d, J = 5.3 Hz), 4.29 (1H, q, J = 6.4 Hz), 4.18 – 4.23 (1H, m), 3.99 (3H, s), 3.58 – 3.70 (17H, m), 3.35 (2H, t, J = 5.3 Hz), 3.01 (1H, d, J = 18.4 Hz), 2.84 (1H, d, J = 18.4 Hz), 2.35 (1H, d, J = 14.3 Hz), 2.11 – 2.17 (1H, m), 2.00

(1H, m), 1.77 (1H, dd, J = 13.2, 4.5 Hz), 1.26 (3H, d, J = 6.8 Hz); ^{13}C NMR (150 MHz, MeOD) δ 214.8 (C), 187.9 (C), 187.6 (C), 172.0 (C), 162.4 (C), 157.3 (C), 156.1 (C), 137.2 (CH), 136.2 (C), 135.7 (C), 135.1 (C), 121.4 (C), 120.5 (CH), 120.2 (CH), 112.3 (C), 112.1 (C), 102.1 (CH), 77.3 (C), 71.9 (CH_2), 71.6 (CH_2), 71.5 (CH_2), 71.5 (CH_2), 71.3 (CH_2), 71.2 (CH_2), 71.1 (CH), 71.0 (CH_2), 69.8 (CH), 68.6 (CH), 65.7 (CH_2), 57.1 (CH_3), 51.7 (CH_2), 46.7 (CH), 37.3 (CH_2), 34.0 (CH_2), 30.7 (CH_2), 17.3 (CH_3); IR (solid) 3405, 3341, 2917, 2100, 1650, 1615, 1578 cm^{-1}; LRMS (ES$^+$) 825 (100, [M+Na]$^+$); HRMS (ES$^+$) calcd. for $C_{37}H_{46}N_4O_{16}Na$ [M+Na]$^+$ 825.2808, observed 825.2807.

4-(6-(Pyrimidin-2-yl)-1,2,4,5-tetrazin-3-yl)benzoic acid 150[220]

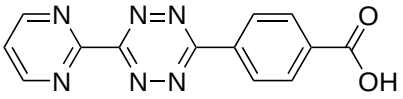

To a solution of 2-pyrimidinecarbonitrile **148** (3.6 g, 34 mmol) in 20 mL ethanol were added 4-cyanobenzoic acid **149** (5.0 g, 34 mmol) and hydrazine monohydrate (8.5 g, 8.3 mL, 0.17 mol). Then the solution was stirred and heated under reflux for 16 h. After cooling to 20 °C, the solid was collected by filtration and washed with acetone (2 × 50 mL). To the remaining solid was added acetic acid (100 mL) followed by an aqueous solution of $NaNO_2$ (3.5 g, 51 mmol) at 5 °C and the reaction mixture stirred at 20 °C for 2 h. The purple colored tetrazine was collected and washed with water (3 × 20 mL). The solid was added into nearly boiled DMF and kept at this temperature for another 5 min. The DMF solution was filtered whilst it was hot. The filtrate was collected and dried *in vacuo* to yield 4-(6-(pyrimidin-2-yl)-1,2,4,5-tetrazin-3-yl)benzoic acid **150** (0.80 g, 2.7 mmol, 8%) as a purple solid: ^{1}H NMR (600 MHz, DMSO-d_6) δ 13.35 (br. s, 1H), 9.21 (d, J = 4.9 Hz, 2H), 8.71 (d, J = 8.4 Hz, 2H), 8.25 (d, J = 8.4 Hz, 2H), 7.85 (t, J = 4.9 Hz, 1H); ^{13}C NMR (150 MHz, DMSO-d_6) δ 166.8 (C), 163.2 (C), 163.0 (C), 159.1 (C), 158.6 (CH), 135.4 (C), 130.3 (CH), 128.4 (CH), 127.9 (C), 123.1 (CH); LRMS (ES$^-$) 279 (100, [M−H]$^-$).

2,5-Dioxopyrrolidin-1-yl 6-(6-(pyrimidin-2-yl)-1,2,4,5-tetrazin-3-yl)benzoate 151[248]

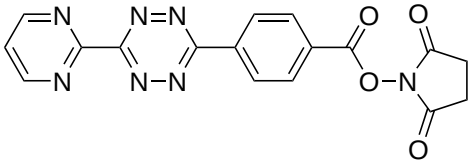

To a solution of 4-(6-(pyrimidin-2-yl)-1,2,4,5-tetrazin-3-yl)benzoic acid **150** (0.10 g, 0.36 mmol) and 1-ethyl-3-(3-dimethylaminopropyl)carbodiimide hydrochloride (83 mg, 0.43 mmol) in DMSO/pyridine (19:1, 5 mL) was added *N*-hydroxysuccinimide (62 mg, 0.54 mmol) and the reaction mixture was stirred at 40 °C for 3 h. Then, the reaction mixture was diluted with H_2O (50 mL), extracted with CH_2Cl_2 (1 × 30 mL), washed with brine (3 × 20 mL), the combined organic layers were dried ($MgSO_4$) and concentrated *in vacuo*. The crude residue was then redissolved in CH_2Cl_2 (7 mL) and precipitated with Et_2O (50 mL). The precipitate was collected by filtration, washed with Et_2O (50 mL) and dried *in vacuo* to yield 2,5-dioxopyrrolidin-1-yl 6-(6-(pyrimidin-2-yl)-1,2,4,5-tetrazin-3-yl)benzoate **151** (0.12 g, 32 mmol, 88%) as a red solid: ^{1}H NMR (600 MHz, DMSO-d_6) δ 9.22 (d, J = 4.9 Hz, 2H), 8.85 (d, J = 8.2 Hz, 2H), 8.43 (d, J = 8.2 Hz, 2H), 7.86 (t, J = 4.9 Hz, 1H), 2.94 (s, 4H); ^{13}C NMR (150 MHz, DMSO-d_6) δ 170.3 (C), 163.0 (C), 161.4 (C), 159.1 (C), 158.6 (CH), 137.8 (C), 131.1 (CH), 129.1 (CH), 127.9 (C), 123.2 (CH), 25.6 (CH_2); LRMS (ES^+) 400 (100, $[M+Na]^+$).

***N,N*'-(((Oxybis(ethane-2,1-diyl))bis(oxy))bis(propane-3,1-diyl))bis(4-(6-(pyrimidin-2-yl)-1,2,4,5-tetrazin-3-yl)benzamide) 152a**

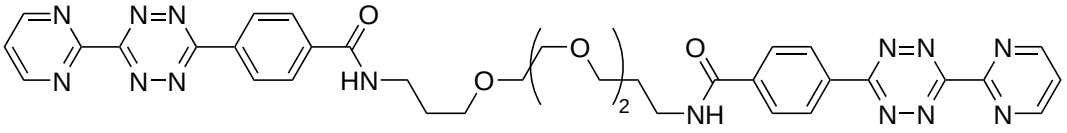

To a solution of 4,7,10-trioxa-1,13-tridecanediamine **82** (26 mg, 0.12 mmol) in DMSO/pyridine (19:1, 5 mL) was added 2,5-dioxopyrrolidin-1-yl 6-(6-(pyrimidin-2-yl)-1,2,4,5-tetrazin-3-yl)benzoate **151** (80 mg, 24 mmol) and the reaction mixture was stirred at 20 °C for 16 h. Then, the reaction mixture was diluted with H_2O (50 mL), extracted with CH_2Cl_2 (1×30 mL), washed with brine (3 × 20 mL), the combined organic layers were dried ($MgSO_4$) and concentrated *in vacuo*. Purification by flash column chromatography

(5% MeOH/CH_2Cl_2) yielded *N,N'*-(((oxybis(ethane-2,1-diyl))bis(oxy))bis(propane-3,1-diyl))bis(4-(6-(pyrimidin-2-yl)-1,2,4,5-tetrazin-3-yl)benzamide) **152a** (37 mg, 0.05 mmol, 41%) as a purple solid: ^{1}H NMR (600 MHz, $CDCl_3$) δ 9.13 (d, J = 4.9 Hz, 4H), 8.78 (d, J = 8.4 Hz, 4H), 8.09 (d, J = 8.4 Hz, 4H), 7.59 (t, J = 4.9 Hz, 2H), 7.50 (br. s, 2H), 3.75 – 3.58 (m, 16H), 1.96 – 1.88 (m, 4H); ^{13}C NMR (150 MHz, $CDCl_3$) δ 166.3 (C), 164.2 (C), 163.3 (C), 159.5 (C), 158.6 (CH), 139.2 (C), 133.7 (CH), 129.0 (CH), 128.2 (CH), 122.7 (CH), 71.0 (CH_2), 70.5 (CH_2), 70.3 (CH_2), 39.4 (CH_2), 28.9 (CH_2); IR (solid) 3292, 2962, 1632, 1561, 1539 cm^{-1}; LRMS (ES$^+$) 767 (100, [M+Na]$^+$); HRMS (ES$^+$) calcd. for $C_{36}H_{37}N_{14}O_5$ [M+H]$^+$ 745.3071, observed 745.3074.

***N,N'*-(3,6,9,12,15,18,21,24,27,30,33,36,39,42,45,48,51,54,57-Nonadecaoxa nonapentacontane-1,59-diyl)bis(4-(6-(pyrimidin-2-yl)-1,2,4,5-tetrazin-3-yl) benzamide) 152b**

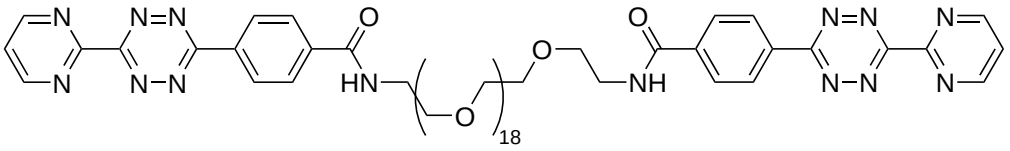

To a solution of *O,O'*-bis(2-aminoethyl)octadecaethylene glycol (0.11 g, 0.12 mmol) in DMSO/pyridine (19:1, 5 mL) was added 2,5-dioxopyrrolidin-1-yl 6-(6-(pyrimidin-2-yl)-1,2,4,5-tetrazin-3-yl)benzoate **151** (80 mg, 24 mmol) and the reaction mixture was stirred at 20 °C for 16 h. Then, the reaction mixture was diluted with H_2O (50 mL), extracted with CH_2Cl_2 (1×30 mL), washed with brine (3 × 20 mL), the combined organic layers were dried ($MgSO_4$) and concentrated *in vacuo*. Purification by flash column chromatography (5% MeOH/CH_2Cl_2) yielded *N,N'*-(3,6,9,12,15,18,21,24,27,30,33,36,39,42,45,48,51,54,57-nonadecaoxanonapentacontane-1,59-diyl)bis(4-(6-(pyrimidin-2-yl)-1,2,4,5-tetrazin-3-yl) benzamide) **152b** (82 mg, 0.04 mmol, 26%) as a purple solid: ^{1}H NMR (600 MHz, $CDCl_3$) δ 9.15 (d, J = 4.9 Hz, 4H), 8.80 (d, J = 8.3 Hz, 4H), 8.11 (d, J = 8.3 Hz, 4H), 7.61 (t, J = 4.9 Hz, 2H), 7.37 (br. s, 2H), 3.79 – 3.49 (m, 80H); ^{13}C NMR (150 MHz, $CDCl_3$) δ 166.6 (C), 164.2 (C), 163.3 (C), 159.5 (C), 158.6 (CH), 139.0 (C), 133.8 (CH), 129.0 (CH), 128.4 (CH), 122.8 (CH), 70.6 (CH_2), 70.6 (CH_2), 70.4 (CH_2), 69.9 (CH_2), 40.3 (CH_2); IR (solid) 3484, 2868, 1650, 1546 cm^{-1}; LRMS (ES$^+$) 1444 (100, [M+Na]$^+$); HRMS (ES$^+$) calcd. for $C_{66}H_{97}N_{14}O_{21}$ [M+H]$^+$ 1421.6953 observed 1421.6955.

***N,N'*-(4,7,10,13,16,19,22,25,28,31,34,37,40,43,46,49,52,55,58,61,64,67,70,73,76,79,82,85,88,91,94,97-Dotriacontaoxahectane-1,100-diyl)bis(4-(6-(pyrimidin-2-yl)-1,2,4,5-tetrazin-3-yl)benzamide) 152c**

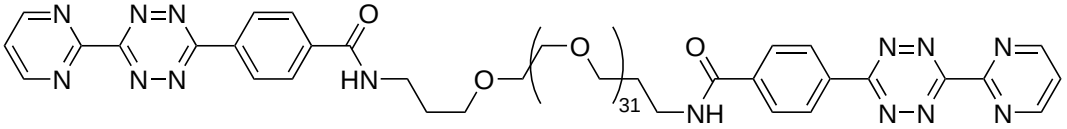

To a solution of *O,O'*-bis(3-aminopropyl)polyethylene glycol 1500 (0.18 g, 0.12 mmol) in DMSO/pyridine (19:1, 5 mL) was added 2,5-dioxopyrrolidin-1-yl 6-(6-(pyrimidin-2-yl)-1,2,4,5-tetrazin-3-yl)benzoate **151** (80 mg, 24 mmol) and the reaction mixture was stirred at 20 °C for 16 h. Then, the reaction mixture was diluted with H_2O (50 mL), extracted with CH_2Cl_2 (1×30 mL), washed with brine (3 × 20 mL), the combined organic layers were dried ($MgSO_4$) and concentrated *in vacuo*. Purification by flash column chromatography (5% MeOH/CH_2Cl_2) yielded *N,N'*-(4,7,10,13,16,19,22,25,28,31,34,37,40,43,46,49,52,55,58,61,64,67,70,73,76,79,82,85,88,91,94,97-dotriacontaoxahectane-1,100-diyl)bis(4-(6-(pyrimidin-2-yl)-1,2,4,5-tetrazin-3-yl)benzamide) **152c** (0.19 g, 0.09 mmol, 71%) as a purple solid: ^{1}H NMR (600 MHz, $CDCl_3$) δ 9.11 (d, J = 4.9 Hz, 4H), 8.76 (d, J = 8.3 Hz, 4H), 8.04 (d, J = 8.3 Hz, 4H), 7.58 (t, J = 4.9 Hz, 2H), 7.50 (br. s, 2H), 3.76 – 3.48 (m, 130H), 1.90 (quint., J = 5.7 Hz, 4H); ^{13}C NMR (150 MHz, $CDCl_3$) δ 166.1 (C), 164.1 (C), 163.2 (C), 159.5 (C), 158.5 (CH), 139.2 (C), 133.6 (CH), 128.8 (CH), 128.2 (CH), 122.7 (CH), 70.8 (CH_2), 70.6 (CH_2), 70.5 (CH_2), 70.3 (CH_2), 39.3 (CH_2), 28.7 (CH_2); IR (solid) 2921, 1656, 1562 cm^{-1}; LRMS (MALDI) 2024±44 (100, [M]).

1,2-Diethyl-1,2-dihydro-pyridazine-3,6-dione 102[52]

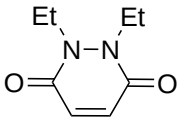

To a solution of maleic anhydride **57** (98 mg, 1.0 mmol) in glacial AcOH (3 mL) was added *N,N'*-diethylhydrazine·2HCl (0.16 g, 1.0 mmol) and the reaction mixture heated at 130 °C for 16 h. The solvent was removed *in vacuo* and the crude residue purified by column chromatography (50% EtOAc/petrol to neat EtOAc) to give 1,2-diethyl-1,2-dihydro-pyridazine-3,6-dione **102** (0.12 g, 0.72 mmol, 72%) as a white solid: ^{1}H NMR (600 MHz, $CDCl_3$) δ 6.85 (s, 2H), 4.11 (q, J = 7.0 Hz, 4H), 1.25 (t, J = 7.0 Hz, 6H); ^{13}C

NMR (150 MHz, $CDCl_3$) δ 157.6 (C), 134.7 (CH), 40.2 (CH_2), 13.3 (CH_3); IR (solid) 2984, 1636, 1590 cm^{-1}; LRMS (CI) 169 (100, $[M+H]^+$); HRMS (CI) calcd for $C_8H_{13}N_2O_2$ $[M+H]^+$ 169.0977, observed 169.0980.

4-Bromo-1,2-diethyl-1,2-dihydro-pyridazine-3,6-dione 103[52]

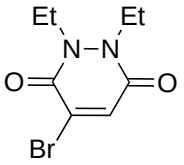

To a solution of 1,2-diethyl-1,2-dihydro-pyridazine-3,6-dione **102** (0.17 g, 1.0 mmol) in CH_2Cl_2 (3 mL) was added Br_2 (1.6 g, 0.51 mL, 10 mmol) and the reaction mixture stirred at 20 °C for 16 h. The solvent and excess Br_2 were removed *in vacuo* and then NEt_3 (0.41 g, 0.56 mL, 4.0 mmol) and CH_2Cl_2 (3 mL) were added and the reaction mixture stirred at 20 °C for 16 h. The solvent was removed *in vacuo* and the crude residue purified by column chromatography (50% EtOAc/petrol to neat EtOAc) to give 4-bromo-1,2-diethyl-1,2-dihydro-pyridazine-3,6-dione **103** (0.23 g, 0.92 mmol, 92%) as a yellow solid: m.p. 80 – 82 °C; ^{1}H NMR (600 MHz, $CDCl_3$) δ 7.31 (s, 1H), 4.14 (q, J = 7.0 Hz, 2H), 4.07 (q, J = 7.0 Hz, 2H), 1.26 (t, J = 7.0 Hz, 3H), 1.22 (t, J = 7.0 Hz, 3H); ^{13}C NMR (150 MHz, $CDCl_3$) δ 156.2 (C), 154.3 (C), 136.0 (CH), 133.7 (C), 41.9 (CH_2), 40.7 (CH_2), 13.3 (CH_3), 13.3 (CH_3); IR (solid) 3058, 2979, 2938, 1631, 1595 cm^{-1}; LRMS (CI) 249 (100, $[M^{81}Br+H]^+$), 247 (100, $[M^{79}Br+H]^+$); HRMS (CI) calcd for $C_8H_{12}BrN_2O_2$ $[M^{81}Br+H]^+$ 249.0082, observed 249.0086.

4,5-Dibromo-1,2-diethyl-1,2-dihydro-pyridazine-3,6-dione 104[52]

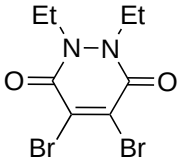

To a solution of 4-bromo-1,2-diethyl-1,2-dihydro-pyridazine-3,6-dione **103** (0.25 mg, 1.0 mmol) in CH_2Cl_2 (3 mL) was added Br_2 (1.6 g, 0.51 mL, 10 mmol) and the reaction mixture stirred at 50 °C for 72 h. The solvent and excess Br_2 were removed *in vacuo* and then NEt_3 (0.41 g, 0.56 mL, 4.0 mmol) and CH_2Cl_2 (3 mL) were added and the reaction mixture stirred at 20 °C for 16 h. The solvent was removed *in vacuo* and the crude residue purified by column chromatography (50% EtOAc/petrol to neat EtOAc)

to give 4,5-dibromo-1,2-diethyl-1,2-dihydro-pyridazine-3,6-dione **104** (0.30 g, 0.91 mmol, 91%) as a yellow solid: m.p. 112 – 114 °C ^{1}H NMR (600 MHz, $CDCl_3$) δ 4.17 (q, J = 7.0 Hz, 4H), 1.28 (t, J = 7.0 Hz, 6H); ^{1}C NMR (150 MHz, $CDCl_3$) δ 153.3 (C), 136.1 (C), 42.4 (CH_2), 13.2 (CH_3); IR (solid) 2979, 2937, 1630, 1574 cm^{-1}; LRMS (EI) 328 (50, $[M^{81}Br^{81}Br]^{+\bullet}$), 326 (100, $[M^{81}Br^{79}Br]^{+\bullet}$), 324 (50, $[M^{79}Br^{79}Br]^{+\bullet}$); HRMS (EI) calcd for $C_8H_{10}Br_2N_2O_2$ $[M^{79}Br^{79}Br]^{+\bullet}$ 323.9104, observed 323.9097.

Tri-*tert*-butyl 2-methylhydrazine-1,1,2-tricarboxylate 114[181]

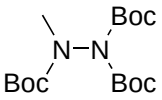

To a solution of methylhydrazine **113** (1.0 g, 1.1 mL 22 mmol), NEt_3 (4.3 g, 6.0 mL, 43 mmol) and DMAP (0.26 g, 2.2 mmol) in CH_2Cl_2 (75 mL) was added Boc_2O (19 g, 87 mmol) and the reaction mixture stirred at 20 °C for 72 h. Then the reaction mixture was diluted with H_2O (80 mL), extracted with EtOAc (3 × 60 mL), the combined organic layers were dried ($MgSO_4$) and concentrated *in vacuo*. The crude residue was purified by flash column chromatography (20% EtOAc/petrol) to afford tri-*tert*-butyl 2-methylhydrazine-1,1,2-tricarboxylate **114** (7.4 g, 22 mmol, 99%) as a yellowish oil: ^{1}H NMR (600 MHz, $CDCl_3$) (major rotamer) δ 3.05 (s, 3H), 1.51 – 1.43 (m, 27H); ^{13}C NMR (150 MHz, $CDCl_3$) (major rotamer) δ 154.0 (C), 150.1 (C) 83.4 (C), 81.4 (C), 35.7 (CH_3), 28.3 (CH_3), 28.1 (CH_3); LRMS (ES^+) 369 (100, $[M+Na]^+$).

Di-*tert*-butyl 1-methylhydrazine-1,2-dicarboxylate 109[180]

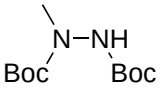

To a solution of tri-*tert*-butyl 2-methylhydrazine-1,1,2-tricarboxylate **114** (2.0 g, 5.8 mmol), in dry MeCN (15 mL) was added $Mg(ClO_4)_2$ (0.27 g, 1.2 mmol) and the reaction mixture stirred at 20 °C for 1 h. Then the reaction mixture was diluted with 10% aq. citric acid (20 mL) and Et_2O (15 mL), extracted with Et_2O (3 × 20 mL), the combined organic layers were dried ($MgSO_4$) and concentrated *in vacuo*. The crude residue was purified by flash column chromatography (15% EtOAc/petrol) to afford di-*tert*-butyl 1-methylhydrazine-1,2-dicarboxylate **109** (1.3 g, 5.2 mmol, 89%) as a white solid: m.p. 54 – 55 °C (*lit. m.p.*[180] 55 – 56 °C); ^{1}H NMR (600 MHz, $CDCl_3$) (major rotamer) δ 6.40

(br. s, 1H), 3.11 (s, 3H), 1.48 – 1.45 (m, 18H); ^{13}C NMR (150 MHz, $CDCl_3$) (major rotamer) δ 155.9 (C), 155.1 (C) 81.3 (C), 81.1 (C), 37.6 (CH_3), 28.3 (CH_3), 28.1 (CH_3); IR (solid) 3316, 2978, 2932, 1701 cm^{-1}; LRMS (ES$^+$) 269 (100, [M+Na]$^+$); HRMS (ES$^+$) calcd. for $C_{11}H_{22}N_2O_4Na$ [M+Na]$^+$ 269.1477, observed 269.1476.

Di-*tert*-butyl 1-(2-(*t*-butoxy)-2-oxoethyl)-2-methylhydrazine-1,2-dicarboxylate 115

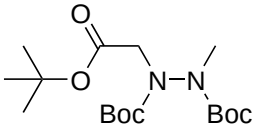

To a solution of di-*tert*-butyl 1-methylhydrazine-1,2-dicarboxylate **109** (0.94 g, 3.8 mmol) in DMF (20 mL) were added caesium carbonate (1.9 g, 5.7 mmol) and *tert*-butyl bromoacetate (1.1 g, 0.84 mL, 5.7 mmol) and the reaction mixture stirred at 20 °C for 16 h. After this time, the reaction mixture was diluted with H_2O (50 mL), extracted with Et_2O (4 × 50 mL), the combined organic layers washed with sat. aq. LiCl (2 × 30 mL), dried ($MgSO_4$), and concentrated *in vacuo*. Purification by flash column chromatography (10% Et_2O/petrol) yielded di-*tert*-butyl 1-(2-(*tert*-butoxy)-2-oxoethyl)-2-methylhydrazine-1,2-dicarboxylate **115** (1.3 g, 3.7 mmol, 98%) as a colourless oil: ^{1}H NMR (600 MHz, $CDCl_3$) δ 4.73 – 4.04 (m, 2H), 3.68 – 3.10 (m, 3H), 1.54 – 1.39 (m, 27H); ^{13}C NMR (150 MHz, $CDCl_3$) (major rotamer) δ 169.2 (C), 155.2 (C), 81.9 (C), 81.6 (C), 81.1 (C), 52.7 (CH_2), 36.8 (CH_3), 28.4 (CH_3), 28.3 (CH_3), 28.2 (CH_3); IR (thin film) 2978, 1748 cm^{-1}; LRMS (ES$^+$) 361 (100, [M+H]$^+$); HRMS (ES$^+$) calcd for $C_{17}H_{33}O_6N_2$ [M+H]$^+$ 361.2339, observed 361.2333.

2-(4,5-Dibromo-2-methyl-3,6-dioxo-3,6-dihydropyridazin-1(2*H*)-yl)acetic acid 116

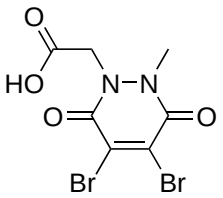

To a solution of di-*tert*-butyl 1-(2-(*tert*-butoxy)-2-oxoethyl)-2-methylhydrazine-1,2-dicarboxylate **115** (1.0 g, 2.8 mmol) in CH_2Cl_2 (10 mL) was added TFA (10 mL) and the reaction mixture stirred at 20 °C for 2 h. After this time, all volatile materials were

removed *in vacuo*. The crude residue was added to a solution of 2,3-dibromomaleic anhydride **58** (0.75 g, 2.8 mmol) in glacial AcOH (40 mL), and the reaction mixture stirred at 20 °C for 16 h heated at 130 °C for 16 h. Then the reaction mixture was concentrated *in vacuo*, and purification by flash column chromatography (3% MeOH/CH_2Cl_2 with 1% AcOH) yielded 2-(4,5-dibromo-2-methyl-3,6-dioxo-3,6-dihydropyridazin-1(2*H*)-yl)acetic acid **116** (0.65 g, 1.9 mmol, 73%) as a white solid: m.p. 210 – 214 °C; ^{1}H NMR (600 MHz, MeOD) δ 4.96 (s, 2H), 3.62 (s, 3H); ^{13}C NMR (150 MHz, MeOD) δ 170.2 (C), 154.8 (C), 154.0 (C), 137.4 (C), 135.7 (C), 49.5 (CH_2), 35.0 (CH_3); IR (solid) 3023, 2969, 1731, 1662 cm^{-1}; LRMS (ES$^-$) 338 (50, [M^{81}Br^{81}Br-H]$^-$), 340 (100, [M^{81}Br^{79}Br-H]$^-$), 342 (50, [M^{79}Br^{79}Br-H]$^-$); HRMS (ES$^-$) calcd for $C_7H_5N_2O_4{}^{79}Br_2$ [M^{79}Br^{79}Br-H]$^-$ 337.8538, observed 337.8540.

Perfluorophenyl 2-(4,5-dibromo-2-methyl-3,6-dioxo-3,6-dihydropyridazin-1(2*H*)-yl)acetate 118

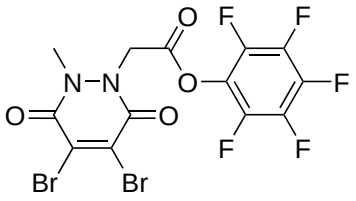

To a solution of 2-(4,5-dibromo-2-methyl-3,6-dioxo-3,6-dihydropyridazin-1(2*H*)-yl)acetic acid **116** (50 mg, 0.15 mmol) in dioxane (5 mL) were added DCC (33 mg, 0.16 mmol) and pentafluorophenol (32 mg, 0.18 mmol). The resulting solution was stirred at 20 °C for 16 h. Then the reaction mixture was diluted with H_2O (15 mL), extracted with EtOAc (3×15 mL), the combined organic layers were washed with sat. aq. sodium bicarbonate (3×10 mL), dried ($MgSO_4$) and concentrated *in vacuo*. The crude residue was purified by flash column chromatography (0 – 2% EtOAc/CH_2Cl_2) to afford perfluorophenyl 2-(4,5-dibromo-2-methyl-3,6-dioxo-3,6-dihydropyridazin-1(2*H*)-yl)acetate **118** (25 mg, 50 µmol, 34%) as a yellowish oil: ^{1}H NMR (500 MHz, $CDCl_3$) δ 5.23 (s, 2H), 3.67 (s, 3H); ^{13}C NMR (125 MHz, $CDCl_3$) δ 163.1 (C), 153.6 (C), 152.8 (C), 137.6 (C), 134.6 (C), 47.6 (CH_2), 34.8 (CH_3).

_N_-(2-(2-(2-Azidoethoxy)ethoxy)ethyl)-2-(4,5-dibromo-2-methyl-3,6-dioxo-3,6-dihydropyridazin-1(2_H_)-yl)acetamide 120

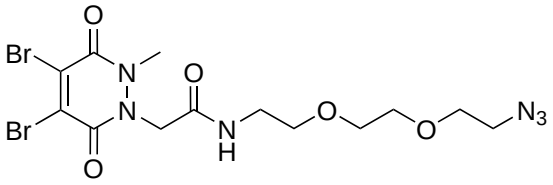

To a solution of perfluorophenyl 2-(4,5-dibromo-2-methyl-3,6-dioxo-3,6-dihydropyridazin-1(2*H*)-yl)acetate **118** (19 mg, 37 µmol) in CH_2Cl_2 (0.5 mL) were added 2-(2-(2-azidoethoxy)ethoxy)ethan-1-amine **119** (9.0 mg, 41 µmol), and NEt_3 (5.6 mg, 5.8 µL, 55 µmol). The resulting solution was stirred at 20 °C for 16 h. Then the reaction mixture was diluted with H_2O (5 mL), extracted with EtOAc (3 × 10 mL), the combined organic layers were washed with sat. aq. sodium bicarbonate (3 × 5 mL), dried ($MgSO_4$) and concentrated *in vacuo*. The crude residue was purified by flash column chromatography (0 – 5% MeOH/CH_2Cl_2) to afford *N*-(2-(2-(2-azidoethoxy)ethoxy)ethyl)-2-(4,5-dibromo-2-methyl-3,6-dioxo-3,6-dihydropyridazin-1(2*H*)-yl)acetamide **120** (15 mg, 30 µmol, 81%) as a yellowish oil: ^{1}H NMR (500 MHz, $CDCl_3$) δ 6.84 (t, J = 5.6 Hz, 1H), 4.73 (s, 2H), 3.72 – 3.61 (m, 14H), 3.60 – 3.56 (m, 2H), 3.48 (td, J = 5.6, 4.6 Hz, 2H), 3.41 (t, J = 4.6 Hz, 2H), 1.74 (s, 2H); ^{13}C NMR (125 MHz, $CDCl_3$) δ 165.4 (C), 152.5 (C), 152.2 (C), 137.0 (C), 134.7 (C), 70.7 (CH_2), 70.5 (CH_2), 70.4 (CH_2), 70.0 (CH_2), 69.4 (CH_2), 50.8 (CH_2), 39.8 (CH_2), 35.0 (CH_3); IR (thin film) 3247, 2965, 2101, 1688, 1634 cm^{-1}; LRMS (ES$^+$) 501 (50, [M^{81}Br^{81}Br+H]$^+$), 499 (100, [M^{81}Br^{79}Br+H]$^+$), 497 (50, [M^{79}Br^{79}Br+H]$^+$); HRMS (ES$^+$) calcd for $C_{13}H_{19}N_6O_5{}^{79}Br_2$ [M^{79}Br^{79}Br+H]$^+$ 496.9784, observed 496.9790.

((1_R_,8_S_,9_s_)-Bicyclo[6.1.0]non-4-yn-9-yl)methyl (2-(2-(2-(4,5-dibromo-2-methyl-3,6-dioxo-3,6-dihydropyridazin-1(2_H_)-yl)acetamido)ethoxy)ethoxy)ethyl)carbamate 121

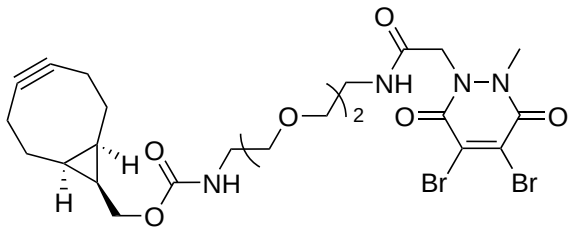

To a solution of 2-(4,5-dibromo-2-methyl-3,6-dioxo-3,6-dihydropyridazin-1(2*H*)-yl)acetic acid **116** (86 mg, 0.25 mmol), PyBOP (0.14 g, 0.28 mmol), and DIPEA (36 mg,

0.28 mmol) in CH_2Cl_2 (5 mL). The resulting solution was stirred at 20 °C for 16 h. Then the reaction mixture was diluted with H_2O (15 mL), extracted with EtOAc (3 × 15 mL), the combined organic layers were dried ($MgSO_4$) and concentrated *in vacuo*. The crude residue was purified by flash column chromatography (neat EtOAc) to afford ((1*R*,8*S*,9*s*)-bicyclo[6.1.0]non-4-yn-9-yl)methyl (2-(2-(2-(2-(4,5-dibromo-2-methyl-3,6-dioxo-3,6-dihydropyridazin-1(2*H*)-yl)acetamido)ethoxy)ethoxy)ethyl)carbamate **121** (87 mg, 0.14 mmol, 54%) as a yellowish oil: ^{1}H NMR (600 MHz, $CDCl_3$) δ 8.34 (br. s, 0.5H), 7.00 (br. s, 0.5H), 5.96 (br. s, 0.5H), 5.29 (br. s, 0.5H), 4.85 – 4.73 (m, 2H), 4.12 (d, J = 8.2 Hz, 2H), 3.76 – 3.50 (m, 11H), 3.50 – 3.43 (m, 2H), 3.40 – 3.30 (m, 2H), 2.31 – 2.17 (m, 6H), 1.61 – 1.51 (m, 2H), 1.41 – 1.24 (m, 1H), 1.01 – 0.85 (m, 2H); ^{13}C NMR (150 MHz, $CDCl_3$) (major rotamer) δ 165.6 (C), 157.8 (C), 153.4 (C), 152.5 (C), 137.0 (C), 134.8 (C), 98.9 (C), 70.8 (CH_2), 70.6 (CH_2), 70.5 (CH_2), 70.3 (CH_2), 70.2 (CH_2), 70.0 (CH_2), 69.6 (CH_2), 69.4 (CH_2), 63.0 (CH_2), 50.9 (CH_2), 40.9 (CH_2), 39.7 (CH_3), 35.0 (CH_2), 29.1 (CH), 21.5 (CH_2), 20.2 (CH), 17.8 (CH_2); IR (thin film) 3338, 2925, 1685, 1633 cm^{-1}; LRMS (ES$^+$) 651 (50, $[M^{81}Br^{81}Br+H]^+$), 649 (100, $[M^{81}Br^{79}Br+H]^+$), 647 (50, $[M^{79}Br^{79}Br+H]^+$); HRMS (ES$^+$) calcd for $C_{24}H_{33}N_4O_7{}^{79}Br_2$ $[M^{79}Br^{79}Br+H]^+$ 647.0716, observed 647.0713.

2-(4-Azidobenzyl)-4-bromo-1-(prop-2-yn-1-yl)-1,2-dihydropyridazine-3,6-dione 100

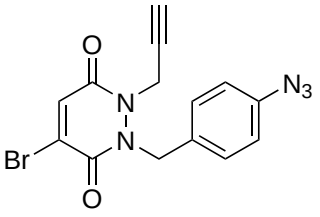

To a solution of di-*tert*-butyl 1-(4-azidobenzyl)-2-(prop-2-yn-1-yl)hydrazine-1,2-dicarboxylate **56** (0.24 mg, 0.59 mmol) in CH_2Cl_2 (9 mL) was added TFA (3 mL) and the reaction mixture stirred at 20 °C for 2 h. After this time, all volatile material was removed *in vacuo* using toluene to form an azeotrope. The crude residue was added to a solution of bromomaleic anhydride (0.13 g, 0.71 mmol) in glacial AcOH (15 mL), and the reaction mixture heated at 130 °C for 16 h. Then the reaction mixture was concentrated *in vacuo*, and purification by flash column chromatography (20% EtOAc/petrol) yielded

an inseparable mixture of regioisomers 2-(4-azidobenzyl)-4-bromo-1-(prop-2-yn-1-yl)-1,2-dihydropyridazine-3,6-dione and 1-(4-azidobenzyl)-4-bromo-2-(prop-2-yn-1-yl)-1,2-dihydropyridazine-3,6-dione **100** (0.13 g, 0.35 mmol, 60%) as an orange oil: ^{1}H NMR (600 MHz, $CDCl_3$) (major regioisomer) δ 7.42 (s, 1H), 7.23 (d, J = 8.3 Hz, 2H), 7.02 (d, J = 8.3 Hz, 2H), 5.47 (s, 2H), 4.68 (d, J = 2.5 Hz, 2H), 2.42 (t, J = 2.5 Hz, 1H); ^{13}C NMR (150 MHz, $CDCl_3$) (major regioisomer) δ 155.8 (C), 154.5 (C), 140.7 (C), 135.9 (CH), 134.6 (C), 131.2 (C), 128.5 (CH), 120.0 (CH), 76.1 (C), 74.7 (CH), 49.9 (CH_2), 35.4 (CH_2); IR (solid) 3299, 3140, 3066, 2970, 2249, 2110, 1637, 1596 cm^{-1}; LRMS (ES$^+$) 384 (100, [M^{81}Br+Na]$^+$), 382 (100, [M^{79}Br+Na]$^+$); HRMS (ES$^+$) calcd for $C_{14}H_{10}N_5O_5{}^{81}BrNa$ [M^{81}Br+Na]$^+$ 383.9897, observed 383.9721.

Methyl (*S*)-(2-(4-azidobenzyl)-3,6-dioxo-1-(prop-2-yn-1-yl)-1,2,3,6-tetrahydropyridazin-4-yl)-*N*-(*tert*-butoxycarbonyl)-L-cysteinate 175

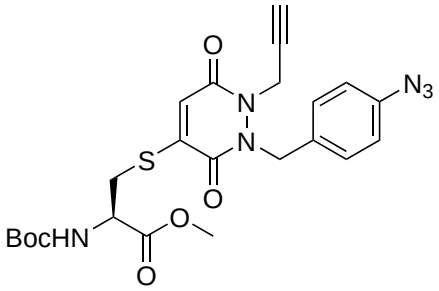

To a mixture of regioisomers 2-(4-azidobenzyl)-4-bromo-1-(prop-2-yn-1-yl)-1,2-dihydropyridazine-3,6-dione and 1-(4-azidobenzyl)-4-bromo-2-(prop-2-yn-1-yl)-1,2-dihydropyridazine-3,6-dione **100** (65 mg, 0.19 mmol) in CH_2Cl_2 (5 mL) were added NEt_3 (0.22 mg, 0.22 mmol) and *N*-(*tert*-butoxycarbonyl)-L-cysteine methyl ester (53 mg, 0.22 mmol) and the mixture was stirred at 20 °C for 2 h. The reaction mixture was then concentrated *in vacuo*, and purification by flash column chromatography (20% EtOAc/petrol) yielded an inseparable mixture of regioisomers methyl (*S*)-(1-(4-azidobenzyl)-3,6-dioxo-1-(prop-2-yn-1-yl)-1,2,3,6-tetrahydropyridazin-4-yl)-*N*-(*tert*-butoxycarbonyl)-L-cysteinate and methyl (*S*)-(2-(4-azidobenzyl)-3,6-dioxo-1-(prop-2-yn-1-yl)-1,2,3,6-tetrahydropyridazin-4-yl)-*N*-(*tert*-butoxycarbonyl)-L-cysteinate **175** (86 mg, 0.17 mmol, 89%) as a yellow viscous oil: ^{1}H NMR (600 MHz, $CDCl_3$) (major regioisomer) δ 7.22 (m, 2H), 7.00 (d, J = 8.4 Hz, 2H), 6.65 (s, 1H), 5.52 – 5.31 (m, 3H), 4.75 – 4.58 (m, 3H), 3.80 (s, 3H), 3.36 (m, J = 5.0 Hz, 1H), 3.24 (m, J = 5.0 Hz, 1H), 2.38 (t, J = 2.5 Hz, 1H), 1.44 (s, 9H); ^{13}C NMR (150 MHz, $CDCl_3$) (major regioisomer) δ 170.5

(C), 156.4 (C), 155.1 (C), 149.9 (C), 140.5 (C), 131.3 (C), 128.5 (CH), 122.8 (CH), 119.9 (CH), 80.9 (C), 76.2 (C), 74.4 (CH), 53.3 (CH_3), 52.0 (CH), 48.1 (CH_2), 35.6 (CH_2), 33.3 (CH_2), 28.4 (CH_3); IR (film) 3289, 2974, 2241, 2109, 1744, 1710, 1628 cm^{-1}; LRMS (ES^+) 537 (100, $[M+Na]^+$); HRMS (ES^+) calcd for $C_{23}H_{26}N_6O_6SNa$ $[M+Na]^+$ 537.1532, observed 537.1533.

Methyl *N*-(*tert*-butoxycarbonyl)-(*S*)-(3-hydroxy-6-oxo-1-(prop-2-yn-1-yl)-1, 6-dihydropyridazin-4-yl)-L-cysteinate 177

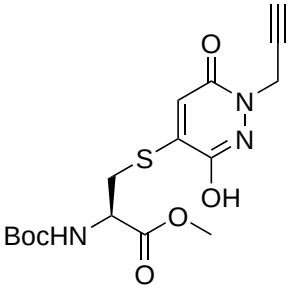

To a an mixture of regioisomers methyl (*S*)-(1-(4-azidobenzyl)-3,6-dioxo-1-(prop-2-yn-1-yl)-1,2,3,6-tetrahydropyridazin-4-yl)-*N*-(*tert*-butoxycarbonyl)-L-cysteinate and methyl (*S*)-(2-(4-azidobenzyl)-3,6-dioxo-1-(prop-2-yn-1-yl)-1,2,3,6-tetrahydropyridazin-4-yl)-*N*-(*tert*-butoxycarbonyl)-L-cysteinate **175** (20 mg, 44 µmol) in DMF (2 mL) was added TCEP·HCl (13 mg, 53 µmol) and the mixture was stirred at 20 °C for 2 h. The reaction mixture was then concentrated *in vacuo*, and purification by flash column chromatography (5% MeOH/CH_2Cl_2) yielded methyl *N*-(*tert*-butoxycarbonyl)-(*S*)-(3-hydroxy-6-oxo-1-(prop-2-yn-1-yl)-1,6-dihydropyridazin-4-yl)-L-cysteinate **177** (14 mg, 36 µmol, 82%) as a yellow oil: ^1H NMR (600 MHz, $CDCl_3$) (major regioisomer) δ 6.80 (s, 1H), 5.42 (d, J = 7.4 Hz, 1H), 4.81 – 4.74 (m, 2H), 4.71 – 4.66 (m, 1H), 3.80 (s, 3H), 3.42 – 3.28 (m, 2H), 2.32 (t, J = 2.5 Hz, 1H), 1.45 (s, 9H); ^{13}C NMR (150 MHz, $CDCl_3$) (major regioisomer) δ 170.5 (C), 156.0 (C), 155.3 (C), 152.0 (C), 147.9 (C), 115.4 (CH), 81.0 (C), 73.1 (CH), 53.2 (CH_3), 52.4 (CH), 40.3 (CH_2), 33.0 (CH_2), 28.4 (CH_3); IR (film) 3295, 2960, 2922, 2851, 2109, 1743, 1708, 1637 cm^{-1}; LRMS (ES^+) 406 (100, $[M+Na]^+$); HRMS (ES^+) calcd for $C_{16}H_{18}N_3O_6SNa$ $[M+Na]^+$ 406.1049, observed 406.1049.

2-(4-Azidobenzyl)-4-(hexylthio)-1-(prop-2-yn-1-yl)-1,2-dihydropyridazine-3,6-dione 176

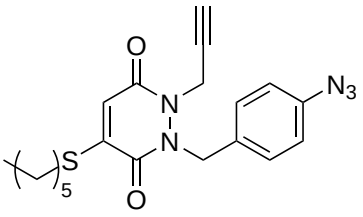

To a an mixture of regioisomers methyl (*S*)-(1-(4-azidobenzyl)-3,6-dioxo-1-(prop-2-yn-1-yl)-1,2,3,6-tetrahydropyridazin-4-yl)-*N*-(*tert*-butoxycarbonyl)-L-cysteinate and methyl (*S*)-(2-(4-azidobenzyl)-3,6-dioxo-1-(prop-2-yn-1-yl)-1,2,3,6-tetrahydropyridazin-4-yl)-*N*-(*tert*-butoxycarbonyl)-L-cysteinate **175** (86 mg, 0.17 mmol) in THF/PBS at pH 7.4 (1:1, 2 mL) was added hexane thiol (0.30 g, 2.6 mmol) and the mixture was stirred at 20 °C for 72 h. The reaction mixture was then concentrated *in vacuo*, and purification by flash column chromatography (20% EtOAc/petrol) yielded an inseparable mixture of regioisomers 2-(4-azidobenzyl)-4-(hexylthio)-1-(prop-2-yn-1-yl)-1,2-dihydropyridazine-3,6-dione and 1-(4-azidobenzyl)-4-(hexylthio)-2-(prop-2-yn-1-yl)-1,2-dihydropyridazine-3,6-dione (47 mg, 0.12 mmol, 71%) as a colourless oil: ^{1}H NMR (600 MHz, $CDCl_3$) (major regioisomer) δ 7.26 – 7.19 (m, 2H), 7.04 – 6.98 (m, 2H), 6.58 (s, 1H), 5.42 (s, 2H), 4.71 (d, J = 2.5 Hz, 2H), 2.80 (t, J = 7.4 Hz, 2H), 2.41 (t, J = 2.5 Hz, 1H), 1.79 – 1.70 (m, 2H), 1.52 – 1.44 (m, 2H), 1.37 – 1.30 (m, 4H), 0.94 – 0.88 (m, 3H); ^{13}C NMR (150 MHz, $CDCl_3$) (major regioisomer) δ 157.0 (C), 155.7 (C), 150.7 (C), 140.3 (C), 131.9 (C), 128.3 (CH), 121.8 (CH), 119.9 (CH), 76.3 (C), 74.5 (CH), 48.1 (CH_2), 35.5 (CH_2), 31.4 (CH_2), 31.0 (CH_2), 28.8 (CH_2), 27.3 (CH_2), 22.6 (CH_2), 14.1 (CH_3); IR (film) 3245, 2955, 2928, 2856, 2243, 2108, 1680, 1631 cm^{-1}; LRMS (ES$^+$) 398 (100, [M+H]$^+$); HRMS (ES$^+$) calcd for $C_{20}H_{24}N_5O_2S$ [M+H]$^+$ 398.1651, observed 398.1654.

***N*-(2-Azidoethyl)-5-(dimethylamino)naphthalene-1-sulfonamide 162**[249]

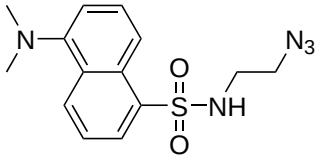

To a solution of dansyl chloride (0.27 g, 1.0 mmol) in CH_2Cl_2 (10 mL) were added 2-bromoethylamine hydrobromide (0.21 g, 1.0 mmol) and NEt_3 (0.28 mL, 2.0 mmol).

The reaction mixture was stirred at 20 °C for 4 h. After this time, all volatile material was removed *in vacuo*. The crude residue was then added to a solution of NaN_3 (0.16 g, 2.5 mmol) in MeCN (10 mL), and the reaction mixture heated at 90 °C for 16 h. Then, the reaction mixture was concentrated *in vacuo*, and purification by flash column chromatography (50% Et_2O/petrol) yielded *N*-(2-azidoethyl)-5-(dimethylamino)naphthalene-1-sulfonamide **162** as a light green oil (0.19 g, 0.59 mmol 59%): ^{1}H NMR (600 MHz, $CDCl_3$) δ 8.57 (d, J = 8.5 Hz, 1H), 8.28 – 8.23 (m, 2H), 7.60 (dd, J = 8.5, 7.3 Hz, 1H), 7.53 (dd, J = 8.5, 7.3 Hz, 1H), 7.21 (d, J = 7.3 Hz, 1H), 4.99 (t, J = 6.4 Hz, 1H), 3.34 – 3.28 (m, 2H), 3.09 – 3.02 (m, 2H), 2.90 (s, 6H); ^{13}C NMR (150 MHz, $CDCl_3$) δ 152.2 (C),134.5 (C), 130.9 (CH), 130.0 (C), 129.8 (CH), 129.6 (C), 128.8 (CH), 123.3 (CH), 118.6 (CH), 115.5 (CH), 51.0 (CH_2), 45.6 (CH_3), 42.5 (CH_2); HRMS (ES$^+$) calcd for $C_{14}H_{18}N_5O_2S$ $[M+H]^+$ 320.1181, observed 320.1184.

_N_-methoxycarbonyl-3-bromomaleimide 106[170]

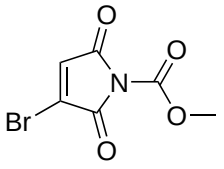

To a solution of 3-bromomaleimide (0.20 g, 1.1 mmol) and *N*-methylmorpholine (0.13 mL, 1.1 mmol) in THF (10 mL) was added methylchloroformate (88 µL, 1.1 mmol) and the reaction mixture was stirred for 30 min at 20 °C. After this time, the reaction mixture was diluted with CH_2Cl_2 (20 mL), the organic phase was washed with H_2O, dried ($MgSO_4$), and concentrated *in vacuo* to yield *N*-methoxycarbonyl-3-bromomaleimide **106** (0.27 g, 1.1 mmol, 100%) as a pale pink solid: m.p. 120 – 122 °C; ^{1}H NMR (600 MHz, $CDCl_3$) δ 7.04 (s, 1H), 4.01 (s, 3H); ^{13}C NMR (150 MHz, $CDCl_3$) δ 163.5 (C), 160.9 (C), 147.6 (C), 133.3 (C), 133.1 (CH), 54.7 (CH_3); IR (solid) 1808, 1763, 1724, 1603, 1438, 1320, 1263, 1070 cm^{-1}.

Di-*tert*-butyl 1-ethylhydrazine-1,2-dicarboxylate 110

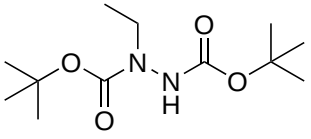

To a solution of di-*tert*-butyl hydrazine-1,2-dicarboxylate **54** (7.0 g, 30 mmol) and caesium carbonate (4.0 g, 12 mmol) in DMF (50 mL) was added bromoethane (0.64 mL,

6.0 mmol) and the reaction mixture stirred at 20 °C for 16 h. After this time, the reaction mixture was diluted with EtOAc (75 mL) and washed with H_2O (3 × 40 mL) and brine (3 × 30 mL). The organic phase was then concentrated *in vacuo*, and cold hexane was added to the crude residue to precipitate out and recover the excess di-*tert*-butyl hydrazine-1,2-dicarboxylate **54** as a white solid through recrystallisation and filtration. The filtrate was then concentrated further *in vacuo*, and purification by flash column chromatography (5 – 15% EtOAc/petrol) yielded di-*tert*-butyl 1-ethylhydrazine-1,2-dicarboxylate **110** (0.64 g, 2.5 mmol, 41%) as a white crystalline solid: m.p. 54 – 57 °C; ^{1}H NMR (600 MHz, $CDCl_3$) δ 6.15 (br. s, 1H), 3.49 (m, 2H), 1.48 – 1.45 (m, 18H), 1.14 (t, J = 7.3 Hz, 3H); ^{13}C NMR (150 MHz, $CDCl_3$) δ 155.3 (C), 81.2 (C), 81.0 (C), 45.8 (CH_2), 44.1 (CH_2), 28.4 (CH_3), 28.3 (CH_3), 12.7 (CH_3); IR (solid) 3313, 2978, 2934, 1706 cm^{-1}; LRMS (ES$^+$) 261 (100, [M+H]$^+$); HRMS (ES$^+$) calcd for $C_{12}H_{24}N_2O_4$ [M+H]$^+$ 261.1814, observed 261.1813.

Di-*tert*-butyl 1,2-diethylhydrazine-1,2-dicarboxylate 112

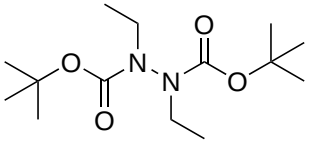

To a solution of di-*tert*-butyl hydrazine-1,2-dicarboxylate **54** (1.0 g, 4.3 mmol) and caesium carbonate (5.6 g, 17 mmol) in DMF (20 mL) was added bromoethane (1.1 g, 10 mmol) and the reaction mixture stirred at 20 °C for 24 h. After this time, the reaction mixture was diluted with EtOAc (50 mL) and washed with H_2O (4 × 20 mL) and brine (2 × 20 mL). The organic phase was then concentrated *in vacuo*, and purification by flash column chromatography (50% EtOAc/petrol) yielded di-*tert*-butyl 1,2-diethylhydrazine-1,2-dicarboxylate **112** (1.1 g, 3.8 mmol, 88%) as a colourless oil. ^{1}H NMR (300 MHz, $CDCl_3$) δ 3.57 – 3.33 (m, 4H), 1.50 – 1.39 (m, 18H), 1.16 (t, J = 7.2 Hz, 6H); ^{13}C NMR (75 MHz, $CDCl_3$) δ 155.1 (C), 80.6 (C), 46.37 (CH_2), 44.37 (CH_2), 28.35 (CH_3), 28.27 (CH_3), 13.56 (CH_3), 12.95 (CH_3); IR (thin film) 2980, 2927, 2881, 1698 cm^{-1}; LRMS (ES$^+$) 288 (100, [M+H]$^+$); HRMS (ES$^+$) calcd for $C_{16}H_{32}N_2O$ [M+H]$^+$ 288.2049, observed 288.2054.

A.3 Protein modification

A.3.1 Antibody modification

A.3.1.1 Antibody digestion

Attempted preparation of a trastuzumab Fab using the protocol described by K. L. Bennett *et al.*[191]

In accordance with the report by K. L. Bennett *et al.*,[191] trastuzumab **19** (6.4 mg·mL^{-1}) in digestion buffer was reacted with a 1/10 amount (wt/wt) of immobilised papain (250 µg·mL^{-1} of gel) for 20 h at 37 °C under nitrogen in a buffer containing 20 mM sodium phosphate monobasic, 10 mM disodium EDTA and 80 mM cysteine·HCl (pH 7.0). The cysteine·HCl was incorporated immediately before trastuzumab digestion. After digestion, the mixture was centrifuged at 200 *g* for 5 min and the supernatant was removed for purification. The supernatant was concentrated to a volume of 200 µL using a diafiltration column (30 kDa MWCO) to purify it from low-molecular-weight proteolytic contaminants, and buffer exchanged into phosphate-buffered saline (PBS, pH 7.0) by passage through diafiltration columns (30 kDa MWCO) four times with excessive PBS (pH 7.0). Finally, the sample was analysed by LCMS and revealed a mixture of Fab products, LCMS: observed masses: 47 309 and 47 675 Da.

Preparation of trastuzumab Fab using sequential digests with pepsin and papain

Immobilised pepsin (0.15 mL) was washed with digestion buffer (20 mM sodium acetate trihydrate, pH 3.1) four times and trastuzumab **19** (0.5 mL, 6.4 mg·mL^{-1} in digestion buffer) was added. The mixture was incubated for 5 h at 37 °C whilst shaking (1100 rpm). The resin was separated from the digest using a filter column, and washed with digest buffer (50 mM phosphate, 1 mM EDTA, 150 mM NaCl, pH 6.8) three times. The digest was combined with the washes and the volume adjusted to 0.5 mL. The sample was analysed by LCMS and revealed formation of F(ab')$_2$ **125**, LCMS: observed mass: 97 303 Da. After this, papain (1.0 mL, 0.25 mg·mL^{-1}) was activated with 10 mM DTT (in digest buffer: 50 mM phosphate, 1 mM EDTA, 150 mM NaCl, pH 6.8) under an argon atmosphere whilst shaking (1100 rpm) for 1 h at 25 °C in the dark. The resin was washed with digest buffer (without DTT) four times and the 0.5 mL of F(ab')$_2$ **125**

added. The mixture was incubated for 16 h at 37 °C whilst shaking (1100 rpm) in the dark. Then the resin was separated from the digest using a filter column, and washed with PBS (pH 7.0) three times. The digest was combined with the washes and the buffer was exchanged completely for PBS (pH 7.4) using diafiltration columns (10 kDa MWCO) and the volume adjusted to 0.4 mL. The digest was analysed by SDS-PAGE and LCMS to reveal formation of a single Fab_{Her} fragment **127**: observed mass 47 650 Da. The concentration of Fab_{Her} was determined by UV/VIS using a molecular extinction coefficient of $\varepsilon_{280} = 68\,590\,\text{M}^{-1}\cdot\text{cm}^{-1}$. [Fab] = $3.3\,\text{mg}\cdot\text{mL}^{-1}$ (0.40 mL, 64%).

Preparation of rituximab Fab using digest with papain

Immobilised papain (0.3 mL, $0.25\,\text{mg}\cdot\text{mL}^{-1}$) was activated with 10 mM DTT (in digest buffer: 50 mM phosphate, 1 mM EDTA, 150 mM NaCl, pH 6.8) under an argon atmosphere whilst shaking (1100 rpm) for 1 h at 25 °C in the dark. The resin was washed with digest buffer (without DTT) four times and rituximab **122** (3 mg in 0.5 mL of digest buffer) was added. The mixture was incubated for 16 h at 37 °C whilst shaking (1100 rpm) in the dark. Then the resin was separated from the digest using a filter column, and washed with PBS (pH 7.0) three times. The digest was combined with the washes and the buffer was exchanged completely for PBS (pH 7.4) using diafiltration columns (10 kDa MWCO) and the volume adjusted to 1.5 mL. Then, the sample was applied to a NAb protein A column (Thermo Scientific) and incubated at 20 °C under constant agitation for 1 h. The Fab fraction, Fab_{Rit} **123**, was eluted according to manufacturers' protocol, the column washed three times with PBS (pH 7.4) and the Fc fraction, Fc_{Rit} **124**, eluted four times with 0.2 M glycine·HCl, pH 2.5, which was neutralised with 10% of the volume of a 1 M Tris, pH 8.5 solution. The Fab_{Rit} **123** fraction was combined with the washes and both Fab_{Rit} and Fc_{Rit} solutions were buffer exchanged into PBS using diafiltration columns (10 kDa MWCO). The digests were analysed by SDS-PAGE and LCMS to reveal formation of Fab_{Rit} **123**: observed mass 47 185 Da, and glycosylated Fc_{Rit} **124**: observed mass 52 922 Da. The concentration of Fab_{Rit} **123** was determined by UV/VIS using a molecular extinction coefficient of $\varepsilon_{280} = 82\,905\,\text{M}^{-1}\cdot\text{cm}^{-1}$.

A.3.1.2 General procedures

General procedure for the preparation of the Fab_{Her}-Pyridazinedione conjugate (Fab_{Her}-PD)

To a solution of Fab_{Her} **127** (50 µL, 30 µM, 1.4 mg·mL^{-1}, 1 eq.) in borate buffer (25 mM sodium borate, 25 mM NaCl, 1 mM EDTA, pH 8.0) was added TCEP (final concentration 90 µM, 3 eq.) and the reaction mixture incubated at 37 °C for 90 min. After this time, was added a solution of pyridazinedione in DMF (final concentration 1.5 mM, 5 eq.) and the reaction mixture incubated at 37 °C for 1 h. The excess reagents were then removed by repeated diafiltration into fresh buffer using VivaSpin sample concentrators (GE Healthcare, 10 000 MWCO). Following this, analysis by LCMS revealed > 99% conversion to the conjugate.

General procedure for the preparation of the Her-Pyridazinedione conjugate (Her-PD)

To a solution of Fab_{Her} **127** (50 µL, 30 µM, 1.4 mg·mL^{-1}, 1 eq.) in borate buffer (25 mM sodium borate, 25 mM NaCl, 1 mM EDTA, pH 8.0) was added TCEP (final concentration 90 µM, 3 eq.) and the reaction mixture incubated at 37 °C for 90 min. After this time, was added a solution of pyridazinedione in DMF (final concentration 1.5 mM, 5 eq.) and the reaction mixture incubated at 37 °C for 1 h. The excess reagents were then removed by repeated diafiltration into fresh buffer using VivaSpin sample concentrators (GE Healthcare, 10 000 MWCO). Following this, analysis by SDS-PAGE and UV-Vis revealed > 95% conversion to the conjugate.

General procedure for Azide–Alkyne Huisgen Cycloaddition (CuAAC)

To a solution of "clickable" Fab_{Her}-Pyridazinedione **137** (50 µL, 42 µM, 2 mg·mL^{-1}) in PB (pH 7.4) containing tris(3-hydroxypropyltriazolylmethyl)amine (THPTA) (500 µM), $CuSO_4$ (100 µM) was added a cargo molecule (azide or alkyne) (final concentration 100 µM, 5 eq.) and sodium ascorbate (final concentration 5 mM) and the reaction mixture incubated at 25 °C for 1 h. The excess reagents were then removed by repeated diafiltration into fresh buffer using VivaSpin sample concentrators (GE Healthcare, 10 000 MWCO). Following this, analysis by LCMS revealed > 95% conversion to the conjugate.

General procedure for Strain-Promoted Azide–Alkyne Cycloaddition (SPAAC)

To a solution of "clickable" Fab_{Her}-Pyridazinedione **137** (50 µL, 21 µM, 1.0 mg·mL^{-1}) in PBS, PB, or BBS was added a cargo molecule (azide) and the reaction mixture incubated at 25 °C for 3 – 6 h. Following this, analysis by LCMS revealed > 95% conversion to the conjugate. The excess reagents were then removed by repeated diafiltration into fresh buffer using VivaSpin sample concentrators (GE Healthcare, 10 000 MWCO).

A.3.1.3 Preparation of Fab-PD constructs

Vide supra, Figure 2.3, page 51 for the structure of the PDs.

Preparation of Fab_{Her}-Diet 131

The general procedure for the preparation of a Fab_{Her}-PD conjugate was followed with Diet PD **104** as the bridging reagent.
Observed mass: 47 822 Da. Expected mass: 47 820 Da.

Preparation of Fab_{Her}-AzideAlkyne-Pyridazinedione conjugate (Fab_{Her}-Azal 137a)

The general procedure for the preparation of a Fab_{Her}-PD conjugate was followed with Azal PD **61** as the bridging reagent.
Observed mass: 47 925 Da. Expected mass: 47 924 Da.

Preparation of Fab_{Her}-PEGAzideAlkyne-Pyridazinedione conjugate (Fab_{Her}-Pazal 137b)

The general procedure for a preparation of the Fab_{Her}-PD conjugate was followed with Pazal PD **69** as the bridging reagent.
Observed mass: 47 994 Da. Expected mass: 47 994 Da.

Preparation of Fab_{Her}-AlkyneAcid-Pyridazinedione conjugate (Fab_{Her}-Alkac 137d)

The general procedure for a preparation of the Fab_{Her}-PD conjugate was followed with Alkac PD **81** as the bridging reagent.
Observed mass: 47 866 Da. Expected mass: 47 866 Da.

Preparation of Fab_{Her}-AzideMethyl-Pyridazinedione conjugate (Fab_{Her}-Azime)

The general procedure for a preparation of the Fab_{Her}-PD conjugate was followed with Azime PD **120** as the bridging reagent.
Observed mass: 47 977 Da. Expected mass: 47 974 Da.

Preparation of Fab_{Her}-BCN-MethylStrainedAlkyne-Pyridazinedione conjugate (Fab_{Her}-Mestra 137g)

The general procedure for a preparation of the Fab_{Her}-PD conjugate was followed with Mestra PD **121** as the bridging reagent.
Observed mass: 48 090 Da. Expected mass: 48 089 Da.

Preparation of Fab_{Her}-MFCO-AlkyneStrainedAlkyne-Pyridazinedione conjugate (Fab_{Her}-MFCOAstra 137c)

The general procedure for a preparation of the Fab_{Her}-PD conjugate was followed with MFCOAstra PD **79** as the bridging reagent.
Observed mass: 48 418 Da. Expected mass: 48 420 Da.

Preparation of Fab_{Her}-Soluble-AlkyneStrainedAlkyne-Pyridazinedione conjugate (Fab_{Her}-Solastra 137e)

The general procedure for a preparation of the Fab_{Her}-PD conjugate was followed with Solastra PD **85** as the bridging reagent.
Observed mass: 48 211 Da. Expected mass: 48 212 Da.

Preparation of Fab_{Her}-BCN-AlkyneStrainedAlkyne-Pyridazinedione conjugate (Fab_{Her}-BCNAstra 137f)

The general procedure for a preparation of the Fab_{Her}-PD conjugate was followed with BCNAstra PD **98** as the bridging reagent.
Observed mass: 48 174 Da. Expected mass: 48 172 Da.

A.3.1.4 Preparation of functionalised Fab_{Her}-PD

Preparation of Fab_{Her}-Azal-PEG_4 conjugate

The general procedure for CuAAC was followed with PEG_4-N_3 **64** as the cargo molecule and Fab_{Her}-Azal **137a** as the "clickable" Fab_{Her}-PD component.
Observed mass: 48 148 Da. Expected mass: 48 143 Da.

Preparation of Fab_{Her}-Alkac-PEG_4 conjugate 157

The general procedure for CuAAC was followed with $N_3-PEG_4-NH_2$ **119** as the cargo molecule and Fab_{Her}-Alkac as the "clickable" Fab_{Her}-PD component.
Observed mass: 48 036 Da. Expected mass: 48 040 Da.

Preparation of Fab_{Her}-Azime-Mestra conjugate

The general procedure for SPAAC was followed with Mestra PD **121** as the cargo molecule and Fab_{Her}-Azime as the "clickable" Fab_{Her}-PD component.
Observed mass: 48 614 Da. Expected mass: 48 620 Da.

Preparation of Fab_{Her}-Mestra-PEG_4 conjugate

The general procedure for SPAAC was followed with $N_3-PEG_4-NH_2$ **119** as the cargo molecule and Fab_{Her}-Mestra **137g** as the "clickable" Fab_{Her}-PD component.
Observed mass: 48 318 Da. Expected mass: 48 319 Da.

Preparation of Fab_{Her}-Mestra-Tetrazine conjugate 153

The general procedure for SPAAC was followed with tetrazine **152a** as the cargo molecule and Fab_{Her}-Mestra **137g** as the "clickable" Fab_{Her}-PD component.
Observed mass: 48 807 Da. Expected mass: 48 802 Da.

Preparation of Fab_{Her}-MFCOAstra-PEG_4 conjugate 155

The general procedure for SPAAC was followed with PEG_4-N_3 **64** as the cargo molecule and Fab_{Her}-MFCOAstra **137c** as the "clickable" Fab_{Her}-PD component.
Observed mass: 48 640 Da. Expected mass: 48 639 Da.

Preparation of Fab_{Her}-MFCOAstra-Dox

The general procedure for SPAAC was followed with Dox−PEG_4−N_3 **147** as the cargo molecule and Fab_{Her}-MFCOAstra **137c** as the "clickable" Fab_{Her}-PD component.
Observed mass: 49 253 Da. Expected mass: 49 257 Da.

Preparation of Fab_{Her}-Solastra-PEG_4 conjugate 156

The general procedure for SPAAC was followed with N_3−PEG_4−NH_2 **119** as the cargo molecule and Fab_{Her}-Solastra **137e** as the "clickable" Fab_{Her}-PD component.
Observed mass: 48 432 Da. Expected mass: 48 431 Da.

Preparation of Fab_{Her}-Solastra-AlexaFluor conjugate 181

The general procedure for SPAAC was followed with AlexaFluor488-Azide (Molecular Probes) **167** as the cargo molecule and Fab_{Her}-Solastra **137e** as the "clickable" Fab_{Her}-PD component.
Observed mass: 48 871 Da. Expected mass: 48 871 Da.

Preparation of Fab_{Her}-Solastra-Dox

The general procedure for SPAAC was followed with Dox−PEG_4−N_3 **147** as the cargo molecule and Fab_{Her}-Solastra **137e** as the "clickable" Fab_{Her}-PD component.
Observed mass: 49 016 Da. Expected mass: 49 013 Da.

Preparation of Fab_{Her}-BCNAstra-PEG_4 conjugate 155

The general procedure for SPAAC was followed with N_3−PEG_4−NH_2 **119** as the cargo molecule and Fab_{Her}-BCNAstra **137f** as the "clickable" Fab_{Her}-PD component.
Observed mass: 48 348 Da. Expected mass: 48 348 Da.

A.3.1.5 Preparation of dually functionalised Fab_{Her}-PD

Preparation of Fab_{Her}-MFCOAstra-PEG_4-PEG_4 conjugate

The general procedure for CuAAC was followed with PEG_4−N_3 **64** as the cargo molecule and Fab_{Her}-MFCOAstra-PEG_4 as the "clickable" Fab_{Her}-PD component.
Observed mass: 48 880 Da. Expected mass: 48 882 Da.

Preparation of Fab_{Her}-Solastra-PEG_4-Cy5 conjugate 158

The general procedure for CuAAC was followed with sulfo-Cy5 **145** as the cargo molecule and Fab_{Her}-Solastra-PEG_4 as the "clickable" Fab_{Her}-PD component.
Observed mass: 49 175 Da. Expected mass: 49 176 Da.

Preparation of Fab_{Her}-Solastra-Dox-PEG_{20k} 159

The general procedure for CuAAC was followed with $PEG_{20k}-N_3$ **144** as the cargo molecule and Fab_{Her}-Solastra-Dox as the "clickable" Fab_{Her}-PD component.

A.3.1.6 Other

Digestion of misbridged Her-Diet 130

The pepsin digestion procedure for trastuzumab **19** was followed with misbridged Her-Diet **130** as the antibody component. This yielded $F(ab)'_{Her}$-Diet **132**.
Observed mass: 48 989 Da. Expected mass: 48 993 Da.

Preparation of Fab_{Rit}-Diet

The general procedure for the preparation of a Fab_{Her}-PD conjugate was followed with Fab_{Rit} **123** and Diet PD **104** as the bridging reagent.
Observed mass: 47 350 Da. Expected mass: 47 351 Da.

Preparation of Fab_{Rit}-AzideAlkyne-Pyridazinedione conjugate (Fab_{Rit}-Azal)

The general procedure for the preparation of a Fab_{Her}-PD conjugate was followed with Fab_{Rit} **123** and Azal PD **61** as the bridging reagent.
Observed mass: 47 464 Da. Expected mass: 47 464 Da.

A.3.1.7 Stability and selectivity

Stability after 8 months at 4 °C

Fab_{Her}-Diet **131**, Fab_{Her}-PEG_{20k}-Dox **159** and Her-Solastra-Dox-Cy5 **161** (50 µL, 30 µM) were buffer exchanged into PBS (pH 7.4) by repeated diafiltration into fresh buffer using VivaSpin sample concentrators (GE Healthcare, 10 000 MWCO) and were incubated at 4 °C for *ca.* 8 months. Following this, analysis by LCMS revealed no trace of degradation

of Fab_{Her}-Diet **131** (expected mass: 47 820 Da, observed mass: 47 822 Da, *vide supra*, Figure 5.2b, page 88) and analysis by SDS-PAGE showed no degradation of the three conjugates **131**, **159** and **161** (*vide supra*, Figure 5.2a and Figure 5.3a and b respectively, page 88).

Stability under acidic pH

Fab_{Her}-Diet **131**, Fab_{Her}-PEG_{20k}-Dox **159** and Her-Solastra-Dox-Cy5 **161** (50 µL, 30 µM) were buffer exchanged into acetate buffer (20 mM sodium acetate trihydrate, pH 3.1) by repeated diafiltration into fresh buffer using VivaSpin sample concentrators (GE Healthcare, 10 000 MWCO) and were incubated at 37 °C for 24 h. Following this, analysis by LCMS revealed no trace of degradation of Fab_{Her}-Diet **131** (expected mass: 47 820 Da, observed mass: 47 822 Da, *vide supra*, Figure 5.2c, page 88) and analysis by SDS-PAGE showed no degradation of the three conjugates **131**, **159** and **161** (*vide supra*, Figure 5.2a and Figure 5.3a and b respectively, page 88).

Stability under basic pH

Fab_{Her}-Diet **131**, Fab_{Her}-PEG_{20k}-Dox **159** and Her-Solastra-Dox-Cy5 **161** (50 µL, 30 µM) were buffer exchanged into BBS (pH 9) by repeated diafiltration into fresh buffer using VivaSpin sample concentrators (GE Healthcare, 10 000 MWCO) and were incubated at 37 °C for 24 h. Following this, analysis by LCMS revealed no trace of degradation of Fab_{Her}-Diet **131** (expected mass: 47 820 Da, observed mass: 47 826 Da, *vide supra*, Figure 5.2d, page 88) and analysis by SDS-PAGE showed no degradation of the three conjugates **131**, **159** and **161** (*vide supra*, Figure 5.2a and Figure 5.3a and b respectively, page 88).

Stability in blood plasma mimicking conditions

Fab_{Her}-Diet **131**, Fab_{Her}-PEG_{20k}-Dox **159** and Her-Solastra-Dox-Cy5 **161** (200 µL, 40 µM) were buffer exchanged into SBF by repeated diafiltration into fresh buffer using VivaSpin sample concentrators (GE Healthcare, 10 000 MWCO) then, human serum albumin (HSA) (final concentration 600 µM) and glutathione (GSH) (final concentration 20 µM) were added. The resulting solutions were then incubated at 37 °C for 7 days. Following this, analysis by SDS-PAGE showed no reaction of the three conjugates **131**, **159** and **161** with GSH or HSA (*vide supra*, Figure 5.4 and Figure 5.5a and b respectively, page 89).

Selectivity control in the absence of TCEP

A solution of Fab_{Her} **127** (50 µL, 30 µM, 1 eq.) in BBS (25 mM sodium borate, 25 mM, 0.5 mM EDTA, pH 8.0) was incubated at 37 °C for 90 min. After this time was added a solution of Solastra PD **85** in DMF (final concentration 1.5 mM, 5 eq.) and the reaction mixture incubated at 37 °C for 1 h. The excess reagents were then removed by repeated diafiltration into fresh buffer using VivaSpin sample concentrators (GE Healthcare, 10 000 MWCO). Following this, analysis by LCMS revealed that no reaction occurred on Fab_{Her} **127** (expected mass: 47 652 Da, observed mass: 47 656 Da).

A.3.2 GFP modification

A.3.2.1 Cloning and expression of protein

The gene for GFP_{S147C} **140** in the vector pNIC28-Bsa4 was generated by Dr Rachel Morgan as described previously.[250]

Sequence:

MHHHHHHSSGVDLGTDNLYFQSMRKGEELFTGVVPILVELDGDVNGHKFSVRG
EGEGDATNGKLTLKFICTTGKLPVPWPTLVTTLTYGVQCFARYPDHMKQHDF
FKSAMPEGYVQERTISFKDDGTYKTRAEVKFEGDTLVNRIELKGIDFKEDGNIL
GHKLEYNFN*C*HNVYITADKQKNGIKANFKIRHNVEDGSVQLADHYQQNTPIGD
GPVLLPDNHYLSTQSVLSKDPNEKRDHMVLLEFVTAAGITHGMDELYK

Expected mass: 29 341 Da. Observed mass: 29 332 Da.

A.3.2.2 Preparation of GFP_{S147C}-PD

Pre-treatment procedure for reaction with GFP_{S147C} 140

Immediately prior to conjugation with GFP_{S147C} **140**, TCEP (10 µL, 10 mM as a solution in water, per 100 µL of protein (1.0 mg·mL^{-1} solution)) was added, incubated on ice for 1 h and the excess reducing agent removed by repeated diafiltration into fresh buffer (100 mM sodium phosphate, pH 8.0) using VivaSpin sample concentrators (GE Healthcare, 3000 MWCO).

Reaction of GFP_{S147C} 140 with 1,2-diethyl-1,2-dihydropyridazine-3,6-dione 102

1,2-Diethyl-1,2-dihydropyridazine-3,6-dione **102** (5 µL, 340 µM in DMF, 10 eq.) was added to GFP_{S147C} **140** (100 µL, 1.0 mg·mL^{-1}, 34 µM) in sodium phosphate buffer (100 mM, pH 8.0). The reaction mixture was incubated at 37 °C for 1 h. Excess reagents were removed by repeated diafiltration into fresh buffer (100 mM sodium phosphate, pH 8.0) using VivaSpin sample concentrators (GE Healthcare, 3000 MWCO). The samples were analysed by LCMS.
Expected mass: 29 501 Da. Observed mass: 29 503 Da.

Analogous reaction conditions when applied to 1-methyl-1,2-dihydropyridazine-3,6-dione **173** in place of 1,2-diethyl-1,2-dihydropyridazine-3,6-dione **102** showed no reaction, even after 16 h and 72 h time points.

Reaction of GFP_{S147C} 140 with 2-(4-azidobenzyl)-4-bromo-1-(prop-2-yn-1-yl)-1,2-dihydropyridazine-3,6-dione (mBr-Azal PD) 100 — Preparation of GFP_{S147C}-Azal 178

2-(4-Azidobenzyl)-4-bromo-1-(prop-2-yn-1-yl)-1,2-dihydropyridazine-3,6-dione (mBr-Azal PD) **100** (5 µL, 340 µM in DMF, 10 eq.) was added to GFP_{S147C} **140** (100 µL, 1.0 mg·mL^{-1}, 34 µM) in sodium phosphate buffer (100 mM, pH 8.0). The reaction mixture was incubated at 37 °C for 1 h. Excess reagents were removed by repeated diafiltration into fresh buffer (100 mM sodium phosphate, pH 8.0) using VivaSpin sample concentrators (GE Healthcare, 3000 MWCO). The samples were analysed by LCMS.
Expected mass: 29 612 Da. Observed mass: 29 613 Da.

A.3.2.3 Stability of GFP_{S147C}-PD

Reduction of GFP_{S147C}-Azal 178 with TCEP — Preparation of GFP_{S147C}-AlkOH 179

TCEP (10 µL, final concentration 340 µM, 10 eq.) was added to conjugate GFP_{S147C}-Azal **178** (90 µL, 1.0 mg·mL^{-1}, 34 µM) in sodium phosphate buffer (100 mM, pH 8.0). The reaction was incubated at 37 °C for 1.5 h. Excess reagents were removed by repeated diafiltration into fresh buffer (100 mM sodium phosphate, pH 8.0) using VivaSpin sample

concentrators (GE Healthcare, 3000 MWCO). The samples were analysed by LCMS.
Expected mass: 29 482 Da. Observed mass: 29 484 Da.

Reaction of GFP_{S147C}-Azal 178 with glutathione

Glutathione (10 µL, 5.0 mM) was added to conjugate GFP_{S147C}-Azal **178** (90 µL, 1.0 mg·mL^{-1}, 34 µM) in sodium phosphate buffer (100 mM, pH 7.4). The reaction was incubated at 37 °C for 72 h and then analysed by LCMS.
Expected mass: 29 332 Da. Observed mass: 29 336 Da.

Reaction of GFP_{S147C}-AlkOH 179 with glutathione

Glutathione (10 µL, 5.0 mM) was added to conjugate GFP_{S147C}-AlkOH **179** (90 µL, 1.0 mg·mL^{-1}, 34 µM) in sodium phosphate buffer (100 mM, pH 7.4). The reaction was incubated at 37 °C for 72 h and then analysed by LCMS.
Expected mass: 29 482 Da. Observed mass: 29 481 Da.

A.3.2.4 Preparation of functionalised GFP_{S147C}-AlkOH

Reaction of GFP_{S147C}-AlkOH 179 with benzyl azide

Tris(3-hydroxypropyltriazolylmethyl)amine (THPTA) (1.2 µL, 20 mM) was added to a solution of CuBr (2.4 µL, 3.0 mg·mL^{-1} in acetonitrile). GFP_{S147C}-AlkOH **179** (60 µL, 1.0 mg·mL^{-1}, 34 µM) in sodium phosphate buffer (100 mM, pH 8.0) was added to the premixed copper solution. Benzyl azide (3 µL, 6.8 mM, 10 eq.) was added to the reaction mixture and the mixture was incubated at 37 °C for 4 h. Excess reagents were removed by repeated diafiltration into fresh buffer (100 mM sodium phosphate, 5 mM EDTA, pH 8.0) using VivaSpin sample concentrators (GE Healthcare, 3000 MWCO). The samples were analysed by LCMS.
Expected mass: 29 615 Da. Observed mass: 29 614 Da.

Reaction of GFP_{S147C}-AlkOH 179 with dansyl azide 162

Tris(3-hydroxypropyltriazolylmethyl)amine (THPTA) (1.2 µL, 20 mM) was added to a solution of CuBr (2.4 µL, 3.0 mg·mL^{-1} in acetonitrile). GFP_{S147C}-AlkOH **179** (60 µL, 1.0 mg·mL^{-1}, 34 µM) in sodium phosphate buffer (100 mM, pH 8.0) was added to the premixed copper solution. Dansyl azide (3 µL, 6.8 mM in DMF, 10 eq.) was added to the reaction mixture and the mixture was incubated at 37 °C for 4 h. Excess reagents were

removed by repeated diafiltration into fresh buffer (100 mM sodium phosphate, 5 mM EDTA, pH 8.0) using VivaSpin sample concentrators (GE Healthcare, 3000 MWCO). The samples were analysed by LCMS.

Expected mass: 29 801 Da. Observed mass: 29 800 Da.

Reaction of GFP_{S147C}-AlkOH 179 with sulfo-cyanine5 azide 145

Tris(3-hydroxypropyltriazolylmethyl)amine (THPTA) (1.2 µL, 20 mM) was added to a solution of CuBr (2.4 µL, 3.0 mg·mL^{-1} in acetonitrile). GFP_{S147C}-AlkOH **179** (60 µL, 1.0 mg·mL^{-1}, 34 µM) in sodium phosphate buffer (100 mM, pH 8.0) was added to the premixed copper solution. Sulfo-cyanine5 azide (3 µL, 6.8 mM in DMF, 10 eq.) was added to the reaction mixture and the mixture was incubated at 37 °C for 4 h. Excess reagents were removed by repeated diafiltration into fresh buffer (100 mM sodium phosphate, 5 mM EDTA, pH 8.0) using VivaSpin sample concentrators (GE Healthcare, 3000 MWCO). The samples were analysed by LCMS.

Expected mass: 30 206 Da. Observed mass: 30 204 Da.

SDS-PAGE gel showing various GFP constructs

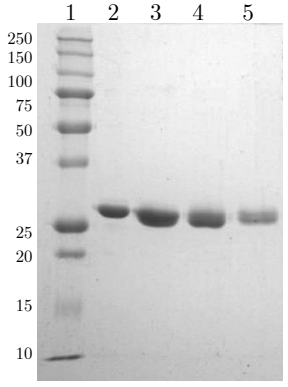

FIGURE A.1: Lane 1 – ladder; 2 – GFP_{S147C} **140**; 3 – GFP_{S147C}-Azal **178**; 4 – GFP_{S147C}-AlkOH **179**; 5 – GFP_{S147C}-AlkOH-Benzyl **180a**.

Appendix B

Acronyms

B.1 Names of Pyridazinediones

	Expanded name (handles)	Number
Azal	**Az**ide–**Al**kyne	**61**
Pazal	**P**EG **Az**ide–**Al**kyne	**69**
MFCO-Astra	**M**ono**f**luoro **C**yclo**o**ctyne-based **A**lkyne–**Str**ained **A**lkyne	**79**
Alkac	**Alk**yne–**Ac**id	**81**
Solastra	**Sol**uble MFCO-**Astra**	**85**
BCN-Astra	**Bic**yclo[6.1.0]**n**onyne-based **A**lkyne–**Str**ained **A**lkyne	**98**
mBr-Azal	**M**ono**br**omo **Azal**	**100**
mBr-Diet	**M**ono**br**omo **Diet**hyl	**103**
Diet	**Diet**hyl	**104**
Azime	**Azi**de **Me**thyl	**120**
BCN-Mestra	**Bic**yclo[6.1.0]**n**onyne-based **Me**thyl–**Str**ained **A**lkyne	**121**

Table B.1: Main acronyms used in this thesis

B.2 Structures of Pyridazinediones

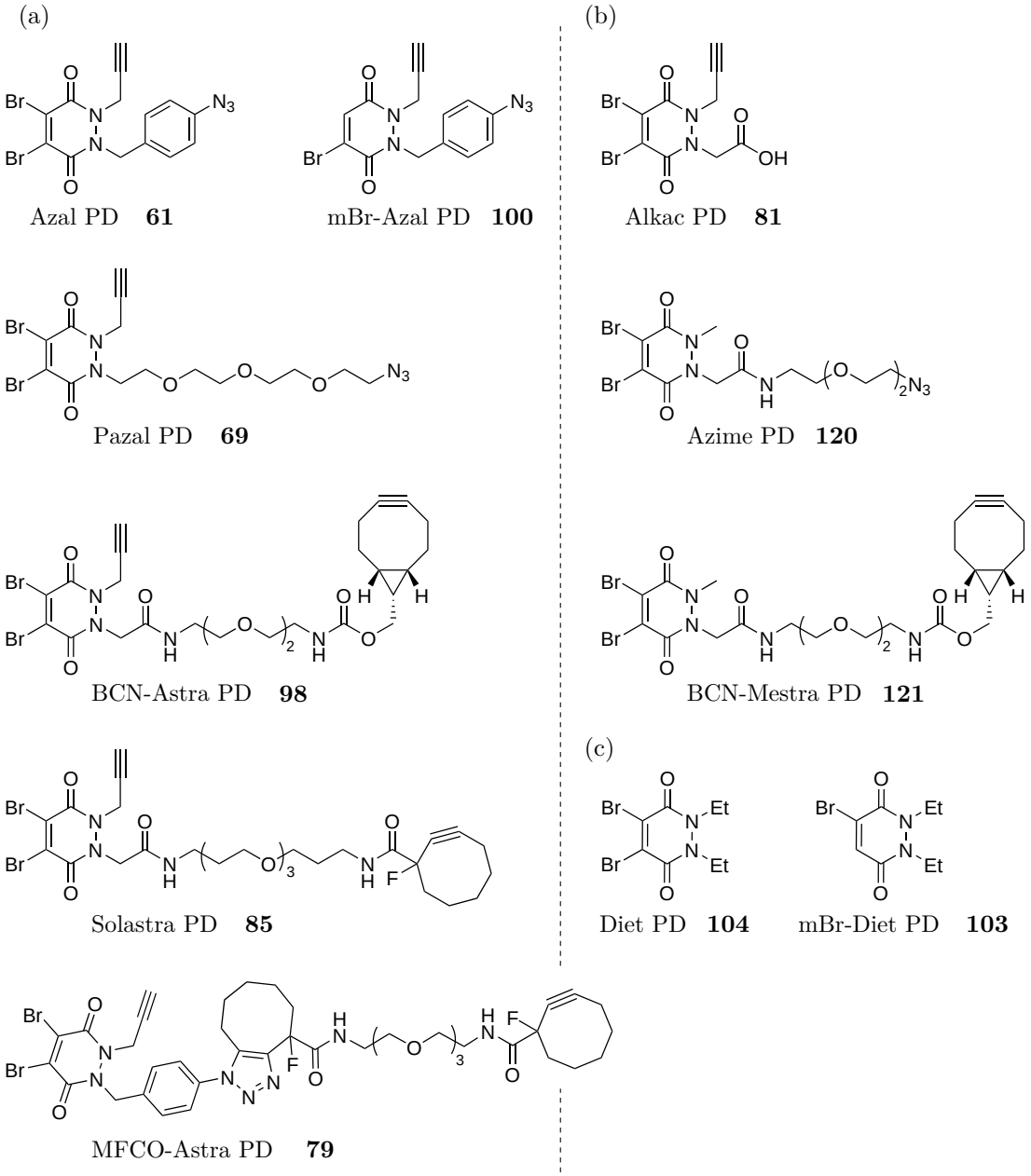

FIGURE B.1: Structure of pyridazinediones prepared with their acronyms with (a) two "clickable" handles; (b) one "clickable" handle; (c) no reactive handle.

Appendix C

Publications

C.1 Peer-reviewed

13. V. Chudasama, A. Maruani and S. Caddick, *Nat. Chem.*, **2016**, DOI: 10.1038/nchem.2415.

12. M. T. W. Lee, A. Maruani, J. R. Baker, S. Caddick and V. Chudasama, *Chem. Sci.*, **2016**, DOI: 10.1039/C5SC02666K.

11. M. T. W. Lee, A. Maruani and V. Chudasama, *J. Chem. Res.*, **2016**, 40, 1 – 9.

10. A. Maruani, H. Savoie, F. Bryden, S. Caddick, R. W. Boyle and V. Chudasama, *Chem. Commun.*, **2015**, 51, 15 304 – 15 307.

9. M. E. B. Smith, M. B. Caspersen, E. Robinson, M. Morais, A. Maruani, J. P. M. Nunes, K. Nicholls, M. J. Saxton, S. Caddick, J. R. Baker and V. Chudasama, *Org. Biomol. Chem.*, **2015**, 13, 7946 – 7949.

8. A. Maruani, M. E. B. Smith, E. Miranda, K. A. Chester, V. Chudasama and S. Caddick, *Nat. Commun.*, **2015**, 6, 6645.

7. A. Maruani, S. Alom, P. Canavelli, M. T. W. Lee, R. E. Morgan, V. Chudasama and S. Caddick, *Chem. Commun.*, **2015**, 51, 5279 – 5282.

6. F. F. Schumacher, J. P. M. Nunes, A. Maruani, V. Chudasama, M. E. B. Smith, K. A. Chester, J. R. Baker and S. Caddick, *Org. Biomol. Chem.*, **2014**, 12, 7261 – 7269.

5. F. Bryden, A. Maruani, H. Savoie, V. Chudasama, M. E. B. Smith, S. Caddick and R. W. Boyle, *Bioconjugate Chem.*, **2014**, 25, 611 – 617.

4. P. Moody, V. Chudasama, R. I. Nathani, A. Maruani, S. Martin, M. E. B. Smith and S. Caddick, *Chem. Commun.*, **2014**, 50, 4898 – 4900.

3. L. Castañeda, A. Maruani, F. F. Schumacher, E. Miranda, V. Chudasama, K. A. Chester, J. R. Baker, M. E. B. Smith and S. Caddick, *Chem. Commun.*, **2013**, 49, 8187 – 8189.

2. L. Castañeda, Z. V. F. Wright, C. Marculescu, T. M. Tran, V. Chudasama, A. Maruani, E. A. Hull, J. P. M. Nunes, R. J. Fitzmaurice, M. E. B. Smith, L. Jones, S. Caddick, and J. R. Baker, *Tetrahedron Lett.*, **2013**, 54, 3493 – 3495.

C.2 Patent

1. F. F. Schumacher, M. E. B. Smith, J. R. Baker, S. Caddick, V. Chudasama and A. Maruani, *WIPO Patent Application WO/2013/132268*, **2013**.

Bibliography

(1) E. S. Lander, L. M. Linton, B. Birren *et al.*, *Nature*, 2001, **409**, 860 – 921.

(2) J. C. Venter, M. D. Adams, E. W. Myers *et al.*, *Science*, 2001, **291**, 1304 – 1351.

(3) O. N. Jensen, *Curr. Opin. Chem. Biol.*, 2004, **8**, 33 – 41.

(4) S. I. van Kasteren, H. B. Kramer, H. H. Jensen *et al.*, *Nature*, 2007, **446**, 1105 – 1109.

(5) C. D. Spicer and B. G. Davis, *Nat. Commun.*, 2014, **5**, 4740.

(6) S. Girouard, M. H. Houle, A. Grandbois, J. W. Keillor and S. W. Michnick, *J. Am. Chem. Soc.*, 2005, **127**, 559 – 566.

(7) D. H. Dube and C. R. Bertozzi, *Nat. Rev. Drug Discov.*, 2005, **4**, 477 – 488.

(8) S. Jevševar, M. Kunstelj and V. G. Porekar, *Biotechnol. J.*, 2010, **5**, 113 – 128.

(9) R. D. Astronomo, H. K. Lee, C. N. Scanlan *et al.*, *J. Virol.*, 2008, **82**, 6359 – 6368.

(10) L. M. Krug, G. Ragupathi, K. K. Ng *et al.*, *Clin. Cancer Res.*, 2004, **10**, 916 – 923.

(11) L. Schofield, M. C. Hewitt, K. Evans, M.-A. Siomos and P. H. Seeberger, *Nature*, 2002, **418**, 785 – 789.

(12) J. J. Day, B. V. Marquez, H. E. Beck, T. A. Aweda, P. D. Gawande and C. F. Meares, *Curr. Opin. Chem. Biol.*, 2010, **14**, 803 – 809.

(13) I. S. Carrico, *Chem. Soc. Rev.*, 2008, **37**, 1423 – 1431.

(14) E. Y. Chi, S. Krishnan, T. W. Randolph and J. F. Carpenter, *Pharm. Res.*, 2003, **20**, 1325 – 1336.

(15) C. P. Hackenberger and D. Schwarzer, *Angew. Chem., Int. Ed. Engl.*, 2008, **47**, 10030 – 10074.

(16) A. J. de Graaf, M. Kooijman, W. E. Hennink and E. Mastrobattista, *Bioconjugate Chem.*, 2009, **20**, 1281 – 1295.

(17) E. M. Sletten and C. R. Bertozzi, *Angew. Chem., Int. Ed. Engl.*, 2009, **48**, 6974 – 6998.

(18) M. B. Francis and I. S. Carrico, *Curr. Opin. Chem. Biol.*, 2010, **14**, 771 – 773.

(19) N. Stephanopoulos and M. B. Francis, *Nat. Chem. Biol.*, 2011, **7**, 876 – 884.

(20) J. Tuls, L. Geren and F. Millett, eng, *J. Biol. Chem.*, 1989, **264**, 16421 – 16425.

(21) J. M. Hooker, A. P. Esser-Kahn and M. B. Francis, eng, *J. Am. Chem. Soc.*, 2006, **128**, 15558 – 15559.

(22) J. C. Gildersleeve, O. Oyelaran, J. T. Simpson and B. Allred, eng, *Bioconjug. Chem.*, 2008, **19**, 1485 – 1490.

(23) P. M. S. D. Cal, J. B. Vicente, E. Pires *et al.*, *J. Am. Chem. Soc.*, 2012, **134**, 10299 – 10305.

(24) G. E. Means and R. E. Feeney, *Bioconjugate Chem.*, 1990, **1**, 2 – 12.

(25) R. Lundblad, *Chemical Reagents for Protein Modification*, CRC Press, Boca Raton, Florida, 3rd edn., 2005.

(26) E. Garanger, R. Weissleder and L. Josephson, *Bioconjugate Chem.*, 2009, **20**, 170 – 173.

(27) S. Jeger, K. Zimmermann, A. Blanc *et al.*, *Angew. Chem., Int. Ed. Engl.*, 2010, **49**, 9995 – 9997.

(28) D. Willner, P. A. Trail, S. J. Hofstead *et al.*, *Bioconjugate Chem.*, 1993, **4**, 521 – 527.

(29) J. R. Adair, P. W. Howard, J. A. Hartley, D. G. Williams and K. A. Chester, *Expert Opin. Biol. Ther.*, 2012, **12**, 1191 – 1206.

(30) S. Kubetzko, C. A. Sarkar and A. Plückthun, *Mol. Pharmacol.*, 2005, **68**, 1439 – 1454.

(31) M. Link, X. Li, J. Kleim and O. S. Wolfbeis, *Eur. J. Org. Chem.*, 2010, **2010**, 6922 – 6927.

(32) A. Wakankar, Y. Chen, Y. Gokarn and F. S. Jacobson, *MAbs*, 2011, **3**, 161 – 172.

(33) F. M. Veronese and G. Pasut, *Drug Discov. Today*, 2005, **10**, 1451 – 1458.

(34) X. Chen, K. Muthoosamy, A. Pfisterer, B. Neumann and T. Weil, *Bioconjugate Chem.*, 2012, **23**, 500 – 508.

(35) R. Bhattacharyya, D. Pal and P. Chakrabarti, *Protein Eng. Des. Sel.*, 2004, **17**, 795 – 808.

(36) M. T. Petersen, P. H. Jonson and S. B. Petersen, *Protein Eng.*, 1999, **12**, 535 – 548.

(37) R. A. Bednar, *Biochemistry (Mosc.)*, 1990, **29**, 3684 – 3690.

(38) D. J. Betting, K. Kafi, A. Abdollahi-Fard, S. A. Hurvitz and J. M. Timmerman, *J. Immunol.*, 2008, **181**, 4131 – 4140.

(39) Y. Zhang, V. S. Bhatt, G. Sun, P. G. Wang and A. F. Palmer, *Bioconjugate Chem.*, 2008, **19**, 2221 – 2230.

(40) I. Shin, H. J. Jung and M. R. Lee, *Tetrahedron Lett.*, 2001, **42**, 1325 – 1328.

(41) C. Lind, R. Gerdes, Y. Hamnell *et al.*, *Arch. Biochem. Biophys.*, 2002, **406**, 229 – 240.

(42) A. Denicola-Seoane and B. M. Anderson, *Biochim. Biophys. Acta*, 1990, **1040**, 84 – 88.

(43) M. Esmann, P. C. Sar, K. Hideg and D. Marsh, *Anal. Biochem.*, 1993, **213**, 336 – 348.

(44) J. A. Thomas, Y. C. Chai and C. H. Jung, *Oxygen Radicals in Biological Systems, Part C (Methods in Enzymology) – Protein S-Thiolation and Dethiolation*, Academic Press, 1994, vol. 233, pp. 385 – 395.

(45) S. Trapp, S. Haider, P. Jones, M. S. P. Sansom and F. M. Ashcroft, *EMBO J.*, 2003, **22**, 2903 – 2912.

(46) J. M. May, *J. Biol. Chem.*, 1988, **263**, 13635 – 13640.

(47) H. H. Winkler, R. M. Daugherty and J. P. Audia, *Biochemistry (Mosc.)*, 2003, **42**, 12562 – 12569.

(48) C. P. Ryan, Ph.D. Thesis, University College London, 2010.

(49) *Maleimide Functionalized*, http://www.sigmaaldrich.com/materials-science/material-science-products.html?TablePage=112250210 (accessed June 2015).

(50) L. M. Tedaldi, M. E. Smith, R. I. Nathani and J. R. Baker, *Chem. Commun.*, 2009, 6583 – 6585.

(51) M. E. Smith, F. F. Schumacher, C. P. Ryan *et al.*, *J. Am. Chem. Soc.*, 2010, **132**, 1960 – 1965.

(52) V. Chudasama, M. E. Smith, F. F. Schumacher *et al.*, *Chem. Commun.*, 2011, **47**, 8781 – 8783.

(53) C. S. Sevier and C. A. Kaiser, *Nat. Rev. Mol. Cell Biol.*, 2002, **3**, 836 – 847.

(54) M. Mucke and F. X. Schmid, *J. Mol. Biol.*, 1994, **239**, 713 – 725.

(55) S. Shaunak, A. Godwin, J. W. Choi *et al.*, *Nat. Chem. Biol.*, 2006, **2**, 312 – 313.

(56) F. F. Schumacher, M. Nobles, C. P. Ryan *et al.*, *Bioconjugate Chem.*, 2011, **22**, 132 – 136.

(57) P. Moody, M. E. B. Smith, C. P. Ryan *et al.*, *ChemBioChem*, 2012, **13**, 39 – 41.

(58) R. A. Rhoades and R. G. Pflanzer, *Human Physiology*, Cengage Learning, 2002.

(59) C. Janeway, P. Travers, M. Walport and M. Shlomchik, *Immunobiology*, Garland Science, 5$^{\text{th}}$ edn., 2001.

(60) R. K. Jain, *Cancer Res.*, 1990, **50**, 814 – 819.

(61) T. Yokota, D. E. Milenic, M. Whitlow and J. Schlom, *Cancer Res.*, 1992, **52**, 3402 – 3408.

(62) A. J. Cumber, E. S. Ward, G Winter, G. D. Parnell and E. J. Wawrzynczak, *J. Immunol.*, 1992, **149**, 120 – 126.

(63) L. J. Holt, A. Basran, K. Jones *et al.*, *Protein Eng. Des. Sel.*, 2008, **21**, 283 – 288.

(64) J. M. Harris and R. B. Chess, *Nat. Rev. Drug Discov.*, 2003, **2**, 214 – 221.

(65) T. Suzuki, N. Kanbara, T. Tomono, N. Hayashi and I. Shinohara, *Biochim. Biophys. Acta*, 1984, **788**, 248 – 255.

(66) P. Caliceti and F. M. Veronese, *Adv. Drug Deliv. Rev.*, 2003, **55**, 1261 – 1277.

(67) A. Jain and S. K. Jain, *Crit. Rev. Ther. Drug Carrier Syst.*, 2008, **25**, 403 – 447.

(68) I. Buchwalow, V. Samoilova, W. Boecker and M. Tiemann, *Sci. Rep.*, 2011, **1**, 28.

(69) *Advantages of Antibody Fragments*, http://www.piercenet.com/method/antibody-fragmentation (accessed June 2015).

(70) A. L. Nelson and J. M. Reichert, *Nat. Biotechnol.*, 2009, **27**, 331 – 337.

(71) A. L. Nelson, *MAbs*, 2010, **2**, 77 – 83.

(72) C. Rao, *Immunology: A Textbook*, Narosa Publishing House, 2005.

(73) L. Griffin and A. Lawson, *Clinical & Experimental Immunology*, 2011, **165**, 285 – 291.

(74) P. Ehrlich, *Br. Med. J.*, 1913, **2**, 353 – 359.

(75) G. Mathe, T. B. Loc and J. Bernard, *C. r. hebd. séances Acad. sci.*, 1958, **246**, 1626 – 1628.

(76) T. Ghose and S. P. Nigam, *Cancer*, 1972, **29**, 1398 – 1400.

(77) G. F. Rowland, G. J. Oneill and D. A. L. Davies, *Nature*, 1975, **255**, 487 – 488.

(78) C. H. J. Ford, C. E. Newman, J. R. Johnson *et al.*, *Br. J. Cancer*, 1983, **47**, 35 – 42.

(79) P. A. Trail, D. Willner, S. J. Lasch *et al.*, *Science*, 1993, **261**, 212 – 215.

(80) G. A. Pietersz and K. Krauer, *J. Drug Target.*, 1994, **2**, 183 – 215.

(81) M. L. Linenberger, T. Hong, D. Flowers *et al.*, *Blood*, 2001, **98**, 988 – 994.

(82) A. Younes, N. L. Bartlett, J. P. Leonard *et al.*, *N. Engl. J. Med.*, 2010, **363**, 1812 – 1821.

(83) P. D. Senter and E. L. Sievers, *Nat. Biotechnol.*, 2012, **30**, 631 – 637.

(84) S. Verma, D. Miles, L. Gianni *et al.*, *N. Engl. J. Med.*, 2012, **367**, 1783 – 1791.

(85) P. M. LoRusso, D. Weiss, E. Guardino, S. Girish and M. X. Sliwkowski, *Clin. Cancer Res.*, 2011, **17**, 6437 – 6447.

(86) A. Mullard, *Nat. Rev. Drug Discov.*, 2013, **12**, 329 – 332.

(87) K. J. Hamblett, P. D. Senter, D. F. Chace *et al.*, *Clin. Cancer Res.*, 2004, **10**, 7063 – 70.

(88) A. C. Stan, D. L. Radu, S. Casares, C. A. Bona and T. D. Brumeanu, *Cancer Res.*, 1999, **59**, 115 – 21.

(89) P. Strop, S.-H. Liu, M. Dorywalska *et al.*, *Chem. Biol.*, 2013, **20**, 161 – 167.

(90) A. Lyons, D. J. King, R. J. Owens *et al.*, *Protein Eng.*, 1990, **3**, 703 – 708.

(91) J. R. Junutula, H. Raab, S. Clark *et al.*, *Nat. Biotechnol.*, 2008, **26**, 925 – 932.

(92) M. Sunbul and J. Yin, *Org. Biomol. Chem.*, 2009, **7**, 3361 – 3371.

(93) T. S. Young, I. Ahmad, J. A. Yin and P. G. Schultz, *J. Mol. Biol.*, 2010, **395**, 361 – 374.

(94) D. Rabuka, J. S. Rush, G. W. deHart, P. Wu and C. R. Bertozzi, *Nat. Protoc.*, 2012, **7**, 1052 – 1067.

(95) J. Y. Axup, K. M. Bajjuri, M. Ritland *et al.*, *Proc. Natl. Acad. Sci. U. S. A.*, 2012, **109**, 16101 – 16106.

(96) J. R. Junutula, S. Bhakta, H. Raab *et al.*, *J. Immunol. Methods*, 2008, **332**, 41 – 52.

(97) H. J. Woo, M. M. Lotz, J. U. Jung and A. M. Mercurio, *J. Biol. Chem.*, 1991, **266**, 18419 – 22.

(98) S. K. Wootton and D. Yoo, *J. Virol.*, 2003, **77**, 4546 – 57.

(99) C. S. Greenberg, P. J. Birckbichler and R. H. Rice, *FASEB J.*, 1991, **5**, 3071 – 7.

(100) T. Kanaji, H. Ozaki, T. Takao *et al.*, *J. Biol. Chem.*, 1993, **268**, 11565 – 72.

(101) T. Kashiwagi, K. Yokoyama, K. Ishikawa *et al.*, *J. Biol. Chem.*, 2002, **277**, 44252 – 60.

(102) P. Strop, W. H. Ho, L. M. Boustany *et al.*, *J. Mol. Biol.*, 2012, **420**, 204 – 219.

(103) P. Wu, W. Shui, B. L. Carlson *et al.*, *Proc. Natl. Acad. Sci. U. S. A.*, 2009, **106**, 3000 – 5.

(104) P. M. Drake, A. E. Albers, J. Baker *et al.*, *Bioconjugate Chem.*, 2014, **25**, 1331 – 41.

(105) E. S. Zimmerman, T. H. Heibeck, A. Gill *et al.*, *Bioconjugate Chem.*, 2014, **25**, 351 – 61.

(106) P. Sapra, M. Damelin, J. Dijoseph *et al.*, *Mol. Cancer Ther.*, 2013, **12**, 38 – 47.

(107) F. Tian, Y. Lu, A. Manibusan *et al.*, *Proc. Natl. Acad. Sci. U. S. A.*, 2014, **111**, 1766 – 71.

(108) W. F. Dall'Acqua, K. E. Cook, M. M. Damschroder, R. M. Woods and H. Wu, *J. Immunol.*, 2006, **177**, 1129 – 1138.

(109) M. M. Sun, K. S. Beam, C. G. Cerveny *et al.*, *Bioconjugate Chem.*, 2005, **16**, 1282 – 90.

(110) S. O. Doronina, B. E. Toki, M. Y. Torgov *et al.*, *Nat. Biotechnol.*, 2003, **21**, 778 – 84.

(111) N. S. Beckley, K. P. Lazzareschi, H.-W. Chih, V. K. Sharma and H. L. Flores, *Bioconjugate Chem.*, 2013, **24**, 1674 – 1683.

(112) A. D. Baldwin and K. L. Kiick, *Bioconjugate Chem.*, 2011, **22**, 1946 – 1953.

(113) B.-Q. Shen, K. Xu, L. Liu *et al.*, *Nat. Biotechnol.*, 2012, **30**, 184 – 189.

(114) M. E. B. Smith, M. B. Caspersen, E. Robinson *et al.*, *Org. Biomol. Chem.*, 2015, 7946 – 7949.

(115) R. P. Lyon, J. R. Setter, T. D. Bovee *et al.*, *Nat. Biotechnol.*, 2014, **32**, 1059 – 62.

(116) L. N. Tumey, M. Charati, T. He *et al.*, *Bioconjugate Chem.*, 2014, **25**, 1871 – 1880.

(117) C. P. Ryan, M. E. Smith, F. F. Schumacher *et al.*, *Chem. Commun.*, 2011, **47**, 5452 – 5454.

(118) G. Badescu, P. Bryant, M. Bird *et al.*, *Bioconjugate Chem.*, 2014, **25**, 1124 – 36.

(119) F. F. Schumacher, J. P. M. Nunes, A. Maruani *et al.*, *Org. Biomol. Chem.*, 2014, **12**, 7261 – 7269.

(120) J. P. M. Nunes, M. Morais, V. Vassileva *et al.*, *Chem. Commun.*, 2015, **51**, 10624 – 10627.

(121) L. M. Hinman, P. R. Hamann, R. Wallace, A. T. Menendez, F. E. Durr and J. Upeslacis, *Cancer Res.*, 1993, **53**, 3336 – 42.

(122) P. R. Hamann, L. M. Hinman, C. F. Beyer *et al.*, *Bioconjugate Chem.*, 2005, **16**, 346 – 53.

(123) W. Wang, J. Vlasak, Y. Li *et al.*, *Mol. Immunol.*, 2011, **48**, 860 – 6.

(124) Q. Zhou, J. E. Stefano, C. Manning *et al.*, *Bioconjugate Chem.*, 2014, **25**, 510 – 20.

(125) X. Li, T. Fang and G. J. Boons, *Angew. Chem., Int. Ed. Engl.*, 2014, **53**, 7179 – 82.

(126) R. Jefferis, *Biotechnol. Prog.*, 2005, **21**, 11 – 6.

(127) H. C. Kolb, M. G. Finn and K. B. Sharpless, *Angew. Chem., Int. Ed.*, 2001, **40**, 2004 – 2021.

(128) K. Nwe and M. W. Brechbiel, *Cancer Biother. Radiopharm.*, 2009, **24**, 289 – 302.

(129) S. I. Presolski, V. P. Hong and M. Finn, *Curr. Protoc. Chem. Biol.*, 2011, **3**, 153 – 162.

(130) C. Besanceney-Webler, H. Jiang, T. Zheng *et al.*, *Angew. Chem., Int. Ed.*, 2011, **50**, 8051 – 8056.

(131) D. M. Beal and L. H. Jones, *Angew. Chem., Int. Ed. Engl.*, 2012, **51**, 6320 – 6326.

(132) C. S. McKay and M. Finn, *Chem. Biol.*, 2014, **21**, 1075 – 1101.

(133) M. Zheng, L. Zheng, P. Zhang, J. Li and Y. Zhang, *Molecules*, 2015, **20**, 3190 – 3205.

(134) O. Dimroth, *Ber. Dtsch. Chem. Ges.*, 1902, **35**, 1029 – 1038.

(135) R. Huisgen, *Proc. Chem. Soc.*, 1961, 357 – 396.

(136) V. V. Rostovtsev, L. G. Green, V. V. Fokin and K. B. Sharpless, *Angew. Chem., Int. Ed.*, 2002, **41**, 2596 – 2599.

(137) C. W. Tornøe, C. Christensen and M. Meldal, *J. Org. Chem.*, 2002, **67**, 3057 – 3064.

(138) V. Hong, S. I. Presolski, C. Ma and M. G. Finn, *Angew. Chem., Int. Ed.*, 2009, **48**, 9879 – 9883.

(139) D. C. Kennedy, C. S. McKay, M. C. B. Legault *et al.*, *J. Am. Chem. Soc.*, 2011, **133**, 17993 – 18001.

(140) N. J. Agard, J. A. Prescher and C. R. Bertozzi, *J. Am. Chem. Soc.*, 2004, **126**, 15046 – 15047.

(141) D. Banerjee, A. P. Liu, N. R. Voss, S. L. Schmid and M. G. Finn, *ChemBioChem*, 2010, **11**, 1273 – 1279.

(142) N. Stephanopoulos, G. J. Tong, S. C. Hsiao and M. B. Francis, *ACS Nano*, 2010, **4**, 6014 – 6020.

(143) I. K. Oh, H. Mok and T. G. Park, *Bioconjugate Chem.*, 2006, **17**, 721 – 727.

(144) V. Ratner, E. Kahana, M. Eichler and E. Haas, *Bioconjugate Chem.*, 2002, **13**, 1163 – 1170.

(145) R. I. Nathani, P. Moody, V. Chudasama, M. E. B. Smith, R. J. Fitzmaurice and S. Caddick, *Chem. Sci.*, 2013, **4**, 3455.

(146) P. Moody, V. Chudasama, R. I. Nathani *et al.*, *Chem. Commun.*, 2014, **50**, 4898.

(147) J. M. Antos, G. L. Chew, C. P. Guimaraes *et al.*, *J. Am. Chem. Soc.*, 2009, **131**, 10800 – 10801.

(148) M. Simon, U. Zangemeister-Wittke and A. Plückthun, *Bioconjugate Chem.*, 2012, **23**, 279 – 286.

(149) M. Mühlberg, M. G. Hoesl, C. Kuehne, J. Dernedde, N. Budisa and C. P. R. Hackenberger, *Beilstein J. Org. Chem.*, 2015, **11**, 784 – 791.

(150) R. Jiang, L. Wang, J. Weingart and X.-L. Sun, *ChemBioChem*, 2013, **15**, 42 – 46.

(151) A. Watzke, M. Köhn, M. Gutierrez-Rodriguez *et al.*, *Angew. Chem., Int. Ed.*, 2006, **45**, 1408 – 1412.

(152) R. P. Temming, L. Eggermont, M. B. van Eldijk, J. C. M. van Hest and F. L. van Delft, *Org. Biomol. Chem.*, 2013, **11**, 2772.

(153) M. Rashidian, S. C. Kumarapperuma, K. Gabrielse, A. Fegan, C. R. Wagner and M. D. Distefano, *J. Am. Chem. Soc.*, 2013, **135**, 16388 – 16396.

(154) D. M. Beal, V. E. Albrow, G. Burslem *et al.*, *Org. Biomol. Chem.*, 2012, **10**, 548 – 554.

(155) A. Maruani, M. E. B. Smith, E. Miranda, K. A. Chester, V. Chudasama and S. Caddick, *Nat. Commun.*, 2015.

(156) L. Wang and P. G. Schultz, *Angew. Chem., Int. Ed.*, 2005, **44**, 34 – 66.

(157) J. M. Chalker, G. J. L. Bernardes and B. G. Davis, *Acc. Chem. Res.*, 2011, **44**, 730 – 741.

(158) H. Neumann, K. Wang, L. Davis, M. Garcia-Alai and J. W. Chin, *Nature*, 2010, **464**, 441 – 444.

(159) W. Wan, Y. Huang, Z. Wang *et al.*, *Angew. Chem., Int. Ed.*, 2010, **49**, 3211 – 3214.

(160) B. Wu, Z. Wang, Y. Huang and W. R. Liu, *ChemBioChem*, 2012, **13**, 1405 – 1408.

(161) I. Nikić, T. Plass, O. Schraidt *et al.*, *Angew. Chem., Int. Ed.*, 2014, **53**, 2245 – 2249.

(162) T. Mukai, A. Hayashi, F. Iraha *et al.*, *Nucleic Acids Res.*, 2010, **38**, 8188 – 8195.

(163) D. B. F. Johnson, J. Xu, Z. Shen *et al.*, *Nat. Chem. Biol.*, 2011, **7**, 779 – 786.

(164) M. J. Lajoie, A. J. Rovner, D. B. Goodman *et al.*, *Science*, 2013, **342**, 357 – 360.

(165) S. Nehring, N. Budisa and B. Wiltschi, *PLOS ONE*, 2012, **7**, ed. D. Jones, 31992.

(166) E. M. Brustad, E. A. Lemke, P. G. Schultz and A. A. Deniz, *J. Am. Chem. Soc.*, 2008, **130**, 17664 – 17665.

(167) C. Gill, G. Jadhav, M. Shaikh *et al.*, *Bioorg. Med. Chem. Lett.*, 2008, **18**, 6244 – 6247.

(168) R. Mornet, N. J. Leonard, J. B. Theiler and M. Doree, *J. Chem. Soc., Perkin Trans. 1*, 1984, 879 – 885.

(169) L. K. Rasmussen, *J. Org. Chem.*, 2006, **71**, 3627 – 3629.

(170) L. Castañeda, Z. V. F. Wright, C. Marculescu *et al.*, *Tetrahedron Lett.*, 2013, **54**, 3493 – 3495.

(171) S. Svedhem, C.-Å. Hollander, J. Shi, P. Konradsson, B. Liedberg and S. C. T. Svensson, *J. Org. Chem.*, 2001, **66**, 4494 – 4503.

(172) M. K. Schultz, S. G. Parameswarappa and F. C. Pigge, *Org. Lett.*, 2010, **12**, 2398 – 2401.

(173) K. K. Sadhu, S. Mizukami, S. Watanabe and K. Kikuchi, *Chem. Commun.*, 2010, **46**, 7403.

(174) C. Dai, L. Cazares, B. Wang *et al.*, *Cellular recognition conjugates and methods of use for the histological analysis of cancer tissue using maldi-ms imaging*, WO Patent App. PCT/US2012/047,557, 2013.

(175) J. Dommerholt, S. Schmidt, R. Temming *et al.*, *Angew. Chem., Int. Ed.*, 2010, **49**, 9422 – 9425.

(176) K. Lang, L. Davis, S. Wallace *et al.*, *J. Am. Chem. Soc.*, 2012, **134**, 10317 – 10320.

(177) D. Wang, W. Chen, Y. Zheng *et al.*, *Org. Biomol. Chem.*, 2014, **12**, 3950.

(178) J. D. Thomas, H. Cui, P. J. North, T. Hofer, C. Rader and J. Burke, T. R., *Bioconjugate Chem.*, 2012, **23**, 2007 – 2013.

(179) M. R. Karver, R. Weissleder and S. A. Hilderbrand, *Angew. Chem., Int. Ed. Engl.*, 2012, **51**, 920 – 922.

(180) J. A. Stafford, M. F. Brackeen, D. S. Karanewsky and N. L. Valvano, *Tetrahedron Lett.*, 1993, **34**, 7873 – 7876.

(181) O. Tšubrik and U. Mäeorg, *Org. Lett.*, 2001, **3**, 2297 – 2299.

(182) J. Bange, E. Zwick and A. Ullrich, *Nat. Med.*, 2001, **7**, 548 – 552.

(183) C. A. Hudis, *N. Engl. J. Med.*, 2007, **357**, 39 – 51.

(184) T. Kute, C. M. Lack, M. Willingham *et al.*, *Cytometry*, 2004, **57A**, 86 – 93.

(185) J. Albanell, J. Codony, A. Rovira, B. n. Mellado and P. Gascón, in *New Trends in Cancer for the 21st Century*, ed. A. Llombart-Bosch and V. Felipo, Springer US, 2003, vol. 532, pp. 253 – 268.

(186) H.-S. Cho, K. Mason, K. X. Ramyar *et al.*, *Nature*, 2003, **421**, 756 – 760.

(187) L. Vecchione, M. Orditura, F. Ciardiello and F. De Vita, *Expert Opin. Invest. Drugs*, 2009, **18**, 945 – 955.

(188) A. D. Santin, S. Bellone, J. J. Roman, J. K. McKenney and S. Pecorelli, *Int. J. Gynaecol. Obstet.*, 2008, **102**, 128 – 131.

(189) US FDA, *FDA approves new treatment for late stage breast cancer*, press release, Feb. 22, 2013.

(190) A. Coulter and R. Harris, *J. Immunol. Methods*, 1983, **59**, 199 – 203.

(191) K. L. Bennett, S. V. Smith, R. J. W. Truscott and M. M. Sheil, *Anal. Biochem.*, 1997, **245**, 17 – 27.

(192) L. Castañeda, A. Maruani, F. F. Schumacher *et al.*, *Chem. Commun.*, 2013, **49**, 8187 – 8189.

(193) B. Pal, P. K. Pradhan, P. Jaisankar and V. S. Giri, *Synthesis*, 2003, 1549 – 1552.

(194) F. F. Schumacher, Ph.D. Thesis, University College London, 2012.

(195) S. Brocchini, S. Balan, A. Godwin, J.-W. Choi, M. Zloh and S. Shaunak, *Nat. Protoc.*, 2006, **1**, 2241 – 2252.

(196) S. Brocchini, A. Godwin, S. Balan, J. W. Choi, M. Zloh and S. Shaunak, *Adv. Drug Deliv. Rev.*, 2008, **60**, 3 – 12.

(197) S. Balan, J.-w. Choi, A. Godwin *et al.*, *Bioconjugate Chem.*, 2007, **18**, 61 – 76.

(198) J. M. Chalker, G. J. Bernardes, Y. A. Lin and B. G. Davis, *Chem. Asian J.*, 2009, **4**, 630 – 640.

(199) A. Maruani, S. Alom, P. Canavelli *et al.*, *Chem. Commun.*, 2015, **51**, 5279–5282.

(200) S. S. Kelkar and T. M. Reineke, *Bioconjugate Chem.*, 2011, **22**, 1879 – 1903.

(201) P. Wang and A. Moore, *Imaging Med.*, 2014, **6**, 25 – 39.

(202) S. M. Janib, A. S. Moses and J. A. MacKay, *Adv. Drug Deliv. Rev.*, 2010, **62**, 1052 – 1063.

(203) J. V. Jokerst and S. S. Gambhir, *Acc. Chem. Res.*, 2011, **44**, 1050 – 1060.

(204) X. Ma, Y. Zhao and X.-J. Liang, *Acc. Chem. Res.*, 2011, **44**, 1114 – 1122.

(205) F. L. Thorp-Greenwood and M. P. Coogan, *Dalton Trans.*, 2011, **40**, 6129.

(206) N. Crawley, M. Thompson and A. Romaschin, *Anal. Chem.*, 2014, **86**, 130 – 160.

(207) C. Hess, D. Venetz and D. Neri, *Med. Chem. Commun.*, 2014, **5**, 408.

(208) M. M. Schmidt and K. D. Wittrup, *Mol. Cancer Ther.*, 2009, **8**, 2861 – 2871.

(209) G. M. Thurber, M. M. Schmidt and K. D. Wittrup, *Adv. Drug Deliv. Rev.*, 2008, **60**, 1421 – 1434.

(210) P. Holliger and P. J. Hudson, *Nat. Biotechnol.*, 2005, **23**, 1126 – 1136.

(211) D. E. Milenic, T. Yokota, D. R. Filpula *et al.*, *Cancer Res.*, 1991, **51**, 6363 – 6371.

(212) L. E. Williams, A. M. Wu, P. J. Yazaki *et al.*, *Cancer Biother. Radiopharm.*, 2001, **16**, 25 – 35.

(213) L. J. Holt, C. Herring, L. S. Jespers, B. P. Woolven and I. M. Tomlinson, *Trends Biotechnol.*, 2003, **21**, 484 – 490.

(214) W. M. Deen, M. J. Lazzara and B. D. Myers, *Am. J. Physiol. Renal Physiol.*, 2001, **281**, 579 – 596.

(215) R. Webster, V. Elliott, B. K. Park, D. Walker, M. Hankin and P. Taupin, in *PEGylated protein drugs: Basic science and clinical applications*, Springer, 2009, pp. 127 – 146.

(216) A. P. Chapman, P. Antoniw, M. Spitali, S. West, S. Stephens and D. J. King, *Nat. Biotechnol.*, 1999, **17**, 780 – 783.

(217) K. Yang, A. Basu, M. Wang *et al.*, *Protein Eng. Des. Sel.*, 2003, **16**, 761 – 770.

(218) C. S. Fishburn, *J. Pharm. Sci.*, 2008, **97**, 4167 – 4183.

(219) T. Kämpchen, W. Massa, W. Overheu, R. Schmidt and G. Seitz, *Chem. Ber.*, 1982, **115**, 683 – 694.

(220) W. Chen, D. Wang, C. Dai, D. Hamelberg and B. Wang, *Chem. Commun.*, 2012, **48**, 1736 – 1738.

(221) A. Niederwieser, A.-K. Späte, L. D. Nguyen, C. Jüngst, W. Reutter and V. Wittmann, *Angew. Chem., Int. Ed.*, 2013, **52**, 4265 – 4268.

(222) M. R. Karver, R. Weissleder and S. A. Hilderbrand, *Bioconjugate Chem.*, 2011, **22**, 2263 – 2270.

(223) A. Krebs and H. Kimling, *Tetrahedron Lett.*, 1970, **11**, 761 – 764.

(224) G. Wittig and S. Fischer, *Chem. Ber.*, 1972, **105**, 3542 – 3552.

(225) E. A. Hull, Ph.D. Thesis, University College London, 2014.

(226) A. G. Polson, J. Calemine-Fenaux, P. Chan *et al.*, *Cancer Res.*, 2009, **69**, 2358 – 2364.

(227) B. Gorovits and C. Krinos-Fiorotti, *Cancer Immunol. Immunother.*, Feb. 2013, **62**, 217 – 223.

(228) P. M. S. D. Cal, G. J. L. Bernardes and P. M. P. Gois, *Angew. Chem., Int. Ed. Engl.*, 2014, **53**, 10585 – 10587.

(229) R. V. J. Chari, M. L. Miller and W. C. Widdison, *Angew. Chem., Int. Ed. Engl.*, 2014, **53**, 3796 – 3827.

(230) L. Ducry and B. Stump, *Bioconjugate Chem.*, 2010, **21**, 5 – 13.

(231) M. N. Saleh, S. Sugarman, J. Murray *et al.*, *J. Clin. Oncol.*, 2000, **18**, 2282 – 2292.

(232) C. Liu, B. M. Tadayoni, L. A. Bourret *et al.*, *Proc. Natl. Acad. Sci. U. S. A.*, 1996, **93**, 8618 – 8623.

(233) R. V. Chari, K. A. Jackel, L. A. Bourret *et al.*, *Cancer Res.*, 1995, **55**, 4079 – 4084.

(234) I. Ojima, X. Geng, X. Wu *et al.*, *J. Med. Chem.*, 2002, **45**, 5620 – 5623.

(235) F. Michelet, R. Gueguen, P. Leroy, M. Wellman, A. Nicolas and G. Siest, *Clin. Chem.*, 1995, **41**, 1509 – 1517.

(236) S. Jalota, S. B. Bhaduri and A. C. Tas, *Mater. Sci. Eng. C*, 2008, **28**, 129 – 140.

(237) N. A. Burton, D. V. S. Green, I. H. Millier, P. J. Taylor, M. A. Vincent and S. Woodcock, *J. Chem. Soc., Perkin Trans. 2*, 1993, 331.

(238) H. Feuer, G. B. Silverman, H. P. Angstadt and A. R. Fauke, *J. Org. Chem.*, 1962, **27**, 2081–2084.

(239) D. M. Miller and R. W. White, *Can. J. Chem.*, 1956, **34**, 1510–1512.

(240) P. L. Carl, P. K. Chakravarty and J. A. Katzenellenbogen, *J. Med. Chem.*, 1981, **24**, 479 – 480.

(241) *Herceptin – Description*, www.fda.gov — ucm092760.pdf.

(242) M. Das, R. Jain, A. K. Agrawal, K. Thanki and S. Jain, *Bioconjugate Chem.*, 2014, **25**, 501 – 509.

(243) D. Thiyagarajan, S. Goswami, C. Kar, G. Das and A. Ramesh, *Chem. Commun.*, 2014, **50**, 7434.

(244) L. L. Silver, *Clin. Microbiol. Rev.*, 2011, **24**, 71 – 109.

(245) K. M. G. O'Connell, J. T. Hodgkinson, H. F. Sore, M. Welch, G. P. C. Salmond and D. R. Spring, *Angew. Chem., Int. Ed.*, 2013, **52**, 10706 – 10733.

(246) H. E. Colley, V. Hearnden, M. Avila-Olias *et al.*, *Mol. Pharm.*, 2014, **11**, 1176 – 1188.

(247) M. Dubernet, V. Caubert, J. Guillard and M. C. Viaud-Massuard, *Tetrahedron*, 2005, **61**, 4585 – 4593.

(248) H. S. G. Beckmann, A. Niederwieser, M. Wiessler and V. Wittmann, *Chem. – Eur. J.*, 2012, **18**, 6548 – 6554.

(249) R. Yan, K. Sander, E. Galante *et al.*, *J. Am. Chem. Soc.*, 2013, **135**, 703 – 709.

(250) R. Nathani, P. Moody, M. E. B. Smith, R. J. Fitzmaurice and S. Caddick, *ChemBioChem*, 2012, **13**, 1283 – 1285.